IMPROVING ENERGY USE, DEMAND AND VISUAL COMFORT IN COMMERICAL BUILDINGS USING LIGHTING AND SHADING CONTROLS

By

Soham Vanage

A DISSERTATION

Submitted to
Michigan State University
in partial fulfillment of the requirements
for the degree of

Civil Engineering – Doctor of Philosophy

2023

ABSTRACT

Windows provide occupants with natural light and a view of the outside, enhancing productivity, which is important as people spend approximately 90% of their time indoors. This is especially the case during and after the COVID-19 pandemic. Automated controls for window shading systems can be used to control solar radiation and daylight entering the space. Lighting controls can reduce lighting requirements, providing energy savings and better visual comfort for occupants than manual controls, which are seldom used effectively.

Past studies have explored automated lighting and shading control strategies, and reported energy savings and visual comfort improvements over their baselines. However, the assumptions for baseline models differ across different studies, making it difficult to compare these automated controls. Thus, this research uses a multi-step modeling process, including daylighting and energy simulations using RADIANCE and EnergyPlus, respectively (i) to compare existing control strategies using the same building inputs (baseline model) for a prototypical small office building, (ii) to develop and evaluate the effectiveness of a novel integrated control strategy that uses variables such as occupancy, HVAC state, solar radiation entering the space, time of day for control, and others variables. (iii) to develop a parametric model to investgate the impact of different input variables such as building form factor, window-to-wall ratio for all different orientations, shade properties such as openness factor, and shade overhang depth on energy performance and visual comfort.

On top of improving energy efficiency and visual comfort in buildings, managing demand at the grid level is becoming more important as renewable energy gets added to the generation mix. Instead of adding more generation to balance the grid, usually using new fossil fuel-based generation, the other approach to balance the grid is to use existing building loads and reduce their

demand during specific hours (also known as demand-side Flexibility Services (FS)). As buildings become smarter with the adoption of new technologies for sensing and control, more integration between buildings and the electric grid is possible. Building loads such as air conditioning and lighting in commercial buildings have the potential to provide demand-side FS. In particular, demand-side flexibility using lighting loads is not well studied in the literature. In commercial buildings, lighting accounts for approximately 10-15% of the load at any time. Past studies have shown that lighting can be dimmed by 15-20% without causing visual discomfort to the occupants. The forth objective thus of theis study (iv) if to improve the existing literature by providing building level and grid level estimates for using lighting loads for all the common commercial building types as demand-side Flexible Services (FS) for three future scenarios in the Midwest region.

Dedicated to my mother Kalpana Vanage for her endless support

ACKNOWLEDGEMENTS

I would like to thank and express my gratitude to many who helped me along the way on this journey without whom this work would not be possible.

Firstly, I would like to thank my major advisor, Dr. Kristen Cetin, for believing in me and providing me with the opportunity to work on this research. Her guidance, support, direction, and encouraging words throughout my journey at both Iowa State University and Michigan State University has helped me progress and learn valuable research skills. Her ability to listen patiently, open-mindedness and work ethic is what is most admirable. She is and will continue to be a great mentor and role model for me both academically and personally. Lastly, I am also grateful for her incredible patience with my writing skills, which she has helped me hone over the last 5 years. Besides my advisor, I would also like to thank the members of my PhD committee, Dr. Annick Anctil, Dr. Joydeep Mitra and Dr. Subir Biswas for their suggestions, feedback, and contributions to this research.

Throughout my research journey, I had the opportunity to pursue a few internships and I would like to express my gratitude towards several supervisors and co-workers. In particular, Matt Hein and Bill Khols from Cedar Falls Utilities, Som Shreshta from Oak Ridge National Lab and Lincoln Harmer, Muhannad Al-Haddad and MJ Ayyampudur from KW Engineering for supporting and believing in me, providing me with challenging projects and making the internships a memorable and fun experience. These opportunities have shaped me and helped me gain valuable industry experience. I would especially like to express my gratitude to my manager, Matt Hein, at Cedar Falls utilities for being flexible, supporting me and keeping me motivated through the last stint of my PHD journey, as I worked on finishing up this dissertation and journal publications.

I am also thankful to my research colleagues and friends, Debrudra Mita, Hao Dong, Yiyi Chu, Niraj Kunwar, Emily Kawka and Elham Jahani for their support, suggestions, patience, and help as I navigated various aspects of graduate student life. I would also like to thank my roommates and friends (both in Michigan and Iowa) Oyendrila Dobe, Ritam Ganguly, Debrudra Mitra, Abhijeet Kulkarni, Saurabh Aykar, Srijita Chandra, Pushkar Velenkar, Hermab Tilak and several others for encouraging words and making my graduate experience fun.

Lastly, I would like to thank my mother, Kalpana Vanage, and my grandparents, Vasant and Vanita Chandane, for their sacrifices, unconditional support, and belief in me that made everything possible.

TABLE OF CONTENTS

CHAPTER 1 – GENERAL INTRODUCTION

1.1 Research big picture, literature review, and research goals

The Greenhouse Gas (GHG) emissions (CO_2 equivalent) for the entire planet due to human activity are approximately 50 billion metric tons (Bmt) each year (Ritchie et. al. 2020). The annual emissions requirements for GHG emissions by the year 2100 for the two most likely pathways by the Intergovernmental Panel on Climate Change (IPCC) (Representative Concentration Pathway RCP 4.5, and RCP 6.0) are approximately 65 are 25 Bmt of CO_2 equivalent, (Socrates, et. al. 2018), respectively. These two pathways (RCP 4.5 and RCP 6.0) thus correspond to limiting the annual emissions increase by 30% and a reduction of 50% in GHG emissions, respectively, as compared to current annual emission levels. The RCP 4.5 and RCP 6.0 scenarios are associated with a projected increase in global average temperature by 1.7-3.2˚C and 2.0-3.7˚C, respectively (Neil 2017). The catastrophic impact of these temperature increases on various socio-economic and natural systems is studied extensively by IPCC (IPCC 2007).

From the global emissions of 50 Bmt each year, the United States is responsible for approximately 6.5 Bmt, or 13% of the worldwide emission each year. The current pledge by the United States aims to reduce GHG emissions by 50% by the end of 2050 (Target: 3.7 Bmt/year) compared to 2005 levels (7.4 Bmt). Thus, the aim is to reduce the annual GHG emission levels by approximately 2.8 Bmt of CO_2 equivalent (6.5 – 3.7 = 2.8 Bmt) in the next 30 years. From the 6.5 Bmt of CO_2 equivalent, CO_2 is responsible for 5.1 Bmt (~ 80% of the emissions) (US EPA 2015), while other greenhouse gases such as methane, nitrous oxide, and fluorinated gases are responsible for the rest.

The total CO_2 emission for the U.S. in 2020 decreased from 5.1 to 4.5 billion tons of CO_2 (11 % reduction) compared to 2019 during the pandemic. In 2020, of the 4.5 Bmt of CO_2 from all energy

can be classified into four sectors, specifically transportation (37%), industrial (28%), residential (19%), and commercial (16%), as shown in Figure 1-1 (top right). Further, the emission associated with just electricity generation for these sectors accounted for around 1.45 Bmt, mostly related to the industrial, commercial, and residential sectors. (Note: this is ignoring the transportation sector and non-electric energy needs from the other sectors due to other sources such as fossil fuels like natural gas and propane).

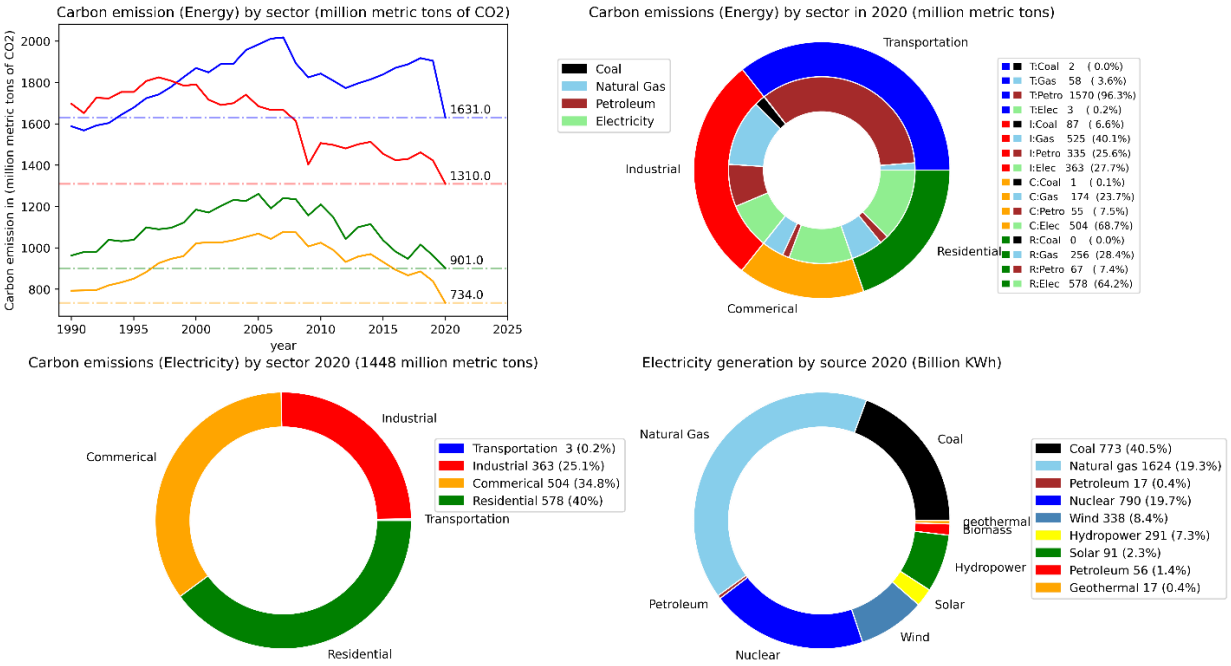

Figure 1-1 CO_2 emissions (million metric tons) by sector (top left), by source (top right), emission for electricity generation (bottom left) and electricity generation in billion kWh by source (bottom right) for the year 2020 in the United States (US EIA 2022) (US EIA 2019)

The sources used for electricity generation are dominated by fossil fuel-powered plants. These include natural gas and coal, which currently account for around 60%, nuclear accounts for another 20%, and the remaining 20% is from all renewable sources combined such as wind, solar, hydropower, biomass, geothermal, and other sources (US EIA 2019) (as shown in Figure 1-1, bottom right). Switching from fossil fuel sources for energy generation to renewable sources reduces the life cycle CO_2 equivalent/kWh by a factor of 15 for a switch from coal to solar, and by

a factor of 10 for a switch from natural gas to solar, which are two current primary fossil fuels used for electricity generation. These factors are even higher for switching from coal to wind/nuclear (factor of 70) and from natural gas to wind/nuclear (factor of 40), as shown in Figure 1-2. However, these renewable generation sources also have their own drawbacks [Abbas, et al.2022]

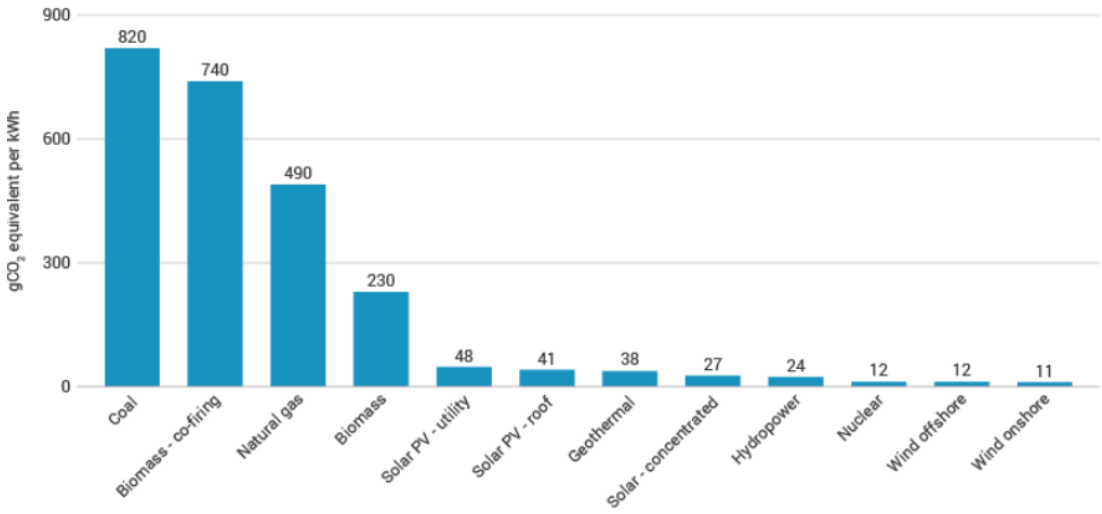

Figure 1-2 Life cycle emissions in (gCO_2 equivalent/kWh) from various generation sources (Thomas, et. al. 2014)

Commercial buildings account for approximately 20% of the energy use (18 quadrillion Btu), 30% of the electricity consumption (1.2 trillion kWh), and around 880 million metric tons of CO_2 emissions (US EIA 2022). Thus, the commercial building sector provides substantial opportunity for reduction in carbon emissions both by improving energy efficiency and providing demand flexibility. The primary commercial building electricity end uses include lighting, refrigeration, ventilation, cooling, computers, and office equipment, as shown in Figure 3. From these loads, lighting accounts for a total of 0.20 trillion kWh (lighting = 17% of 1.2 trillion kWh) and roughly 85 million tons of CO_2 emissions (17 % of 504 million metric tons). Thus, the project aims to reduce a portion of 85 million tons of CO2 (around 1% of the US CO_2 emissions and 0.14% of the world's CO_2 emissions) using various energy-saving and demand strategies.

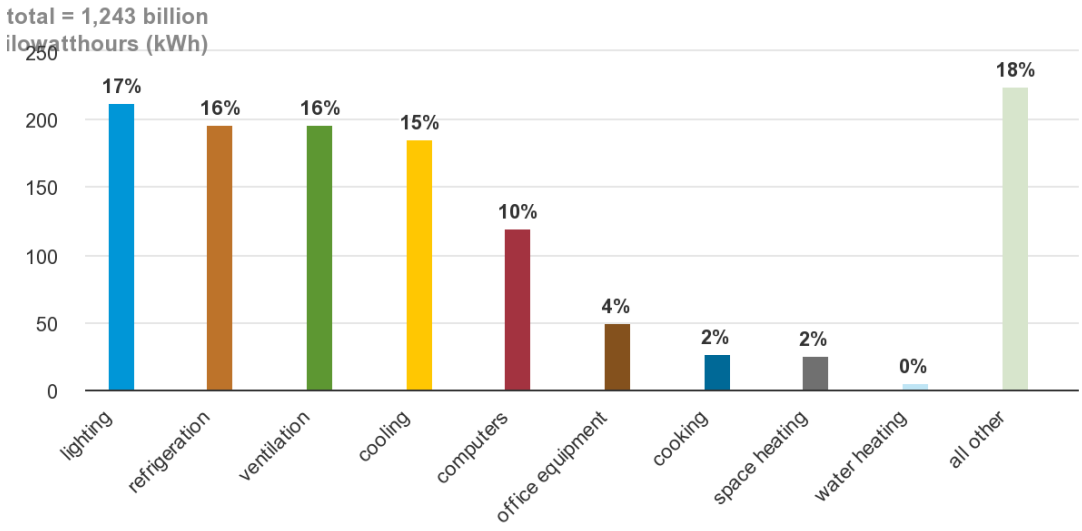

Figure 1-3 Electricity use in commercial buildings by end-uses (US EIA CBECS 2018)

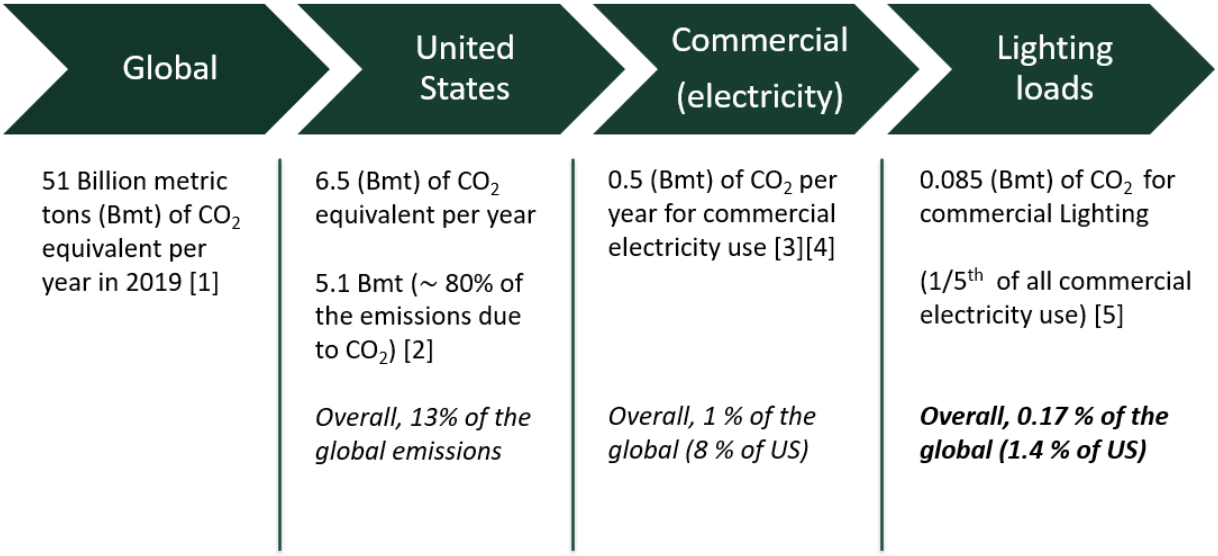

Figure 1-4 Carbon emissions in Billion metric tons CO_2 equivalent at different scales

Windows allow solar radiation and natural light to enter the building which can affect the lighting energy consumption. Incoming solar radiation can also significantly increase or reduce a building's energy consumption based on whether this occurs in a cooling, or a heating dominated season. Windows also allows daylight into the room, where low levels of daylight can increase the lighting energy consumption whereas too much daylight can cause visual discomfort to the occupants.

Further, windows provide occupants with natural light, a view to the outside, and enhance productivity (Edwards & Torcellini, 2002) (Shishegar & Boubekri, 2016) and provide a sense of well-being which is important considering people spend approximately 90% of their time indoors (Mitra et al., 2022), especially after the COVID-19 pandemic.

Although most building have shading devices such as roller shades and Venetian blinds to control daylight and solar radiation entering the space, these shading devices are operated manually and not used effectively. Rea (1984) found that occupants often close the blinds when excessive light or light-causing glare enters the space but are less likely to open the shades again when the unwanted lighting conditions no longer occur. Based on Sanati & Utzinger (2013) occupants do not adjust shading devices frequently, and once the shades are lowered, they are left in place for days or even weeks leading to reduced lighting energy savings from natural light.

To facilitate the development of these automated controls for lighting and shading systems visual comfort for occupants needs to be evaluated. All the developed visual comfort metrics are extensively summarized in these review studies (Vasquez et al., 2022)(Carlucci et al., 2015)(Sadeghi et al., 2016)(Da Silva et al., 2012). These metrics are used both as input variable thresholds for shading and lighting levels and/or to evaluate the performance of a control strategy. The common visual comfort metrics used in past studies include glare indices (Xiong and Tzempelikos, 2016 ; Da Silva et al., 2012 ; Shen et al., 2014 ; de Vries et al., 2021; Kunwar and Bhandari, 2020 ; Bian et al., 2020), vertical illuminance inside the building (Bian et al., 2020; de Vries et al., 2021; Kunwar & Bhandari, 2020; Shen 2012; Xiong and Tzempelikos, 2016). For solar radiation-based control, a solar radiation threshold is used to control the radiation entering the space (Tzempelikos and Athienitis, 2007; Wankanapon and Mistrick ,2011; Shen 2012; Shen and Tzempelikos, 2012; A. Atzeri et al., 2018). Usually, this value ranges from 20 W/m^2 to 400

W/m^2. In addition to using visual comfort criterion or solar radiation entering the space, some studies have also used factors such as occupant behavior (Bourgeois et al., 2006)(Athanassios Tzempelikos & Athienitis, 2007)(Da Silva et al., 2012)(E. Shen et al., 2014), sun tracking (de Vries et al., 2021; E. Shen et al., 2014), indoor temperature (Karlsen et al., 2016), HVAC state (heating/cooling mode) and different controls for day and night (E. Shen et al., 2014) to develop shading and lighting controls.

Even though various studies, such as those highlighted above, have explored automated controls strategies and presented energy saving and visual comfort improvements, research that compares all existing control strategies using a typical/common baseline model is lacking for combined lighting and shade control strategies. A meta-analysis that can quantify and estimate the visual comfort and energy savings improvements for shading and lighting controls for all the existing control strategies can be very challenging as these studies have different assumptions for baseline models including assumptions for the input variables such as room sizes (depth and width), window size (height, width, and WWR (with/without split windows)), window orientation (simultaneous windows in two directions), glazing material properties, shade material properties, and climate zones of the building. Thus, there is merit in comparing existing control strategies using the same baseline model by developing a daylighting and energy model. This research also proposes an a novel Integrated Control Strategy (IGS), which accounts for variables such as occupancy, HVAC state, solar radiation entering the space, time of day for control and other variabes to further optimze the enrgy savings and improvement in visual comfort.

As mentioned above the energy and daylighting model results are very sensitive to the building input variables. Thus, the studies proposing different automated control strategies typically provide some sensitivity analysis for a few input variables. Another approach to explore the impact of input

variables is to use a parametric/optimization study that can show the influence of possible combination of all the variables at once as opposed to sensitivity analysis where a particular variable is changed while all others are fixed. Thus, an energy and daylighting model is developed using six (6) input variables such as WWR for all four orientations, shade material openness factor, and the length overhang depth to evaluate the best-case scenarios for (Useful Daylight Illuminance) UDI, (Energy Use intensity) EUI, view to the outside, and improvement in thermal comfort. This process is repeated nine (9) times for different building form factors to estimate the variation in results as the building form factor is changed.

In addition to improving energy efficiency and visual comfort in buildings, managing demand at the grid level is becoming more important as renewable generation sources are added to the generation mix. Electricity generation due to renewable resources such as wind and solar combined is projected to represent 36% of the total energy generation in 2050 (U.S. EIA Energy Outlook 2022). These renewable energy generation sources are highly variable throughout the day and between seasons. Furthermore, the generation sources do not match exactly with electricity demand in terms of when electricity is produced versus consumed. With limited grid-level storage, electricity generation needs to be balanced with electricity demand in real-time. This variability is usually addressed using various grid-based services known as Flexibility Services (FS).

Currently, these FS are dependent mostly on non-renewable sources (MISO 2020), such as natural gas and oil. However, with reductions in non-renewable sources in the generation mix, compounded with more FS requirements due to increases in variable generation such as solar and wind, there is a need to provide FS using sources other than non-renewable generation sources. Further, with more renewable energy generation sources, FS will not only be needed during peak demand periods but also throughout the day. Furthermore, the transmission flow patterns

significantly change with distributed renewable energy as compared to current transmission patterns dominated by non-renewable energy sources where the flow of electricity is from the power generation plant to the consumers. Therefore, this possibly requires more transmission infrastructure in the future as more distributed renewable energy is added to the grid.

Demand-side FS thus can help provide load flexibility and reduce capital investment for transmission and distribution systems by modulating loads in existing buildings to match available supply. Various types of loads in commercial and residential buildings can potentially provide these FS. These loads can be broadly classified into two categories, including activity-driven loads (ADLs) and thermostatically controlled loads (TCLs) (Kunwar el al. 2021). ADLs are generally loads from appliances that are largely influenced by occupant activities, such as clothes washers, dryers, dishwashers, lighting, and electric vehicles. TCLs include electricity-consuming appliances such as HVAC (Heating, Ventilation and Air Conditioning) systems and water heaters, which are largely controlled by a thermostat. These different types of loads have different response times, total capacity reduction potential, time-of-day availabilities, and technology penetration levels. Thus, there is a need to study these loads separately.

In commercial buildings, lighting loads present a unique opportunity as lighting accounts for approximately 10-15% of the load at any given time. Past studies have shown that lighting can be dimmed by 15-20% without causing visual discomfort to the occupants. Thus, lighting loads have the potential to act as fast acting demand side flexibility services as they can be dimmed instantaneously. Without any lighting-based controls, lighting loads (ADLs) in commercial buildings are generally dependent on the space type (e.g., open office, library, surgery rooms), the operating schedule of the building, the age of the building, and/or the lighting efficiency. Therefore, without any controls, lighting loads generally have consistent use patterns, with the

stronger predictors being the day of the week (weekdays/weekends) and time of day, with some minor seasonal variations due to changes in sunrise and sunset times. However, for perimeter zones with lighting-based controls, the lighting loads also depend on daylight available in space. For that reason, estimating the potential for lighting loads flexible loads can be challenging as if the lights are already switched off using daylighting controls, they are not available as flexible loads.

In particular, demand-side flexibility using lighting loads is not well studied in the literature as other building loads such as Heating Ventilation and Air Conditioning (HVAC). Thus, there is a need to develop estimates on how much potential there is in lighting loads as flexible services both at building level and at the grid level estimates for using lighting loads. These results can be used as inputs for grid levels models to predict future generation, transmission, and distribution investments for future high renewable energy scenarios.

1.2 Research Objectives

This proposed research consists of three primary Focus Areas. These are discussed in further detail below (see Figure 1-5).

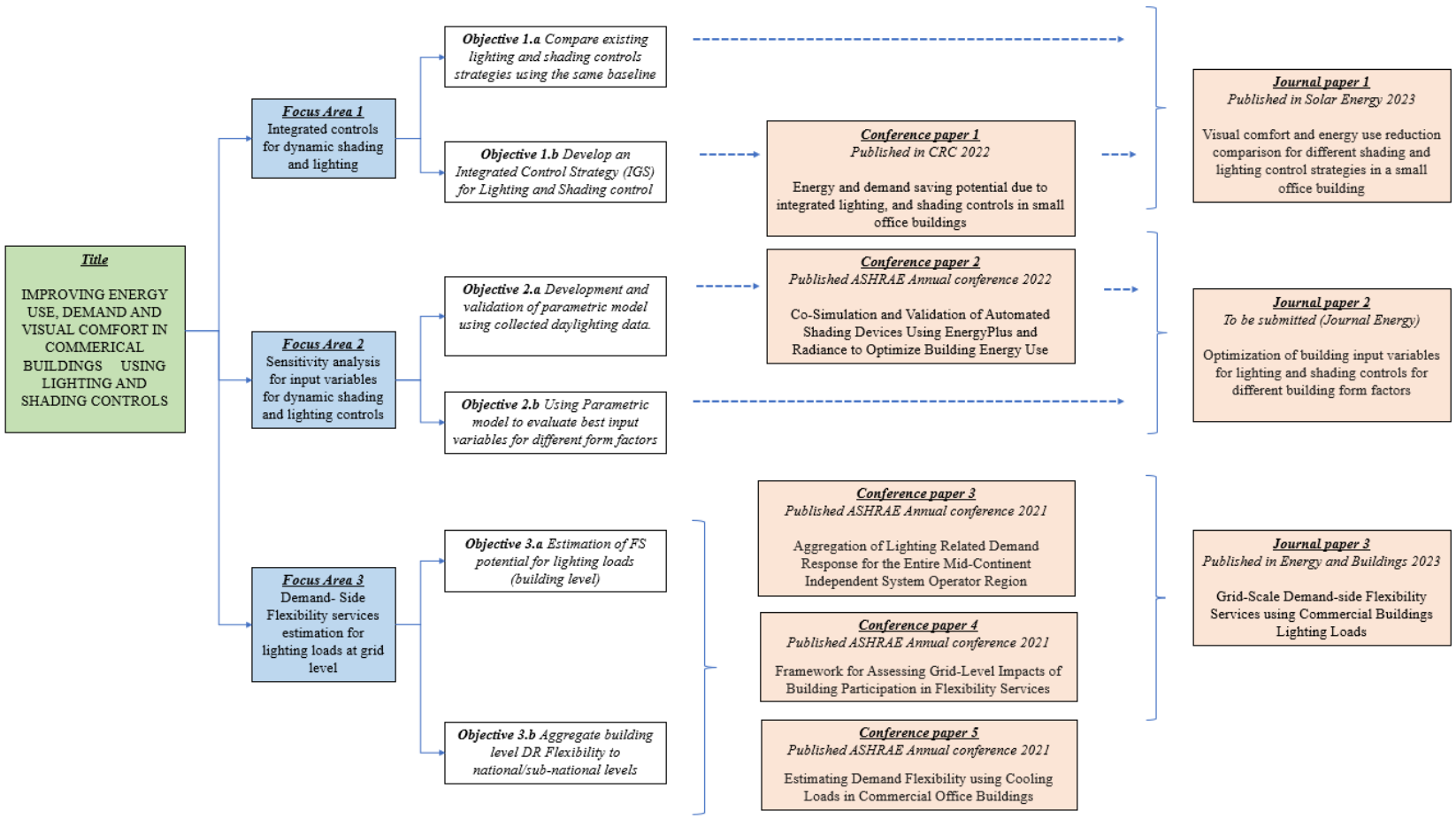

Figure 1-5 Diagram of research organization

1.2.1 Focus Area 1: Integrated controls for dynamic shading and lighting

The goal of Focus Area 1 is to develop lighting and shading control strategies for dynamic fenestration systems to estimate the amount of energy savings and demand reduction potential in a typical office building. The most common shading devices used in office buildings include roller shades and venetian blinds. Various control strategies adjust shading and lighting levels based on multiple input variables such as weather data, which calculates incoming daylight and other visual comfort metrics. The research questions addressed, or goals for Focus Area 1 include:

1. How do existing lighting and shading control strategies compare with each other in terms of performance?
2. Can the existing control strategies be further modified to develop integrated control strategies to maximize energy savings and visual comfort improvements?

Objective 1.a Compare existing lighting and shading controls strategies using the same baseline

This objective aims to recreate and test existing lighting and shading control strategies in the existing recent literature and compare them using the same baseline conditions. Past studies that have explored automated lighting and shading control strategies typically report energy savings and visual comfort improvements over their respective baselines. However, across different studies, the assumptions for baseline models differ. For instance, these actual buildings usually have different room sizes (depth and width), different window locations (height, width, and WWR (with/without split windows), window orientation (simultaneous windows in two directions), glazing properties and climate zones of the building location. As different studies have different assumptions for these input variables, comparing percent improvement in energy savings due to the implemented control strategies across different papers can be challenging. Objective 1.a works

to bridge this gap using a single baseline model to compare existing control strategies for different zone orientation and climate zones.

Objective 1.b Develop an Integrated Control Strategy (IGS) for Lighting and Shading Control

Various input variables can be used to control shading devices, such as position, sun, solar radiation, available daylight, and occupancy, both individually and in combination. A novel Integrated Control Strategy (IGS), which accounts for variables such as occupancy, HVAC state, solar radiation entering the space, and time of day for control. This study uses a multi-step modeling process, including daylighting and energy simulations using RADIANCE and EnergyPlus, respectively, in a Ladybug and Honeybee plugin environment. The results for the IGS control strategy are than compared to the existing control strategies developed in Objective 1.a.

1.2.2 Focus Area 2: Sensitivity analysis for input variables for dynamic shading and lighting controls

The objective of this Focus Area is to explore the sensitivity of different building input variables and their impact on the output metrics for combined shading and lighting control strategies. The best strategy from Focus Area 1 is chosen for this purpose. Focus Area 2 is split between two objectives model development and validation and development of parametric model to test sensitivity for various input variables. The research questions addressed, or goals for Focus Area 2 include:

1. What are the best values for input variables such as WWR, shade openness and shade overhang depth for optimum energy saving, visual comfort, and thermal comfort?
2. What is the impact of building form factor on energy saving, visual comfort and thermal comfort?

Objective 2.a Development and validation of parametric model using collected daylighting data

The daylighting model developed for Objective 2.b first needs to be validated with collected illuminance data for a real test building located in Ankeny, Iowa to estimate the values of fixed variables such as wall, ceiling, and floor reflectivity. Illuminance data at different points in the test room is collected for three different orientations for the test building for a period of 10 days each. The validation of the model also provides further confidence that the current model setup used for daylighting and energy simulation using RADIANCE and EnergyPlus with Ladybug tools as the interface will provide satisfactory results for the parametric model without errors.

Objective 2.b Using Parametric model to evaluate best input variables for different form factors

The energy consumption and the visual comfort results for Objectives 1.a and 1.b depend on various factors and variables that represent the physical characteristics of the buildings such as: window-to-wall ratio, room geometry, surface reflectance, window glazing type (double pane/low-e) and shade properties (% openness factor, color, material), zone orientation (N, W, S, E), and building location. Parametric/optimization methods in the past have typically used Energy Use Intensity (EUI) and visual comfort metrics such as UDI (Useful Daylight Illuminance) to estimate the ideal combination of these variables. However, output metrics such as view to outside, glare, and thermal comfort are typically ignored. This study aims to build a parametric model using various variables such as WWR for all four orientations, shade material property (openness factor), and the length of the building overhang depth to estimate best-case scenarios for UDI, EUI, view to the outside, and thermal comfort using PMV (Predicted Mean Vote) for a shade control strategy that uses glare-based control.

1.2.3 Focus Area 3: Demand-Side Flexibility services estimation for lighting loads at grid level

The main goal of this Focus Area 3 is to assess the demand reduction potential of lighting loads as Flexible Services, by the time of day. This is then to be aggregated to county, state, and grid-level estimates of impact of such controls on grid operations and needs. There are several major research questions to be addressed in Focus Area 3 including the following:

1. Can lighting loads in commercial buildings be used as demand-side flexible loads, and what is the potential?
2. How can building level lighting loads be aggregated to the county, state, and grid-level using various building stock datasets that are available, to estimate commercial building lighting load contributions at different scales?

Objective 3.a Estimation of FS potential for lighting loads (building level)

This objective focuses on estimating the FS potential for lighting loads using lighting dimming controls for different types of commercial buildings. EnergyPlus is used as the tool to balance sufficient daylight and/or artificial light is availability in a space, with the ability to reduce artificial lighting use for demand flexibility. This is accomplished by reducing artificial lighting levels by 20 % [37-39], which is considered an acceptable value for lighting level reduction for a short period during DR events. Building level estimates for demand saving potential for DOE Commercial Prototype and Reference building models for different energy code versions are then evaluated.

Objective 3.b Aggregate building level DR Flexibility to national/sub-national levels

This objective focuses on scaling building level results spatially to county, state, and grid level. To scale the building level data, factors such as building age, type, population distribution, building

energy code adoption year, and percent of building retrofitted are considered as input variables. The gird level data for lighting loads that can act as flexible loads can be used as inputs for grid levels models to predict future generation, transmission, and distribution investments for future high renewable energy scenarios.

1.3 Research Organization

The research is organized into six chapters. Chapter 1 provides an introduction and outlines the research organization. Chapter 2 discusses Focus Area 1. More specifically this chapter discusses the methodology for developing and modeling an integrated control strategy for lighting and shading systems. The modeled control strategy is then compared to existing control strategies in the literature to highlight the improvement using preliminary results such as energy savings and improvements in visual comfort. Chapter 3 discusses Focus Area 2. This chapter integrates the best model developed in Chapter 2 and explores sensitivity to various input variables such as WWR, shade openness factor, and the length shade overhang to estimate its effect on the lighting and shading controls. Chapter 4 discusses Focus Area 3 and is independently developed from Focus Area 1 and 2. Its primary aim is to develop a methodology to scale up building-level results for demand side flexibility potential using lighting loads to the grid scale. This uses lighting without any shading controls to estimate the load flexibility by the hour of the day that will be used if the grid consumption is over the grid production (a likely case for high renewable energy penetration case). Finally, Chapter 5 provides conclusions for all the Focus Areas, limitations of current research work, significant contributions, and suggestions for future work. Chapter 6 provides a list of publications based on the current research.

REFERENCES

Azarpour, Abbas, et al. "Current status and future prospects of renewable and sustainable energy in North America: Progress and challenges." Energy Conversion and Management 269 (2022): 115945

Atzeri, A., Cappelletti, F., & Gasparella, A. (2014). Internal versus external shading devices performance in office buildings. Energy Procedia, 45, 463–472. https://doi.org/10.1016/j.egypro.2014.01.050

Atzeri, A. M., Gasparella, A., Cappelletti, F., & Tzempelikos, A. (2018). Comfort and energy performance analysis of different glazing systems coupled with three shading control strategies. Science and Technology for the Built Environment, 24(5), 545–558. https://doi.org/10.1080/23744731.2018.1449517

Bian, Y., Dai, Q., Ma, Y., & Liu, L. (2020). Variable set points of glare control strategy for side-lit spaces: Daylight glare tolerance by time of day. Solar Energy, 201(March), 268–278. https://doi.org/10.1016/j.solener.2020.03.016

Bourgeois, D., Reinhart, C., & Macdonald, I. (2006a). Adding advanced behavioural models in whole building energy simulation : A study on the total energy impact of manual and automated lighting control. 38, 814–823. https://doi.org/10.1016/j.enbuild.2006.03.002

Bourgeois, D., Reinhart, C., & Macdonald, I. (2006b). Adding advanced behavioural models in whole building energy simulation: A study on the total energy impact of manual and automated lighting control. Energy and Buildings, 38(7), 814–823. https://doi.org/10.1016/j.enbuild.2006.03.002

Bruckner, Thomas, et al. "Energy systems." (2014).

Carlucci, S., Causone, F., De Rosa, F., & Pagliano, L. (2015). A review of indices for assessing visual comfort with a view to their use in optimization processes to support building integrated design. Renewable and Sustainable Energy Reviews, 47(7491), 1016–1033. https://doi.org/10.1016/j.rser.2015.03.062

Craik, Neil. Developing a national strategy for climate engineering research in Canada. Centre for International Governance Innovation., 2017.

Change, Climate. "Working Group II: Impacts, adaptation and vulnerability." Geneva: Intergovernmental Panel on Climate Change (2007).

Da Silva, P. C., Leal, V., & Andersen, M. (2012a). Influence of shading control patterns on the energy assessment of office spaces. Energy and Buildings, 50, 35–48. https://doi.org/10.1016/j.enbuild.2012.03.019

Da Silva, P. C., Leal, V., & Andersen, M. (2012b). Influence of shading control patterns on the energy assessment of office spaces. Energy and Buildings, 50, 35–48. https://doi.org/10.1016/j.enbuild.2012.03.019

de Vries, S. B., Loonen, R. C. G. M., & Hensen, J. L. M. (2021). Simulation-aided development of automated solar shading control strategies using performance mapping and statistical classification. Journal of Building Performance Simulation, 14(6), 770–792. https://doi.org/10.1080/19401493.2021.1887355

Edwards, L., & Torcellini, P. (2002). A Literature Review of the Effects of Natural Light on Building Occupants A Literature Review of the Effects of Natural Light on Building Occupants. Contract, July, 55.

Jakubiec, J. A. (2016). Building a Database of Opaque Materials for Lighting Simulation. Los Angeles, 2015, 6. http://files/20276/Jakubiec - 2016 - Building a Database of Opaque Materials for Lighti.pdf

Karlsen, L., Heiselberg, P., Bryn, I., & Johra, H. (2016). Solar shading control strategy for office buildings in cold climate. Energy and Buildings, 118(0130), 316–328. https://doi.org/10.1016/j.enbuild.2016.03.014

Konstantoglou, M., & Tsangrassoulis, A. (2016). Dynamic operation of daylighting and shading systems: A literature review. Renewable and Sustainable Energy Reviews, 60, 268–283. https://doi.org/10.1016/j.rser.2015.12.246

Konstantzos, I., Tzempelikos, A., & Chan, Y. C. (2015). Experimental and simulation analysis of daylight glare probability inoffices with dynamic window shades. Building and Environment, 87, 244–254. https://doi.org/10.1016/j.buildenv.2015.02.007

Kunwar, N., & Bhandari, M. (2020). A comprehensive analysis of energy and daylighting impact of window shading systems and control strategies on commercial buildings in the United States. Energies, 13(9). https://doi.org/10.3390/en13092401

Kypreos, Socrates, et al. "Efficient and Equitable Climate Change Policies." Systems 6.2 (2018): 10.

MISO 2020, Available: https://cdn.misoenergy.org/MISO%20FORWARD_2020433101.pdf

Mitra, D., Chu, Y., & Cetin, K. (2022). COVID-19 impacts on residential occupancy schedules and activities in U . S . Homes in 2020 using ATUS. Applied Energy, 324(August), 119765. https://doi.org/10.1016/j.apenergy.2022.119765

Rea, M. S. (1984). Window blind occlusion: a pilot study. Building and Environment, 19(2), 133–137. https://doi.org/10.1016/0360-1323(84)90038-6

Ritchie, Hannah, and Max Roser. "CO_2 and greenhouse gas emissions." Our world in data (2020).

Sanati, L., & Utzinger, M. (2013). The effect of window shading design on occupant use of blinds and electric lighting. Building and Environment, 64, 67–76. https://doi.org/10.1016/j.buildenv.2013.02.013

Shen, E., Hu, J., & Patel, M. (2014). Energy and visual comfort analysis of lighting and daylight control strategies. Building and Environment, 78, 155–170. https://doi.org/10.1016/j.buildenv.2014.04.028

Shen, H., & Tzempelikos, A. (2012). Daylighting and energy analysis of private offices with automated interior roller shades. Solar Energy, 86(2), 681–704. https://doi.org/10.1016/j.solener.2011.11.016

Tzempelikos, Athanasios, & Ph, D. (n.d.). An Experimental and Simulation Study of Lighting Performance in Offices with Automated Roller Shades.

Tzempelikos, Athanasios, & Shen, H. (2013). Comparative control strategies for roller shades with respect to daylighting and energy performance. Building and Environment, 67, 179–192. https://doi.org/10.1016/j.buildenv.2013.05.016

Tzempelikos, Athanassios, & Athienitis, A. K. (2007). The impact of shading design and control on building cooling and lighting demand. 81, 369–382. https://doi.org/10.1016/j.solener.2006.06.015

Vasquez, N. G., Rupp, R. F., Andersen, R. K., & Toftum, J. (2022). Occupants' responses to window views, daylighting and lighting in buildings: A critical review. Building and Environment, 219(February), 109172. https://doi.org/10.1016/j.buildenv.2022.109172

Wankanapon, P., & Mistrick, R. G. (n.d.). Roller Shades and Automatic Lighting Control with Solar Radiation Control Strategies. 35–42.

Xiong, J., & Tzempelikos, A. (2016). Model-based shading and lighting controls considering visual comfort and energy use. Solar Energy, 134, 416–428. https://doi.org/10.1016/j.solener.2016.04.026

U.S. EIA 2018 Commercial Buildings Energy Consumption Survey. Available:https://www.eia.gov/consumption/commercial/data/2018/

US EPA. "Greenhouse Gas Inventory Data Explorer." (2015). Available: https://cfpub.epa.gov/ghgdata/inventoryexplorer/

US EIA 2020: US U.S. Energy-Related Carbon Dioxide Emissions, 2020 : Available: https://www.eia.gov/environment/emissions/carbon/pdf/2020_co2analysis.pdf

US Energy Information Administration. "What is US electricity generation by energy source?" (2019). Available: https://www.eia.gov/tools/faqs/faq.php?id=427&t=3

US EIA 2021 Form-816 "Annual Electric Power Industry Report, Form EIA-816 detailed data

U.S. EIA (2012) Commercial Buildings Energy Consumption Survey. Available:www.eia.gov/consumption/commercial/data/2012

CHAPTER 2 – DEVELOPMENT OF SHADING CONTROL STRATEGIES

Published in Solar Energy

Citation: Vanage, Soham, Hao Dong, and Kristen Cetin. "Visual comfort and energy use reduction comparison for different shading and lighting control strategies in a small office building." *Solar Energy* 265 (2023): 112086.

ABSTRACT

Automated shading and lighting control systems can be used to control solar radiation and daylight entering the space and reduce the lighting requirement, providing both energy savings and better visual comfort for occupants. Past studies that have explored automated lighting and shading control strategies typically report energy savings and visual comfort improvements over their respective baselines. However, across different studies, the assumptions for baseline models differ, as many daylighting studies use an experimental setup to measure various daylighting-based metrics to evaluate the performance of their control strategies in a real building. For instance, these actual buildings usually have different room sizes (depth and width), different window locations (height, width, and WWR (with/without split windows), window orientation (simultaneous windows in two directions), glazing properties and climate zones of the building location. As these input variables affect the result of daylighting studies, comparing percent improvement in energy savings due to the implemented control strategies across different papers can be challenging. This research uses a common baseline to evaluate the differences between a broad diversity of existing lighting and shading control strategies. The author also proposes an Integrated Control Strategy (IGS), which accounts for variables such as occupancy, HVAC state, solar radiation entering the space, and time of day for control. This study uses a multi-step modeling process, including daylighting and energy simulations using RADIANCE and EnergyPlus, respectively, in a Ladybug and Honeybee plugin environment. The results are used to quantify the differences in the existing control strategies to a common baseline model. The results suggest that complex rule based

shading and lighting strategies such as an IGS performs only slightly better (6-12 % decrease in view to the outside, no glare, 82-88% lighting energy savings and 7.5-14.5% total energy savings compared shades fully open) when compared to existing glare metric based control strategy (4.5-9.5 % decrease in view to the outside, no glare, 63-72% lighting energy savings and 7-13% total laod savings compared shades fully open. Thus, if the addition of sensors is needed to support complex shading and lighting controls strategies, these sensors may benefit from being used for multiple purposes in order to justify their use.

2.1 INTRODUCTION

Windows are necessary to provide occupants with natural light, a view to the outside, and to enhance productivity (Edwards & Torcellini, 2002) (Shishegar & Boubekri, 2016) which is important considering people spend approximately 90% of their time indoors (Klepeis et al., 2001) (Mitra et al., 2022). If the light entering through the windows is not adequately controlled, it can cause visual discomfort to the occupants. Windows also allow solar radiation into the space, which can increase or reduce a building's energy consumption based on the cooling or heating season.

Although most building have shading devices such as roller shades and Venetian blinds to control daylight and solar radiation entering the space, these shading devices are operated manually and not used effectively. (Rea, 1984) found that occupants often close the blinds when excessive light or light-causing glare enters the space but are less likely to open the shades again when the unwanted lighting conditions no longer occur. Based on (Sanati & Utzinger, 2013) occupants don't adjust shading devices frequently, and once the shades are lowered, they are left in place for days or even weeks leading to reduced lighting energy savings from natural light. Furthermore, according to (CBECS 2018), only 3.1% of buildings have multilevel lighting dimming and only 1.3% of buildings have daylighting controls. Thus, there is a huge opportunity to improve visual

comfort and lighting energy use using automated lighting and shading controls. Some of the already existing rule-based automated lighting and shading strategies are discussed in the literature review section.

2.1.1 Background/ Literature review

Most automated shading control strategies use some visual comfort metrics for control. Multiple review studies have summarized commonly used visual comfort metrics (Carlucci et al., 2015) (Da Silva et al., 2012) (Tabadkani et al., 2020) (Jain & Garg, 2018) used for shade control in detail. Studies such (Seyed, et al. 2020) have done a meta-analysis of how these metrics are used for shading control in different field studies and lab experiments. These metrics are used both as a threshold for shading and lighting levels and/or to evaluate the performance of a control strategy. Commonly used daylighting metrics include Daylight Autonomy (DA), Continuous Daylight Autonomy (cDA), Useful Daylight Illuminance (UDI), Spatial Daylight Autonomy (sDA), and Annual Sunlight Exposure (ASE). For estimating glare, researchers have used Daylight Glare Index (DGI), Unified Glare Rating (UGR), Daylight Glare Probability (DGP), Simplified Daylight Glare Probability (DGPs) and Predicted Glare Sensation Vote (PGSV). Since simulating glare (DGP) can be time extensive, this study uses Simplified Daylight Glare Probability (DGPs) (Weinold 2007) which provides a simple empirical relation between vertical illuminance at the eye level of the occupants and glare. A DGPs value higher than 0.35 (corresponds to 2600 lux at eye level) can cause visual discomfort for occupants. However, DGPs do not accurately calculate glare conditions for low vertical illuminance values especially when direct light hits the eyes such as seeing the sun directly through the shades (Konstantzos et al., 2015).

Several review studies (Tabadkani et al., 2020) (Jain & Garg, 2018) (Konstantoglou & Tsangrassoulis, 2016)(Kunwar et al., 2018) have summarized rule-based automated shading and

lighting control strategies for roller shades. These studies usually use no shades or shades fully closed as the baseline. Several studies also use manually controlled shades as one of the baseline models the evaluate energy and visual comfort difference between manually controlled shades and automated shading control (Bourgeois et al. 2006)(Kunwar and Bhandari, 2020) (Shen et al. 2014). For manual control, factors such as room layout, which is whether the building is an open layout, or a private/closed office space are important when deciding the lighting and shading control strategy. In the case of a private office, the occupant may have full manual control over the shades whereas in cases such as open offices, multiple occupants in the same open office that are located a different distance and orientations from the windows can lead to issues on when the shades need to open or closed. Some studies such as (Tzempelikos and Athienitis, 2007) and (Reinhart 2004) therefore are focused on private office spaces. Moreover, the accessibility of the controller can impact the frequency with which the manual controlled shades are operated (Sadeghi et al., 2016). Several authors have categorized manual control strategies into dynamic manual control strategies (active control) and static manual control strategies (passive control).

For automated shade control, studies use visual comfort metrics or the amount of solar radiation entering space as the criterion to select shade position. The commonly used visual comfort metrics are glare indices (Xiong and Tzempelikos, 2016 ; Da Silva et al., 2012 ; Shen et al., 2014 ; Goovaerts et al., 2017; de Vries et al., 2021; Kunwar and Bhandari, 2020 ; Bian et al., 2020; A. Atzeri et al., 2018; Do and Chan, 2020), vertical illuminance inside the building (Bian et al., 2020; de Vries et al., 2021; Kunwar & Bhandari, 2020; Shen 2012; Xiong and Tzempelikos, 2016), transmitted illuminance (Kunwar & Bhandari, 2020)(Athanasios Tzempelikos & Shen, 2013), or luminance ratio (Bian et al., 2020). For solar radiation-based control, a solar radiation threshold is used to control the radiation entering the space (Tzempelikos and Athienitis, 2007; Wankanapon

and Mistrick ,2011; Shen 2012; Shen and Tzempelikos, 2012; Da Silva et al., 2012; de Vries et al.; A. Atzeri et al., 2018). Usually, this value ranges from 20 W/m^2 to 400 W/m^2. For controls with solar radiation, Work plane Protection Position (WPP) (Shen 2012)(Konstantzos et al., 2015; Kunwar et al., 2019) can be used to close the shades to a certain height based on the sun position such that the direct sunlight does not hit the occupants. Studies also use a fixed solar penetration depth (Lee & Selkowitz, 2006) to prevent direct sunlight from hitting occupants. Furthermore, most studies use shading control with the shades either fully closed or fully open. However, few studies also include controls where shades gradually open or close, stopping when a targeted threshold is met (Lee and Selkowitz, 2006; Xiong and Tzempelikos, 2016; Kunwar et al., 2019). Table 2-1 provides a review of studies that have used automated control strategies for roller shades and highlights the control strategy used with visual comfort metrics thresholds, the performance metrics to evaluate the strategy, and sensitivity to input variables.

In addition to using visual comfort criterion or solar radiation entering the space, some studies use factors such as occupant behavior (Bourgeois et al., 2006)(Athanassios Tzempelikos & Athienitis, 2007)(Da Silva et al., 2012)(E. Shen et al., 2014), sun tracking (de Vries et al., 2021; E. Shen et al., 2014), indoor temperature (Karlsen et al., 2016), HVAC state (heating/cooling mode) and different controls for day and night (E. Shen et al., 2014) to develop integrated shading and lighting controls. Thus, the control strategies in this study are divided into four categories.

Table 2-1 Review of automated control strategies for roller shades

Reference	Baseline case	Shading control	Shading control type	Shade increments	Lighting control	Other variables used for control	Performance metrics	Variable sensitivity
(Bourgeois et al., 2006)	No shades, lighting always on	Active Manual control – Adjust shades to maximize daylight availability	Manual /Independent control	Fully open/fully closed	Work plane illuminance (500 lux)	Occupancy	--Heating, cooling, and lighting EUI	--Building location
(Lee & Selkowitz, 2006)	--	Glare and solar penetration depth	Independent control	Five (5) shade heights	Work plane illuminance (500 lux)	Solar penetration depth	--Lighting energy use	--Sensor distance --Window orientation
(Athanassios Tzempelikos & Athienitis, 2007)	Closed shades: lighting always on	Solar radiation-based control (Shades fully open < 20W/m^2)	Independent control	Fully open/fully closed	Work plane illuminance (500 lux)	Occupancy	--Daylight Availability ratio (DAR) --Work plane illuminance --Heating, cooling, and lighting load	--WWR --Sensor distance to window --Zone orientation
(Wankanapon & Mistrick)	No shades, lighting always on	Solar radiation-based control (Shades fully open < 95/ 189/400 W/m^2)	Independent control	Fully open/fully closed	Work plane illuminance (500 lux)	--	--Heating, cooling, and lighting EUI	--Zone orientation --Shade color --Solar radiation threshold
(Shen and Athanasios Tzempelikos, n.d.)	No shades, no lighting control	Shades close when direct sunlight on facade.	Independent control	Fully open/fully closed	Work plane illuminance (500 lux)	--	-UDI bins (100 - 2000 Lux) -Daylight autonomy	--WWR --Shade openness factor --Sensor location --Zone orientation
(Athanasios Tzempelikos & Shen, 2013)	No shade	S2- (Shades fully open when solar radiation < 20/100/200/400 W/m^2) S3- Transmitted illuminance S4- Transmitted illuminance shade + WPP	Independent control	Fully open/fully closed +WPP	Work plane illuminance (500 lux)	--	-UDI bins (100 - 2000 Lux) -Daylight autonomy	--WWR --Shade openness factor --Zone orientation --Sensor distance
(Iason Konstantzos et al. 2015)	Fully closed shades	S2- WPP control S3- WPP control + work plane illuminance (< 2000 lux)	Independent control	11 positions (10 % increments)	--	--	--DGP --Work plane Illuminance	--Glazing type
(Xiong & Tzempelikos, 2016)	--	Close shades in increments until S1 - Glare with DGP <0.35 S2 - Glare with DGPs Vertical illuminance < 2500 lux) S3- Work plane illuminance < 2000 lux)	Independent control	11 positions (10 % increments)	--	--	--DGP --Work plane Illuminance --Vertical Illuminance	--
(A. M. Atzeri et al., 2018)	No shades	S1- based on work plane illuminance (<500 lux open, 500- 2000 lux maintain, and > 200 lux close S2- Work plan protection height S3- Work plan protection height and Work plane illuminance (< 2000 lux)	Independent control	open, closed, and intermediate shade	Work plane illuminance (500 lux)	-	--Daylight Autonomy (sDA) --Comfort Availability (CA) --Comfort Usability (CU) --Daylight Usability (CU) --Heating, cooling and lighting.	--Glazing size --Glazing transmittance --Zone orientation
(Do & Chan, 2020)	(DGPs < 0.35) at 1 m work plane level	S1- Blinds (based on season) + roller shades (based on glare) S2- Top section - Diffuse roller shades (fully up or fully down) and middle section - Glare-blocking roller shades (Eleven states)	Manual /Independent control	Multi-sectional shades	Work plane illuminance (500 lux)	Blinds and roller shades combined	--cDA and DGPs	--Location --Zone orientation
(Kunwar et al., 2019)	No shades, no lighting control	S1- Solar radiation (<150 W/m2) + vertical illuminance (1830 lux) – sensor at 1 meter S1- Solar radiation (<150 W/m2) + vertical illuminance (1830 lux) - sensor at 3 meters	Independent /Integrated control	Multiple positions	Work plane illuminance (500 lux)	WPP	--Work plane illuminance --UDI, DGPs --Lighting energy	--Zone orientation --Sensor placement --Shade properties
(de Vries et al., 2021)	Solar radiation < 200 W/m2 (fully open/ closed)	AU: Always up AD: Always down SC: Solar cut-off (WPP at 0.75 m) EL: Solar cut-off (WWP at 1.2 m)	Independent control	Multiple positions	Work plane illuminance (500 lux)	--	--DGPs --Vertical Illuminance --Heating, cooling, and lighting EUI	--Sensor placement

Table 2-1 (cont'd)

(Kunwar & Bhandari, 2020)	No shades, no lighting control	(LC): No shade control with lighting dimming (MC): Manual Control (Nezamdoost et al., 2018) (AC1): Window illuminance + solar penetration depth + WPP (Fully open/50% closed/Fully closed) (AC2): DGI < 22 (fully open/fully closed) (AC3): External illuminance on the façade (Fully open/fully closed) (AC4): External illuminance on the façade (5 positions)	Independent control	--	Work plane illuminance (500 lux)	--	--sDA, ASE, DGPs --Heating, cooling, and lighting EUI	--Location --Building vintage --Zone orientation
(Do & Chan, 2021)	Fully closed	DGPs < 0.35 at 1.5 m	Independent control	--	Work plane illuminance (500 lux)	--	--lighting energy saving --glare prevention --view	--Glazing properties --WWR --Shade properties --Zone orientation
(A. Atzeri et al., 2014;)	--	S1 – Solar Radiation al radiation on the window surface > 150 W m2 S2 - Daylight Glare Index (DGI) > 22	Independent control	Internal vs external shades	--	--	--Heating, cooling, and lighting --PM_V (Predicted Mean Vote when solar irradiation hits the occupant)	-Interval vs external shades -WWR -Glazing type -Shading type

2.1.1 Research gap and goals

Previous studies such as (Gentile & Dubois, 2017) (Williams et al., 2012) have simulated lighting controls in different commercial buildings to estimate the percentage saving associated with various lighting control strategies using the same baseline case. These included daylighting-based control, occupancy-based lighting control, personal tuning, and institutional tuning.

However, research that compares all existing control strategies using a typical/common baseline case is lacking for combined lighting and shade control strategies. A meta-analysis that can quantify and estimate the visual comfort and energy savings improvements for shading and lighting controls for all the existing control strategies can be very challenging as these studies have different assumptions for baseline models and use different metrics for comparing the results of these different control strategies. In most cases, the baseline models differ because many daylighting studies use an experimental setup to measure various daylighting-based metrics to evaluate the performance of their control strategies in a real building. For these actual buildings, the input variables such as room sizes (depth and width), window size (height, width, and WWR (with/without split windows)), window orientation (simultaneous windows in two directions), glazing material properties, shade material properties, and climate zones of the building are different. Table 2-2 shows the input values for baseline building used for existing automated control studies.

Although these studies show the sensitivity to performance metrics for various input variables, comparing percent improvement in visual comfort or/and energy savings due to the implemented control strategies across different papers still can be very challenging. Some studies, such as (E. Shen et al., 2014) (Da Silva et al., 2012a) have compared control strategies for Venetian blinds. However, studies involving roller shades that compare all the existing control strategies are

lacking. Only a few studies involving roller shades have compared control strategies with the shades opening and closing in small increments (as opposed to just fully open and fully closed) with integrated controls, as shown in Table 2-1. This research provides an additional point of reference when comparing a wide variety of control strategies involving roller shades using a typical US DOE small office building model.

Table 2-2 Review of input variables used for automated control strategies

Reference	(Box model/ prototype model/real building)	Measured data/ simulated model	Room size/ Area	Window properties			Window Orientation	Window Properties	Shade properties	Lighting (LPD)	Location/Climate zones	Performance metrics reported
				WWR	Window -sill height	Window size						
(Bourgeois et al., 2006a)	Real building/ Box model	Simulated	W = 5 m, H = 3 m	-	0.95 m	1.68 m high	South facing	Tvis = 0.69	Tvis= 0.16	15 W/m^2	Quebec City, Canada Rome, Italy	--Heating, cooling, and lighting EUI
(Lee & Selkowitz, 2006)	Real Building	Measured	(13.3 m * 23.6 m * 3.15 m)	76%	0.76 m	-	West and south facing	Tvis = 0.75	Tvis = 0.06	16 W/m^2	New York city	--Lighting energy use
(Athanassios Tzempelikos & Athienitis, 2007)	Box model	Simulation	(3 m * 3 m * 3 m)	(5% - 80%)	-	-	South, North, East, and West	-	Tvis = 0.10	15 W/m^2	Montreal, Canada	--Daylight Availability ratio --Work plane illuminance --Cooling heating and lighting load
(Wankanapon & Mistrick, n.d.)	Box model	Simulation	(3 m * 4.6 m * 3.7 m)	40%	-	-	South, North, East, and West	Tvis = (0.7/0.48)	Tvis = 0.14/0.04	9.9 W/m^2	Minneapolis, MN and Houston, TX	--Heating, cooling, and lighting EUI
(Shen and Athanasios Tzempelikos, n.d.)	Box model	Simulation	(3 m * 4 m * 3 m) (30 m * 40 m * 3 m)	(15%, 30%, 50% and 70%)	0.8 m	(1.5 * 1.2 m) (2.0 * 1.8 m) (3.0 * 2.0 m) (4.0 * 2.1 m)	South, North, East, and West		1%, 3%, 7% and 10 % openness	-	Chicago, IL Philadelphia, PA Los Angeles CA	-UDI bins (100 - 2000 Lux) -Daylight autonomy
(Athanasios Tzempelikos & Shen, 2013)	Box model	Simulation	(4 m * 4 m * 3 m)	(20%, 40% and 60%)	-	(3.0 * 1.6 m)	South, North, East, and West	Tvis = (0.75/0.484)	5%, 10% and 15% openness	10 W/m^2	Philadelphia, PA	--% times shades open --UDI, DA --Cooling, heating, and lighting EUI
(Konstantzos et al. 2015)	Real building	Measured data	(5 m * 5.2 m * 3.4 m)	60%	-	-	South	Tvis = (0.65/0.786)	Tvis = 0.05	-	West Lafayette, IN	--DGP --Work plane Illuminance
(Xiong & Tzempelikos, 2016)	Real building	Measured data	(5 m * 5.2 m * 3.4 m)	60%	-	-	South	Tvis = (0.65/0.786)	Tvis = 0.05	-	West Lafayette, IN	--DGP --Work plane Illuminance --Vertical Illuminance
(A. M. Atzeri et al., 2018)	Box model	Simulation	(10m * 10 m * 3m)	-	-	(9 * 1.5 m)	South and East	-	-	10.6 W m^2	Rome, Italy	--Daylight Autonomy (sDA) --Comfort Availability (CA) --Comfort Usability (CU) --Heating, cooling, and lighting
(Do & Chan, 2020)	Box model	Simulation	(3 m * 7 m * 3.3 m)	-	0.8	(3 * 2.5 m)	South and west	Tvis = 0.7	Tvis = 0.50/0.01	-	Taipei, New York city	--cDA and DGPs
(Kunwar et al., 2019b)	Test facility	Measured data + simulation	24.7 m^2	48%	-	6.88 m^2	South, East and West	Tvis = 0.8/0.656	Tvis = 0.12/0.01	12 W/m^2	Ankeny, IA	--Work plane illuminance --UDI, DGPs --Lighting energy
(de Vries et al., 2021)	Box Model	Simulation	4.5m (4.5 m * 6 m * 3 m)	80%		-	South	Tvis = 0.82	Tvis = 0.013	10.9 W/m^2	Amsterdam (The Netherlands)	--DGPs --Vertical Illuminance

Table 2-2 (cont'd)

(Kunwar & Bhandari, 2020)	Prototype model	Simulation	4,982 m^2	33%	-	-	South, East and West		VT = 0.12	16.89 W/m^2 and 8.5 W/m^2	Houston (2A) Los Angeles (3B-CA), Washington DC (4A), Seattle (4C), Chicago (5A), and Minneapolis (6A.	
(Do & Chan, 2021)	Box model	Simulation	(12 m × 15 m × 3.3 m)-	(0%, 10%, 20%, 30%, 40% and 50%)	0.825	(12 * 3.3 m)	North, South, West	Tvis = 0.04/0.08/0.10	Tvis = 0.04/0.08/0.10		Taipei	--Lighting energy saving --Glare prevention --View
(A. Atzeri et al., 2014)	Box model	Simulation	100 m^2 (h = 3 m)	-	-	(9 * 1.5 m) (9 * 2.5 m)	(South) (South + North) (East) (East + West)	τvis = 0.439/0.205/ 0.391/0.191	Tvis = 0.16/0.10/0.06	12 W/m^2	Rome, Italy	--Heating, cooling, and lighting --PMV (Predicted Mean Vote when solar irradiation hits the occupant)

The remainder of this research is organized as follows, Section 2 discusses the Baseline Model selection and the overall workflow of the study including the implemented range of shading and lighting strategies. Section 3 includes the results and discussion whereas Section 4 includes the conclusions for the study.

2.2 MODEL SETUP AND WORKFLOW

This section discusses the model setup and inputs for the daylighting and energy model and the implemented shading and lighting strategies. RADIANCE v5.4 is used for the daylighting model, whereas EnergyPlus v8.9.0 is used for the energy model. These two modeling tools are used in a Ladybug and Honeybee v1.1.0 (Ladybug tools) environment, a plugin for Rhino3D, and Grasshopper (Rhino 3D v6.0).

2.2.1 Selection of Baseline Model

The small office building from the U.S. DOE Commercial Prototype Building models (US DOE 2022) was used as the Baseline Model as shown in Figure 2-1. The ASHRAE 90.1-2004 code version is chosen for the study, as its EUI best resembles the EUI of the existing office buildings. Table 2-3 compares the total site EUI for the ASHRAE 90.1-2004 office building with the EUI for existing office buildings from Building Performance Database (BPD) for climate zones 2A, 4A, 5A, and 7.

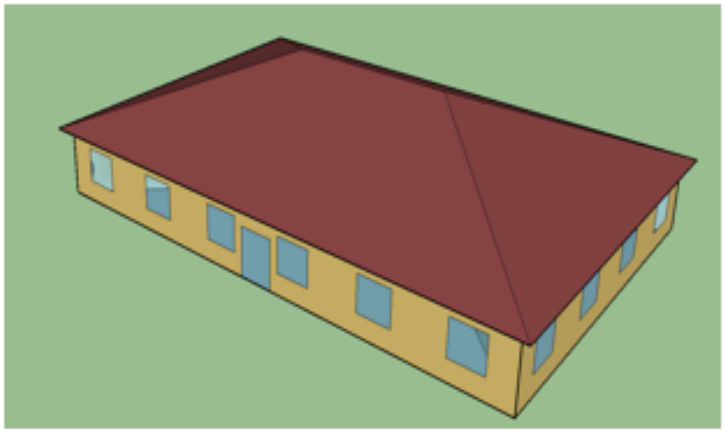

Figure 2-1 ASHRAE 90.1-2004 DOE Commercial Prototype model for small office building

Table 2-3 Energy Use Intensity (EUI) for Prototype Building model in in kWh/m^2

Climate zone	ASHRAE 90.1-2004 model EUI	BPD median EUI (building count)
2A	141.9	176.6 (2730)
4A	129.3	198.7 (8758)
5A	138.8	208.2 (7042)
7	176.6	214.5 (158)

The small office building model has five conditioned zones (four perimeter zones and one core zone). This study is focused on the perimeter zones since shading controls impact these zones. The south-facing and north-facing zones have six windows each (WWR 25%), whereas the east-facing and west-facing zones have four windows each (WWR 20%). The Baseline Model does not have any shading devices or lighting control. The total area of the small office building is 511 m^2. Additional details on the DOE building models are well documented (Deru et al., 2011).

2.2.2 Overall Modeling workflow

The modeling was completed following a three-step process, as shown in Figure 2-2. Step (i) was the zone-level daylight modeling using RADIANCE to generate illuminance values. Step (ii) selecting shade position and lighting level based on the illuminance values generated and the control strategy discussed in Section 2.3. Step (iii) updates the selected shading and lighting levels

in the Baseline Model. The Baseline model and updated model with the control strategy is simulated to compare the differences.

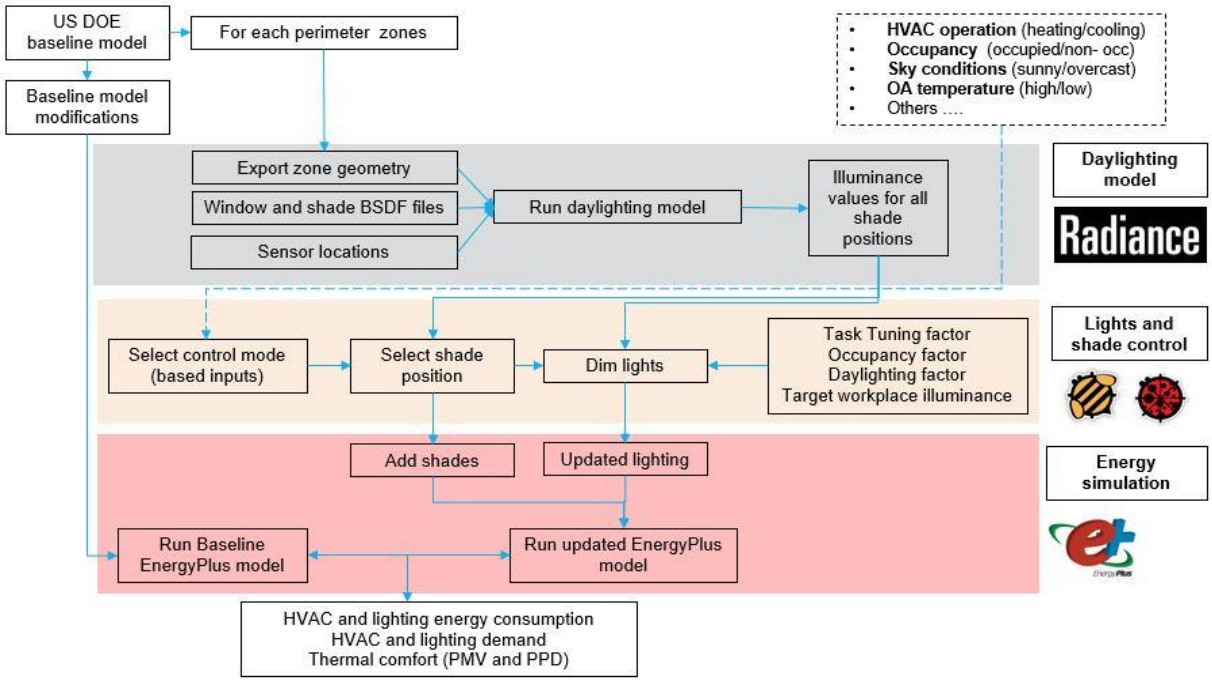

Figure 2-2 Overall modeling workflow

RADIANCE (3-phase matrix method) was used to model the illuminance at sensor points in the room (Figure 2-2), as the model uses dynamic shading devices without any external non-coplanar shading surface such as a window overhang (Subramaniam, 2017). Each perimeter zone was modeled independently. The main inputs used by the daylighting model are explained below.

(i) **Zone geometry** was imported from the DOE Prototype small office building. Typical assumptions for surface reflectance values for opaque surfaces such as walls, floors, and ceiling were used (Jakubiec, 2016).

(ii) **The BSDF files** for windows and shades were generated using WINDOW LBNL v7.7. The layers and properties used for windows are specified in Table 2-4. To mimic the lowering of shades gradually, the exterior windows were divided into ten equal horizontal sections (fully

closed, 90% closed, … 10% closed, fully open), as shown in Figure 2. Thus, the shades were simulated to open or close in increments of 0.15 meters.

Table 2-4 Layers for glazing and its properties

Glazing layers	Thickness (mm)	Visible transmittance	Visible reflectance	Emissivity	Conductivity (W/m-K)
Glass	5.8	0.493	0.378	0.84	1
Air gap	6	-	-	-	-
Glass	5.7	0.771	0.079	0.84	1
Air gap	35	-	-	-	-
Roller shades (5% openness)	0.59	0.57	0.2	0.8	0.3

(iii) **Sensor location:** Illuminance values were determined for two sensor locations. The vertical sensor and the work plane sensor are located 1.6 m away from the window and at a height of 1.2 m and 0.76 m, respectively. The vertical sensor was positioned to face the window while the work plane sensor was positioned to face the ceiling, as shown in Figure 2-3. The distance of 1.6 m was chosen based on the Prototype Building model's (ASHRAE 90.1-2010) default location for daylighting sensor points.

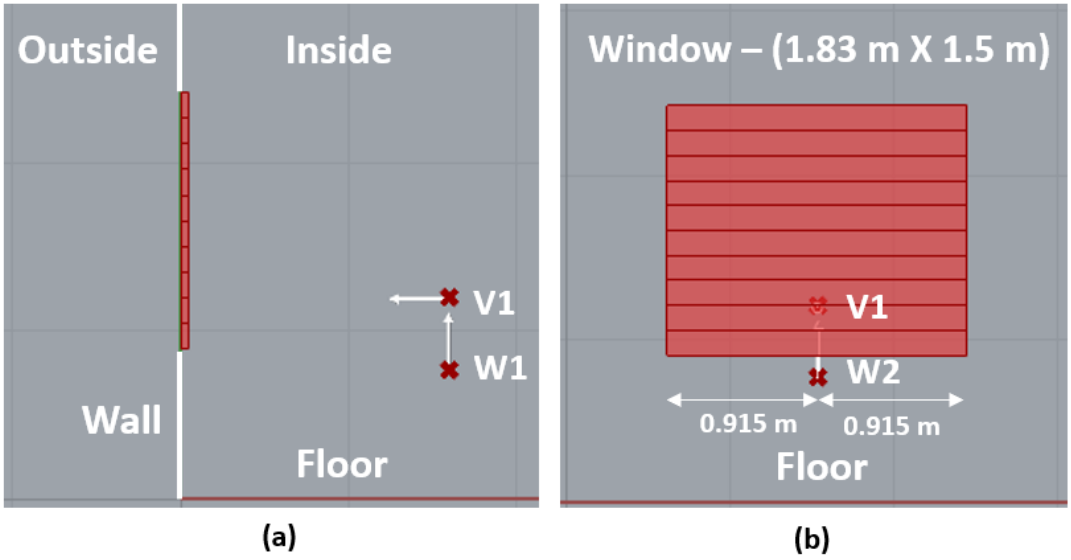

Figure 2-3 (a) side view (b) front view for sensor location with respect to the window

(Note: V1 is a vertical sensor and is located at 1.6 m from the window (height 1.2 m - facing the window), and W1 is the work plane sensor located at 1.6 m from the window (height 0.76 m - facing the ceiling))

The daylighting model generates annual illuminance values for both the vertical and the work-plane sensors for various shade positions. Figure 2-4 shows the illuminance values for the vertical and the work-plane sensors for 11 shade positions (fully closed, 90% closed, 80% closed, … 10% closed, fully open) for the south-facing zone for the summer solstice (20th June). Similarly, Figure 2-5 shows the winter solstice (21st December).

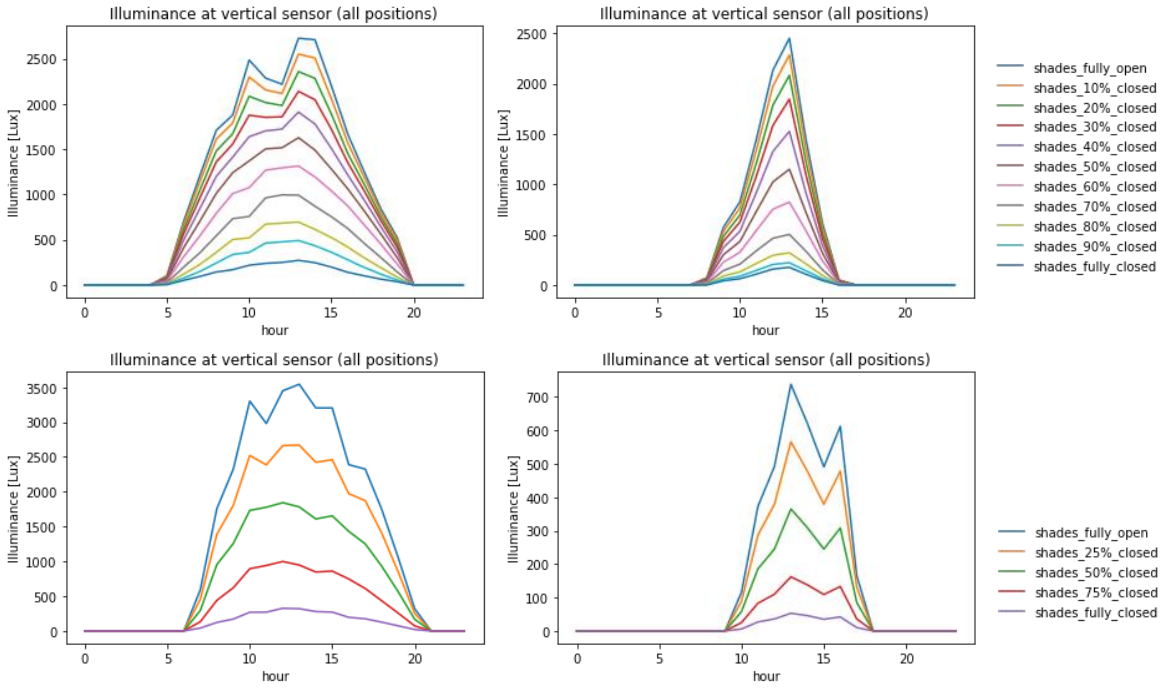

Figure 2-4 Illuminance values for vertical sensor on the summer solstice (left) and winter solstice(right) for small office building (top) and medium office building (bottom) for the south facing zone. *(for medium sized office building the shades are lowered in 5 levels)*

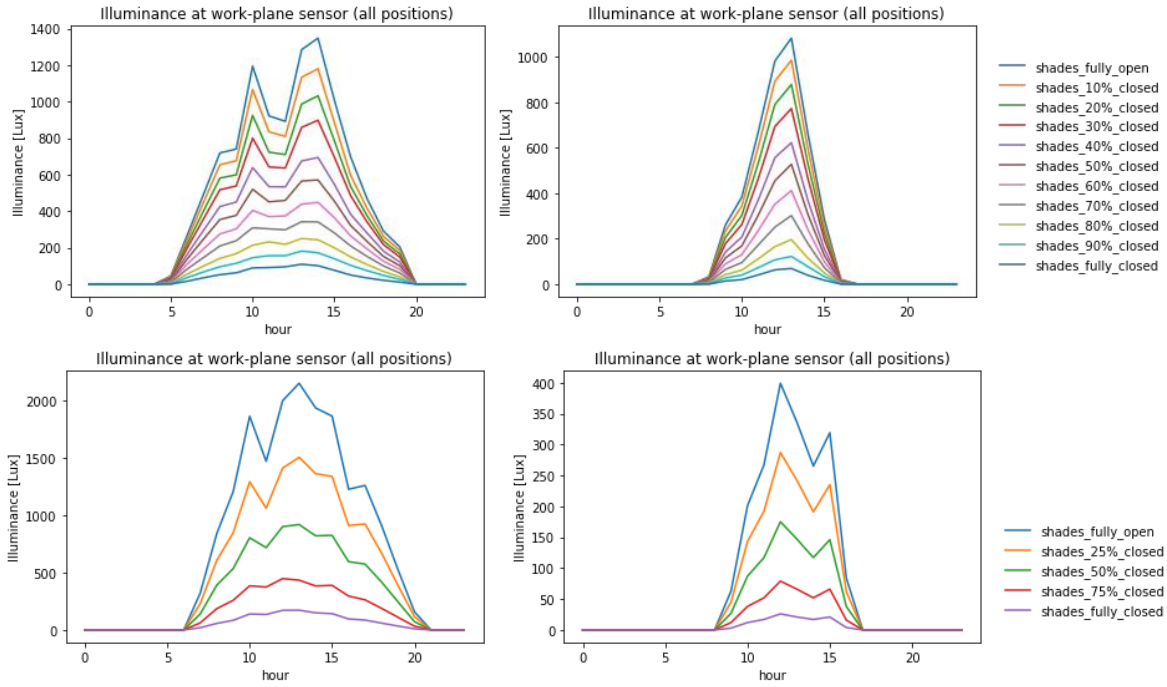

Figure 2-5 Illuminance values for the work-plane sensor on the summer solstice (left) and winter solstice(right) for small office buildings (top) and medium office building (bottom) for the south facing zone

(iv) **Weather data:** TMY3 (Typical Metrological Year) files were used for the daylighting and energy simulation (Wilcox and Marion, 2008). The simulation was run for ASHRAE climate zones CZ2A (Tampa, FL; hot humid); CZ4A (New York City, NY; Mixed Humid), CZ5A (Lansing, MI; cool humid) and CZ7 International Falls, MN; very cold)

2.2.3 Control strategies

Based on the literature review, a range of control strategies to adjust shades and lighting were chosen. A description of control strategies used in this study is listed in Table 2-5. These strategies are divided into four categories (a) Baseline Model (BAM) is a model without any automated controls and is used as a basis of comparison for all the automated control strategies. Two Baseline Models are used, one with the shades fully open and the other with the shades fully closed (b) Manual Control Strategies (MCS), where occupants are assumed to adjust the shading manually. In the current study dynamic manual control strategy is based on (Reinhart 2004). In this strategy,

when direct solar irradiance is higher than 50 W/m2, the shades are closed. The shades remain closed throughout the day and are assumed to be opened each morning by the occupant. (c) Independent Control Strategies (IDS), use a single variable, either solar radiation or glare, as input to automate shades and lighting levels. (d) Integrated Control Strategies (IGS) combines the IDS logic with additional input variables such as Work plane Protection Position (WPP), occupancy-based control, and HVAC state to determine shading and lighting levels. LED lights with an LPD of 6.8 W/m2 are assumed for the control strategies. The LPD values were taken from the DOE Prototype Building model for a small office building (ASHRAE 90.1-2010) for LED lights.

For the Independent control strategy using glare, DGPs (Simplified Daylight Glare Probability) was used [14]. DGPs is a simplified version of DGP (Daylight Glare probability) based only on the vertical illuminance at eye level (Ev) and is calculated using the following equation.

$$DGPs = 6.22 * 10{-}5\ (Ev) + 0.184$$

DGPs value below 0.35 was considered imperceptible, 0.35 - 0.4 perceptible, 0.4 - 0.45 disturbing and above 0.45 are intolerable. Imperceptible DGPs are visually comfortable for the occupants while the other three categories of DGPs can cause visual discomfort. Figure 2-6 and 2-7 shows the DGPs values for all the perimeter zones for a fully open position.

Figure 2-6 DGPs category by percentage for each month for all zones for fully open shade position

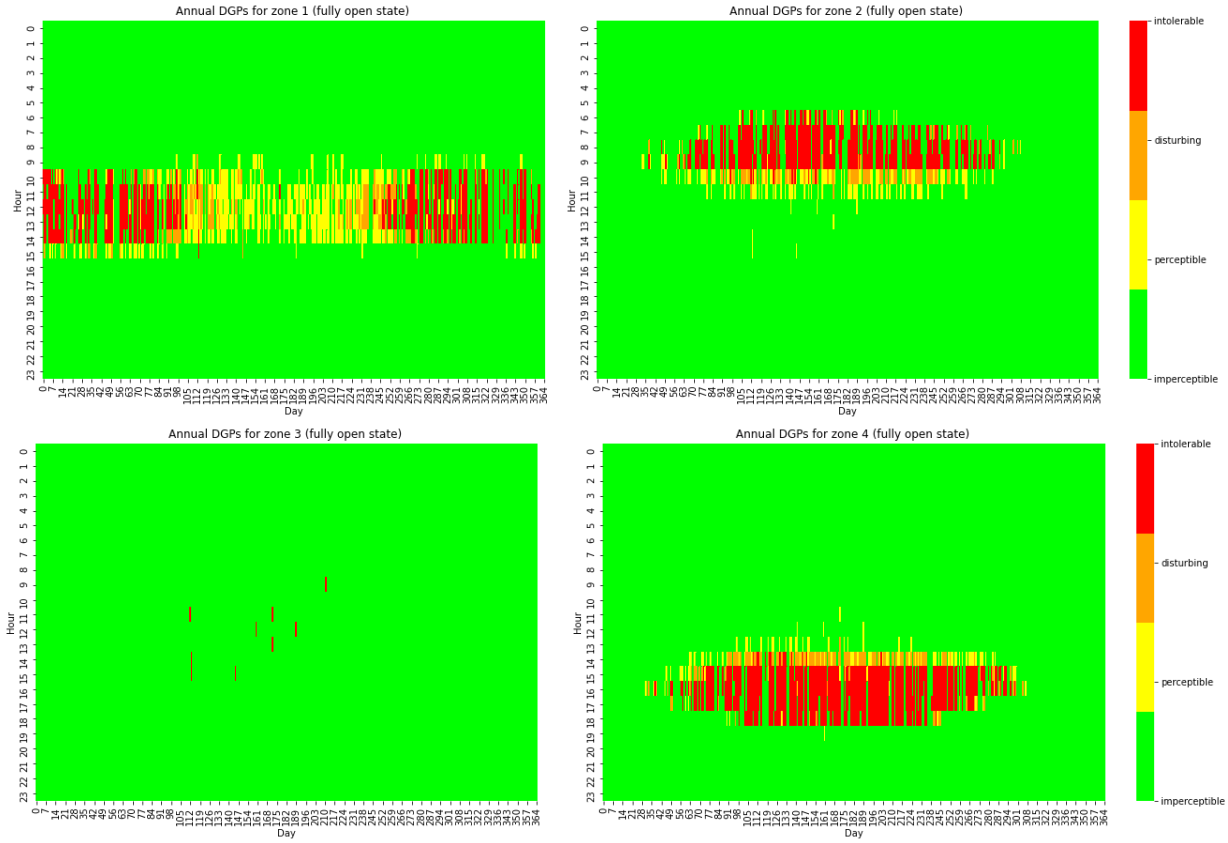

Figure 2-7 Annual DGPs for all zones for fully open shade position
(Note: Zone 1 is south facing, zone 2 is east facing, zone 3 is north facing and zone 4 is west facing)

Table 2-5 Control Strategies compared in the study

Strategy bin	Strategy sub type	Abbreviation	Shading action & threshold	Shading sensor location	Lighting action & threshold	Lighting sensor location	Shade operation description	Sensitivity Analysis
Baseline Model (BAM)	Baseline 1	BAM_1	No shades (fully open)	-	No lighting controls	-	No shades	-
	Baseline 2	BAM_2	Shades fully closed	-	No lighting controls	-	Shades fully closed	-
Manual Control Strategy (MCS)	-	MCS	Manually adjusted by occupants	On the roof, facing up	No lighting controls	-	Shades are fully opened by the occupants each morning and are fully closed and remain closed throughout the day if direct sunlight hits the occupants with direct solar irradiance higher than 50 W/m^2.	Sensitivity for solar radiation threshold (50-250 W/m^2)
Independent Control Strategy (IDS)	No shades with lighting control	IDS_LC	No shades	-	500 lux at W1 [a]	W1 [a]	No shades	-
	Using solar radiation (S)	IDS _SU	Solar radiation > threshold shades are fully closed (else fully open)	On the roof, facing up	500 lux at W1 [a]	W1 [a]	Shades fully close if the solar radiation at the sensor located on the roof is above a threshold value. SU stands for control using **S**olar radiation and a sensor facing **U**p towards the sky.	Sensitivity for solar radiation threshold (50-250 W/m^2)
		IDS _SH		On the roof, facing horizon			Same as IDS_SU, but the sensor faces the horizon. SH stands for control using **S**olar radiation and a sensor facing the **H**orizon.	
	Using glare (G)	IDS_GS	If DGPs > 0.35 shades are fully closed (else fully open)	V1[b]	500 lux at W1 [a]	W1 [a]	Shades are automated to fully close if DGPs is higher than 0.35 at the vertical sensor V1 [a]. GS stands for control using **G**lare control using a **S**ingle window section (that is, shades are either fully open or fully closed).	-
		IDS_GM	If DGPs > 0.35 shade closes in increments of 0.15	V1[b]	500 lux at W1 [a]	W1 [a]	Shades are automated to fully close in increments of 0.15 m if DGPs is higher than 0.35 at the vertical sensor V1 [a]. GM stands for control using **G**lare and **M**ultiple window sections (that is, shades are either fully open, 10% closed, 20% closed, ….90% closed and fully closed).	-
Integrated Control Strategy (IGS)	-	IGS	Based on control modes based on Table 6				Independent Control Strategy with WPP, occupancy, day/night, and HVAC state; detailed operation modes are listed in Table 6. WPP: Shades are lowered to WPP irrespective of illuminance values when the solar radiation is higher than 50 W/m^2. HVAC state: In cooling mode, to maintain visual comfort and minimize the radiation entering the space; in heating mode, to maintain visual comfort and maximize the radiation entering the space. Day/night: Night is sun below the horizon; day is above the horizon. Occupancy control: space is considered unoccupied if the occupancy factor is less than 0.1.	-

Note: [a] for location of W1 and V1, see Figure 2; (All strategies use LED lights with a LPD of 6.8 W/m^2)

The IGS developed by the author, is divided into several control modes based on the binary state of various variables. For instance, visual comfort is not considered during unoccupied modes, and the shade positions are selected to just to minimize or maximize solar radiation entering the space during cooling and heating modes, respectively. Thus, during occupied timesteps visual comfort is given priority. The shades remain fully open or closed during the night based on (E. Shen et al., 2014). Other modes are shown in Table 2-6 and Figure A.1 in Appendix A.

Table 2-6 Control modes variables and strategies for Integrated Control Strategy

Control mode index	Control Mode Variables				Shade and light control strategies			
	HVAC state	Day /Night	Occupied/ Non-occupied	Sunny/ Overcast	Shade control operation	Target vertical illuminance	Lighting control operation	Target work plane illuminance (daylight + artificial)
Mode 1	Cooling	Night	Non-occupied	--	Fully *open* shades	--	Switch off lights	--
Mode 2	Cooling	Night	Occupied	--	Fully *open* shades	--	Limit to target	500 lux
Mode 3	Cooling	Night	Non-occupied	--	Fully *close* shades	--	Switch off lights	--
Mode 4	Cooling	Day	Occupied	Overcast	Range (full open, full close) [a]	2600 lux	Limit to target	500 lux
Mode 5	Cooling	Day	Occupied	Sunny	Range (WPP, full close) [b]	2600 lux	Limit to target	500 lux
Mode 6	Heating	Night	Non-occupied	--	Fully *close* shades	--	Switch off lights	--
Mode 7	Heating	Night	Occupied	--	Fully *close* shades	--	Limit to target	500 lux
Mode 8	Heating	Day	Non-occupied	--	Fully *open* shades	--	Switch off lights	--
Mode 9	Heating	Day	Occupied	Overcast	Range (full open, full close) [a]	2600 lux	Limit to target	500 lux
Mode 10	Heating	Day	Occupied	Sunny	Range (WPP, full close) [b]	2600 lux	Limit to target	500 lux

Note: [a] In Mode 4 and Mode 9 the shades are operated between the fully open position and a fully closed position as it is overcast with no risk of sunlight reaching occupants; [b] In Mode 5 and Mode 10 the shades are operated between the WPP and fully closed position as it is sunny and with risk of sunlight reaching occupants if the shades are opened more than WPP

Figure 2-8 below shows the control modes chosen based in Table 2-6 for the summer solstice (20th June) and winter solstice (21st December) for all four zones. The Figure below highlights the model switching between modes at an hourly level based on the input variables to create a dynamic control model. Figure 2-9 further shows which shade position was selected based on the selected control model for the summer solstice (20th June) and winter solstice (21st December) whereas

Figure 2-10 shows the Shade selection for the entire year for all four zones. For all Figures 2-8, 2-9 and 2-10 zone 1 is south facing, zone 2 is east facing, zone 3 is north facing and zone 4 is west facing)

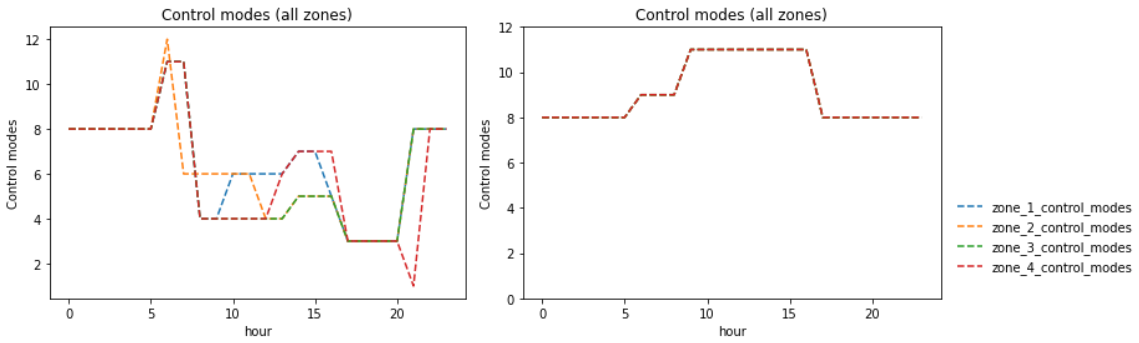

Figure 2-8 Control modes for all perimeter zones on summer (left) and winter (right) solstice

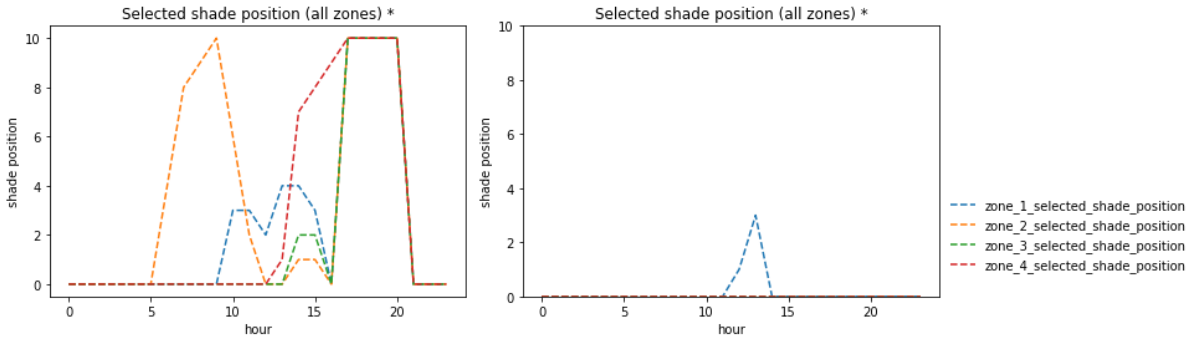

Figure 2-9 Selected shade position for all perimeter zones on summer (left) and winter (right) solstice

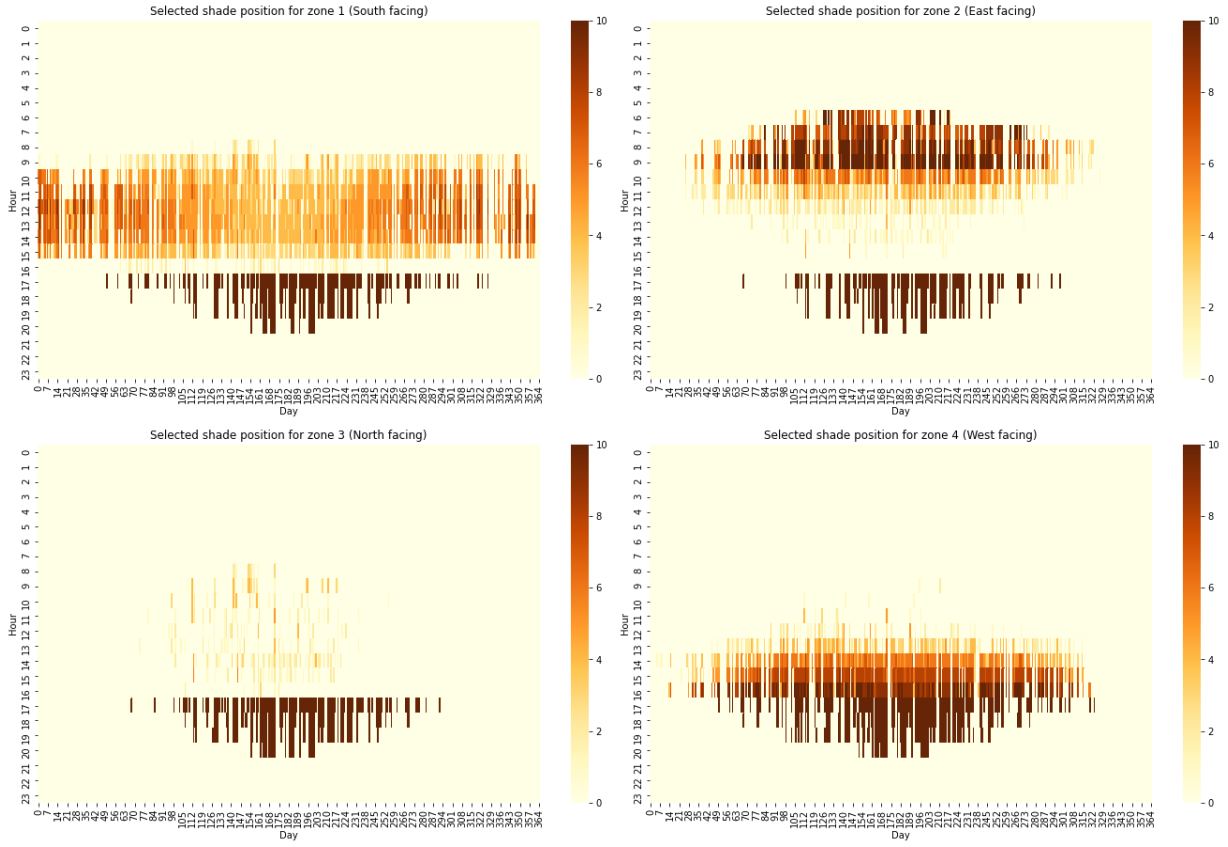

Figure 2-10 Annual selected shade position for all perimeter zones

The shading and lighting action for each control mode is also shown in Table 2-6. Based on the mode, the shades are either fully open or fully closed or a shade position is selected to limit the vertical illuminance value to 2600 lux (equivalent to DGPs > 0.35). For the selected shade position, a lighting level is chosen such that the target work plane illuminance is 500 lux during occupied periods, and lights are switched off during unoccupied periods. The selected shading position and lighting level are updated in the EnergyPlus model and simulated.

2.2.4 Performance metrics

(a) **Percent time's view to the outside:** View to the outside is the percentage of times throughout the year between 8 am and 5 pm when the occupant has a view to the outside. For instance, for BAM_1 (no shades) the view to the outside is 100 %, whereas for BAM_2

(shade fully closed) the view to the outside is 0 %. For all the other control strategies (MCS, IDS, and IGS) the view to the outside is somewhere in between 0 % and 100 %.

(b) **Percent time's glare is perceptible:** Percent of times throughout the year between 8 am and 5 pm when the glare is perceptible (DGPs > 0.35) is calculated at sensor position V1 for all orientations separately. Additional information on the quality of discomfort due to glare is also provided for (i) Perceptible glare (0.35 <= DGPs < 0.4) (ii) disturbing glare (0.4 <= DGPs < 0.45) and (iii) Intolerable glare (GDPs> 0.45).

(c) **Evaluate EUI:** The annual EUI for the entire building is calculated as the summation of cooling, heating, and lighting energy divided by the total area for the entire building. Heating, cooling, and lighting EUI are expressed in kWh/$m^{2.}$ The building assumes Ideal air loads for HVAC calculations.

2.3 RESULTS AND DISCUSSION

The results and discussion section compares the visual comfort and energy use results for ASHRAE CZ5A for four (4) zone orientations (South, East, North, and West) for all the control strategies discussed in Table 2-5. The average visual comfort and energy use values of all the perimeter zones are also compared for four (4) ASHRAE climate zones (CZ2A, CZ4A, CZ5A, and CZ7). The results are organized such that the changes for visual comfort metrics, such as view to the outside and glare, are discussed in Section 3.1.1 for both zone orientation and climate zones whereas the energy use results, such as lighting loads and total loads are compared in Section 3.1.2. Section 3.2 compares and discusses the main insights for the results shown below.

2.3.1 Results

2.3.1.1 Visual Comfort by Zone Orientation and Climate zones

Figures 2-11 and 2-12 (Table 2-7 and 2-8) include the annual percentage of time occupants have a view to the outside and the percentage of time that glare is perceptible (DGPs>0.35) between the operating hours of 8 am to 5 pm. Figures compare the Baseline Models (BAM) to the MCS, IDS, and IGS control strategies. For IDS, various solar radiation thresholds are used. These threshold values are included in each strategy's name in the figure. Each figure (Figures 2-11 and 2-12) is followed by a table below (Table 2-7 and 2-8) that includes the absolute value of the result variable (view to the exterior/glare) for all control strategies and the percent change in performance (in the parenthesis below) of that control strategy to the baseline model BAM_1. The authors show only a percentage difference to the BAM_1. However, percentage change for other control strategies (IDS and IGS) can be calculated to the other Baseline Model (BAM_2) or Manual Control Strategy (MCS) based on values provided in Table 2-11 and 2-12.

In Figure 2-11, the percentage of times when DGPs > 0.35 is shown for each control strategy, additionally information on the quality of discomfort due to glare is also provided in square brackets. This shows when the glare is perceptible (0.35 <= DGPs < 0.4), disturbing (0.4 <= DGPs < 0.45) and intolerable (GDPs> 0.45). For instance [4.5/1.8/8.4] in the table denotes that glare is perceptible for 4.5 % of hours, disturbing for 1.8% of the hours, and intolerable for 8.4 % of hours (with a total for 14.71 % of hours where DGPs > 0.35). Like Figure 2-11 and 2-12 (with Table 2-7 and 2-8) which show results by zone orientation, Figures 2-13 and 2-14 (with Table 2-9 and 2-10) show the results for times viewed to the outside and the percentage times glare exceeds > 0.35 by climate zones.

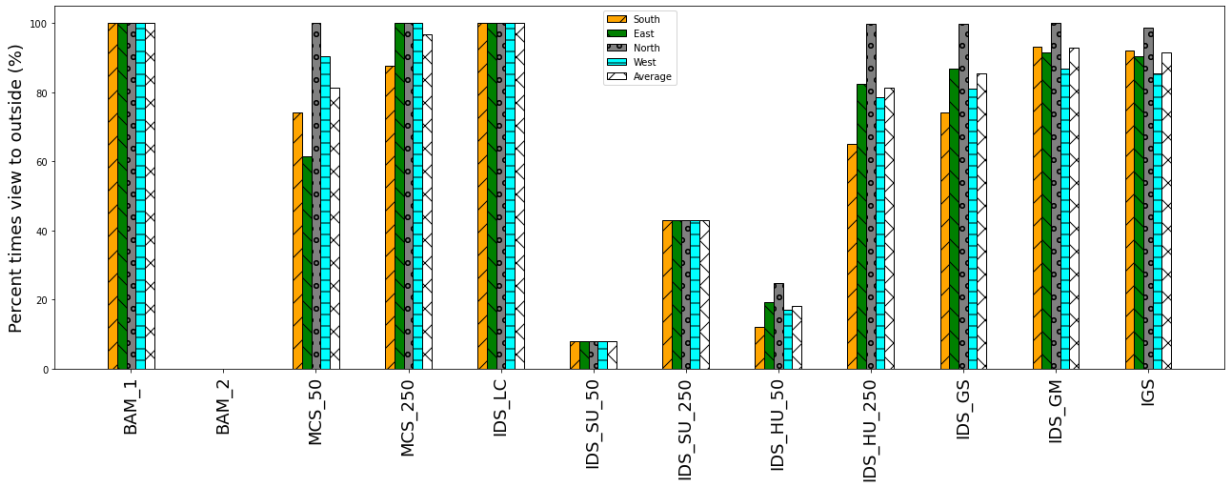

Figure 2-11 Annual percent time occupants have views to the outside from 8 am to 5 pm

Table 2-7 Annual percent time occupants have views to the outside from 8 am to 5 pm *(Note: The value in parentheses is the % change with respect to the BAM_1)*

	BAM_1	BAM_2	MCS_50	MCS_250	IDS_LC	IDS_SU_50	IDS_SU_250	IDS_HU_50	IDS_HU_250	IDS_GS	IDS_GM	IGS
South	100.0	0.0	74.05 (-25.95)	87.73 (-12.27)	100.0 (0.0)	7.89 (-92.11)	43.1 (-56.9)	12.08 (-87.92)	65.04 (-34.96)	74.25 (-25.75)	93.1 (-6.9)	92.05 (-7.95)
East	100.0	0.0	61.37 (-38.63)	100.0 (0.0)	100.0 (0.0)	7.89 (-92.11)	43.1 (-56.9)	19.12 (-80.88)	82.33 (-17.67)	86.9 (-13.1)	91.62 (-8.38)	90.38 (-9.62)
North	100.0	0.0	100.0 (0.0)	100.0 (0.0)	100.0 (0.0)	7.89 (-92.11)	43.1 (-56.9)	24.77 (-75.23)	99.84 (-0.16)	99.89 (-0.11)	100.0 (0.0)	98.68 (-1.32)
West	100.0	0.0	90.49 (-9.51)	100.0 (0.0)	100.0 (0.0)	7.89 (-92.11)	43.1 (-56.9)	17.18 (-82.82)	78.66 (-21.34)	81.1 (-18.9)	86.96 (-13.04)	85.45 (-14.55)
Average	100.0	0.0	81.48 (-18.52)	96.93 (-3.07)	100.0 (0.0)	7.89 (-92.11)	43.1 (-56.9)	18.29 (-81.71)	81.47 (-18.53)	85.53 (-14.47)	92.92 (-7.08)	91.64 (-8.36)

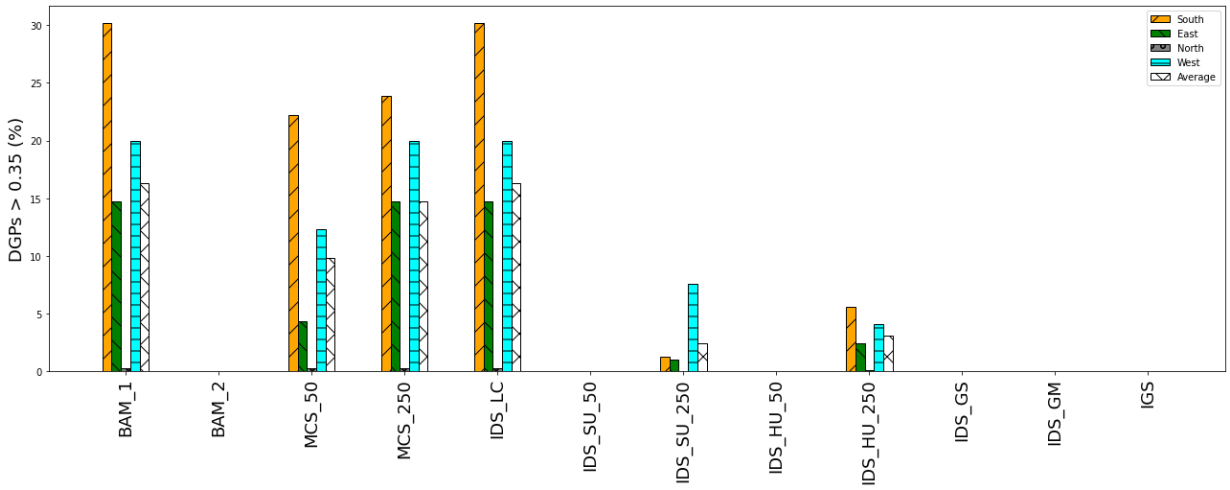

Figure 2-12 Annual percent of time glare occurs (DGPs > 0.35) from 8 am to 5 pm

Table 2-8 Annual percent of time glare occurs (DGPs > 0.35) from 8 am to 5 pm *(Note: The value in parentheses is the % change with respect to the BAM_1)*

	BAM_1	BAM_2	MCS_50	MCS_250	IDS_LC	IDS_SU_50	IDS_SU_250	IDS_HU_50	IDS_HU_250	IDS_GS	IDS_GM	IGS
South	30.16 [12.3/4.1/13.8]	0.0 [0.0/0.0/0.0]	22.22 [11.5/3.4/7.3] (-26.34)	23.84 [11.8/3.6/8.4] (-20.98)	30.16 [12.3/4.1/13.8] (0.0)	0.0 [0.0/0.0/0.0] (-100.0)	1.26 [0.4/0.2/0.6] (-95.82)	0.0 [0.0/0.0/0.0] (-100.0)	5.59 [2.0/1.0/2.5] (-81.47)	0.0 [0.0/0.0/0.0] (-100.0)	0.0 [0.0/0.0/0.0] (-100.0)	0.0 [0.0/0.0/0.0] (-100.0)
East	14.71 [4.5/1.8/8.4]	0.0 [0.0/0.0/0.0]	4.33 [1.3/0.6/2.4] (-70.58)	14.71 [4.5/1.8/8.4] (0.0)	14.71 [4.5/1.8/8.4] (0.0)	0.0 0.0/0.0/0.0] (-100.0)	0.96 [0.5/0.2/0.2] (-93.48)	0.0 [0.0/0.0/0.0] (-100.0)	2.44 [1.0/0.4/1.1] (-83.43)	0.0 [0.0/0.0/0.0] (-100.0)	0.0 [0.0/0.0/0.0] (-100.0)	0.0 [0.0/0.0/0.0] (-100.0)
North	0.22 [0.2/0.0/0.0]	0.0 [0.0/0.0/0.0]	0.22 [0.2/0.0/0.0] (0.0)	0.22 [0.2/0.0/0.0] (0.0)	0.22 [0.2/0.0/0.0] (0.0)	0.0 [0.0/0.0/0.0] (-100.0)	0.0 [0.0/0.0/0.0] (-100.0)	0.0 [0.0/0.0/0.0] (-100.0)	0.08 [0.1/0.0/0.0] (-62.5)	0.0 [0.0/0.0/0.0] (-100.0)	0.0 [0.0/0.0/0.0] (-100.0)	0.0 [0.0/0.0/0.0] (-100.0)
West	19.95 [3.8/2.5/13.6]	0.0 [0.0/0.0/0.0]	12.33 [3.6/2.4/6.2] (-38.19)	19.95 [3.8/2.5/13.6] (0.0)	19.95 [3.8/2.5/13.6] (0.0)	0.0 [0.0/0.0/0.0] (-100.0)	7.53 [0.6/1.0/5.9] (-62.23)	0.0 [0.0/0.0/0.0] (-100.0)	4.03 [1.2/0.5/2.4] (-79.81)	0.0 [0.0/0.0/0.0] (-100.0)	0.0 [0.0/0.0/0.0] (-100.0)	0.0 [0.0/0.0/0.0] (-100.0)
Average	16.26 [5.2/2.1/9.0]	0.0 [0.0/0.0/0.0]	9.77 [4.2/1.6/4.0] (-39.89)	14.68 [5.1/2.0/7.6] (-9.73)	16.26 [5.2/2.1/9.0] (0.0)	0.0 [0.0/0.0/0.0] (-100.0)	2.44 [0.4/0.4/1.7] (-85.0)	0.0 [0.0/0.0/0.0] (-100.0)	3.03 [1.1/0.5/1.5] (-81.34)	0.0 [0.0/0.0/0.0] (-100.0)	0.0 [0.0/0.0/0.0] (-100.0)	0.0 [0.0/0.0/0.0] (-100.0)

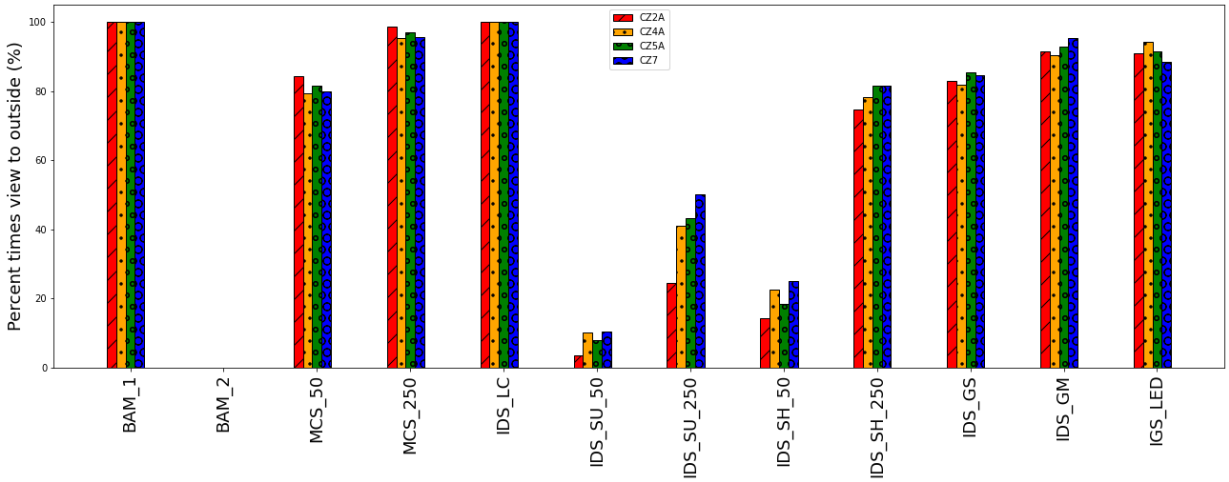

Figure 2-13 Annual percent of times view to the outside from 8 am to 5 pm, by ASHRAE climate zone

Table 2-9 Annual percent of times view to the outside from 8 am to 5 pm, by ASHRAE climate zone *(Note: The value in parentheses is the % change with respect to the BAM_1)*

	BAM_1	BAM_2	MCS_50	MCS_250	IDS_LC	IDS_SU_50	IDS_SU_250	IDS_HU_50	IDS_HU_250	IDS_GS	IDS_GM	IGS
CZ2A	100.0	0.0	84.41 (-15.59)	98.71 (-1.29)	100.0 (0.0)	3.56 (-96.44)	24.41 (-75.59)	14.29 (-85.71)	74.76 (-25.24)	83.03 (-16.97)	91.66 (-8.34)	91.1 (-8.9)
CZ4A	100.0	0.0	79.47 (-20.53)	95.49 (-4.51)	100.0 (0.0)	10.16 (-89.84)	41.07 (-58.93)	22.51 (-77.49)	78.41 (-21.59)	81.8 (-18.2)	90.52 (-9.48)	94.3 (-5.7)
CZ5A	100.0	0.0	81.48 (-18.52)	96.93 (-3.07)	100.0 (0.0)	7.89 (-92.11)	43.1 (-56.9)	18.29 (-81.71)	81.47 (-18.53)	85.53 (-14.47)	92.92 (-7.08)	91.64 (-8.36)
CZ7	100.0	0.0	79.95 (-20.05)	95.64 (-4.36)	100.0 (0.0)	10.49 (-89.51)	50.0 (-50.0)	25.03 (-74.97)	81.64 (-18.36)	84.63 (-15.37)	95.26 (-4.74)	88.61 (-11.39)

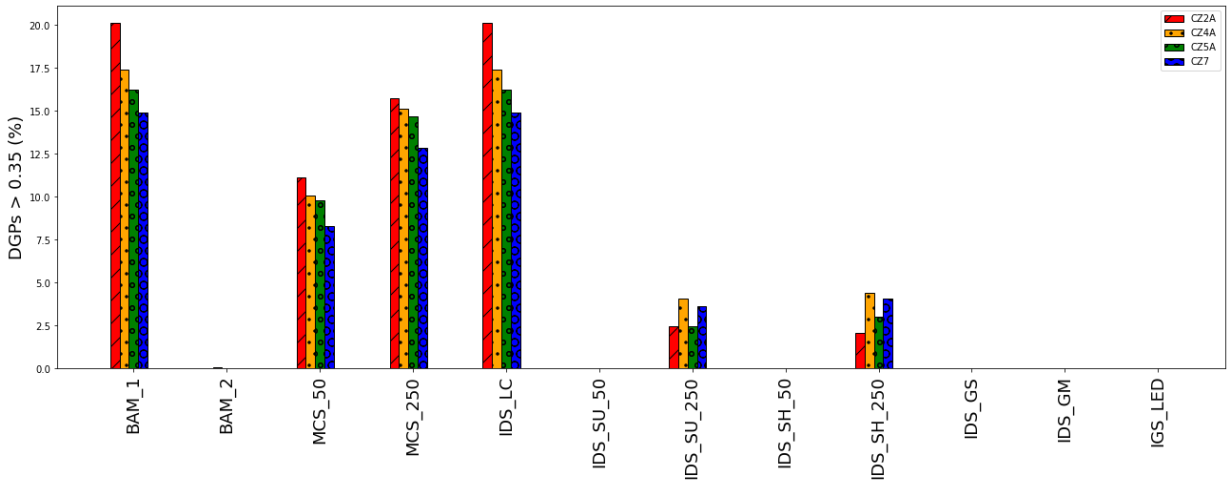

Figure 2-14 Annual percent of times glare (DGPs >0.35) from 8 am to 5 pm, by ASHRAE climate zone

Table 2-10 Annual percent of times glare (DGPs >0.35) from 8 am to 5 pm, by ASHRAE climate zone *(Note: The value in parentheses is the % change with respect to the BAM_1)*

	BAM_1	BAM_2	MCS_50	MCS_250	IDS_LC	IDS_SU_50	IDS_SU_250	IDS_HU_50	IDS_HU_250	IDS_GS	IDS_GM	IGS
CZ2A	20.14 [4.0/2.5/9.9]	0.0 [0.0/0.0/0.0]	11.13 [3.4/2.1/5.6] (-44.73)	15.73 [3.9/2.4/9.4] (-21.87)	20.14 [4.0/2.5/9.9] (0.0)	0.0 [0.0/0.0/0.0] (-100.0)	2.44 [0.4/0.4/1.7] (-87.89)	0.0 [0.0/0.0/0.0] (-100.0)	2.07 [0.6/0.3/1.1] (-89.73)	0.0 [0.0/0.0/0.0] (-100.0)	0.0 [0.0/0.0/0.0] (-100.0)	0.0 [0.0/0.0/0.0] (-100.0)
CZ4A	17.42 [4.5/2.2/10.7]	0.09 [0.0/0.0/0.0]	10.06 [3.8/1.4/4.9] (-42.23)	15.12 [4.5/2.1/8.6] (-13.21)	17.42 [4.5/2.2/10.7] (0.0)	0.0 [0.0/0.0/0.0] (-100.0)	4.08 [0.9/0.5/2.7] (-76.6)	0.0 [0.0/0.0/0.0] (-100.0)	4.4 [1.6/0.6/2.2] (-74.75)	0.0 [0.0/0.0/0.0] (-100.0)	0.0 [0.0/0.0/0.0] (-100.0)	0.0 [0.0/0.0/0.0] (-100.0)
CZ5A	16.26 [5.2/2.1/9.0]	0.0 [0.0/0.0/0.0]	9.77 [4.2/1.6/4.0] (-39.89)	14.68 [5.1/2.0/7.6] (-9.73)	16.26 [5.2/2.1/9.0] (0.0)	0.0 [0.0/0.0/0.0] (-100.0)	2.44 [0.4/0.4/1.7] (-85.0)	0.0 [0.0/0.0/0.0] (-100.0)	3.03 [1.1/0.5/1.5] (-81.34)	0.0 [0.0/0.0/0.0] (-100.0)	0.0 [0.0/0.0/0.0] (-100.0)	0.0 [0.0/0.0/0.0] (-100.0)
CZ7	14.88 [4.0/2.0/8.9]	0.0 [0.0/0.0/0.0]	8.27 [3.2/1.5/3.6] (-44.45)	12.86 [3.8/1.9/7.1] (-13.62)	14.88 [4.0/2.0/8.9] (0.0)	0.0 [0.0/0.0/0.0] (-100.0)	3.61 [0.7/0.4/2.4] (-75.75)	0.0 [0.0/0.0/0.0] (-100.0)	4.05 [1.4/0.6/2.1] (-72.76)	0.0 [0.0/0.0/0.0] (-100.0)	0.0 [0.0/0.0/0.0] (-100.0)	0.0 [0.0/0.0/0.0] (-100.0)

<u>Manual Control Strategy (MCS)</u>: Based on Figures 2-11 and 2-12, if Manual Control Strategy (MCS) is used, on average, there is a reduction in views to the outside by 18% for MCS_50 (most for South and East zone) and 3% for MCS_250 (most for South zone) as compared to BAM_1 for CZ5A. When comparing other climate zones with MCS, on average, the reduction in views to the outside is around 16-20% for MCS_50 and 1-5% for MCS_250.

For CZ5A using MCS_50, the range for glare reduction is 40-70% (mainly East, West, and South), and for MCS_250, a 20% reduction in glare in the South (East, West, and North sides are unaffected). Thus, it is preferable for the East and the South zones to follow an MCS with a lower solar radiation threshold for better visual comfort as compared to a baseline with no shades. No

MCS is necessary for the north side as a view to the outside is maximum, with the percentage times the glare values exceeding the 0.35 threshold being zero. Furthermore, there is an average 45% reduction in glare for all climate zones for MCS_50 and a 10-20% reduction for MCS_250 (highest for CZ2A around 20%).

Independent Control Strategy (IDS): Based on Figure 2-11, IDS_LC, with just lighting control, has the same visual comfort performance as baseline model BAM_1, as neither use shades. Independent Control Strategy with the sensor facing the horizon (IDS_SH_50 and IDS_SH_250) results in more hours with a view to the outside as compared to the sensor facing up (IDS_SU_50 and IDS_SU_250). This change is small between IDS_SH_50 and IDS_SU_50, whereas this change is significant between IDS_SH_250 and IDS_SU_250. Additionally, when comparing climate zones, the percentage of the time with views to the outside for IDS_SU_250 is 25-50% lower as compared to BAM_1, while for IDS_SH_250, it is 75-82% lower as compared to BAM_1. When comparing different climate zones for glare values (shown in Figure 2-13), Independent Control Strategy (IDS_SU_250) has 50-100 more hours with DGPs > 0.35 as compared (IDS_SH_250). Both IDS_SU_50 and IDS_SU_50 have no observed glare conditions. IDS using the glare metric (IDS_GS and IDS_GM) performs better than both IDS using solar radiation (IDS_SH_250 and IDS_SU_250) in terms of both views to the outside and annual glare values for all climate zones. IDS_GM performs slightly better than IDS_GS in providing views to the outside for an additional 300 hours, with glare values being zero in both cases.

Integrated Control Strategy (IGS): Integrated Control Strategy which uses WPP, occupancy, day/night, and HVAC state to select shading and lighting levels when compared to IGS_MS reduces views to the outside by approximately 20-200 hours annually as compared to IDS_GM

based on Figure 2-13. The decrease is most significant for CZ7 and lowest for CZ2A. For both IGS and IDS_GM, the glare values are zero hours annually.

Overall comparison for visual comfort by zone orientation and climate zones

Using the absolute values from Figure 2-11 and Figure 2-12 for percentage of times view to the outdoors and percentage of times glare is present, Table 2-11 and 2-12 are generated to order the performance for each control strategy by zone orientation from more hours of view to the outside to less hours of view to the outside in Table 2-11 and from less hours with glare to more hours of glare in Table 2-12. Top best cases from Table 2-11 and 2-12. Table 2-13 and 2-14 provide similar results by climate zones.

Table 2-11 Summary of results for visual comfort by zone orientation

Control strategy	**Performance order for control strategies (% view to outside)** **More view to the outside ←==========→ Less view to the outside**
South	***IDS_LC_LED*** > ***IDS_GM_LED*** > ***IGS_LED*** > MCS_LED_250 > IDS_GS_LED > MCS_LED_50 > IDS_SH_LED_50 > IDS_SU_LED_50 > IDS_SH_LED_50 > IDS_SU_LED_50
East	***IDS_LC_LED*** > ***MCS_LED_250*** > ***IDS_GM_LED*** > IGS_LED > IDS_GS_LED > IDS_SH_LED_50 > MCS_LED_50 > IDS_SU_LED_50 > IDS_SH_LED_50 > IDS_SU_LED_50
North	***IDS_GM_LED*** > ***IDS_LC_LED*** > ***MCS_LED_250*** > MCS_LED_50 > IDS_GS_LED > IDS_SH_LED_50 > IGS_LED > IDS_SU_LED_50 > IDS_SH_LED_50 > IDS_SU_LED_50
West	***IDS_LC_LED*** > ***MCS_LED_250*** > ***MCS_LED_50*** > IDS_GM_LED > IGS_LED > IDS_GS_LED > IDS_SH_LED_50 > IDS_SU_LED_50 > IDS_SH_LED_50 > IDS_SU_LED_50

Table 2-12 Summary of results for visual comfort by zone orientation

Control strategy	**Performance order for control strategies (% times glare)** **Less hours with glare ←==========→ More hours with glare**
South	***IDS_GM_LED*** > ***IDS_GS_LED*** > ***IDS_SU_LED_50*** > IGS_LED > IDS_SH_LED_50 > IDS_SU_LED_50 > IDS_SH_LED_50 > MCS_LED_50 > MCS_LED_250 > IDS_LC_LED
East	***IDS_GM_LED*** > ***IDS_GS_LED*** > ***IDS_SU_LED_50*** > IGS_LED > IDS_SH_LED_50 > IDS_SU_LED_50 > IDS_SH_LED_50 > MCS_LED_50 > IDS_LC_LED > MCS_LED_250
North	***IDS_GM_LED*** > ***IDS_GS_LED*** > ***IDS_SH_LED_50*** > IDS_SU_LED_50 > IGS_LED > IDS_SU_LED_50 > IDS_LC_LED > IDS_SH_LED_50 > MCS_LED_250 > MCS_LED_50
West	***IDS_GM_LED*** > ***IDS_GS_LED*** > ***IDS_SU_LED_50*** > IGS_LED > IDS_SH_LED_50 > IDS_SH_LED_50 > IDS_SU_LED_50 > MCS_LED_50 > IDS_LC_LED > MCS_LED_250

Table 2-13 Summary of results for visual comfort by climate zones

Control strategy	Performance order for control strategies (% view to outside) More view to the outside ←========== Less view to the outside
CZ2A	***IDS_LC_LED*** > ***MCS_LED_250*** > ***IDS_GM_LED*** > IGS_LED > MCS_LED_50 > IDS_GS_LED > IDS_SH_LED_50 > IDS_SU_LED_50 > IDS_SH_LED_50 > IDS_SU_LED_50
CZ4A	***IDS_LC_LED*** > ***MCS_LED_250*** > ***IGS_LED*** > IDS_GM_LED > IDS_GS_LED > MCS_LED_50 > IDS_SH_LED_50 > IDS_SU_LED_50 > IDS_SH_LED_50 > IDS_SU_LED_50
CZ5A	***IDS_LC_LED*** > ***MCS_LED_250*** > ***IDS_GM_LED*** > IGS_LED > IDS_GS_LED > MCS_LED_50 > IDS_SH_LED_50 > IDS_SU_LED_50 > IDS_SH_LED_50 > IDS_SU_LED_50
CZ7	***IDS_LC_LED*** > ***MCS_LED_250*** > ***IDS_GM_LED*** > IGS_LED > IDS_GS_LED > IDS_SH_LED_50 > MCS_LED_50 > IDS_SU_LED_50 > IDS_SH_LED_50 > IDS_SU_LED_50

Table 2-14 Summary of results for visual comfort by climate zone

Control strategy	Performance order for control strategies (% times glare) Less hours with glare ←========== More hours with glare
CZ2A	***IDS_GM_LED*** > ***IDS_GS_LED*** > ***IGS_LED*** > IDS_SH_LED_50 > IDS_SU_LED_50 > IDS_SH_LED_50 > IDS_SU_LED_50 > MCS_LED_50 > MCS_LED_250 > IDS_LC_LED
CZ4A	***IGS_LED*** > ***IDS_GM_LED*** > ***IDS_GS_LED*** > IDS_SU_LED_50 > IDS_SH_LED_50 > IDS_SU_LED_50 > IDS_SH_LED_50 > MCS_LED_50 > MCS_LED_250 > IDS_LC_LED
CZ5A	***IDS_GM_LED*** > ***IDS_GS_LED*** > ***IDS_SU_LED_50*** > IGS_LED > IDS_SH_LED_50 > IDS_SU_LED_50 > IDS_SH_LED_50 > MCS_LED_50 > MCS_LED_250 > IDS_LC_LED
CZ7	***IDS_GM_LED*** > ***IDS_GS_LED*** > ***IGS_LED*** > IDS_SU_LED_50 > IDS_SH_LED_50 > IDS_SU_LED_50 > IDS_SH_LED_50 > MCS_LED_50 > MCS_LED_250 > IDS_LC_LED

Appendix B provides charts and data for sensitivity to solar radiation threshold for MCS and both the Independent Control Strategies (IDS_SH and IDS_SU) for values ranging from 50 W/m^2 to 250 W/m^2 in increments for 50 W/m^2 for solar radiation both by zone orientation for CZ5A and average values for four ASHRAE climate zones (CZ2A, CZ4A, CZ5A, and CZ7). Further, Appendix B also provides charts for additional visual comfort variables such as Daylight Autonomy (DA), Continuous Daylight Autonomy (cDA), and four Useful Daylight Illuminance (UDI) bins namely $UDI_{100\text{-}500\ lux}$, $UDI_{500\text{-}1000\ lux}$, $UDI_{1000\text{-}2000\ lux}$, and $UDI_{>2000\ lux}$ for both different zone orientation and by climate zones.

2.3.1.2 Energy use by Zone Orientation and Climate zones

Figures 2-15 and 2-16 show the lighting and total loads per zone area, referred to as just lighting EUI and total EUI, respectively. These figures show values for each perimeter zone and an average value for all the perimeter zones. Like Section 3.1.1, each figure (Figures 2-15 and 2-16) is

followed by a Table below (Table 2-15 and 2-16) that includes the percent change in performance for each control strategy to the baseline model BAM_1. Like Figure 2-15 and 2-16 (with Table 2-15 and 2-16), which show results by zone orientation, Figure 2-17 and 2-18 (with Table 2-17 and 2-18) show the results of average lighting and total energy per zone area for all four perimeter zones by climate zones.

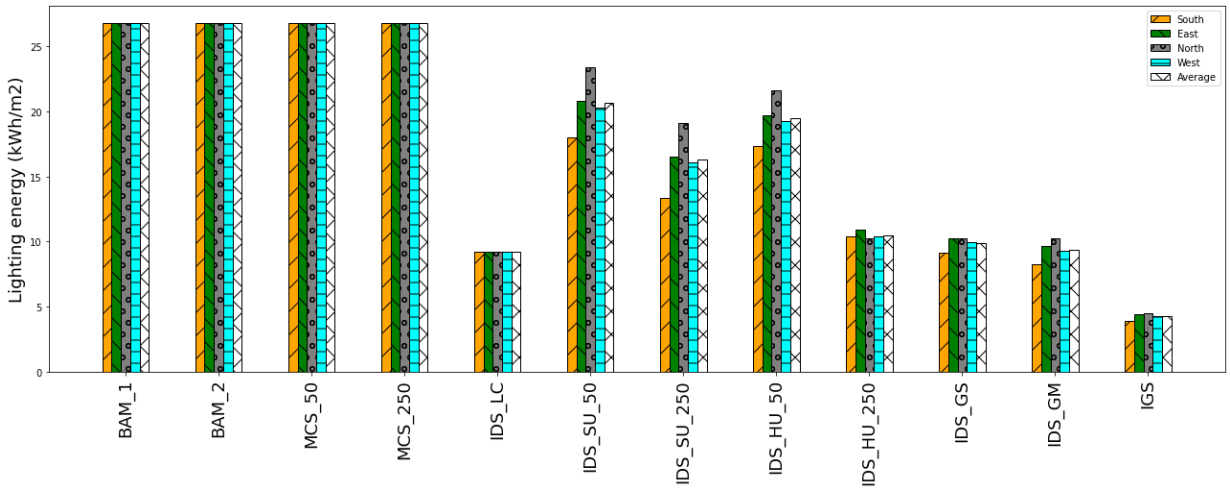

Figure 2-15 Comparison of annual lighting EUI by zone orientation

Table 2-15 Comparison of annual lighting EUI by zone orientation *(Note: The value in parentheses is the % change with respect to the BAM_1)*

	BAM_1	BAM_2	MCS_50	MCS_250	IDS_LC	IDS_SU_50	IDS_SU_250	IDS_HU_50	IDS_HU_250	IDS_GS	IDS_GM	IGS
South	26.75	26.75	26.75 (0.0)	26.75 (0.0)	9.2 (-65.61)	17.97 (-32.82)	13.36 (-50.06)	17.3 (-35.33)	10.39 (-61.16)	9.15 (-65.79)	8.27 (-69.08)	3.89 (-85.46)
East	26.75	26.75	26.75 (0.0)	26.75 (0.0)	9.2 (-65.61)	20.83 (-22.13)	16.54 (-38.17)	19.68 (-26.43)	10.89 (-59.29)	10.21 (-61.83)	9.63 (-64.0)	4.41 (-83.51)
North	26.75	26.75	26.75 (0.0)	26.75 (0.0)	9.2 (-65.61)	23.41 (-12.49)	19.09 (-28.64)	21.64 (-19.1)	10.27 (-61.61)	10.25 (-61.68)	10.23 (-61.76)	4.48 (-83.25)
West	26.75	26.75	26.75 (0.0)	26.75 (0.0)	9.2 (-65.61)	20.26 (-24.26)	16.09 (-39.85)	19.28 (-27.93)	10.38 (-61.2)	9.96 (-62.77)	9.25 (-65.42)	4.26 (-84.07)
Average	26.75	26.75	26.75 (0.0)	26.75 (0.0)	9.2 (-65.61)	20.62 (-22.93)	16.27 (-39.18)	19.48 (-27.2)	10.48 (-60.81)	9.89 (-63.02)	9.34 (-65.07)	4.26 (-84.07)

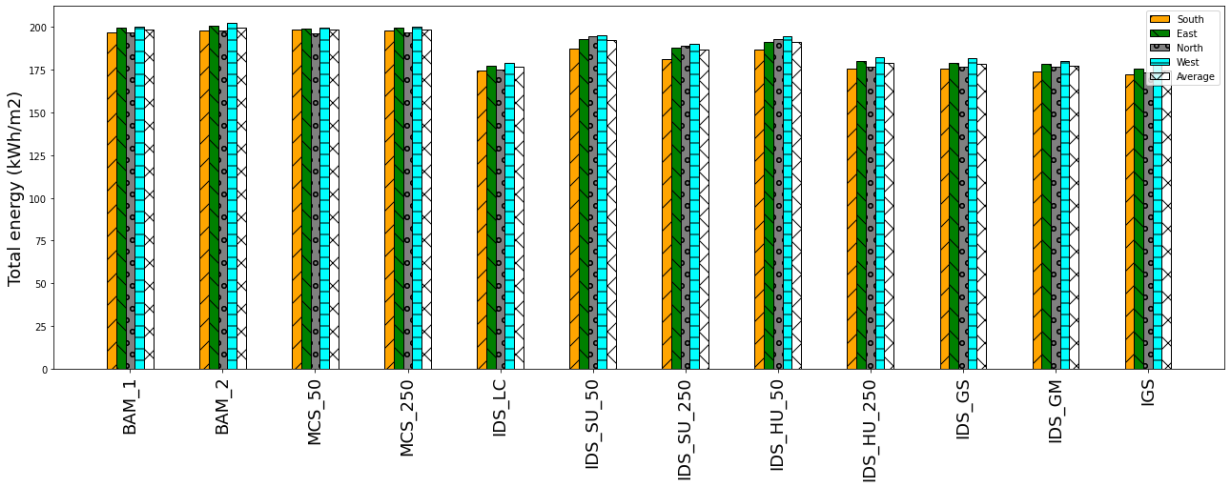

Figure 2-16 Comparison of annual total EUI by zone orientation

Table 2-16 Comparison of annual total EUI by zone orientation *(Note: The value in parentheses is the % change with respect to the BAM_1)*

	BAM_1	BAM_2	MCS_50	MCS_250	IDS_LC	IDS_SU_50	IDS_SU_250	IDS_HU_50	IDS_HU_250	IDS_GS	IDS_GM	IGS
South	196.66	197.92	198.31 (0.84)	197.78 (0.57)	174.65 (-11.19)	187.38 (-4.72)	181.44 (-7.74)	186.7 (-5.06)	175.78 (-10.62)	175.62 (-10.7)	174.25 (-11.4)	172.18 (-12.45)
East	199.83	200.97	198.96 (-0.44)	199.82 (-0.01)	177.15 (-11.35)	193.13 (-3.35)	187.86 (-5.99)	191.32 (-4.26)	180.08 (-9.88)	179.24 (-10.3)	178.5 (-10.67)	175.68 (-12.09)
North	196.82	197.97	196.41 (-0.21)	196.82 (0.0)	175.16 (-11.0)	194.53 (-1.16)	188.96 (-3.99)	192.78 (-2.05)	176.88 (-10.13)	176.82 (-10.16)	176.86 (-10.14)	173.35 (-11.92)
West	200.22	202.24	199.67 (-0.27)	200.17 (-0.02)	179.14 (-10.53)	195.35 (-2.43)	190.02 (-5.09)	194.6 (-2.81)	182.37 (-8.92)	181.9 (-9.15)	180.35 (-9.92)	177.94 (-11.13)
Average	198.38	199.77	198.34 (-0.02)	198.65 (0.13)	176.52 (-11.02)	192.6 (-2.92)	187.07 (-5.7)	191.35 (-3.54)	178.78 (-9.88)	178.4 (-10.08)	177.49 (-10.53)	174.79 (-11.89)

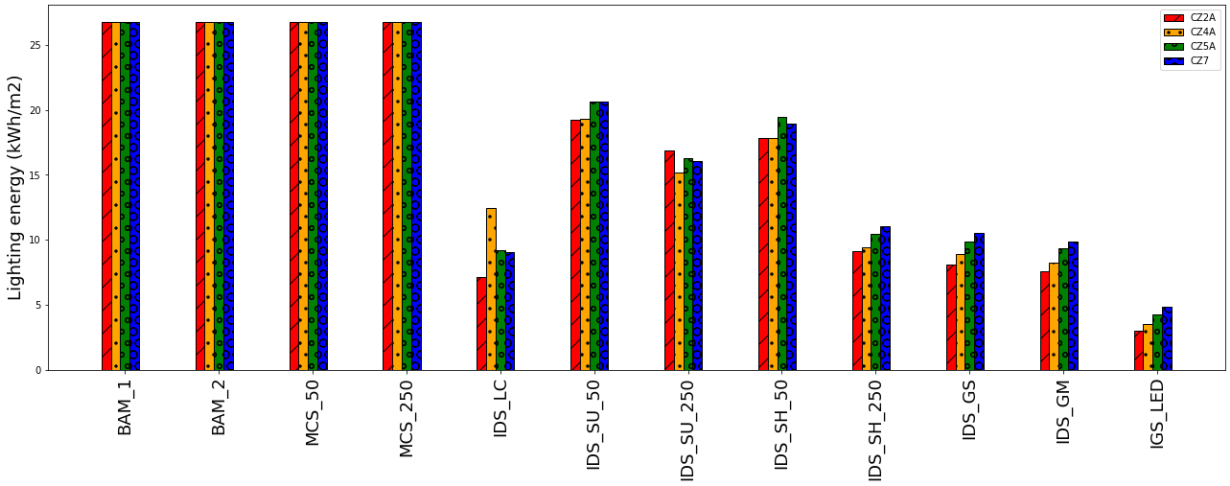

Figure 2-17 Comparison of average annual lighting load by climate zone

Table 2-17: Comparison of average annual lighting load by climate zone *(Note: The value in parentheses is the % change with respect to the BAM_1)*

	BAM_1	BAM_2	MCS_50	MCS_250	IDS_LC	IDS_SU_50	IDS_SU_250	IDS_HU_50	IDS_HU_250	IDS_GS	IDS_GM	IGS
CZ2A	26.75	26.75	26.75 (0.0)	26.75 (0.0)	7.16 (-73.23)	19.27 (-27.97)	16.88 (-36.9)	17.88 (-33.18)	9.16 (-65.75)	8.12 (-69.64)	7.55 (-71.79)	3.04 (-88.65)
CZ4A	26.75	26.75	26.75 (0.0)	26.75 (0.0)	12.45 (-53.46)	19.33 (-27.73)	15.21 (-43.14)	17.87 (-33.21)	9.46 (-64.64)	8.94 (-66.6)	8.24 (-69.19)	3.52 (-86.84)
CZ5A	26.75	26.75	26.75 (0.0)	26.75 (0.0)	9.2 (-65.61)	20.62 (-22.93)	16.27 (-39.18)	19.48 (-27.2)	10.48 (-60.81)	9.89 (-63.02)	9.34 (-65.07)	4.26 (-84.07)
CZ7	26.75	26.75	26.75 (0.0)	26.75 (0.0)	9.03 (-66.24)	20.61 (-22.95)	16.05 (-39.99)	18.93 (-29.21)	11.04 (-58.72)	10.56 (-60.54)	9.88 (-63.08)	4.82 (-81.97)

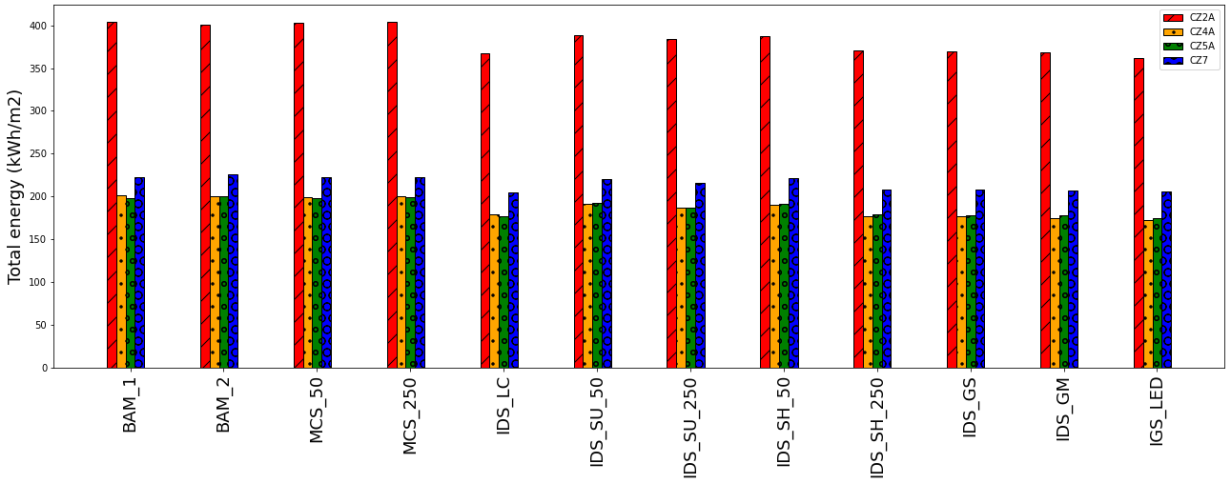

Figure 2-18 Comparison of average annual total load by climate zone

Table 18: Comparison of average annual lighting load by climate zone *(Note: The value in parentheses is the % change with respect to the BAM_1)*

	BAM_1	BAM_2	MCS_50	MCS_250	IDS_LC	IDS_SU_50	IDS_SU_250	IDS_HU_50	IDS_HU_250	IDS_GS	IDS_GM	IGS
CZ2A	403.78	401.3	402.69 (-0.27)	403.76 (-0.01)	367.29 (-9.04)	388.94 (-3.68)	383.82 (-4.95)	387.7 (-3.98)	370.42 (-8.26)	369.05 (-8.6)	368.12 (-8.83)	361.44 (-10.49)
CZ4A	201.28	199.7	199.53 (-0.87)	200.19 (-0.54)	179.1 (-11.02)	190.75 (-5.23)	186.38 (-7.4)	190.4 (-5.4)	176.64 (-12.24)	177.03 (-12.05)	175.03 (-13.04)	172.19 (-14.45)
CZ5A	198.38	199.77	198.34 (-0.02)	198.65 (0.13)	176.52 (-11.02)	192.6 (-2.92)	187.07 (-5.7)	191.35 (-3.54)	178.78 (-9.88)	178.4 (-10.08)	177.49 (-10.53)	174.79 (-11.89)
CZ7	222.25	226.31	222.82 (0.25)	222.84 (0.26)	204.54 (-7.97)	220.68 (-0.71)	215.51 (-3.03)	221.88 (-0.17)	208.37 (-6.25)	207.86 (-6.48)	207.05 (-6.84)	206.16 (-7.24)

Manual Control Strategy (MCS): As shown in Figure 2-15, for CZ5A, the difference between the baseline models with shades fully open (BAM_1) and shades fully closed (BAM_2) is slight. The total EUI for BAM_2, compared to BAM_1, is around 0.6% higher on average for all perimeter zones. The slight increase in total load between BAM_1 and BAM_2 is due to increased solar heat gain in space. The total energy use for MCS_250 is between BAM_1 and BAM_2; The MCS can be used mainly to reduce glare or improve visual comfort in the space without substantially impacting the total load.

Figures 2-17 and 2-18 show the lighting and total EUI for four (4) climate zones. Between BAM_1 and BAM_2, there is only a slight increase or decrease in total EUI depending upon the climate zone (0.6% decrease in CZ2A while 1.8% increase in CZ7). For colder climates, a significant part of the total load comes from heating, and thus, a reduction in solar heat gain increases the total load by 1.8% for CZ7. On the other hand, for CZ2A, a cooling-dominated region, a reduction in solar heat gain reduces the total load slightly by approximately 0.6%. MCS, including both MCS_50 and MCS_250, impacts the total load by 0.25% compared to BAM_1. The main goal of the MCS_50 and MCS_250 is to reduce glare in space.

Independent Control Strategy (IDS): As shown in Figure 2-15, for CZ5A the IDS with no shades and only lighting control (IDS_LC) reduces the lighting load by 65% and total load by 11% as compared to BAM_1 with percent savings similar across all zone orientations. When comparing the average values between climate zones, in CZ4A and CZ5A, IDS_LC reduces the total load by 11% for CZ4A and CZ5A, while for CZ2A and CZ7, the reduction in the total EUI is 8%. Thus, overall, the more extreme weather climates such as CZ2A and CZ7 provide a lower percent reduction in total EUI as compared to the moderate climates such as CZ4A and CZ5A.

When comparing IDS with a solar radiation threshold with sensor facing the horizon (IDS_SH_50 and IDS_SH_250) and with sensor facing up (IDS_SH_50 and IDS_SH_250) for total load savings, the IDS with the sensor facing the horizon (IDS_SH_50 and IDS_SH_250) provides slightly more total load savings as shown in table below Figure 2-15. The trend is similar for all climate zones, with moderate weather climate zones providing the most savings and extreme climate zones providing slightly lower savings when compared to their respective baselines. The values are quantified in Figures 2-17 and 2-18.

When comparing Further, IDS_GS and IDS_GM, when compared to IDS_SH_250, provide a similar but slightly higher total load savings (10.1% reduction for IDS_GS and 10.5% reduction for IDS_GM as compared to BAM_1, as opposed to 9.8% reduction for IDS_SH_250 as compared to BAM_1). The percentage savings for IDS_GS and IDS_GM are similar across all zone orientations. When comparing climate zones, the total EUI savings for IDS_GS and IDS_GM are 6-9% for CZ7/CZ2A and 10-13% for CZ5A/CZ4A as compared to BAM_1. The total load savings for IDS_SH_250 are slightly lower, around 6-8% CZ7/CZ2A and 10-12% CZ5A/CZ4A as compared to BAM_1.

Integrated Control Strategy (IGS): Based on Figure 2-15, for CZ5A the IGS reduces the lighting EUI as compared to IDS_GM (84% reduction for IGS as compared to BAM_1, whereas 65% reduction for IDS_GM as compared to BAM_1). When comparing the total EUI, there is an 11.9% reduction for IGS as compared to BAM_1 which is slightly better than a 10.5% reduction for IDS_GM as compared to BAM_1. The percentage savings for IGS are similar across all zone orientations. When comparing climate zones for IGS a reduction in total EUI for IGS is 7-10% for CZ7/CZ2A and 12-14% for CZ5A/CZ4A as compared to BAM_1. For comparison, the reduction

in total loCCZ4A is 6-9% for CZ7/CZ2A and 10-13% CZ5A/CZ4A reduction for as compared to BAM_1.

Overall comparison for visual comfort by zone orientation and climate zones

Using the absolute load values in Figure 2-15 and 2-16 for lighting and total load, Table 2-19 and 2-20 respectively compares the performance for each control strategy by zone orientation from the lowest energy use to the highest energy use. For both lighting load and total load, the control strategy IGS_LED provides the lowest lighting load of all the control strategies for all zone orientations. Similarly, Using the absolute load values in Figure 2-17 and Figure 2-18, Table 2-21 and 2-22 respectively compares the performance for each control strategy by climate zones from the lowest energy use to the highest energy use. For both lighting load and total load, the control strategy IGS_LED provides the lowest lighting load of all the control strategies for all climate zones.

Table 2-19 Summary of results for energy use by zone orientation

Control strategy	**Performance order for control strategies (by lighting load)** **Low energy use ⟵==========⟶ High energy use**
South	***IGS_LED*** ≥ ***IDS_GM_LED*** ≥ ***IDS_GS_LED*** > IDS_LC_LED > IDS_SH_LED_50 > IDS_SU_LED_50 > IDS_SH_LED_50 > IDS_SU_LED_50 > MCS_LED_250 > MCS_LED_50
East	***IGS_LED*** ≥ ***IDS_LC_LED*** ≥ ***IDS_GM_LED*** > IDS_GS_LED > IDS_SH_LED_50 > IDS_SU_LED_50 > IDS_SH_LED_50 > IDS_SU_LED_50 > MCS_LED_250 > MCS_LED_50
North	***IGS_LED*** ≥ ***IDS_LC_LED*** ≥ ***IDS_GM_LED*** > IDS_GS_LED > IDS_SH_LED_50 > IDS_SU_LED_50 > IDS_SH_LED_50 > IDS_SU_LED_50 > MCS_LED_250 > MCS_LED_50
West	***IGS_LED*** ≥ ***IDS_LC_LED*** ≥ ***IDS_GM_LED*** > IDS_GS_LED > IDS_SH_LED_50 > IDS_SU_LED_50 > IDS_SH_LED_50 > IDS_SU_LED_50 > MCS_LED_250 > MCS_LED_50

Table 2-20 Summary of results for energy use by zone orientation

Control strategy	**Performance order for control strategies (by total load)** **Low energy use ⟵==========⟶ High energy use**
South	***IGS_LED*** ≥ ***IDS_GM_LED*** ≥ ***IDS_LC_LED*** > IDS_GS_LED > IDS_SH_LED_50 > IDS_SU_LED_50 > IDS_SH_LED_50 > IDS_SU_LED_50 > MCS_LED_250 > MCS_LED_50
East	***IGS_LED*** ≥ ***IDS_LC_LED*** ≥ ***IDS_GM_LED*** > IDS_GS_LED > IDS_SH_LED_50 > IDS_SU_LED_50 > IDS_SH_LED_50 > IDS_SU_LED_50 > MCS_LED_50 > MCS_LED_250
North	***IGS_LED*** ≥ ***IDS_LC_LED*** ≥ ***IDS_GS_LED*** > IDS_GM_LED > IDS_SH_LED_50 > IDS_SU_LED_50 > IDS_SH_LED_50 > IDS_SU_LED_50 > MCS_LED_50 > MCS_LED_250
West	***IGS_LED*** ≥ ***IDS_LC_LED*** ≥ ***IDS_GM_LED*** > IDS_GS_LED > IDS_SH_LED_50 > IDS_SU_LED_50 > IDS_SH_LED_50 > IDS_SU_LED_50 > MCS_LED_50 > MCS_LED_250

Table 2-21 Summary of results for energy use by climate zones

Control strategy	Performance order for control strategies (by lighting load) Low energy use ⟵==========⟶ High energy use
CZ2A	***IGS_LED*** > ***IDS_LC_LED*** > ***IDS_GM_LED*** > IDS_GS_LED > IDS_SH_LED_50 > IDS_SU_LED_50 > IDS_SH_LED_50 > IDS_SU_LED_50 > MC_LED_250 > MC_LED_50 > MCS_LED_250 > MCS_LED_50
CZ4A	***IGS_LED*** > ***IDS_GM_LED*** > ***IDS_GS_LED*** > IDS_SH_LED_50 > IDS_LC_LED > IDS_SU_LED_50 > IDS_SH_LED_50 > IDS_SU_LED_50 > MC_LED_250 > MC_LED_50 > MCS_LED_250 > MCS_LED_50
CZ5A	***IGS_LED*** > ***IDS_LC_LED*** > ***IDS_GM_LED*** > IDS_GS_LED > IDS_SH_LED_50 > IDS_SU_LED_50 > IDS_SH_LED_50 > IDS_SU_LED_50 > MC_LED_250 > MC_LED_50 > MCS_LED_250 > MCS_LED_50
CZ7	***IGS_LED*** > ***IDS_LC_LED*** > ***IDS_GM_LED*** > IDS_GS_LED > IDS_SH_LED_50 > IDS_SU_LED_50 > IDS_SH_LED_50 > IDS_SU_LED_50 > MC_LED_250 > MC_LED_50 > MCS_LED_250 > MCS_LED_50

Table 2-22 Summary of results for energy use by climate zones

Control strategy	Performance order for control strategies (by total load) Low energy use ⟵==========⟶ High energy use
CZ2A	***IGS_LED*** > ***IDS_LC_LED*** > ***IDS_GM_LED*** > IDS_GS_LED > IDS_SH_LED_50 > IDS_SU_LED_50 > IDS_SH_LED_50 > IDS_SU_LED_50 > MC_LED_50 > MC_LED_250 > MCS_LED_50 > MCS_LED_250
CZ4A	***IGS_LED*** > ***IDS_GM_LED*** > ***IDS_SH_LED_50*** > IDS_GS_LED > IDS_LC_LED > IDS_SU_LED_50 > IDS_SH_LED_50 > IDS_SU_LED_50 > MC_LED_50 > MC_LED_250 > MCS_LED_50 > MCS_LED_250
CZ5A	***IGS_LED*** > ***IDS_LC_LED*** > ***IDS_GM_LED*** > IDS_GS_LED > IDS_SH_LED_50 > IDS_SU_LED_50 > IDS_SH_LED_50 > IDS_SU_LED_50 > MC_LED_50 > MC_LED_250 > MCS_LED_50 > MCS_LED_250
CZ7	***IDS_LC_LED*** > ***IGS_LED*** > ***IDS_GM_LED*** > IDS_GS_LED > IDS_SH_LED_50 > IDS_SU_LED_50 > IDS_SU_LED_50 > IDS_SH_LED_50 > MC_LED_50 > MC_LED_250 > MCS_LED_50 > MCS_LED_250

Similar to visual comfort metrics, Appendix C provides charts and sensitivity data for cooling, heating, lighting, and total load for MCS and Independent Control Strategy (IDS_SH) and IDS_SU) for values ranging from 50 W/m^2 to 250 W/m^2 in increments for 50 W/m^2 for solar radiation for four ASHRAE climate zones (CZ2A, CZ4A, CZ5A, and CZ7)

2.3.1.3 Overall model comparison by zone orientation

Table 2-23 below shows the best control strategy for three categories (i) all MCS strategies, (ii) all IDS strategies, and (iii) the overall best strategy (MCS, IDS, and IGS) for each performance metric by zone orientation. Thus, the table shows which control strategy has a maximum view to the outside, the lowest glare, and the most energy saving by category. Each category's overall best control strategy varies by zone orientation. When comparing the view to the outside, IDS_LC has the most view to the outside as it does not use any shades. However, for the North zone, MCS_50, MCS_100, MCS_150, MCS_200, MCS_250, IDS_LC, and IDS_GM all provide maximum view

to the outside. The best control strategies for glare are IDS_SU_50, IDS_SH_50, IDS_GS, IDS_GM, and IGS, as they do not cause any glare except for the North zone. In terms of energy use, IGS provides the most total energy savings for all climate zones.

Table 2-23: Overall control strategy comparison by zone orientation (for CZ5A)

Orientation	Performance metric	Best (MCS) strategy	Best (IDS) strategy	Overall best (MCS, IDS and IGS) strategy
South	View	MCS_250	IDS_LC	IDS_LC
	Glare	MCS_100	IDS_SU_50, IDS_SH_50 IDS_GS, IDS_GM	IDS_SU_50, IDS_SH_50 IDS_GS, IDS_GM, IGS
	Total EUI	MCS_250	IDS_GM	IGS
East	View	MCS_250	IDS_LC	IDS_LC
	Glare	MCS_50	IDS_SU_50, IDS_SH_50, IDS_GS, IDS_GM	IDS_SU_50, IDS_SH_50 IDS_GS, IDS_GM, IGS
	Total EUI	MCS_50	IDS_LC	IGS
North	View	MCS_50, MCS_100, MCS_150, MCS_200, MCS_250	IDS_LC, IDS_GM	MCS_50, MCS_100, MCS_150, MCS_200, MCS_250, IDS_LC, IDS_GM
	Glare	MCS_100, MCS_150, MCS_200	IDS_SU_50, IDS_SU_100, IDS_SU_150, IDS_SU_200, IDS_SU_250, IDS_SH_50 IDS_GS, IDS_GM	MCS_100, MCS_150, MCS_200, IDS_SU_50, IDS_SU_100, IDS_SU_150, IDS_SU_200, IDS_SU_250, IDS_SH_50 IDS_GS, IDS_GM, IGS
	Total EUI	MCS_50	IDS_LC	IGS
West	View	MCS_250	IDS_LC	IDS_LC
	Glare	MCS_250	IDS_SU_50, IDS_SH_50 IDS_GS, IDS_GM	IDS_SU_50, IDS_SH_50 IDS_GS, IDS_GM, IGS
	Total EUI	MCS_100	IDS_LC	IGS

2.3.1.4 Overall model comparison by climate zones

Table 2-24 below shows the best control strategy for three categories (i) all MCS strategies, (ii) all IDS strategies, and (iii) the overall best strategy (MCS, IDS, and IGS) for each performance metric by climate zones. The overall best control strategy for each category is consistent between climate zones. For all the climate zones, for view to the outside, IDS_LC has the most view to the outside as it does not use any shades. The best control strategies for glare are IDS_SU_50, IDS_SH_50, IDS_GS, IDS_GM, and IGS, as they do not cause any glare. In terms of energy use, IGS provides the most total energy savings for all climate zones.

Table 2-24: Overall control strategy comparison by climate zones

Orientation	Performance metric	Best (MCS) strategy	Best (IDS) strategy	Overall best (MCS, IDS and IGS) strategy
CZ2A	View	MCS_250	IDS_LC	IDS_LC
	Glare	MCS_50	IDS_SU_50, IDS_SH_50 IDS_GS, IDS_GM	IDS_SU_50, IDS_SH_50 IDS_GS, IDS_GM, IGS
	Total EUI	MCS_50	IDS_LC	IGS
CZ4A	View	MCS_250	IDS_LC	IDS_LC
	Glare	MCS_50	IDS_SU_50, IDS_SH_50 IDS_GS, IDS_GM	IDS_SU_50, IDS_SH_50 IDS_GS, IDS_GM, IGS
	Total EUI	MCS_50	IDS_GM	IGS
CZ5A	View	MCS_250	IDS_LC	IDS_LC
	Glare	MCS_100	IDS_SU_50, IDS_SH_50 IDS_GS, IDS_GM	IDS_SU_50, IDS_SH_50 IDS_GS, IDS_GM, IGS
	Total EUI	MCS_50	IDS_LC	IGS
CZ7	View	MCS_250	IDS_LC	IDS_LC
	Glare	MCS_50	IDS_SU_50, IDS_SH_50 IDS_GS, IDS_GM	IDS_SU_50, IDS_SH_50 IDS_GS, IDS_GM, IGS
	Total EUI	MCS_100	IDS_LC	IDS_LC

2.3.2 Discussion

The research goal of this study was to compare the existing shading and lighting control strategies using a typical/common baseline case. Across existing studies, the visual comfort and energy savings improvements for shading and lighting controls can be very challenging as these studies have different assumptions for baseline models and use different metrics for comparing the results. In most cases, the baseline models differ in the input variables such as room sizes (depth and width), window size (height, width, and WWR (with/without split windows)), window orientation (simultaneous windows in two directions), glazing material properties, shade material properties, and climate zones of the building. To achieve this, a US DOE Prototype Building model for small office buildings was used to compare building performance 4 different types of control strategies (a) Baseline Model (BAM), (b) Manual Control Strategy (MCS), (c) Independent Control Strategy (IDS) using solar radiation and glare and (d) Integrated Control Strategy (IGS) which combines the Independent Control Strategy with other variables such as Work Plane Protection Position

(WPP), occupancy-based control, and HVAC state to select appropriate shading and lighting level targets.

The results of this study allow a single baseline model to compare multiple control strategies for different zone orientation and climate zones. The results provide the following insights. (a) MCS slightly reduces total energy but can improve visual comfort, especially to reduce glare. (b) When using IDS with solar radiation-based control, IDS_SH (sensor facing the horizon) has significantly better energy use and view to the outside, with only a slight increase in glare than IDS_SU (sensor facing directly up). (c) IDS using glare-based control outperforms IDS using solar radiation in terms of reduction in energy use and glare while providing longer views to the outside. (d) For automated shade control using the Independent Control Strategy (IDS), it is advisable to use IDS_GM for a maximum total load reduction of around 10.5% compared to BAM_1 for climate zone 5A. (e) For climate zone 5A, the Integrated Control Strategy (IGS) provides the best total load reduction of all strategies of around 12% savings, with zero glare compared to BAM_1. However, the IGS only provides a small incremental change over IDS_GM (10.5% reduction in total load, with zero glare; views to the outside are only reduced by 7% as compared to BAM_1) while using multiple sensors to determine occupancy, sky condition, and HVAC state. (f) For all control strategies, the trends remain the same for all climate zones, like the results by zone orientation. However, extreme weather climates such as CZ2A and CZ7 provide a lower percent reduction in total load than moderate climates such as CZ4A and CZ5A. A few studies involving roller shades have compared multiple control strategies with the shades opening and closing in small increments (as opposed to just fully open and fully closed) with integrated controls. This research provides an additional point of reference when comparing a wide variety of control strategies involving roller shades using a typical US DOE small office building model.

Even though this study compared various strategies using RADIANCE and EnergyPlus, there are various limitations to this study. These include the following, (a) the minimum timestep for the analysis is one hour due to the significant time taken for RADIANCE simulation for granular timesteps. Studies with more granular timesteps for daylighting and energy simulation can highlight the incremental saving of complex shading and lighting strategies by capturing fluctuating weather conditions. (b) The occupancy schedule used in IGS is based on the DOE model Prototype Building model's hourly occupancy schedule. A stochastic model or a case study can better highlight the impact of occupancy when used as IGS (c). This study used two illuminance sensors, one vertical and one work plane sensor, for the analysis. Controls based on daylight available throughout space using multiple sensors can be used for controlling lighting levels at a fixture-by-fixture level. This can further increase lighting load savings compared to a zone-level model. Thus, spatial-visual comfort metrics such as Spatial Daylight Autonomy and Annual Sunlight Exposure can be used to compare strategies. (d) Sensitivity to other variables, such as shade openness factor and WWR can provide additional information on which strategy performs better and are currently being studied by the author. (e) This study does not assess how these control strategies impact peak loads or thermal discomfort due to direct sunlight entering space and hitting occupants. This is the subject for future work.

2.4 CONCLUSIONS

The study aims to quantify the percent improvement in visual comfort and/or energy savings due to different existing control strategies for roller shades. Comparing shade and lighting control strategies across different studies can be challenging as most existing studies have different baseline model assumptions for variables such as room sizes (depth and width), window size (height, width, and WWR (with/without split windows)), window orientation (simultaneous

windows in two directions), glazing material properties, shade material properties, and climate zones of the building. Thus, this study uses a US DOE Prototype Building model for small office building to compare building performance for (a) Baseline Model (model with and without shades), (b) Manual Control Strategy, (c) Independent Control Strategy using solar radiation and glare and (d) Integrated Control Strategy which combines the Independent Control Strategy with other variables such as Work Plane Protection Position (WPP), occupancy-based control, and HVAC state to select appropriate shading and lighting level targets. Visual comfort metrics such as view to the outside, glare conditions, and energy use metrics such as cooling, heating, lighting, and total EUI are compared for different control strategies. A comparison is shown by zone orientation for Lansing, MI (CZ5A) while the average values for all perimeter zones are compared for four ASHRAE climate zones, Tampa, FL (CZ2A), New York City, NY (CZ4A), Lansing, MI (CZ5A) and International Falls, MN (CZ7). The study concludes that a complex rule-based shading strategy such as an Integrated Control Strategy, which uses HVAC state, occupancy sensors, and time of day for controls, only performs slightly better in terms of both energy use and visual comfort than a control strategy that uses glare to control the shades. Thus, if the addition of sensors is needed to support complex shading and lighting control strategies, these sensors may benefit from being used for multiple purposes in order to justify their use.

REFERENCES

Atzeri, A., Cappelletti, F., & Gasparella, A. (2014). Internal versus external shading devices performance in office buildings. *Energy Procedia*, *45*, 463–472. https://doi.org/10.1016/j.egypro.2014.01.050

Atzeri, A. M., Gasparella, A., Cappelletti, F., & Tzempelikos, A. (2018). Comfort and energy performance analysis of different glazing systems coupled with three shading control strategies. *Science and Technology for the Built Environment*, *24*(5), 545–558. https://doi.org/10.1080/23744731.2018.1449517

Bian, Y., Dai, Q., Ma, Y., & Liu, L. (2020). Variable set points of glare control strategy for side-lit spaces: Daylight glare tolerance by time of day. *Solar Energy*, *201*(March), 268–278. https://doi.org/10.1016/j.solener.2020.03.016

Bourgeois, D., Reinhart, C., & Macdonald, I. (2006a). *Adding advanced behavioural models in whole building energy simulation : A study on the total energy impact of manual and automated lighting control*. *38*, 814–823. https://doi.org/10.1016/j.enbuild.2006.03.002

Bourgeois, D., Reinhart, C., & Macdonald, I. (2006b). Adding advanced behavioural models in whole building energy simulation: A study on the total energy impact of manual and automated lighting control. *Energy and Buildings*, *38*(7), 814–823. https://doi.org/10.1016/j.enbuild.2006.03.002

Carlucci, S., Causone, F., De Rosa, F., & Pagliano, L. (2015). A review of indices for assessing visual comfort with a view to their use in optimization processes to support building integrated design. *Renewable and Sustainable Energy Reviews*, *47*(7491), 1016–1033. https://doi.org/10.1016/j.rser.2015.03.062

Da Silva, P. C., Leal, V., & Andersen, M. (2012a). Influence of shading control patterns on the energy assessment of office spaces. *Energy and Buildings*, *50*, 35–48. https://doi.org/10.1016/j.enbuild.2012.03.019

Da Silva, P. C., Leal, V., & Andersen, M. (2012b). Influence of shading control patterns on the energy assessment of office spaces. *Energy and Buildings*, *50*, 35–48. https://doi.org/10.1016/j.enbuild.2012.03.019

de Vries, S. B., Loonen, R. C. G. M., & Hensen, J. L. M. (2021). Simulation-aided development of automated solar shading control strategies using performance mapping and statistical classification. *Journal of Building Performance Simulation*, *14*(6), 770–792. https://doi.org/10.1080/19401493.2021.1887355

Deru, M., Field, K., Studer, D., Benne, K., Griffith, B., Torcellini, P., Liu, B., Halverson, M., Winiarski, D., Rosenberg, M., Yazdanian, M., Huang, J., & Crawley, D. (2011). U.S. Department of Energy commercial reference building models of the national building stock. *Publications (E)*, *February 2011*, 1–118. http://digitalscholarship.unlv.edu/renew_pubs/44

Do, C. T., & Chan, Y. C. (2020). Evaluation of the effectiveness of a multi-sectional facade with Venetian blinds and roller shades with automated shading control strategies. *Solar Energy*, *212*(October), 241–257. https://doi.org/10.1016/j.solener.2020.11.003

Do, C. T., & Chan, Y. C. (2021). Daylighting performance analysis of a facade combining daylight-redirecting window film and automated roller shade. *Building and Environment*, *191*(October 2020), 107596. https://doi.org/10.1016/j.buildenv.2021.107596

Edwards, L., & Torcellini, P. (2002). A Literature Review of the Effects of Natural Light on Building Occupants A Literature Review of the Effects of Natural Light on Building Occupants. *Contract*, *July*, 55.

Goovaerts, C., Descamps, F., & Jacobs, V. A. (2017). Shading control strategy to avoid visual discomfort by using a low-cost camera: A field study of two cases. *Building and Environment*, *125*, 26–38. https://doi.org/10.1016/j.buildenv.2017.08.030

Jain, S., & Garg, V. (2018). A review of open loop control strategies for shades, blinds and integrated lighting by use of real-time daylight prediction methods. *Building and Environment*, *135*(March), 352–364. https://doi.org/10.1016/j.buildenv.2018.03.018

Jakubiec, J. A. (2016). Building a Database of Opaque Materials for Lighting Simulation. *Los Angeles*, *2015*, 6. http://files/20276/Jakubiec - 2016 - Building a Database of Opaque Materials for Lighti.pdf

Karlsen, L., Heiselberg, P., Bryn, I., & Johra, H. (2016). Solar shading control strategy for office buildings in cold climate. *Energy and Buildings*, *118*(0130), 316–328. https://doi.org/10.1016/j.enbuild.2016.03.014

Klepeis, N. E., Nelson, W. C., Ott, W. R., Robinson, J. P., Tsang, A. M., Switzer, P., Behar, J. V, Hern, C., & Engelmann, W. H. (2001). *Klepeis2001.Pdf*. *September 1998*.

Konstantoglou, M., & Tsangrassoulis, A. (2016). Dynamic operation of daylighting and shading systems: A literature review. *Renewable and Sustainable Energy Reviews*, *60*, 268–283. https://doi.org/10.1016/j.rser.2015.12.246

Konstantzos, I., Tzempelikos, A., & Chan, Y. C. (2015). Experimental and simulation analysis of daylight glare probability inoffices with dynamic window shades. *Building and Environment*, *87*, 244–254. https://doi.org/10.1016/j.buildenv.2015.02.007

Kunwar, N., & Bhandari, M. (2020). A comprehensive analysis of energy and daylighting impact of window shading systems and control strategies on commercial buildings in the United States. *Energies*, *13*(9). https://doi.org/10.3390/en13092401

Kunwar, N., Cetin, K. S., & Passe, U. (2018). Dynamic Shading in Buildings: a Review of Testing Methods and Recent Research Findings. *Current Sustainable/Renewable Energy Reports*, *5*(1), 93–100. https://doi.org/10.1007/s40518-018-0103-y

Kunwar, N., Cetin, K. S., Passe, U., Zhou, X., & Li, Y. (2019a). Full-scale experimental testing

of integrated dynamically-operated roller shades and lighting in perimeter office spaces. *Solar Energy*, *186*(February), 17–28. https://doi.org/10.1016/j.solener.2019.04.069

Kunwar, N., Cetin, K. S., Passe, U., Zhou, X., & Li, Y. (2019b). Full-scale experimental testing of integrated dynamically-operated roller shades and lighting in perimeter office spaces. *Solar Energy*, *186*(March), 17–28. https://doi.org/10.1016/j.solener.2019.04.069

Lee, E. S., & Selkowitz, S. E. (2006). The New York Times Headquarters daylighting mockup: Monitored performance of the daylighting control system. *Energy and Buildings*, *38*(7), 914–929. https://doi.org/10.1016/j.enbuild.2006.03.019

Mitra, D., Chu, Y., & Cetin, K. (2022). COVID-19 impacts on residential occupancy schedules and activities in U . S . Homes in 2020 using ATUS. *Applied Energy*, *324*(August), 119765. https://doi.org/10.1016/j.apenergy.2022.119765

Nezamdoost, A., Mahic, A., & Van Den Wymelenberg, K. (2018). A human factors study to update a recently proposed manual blind use algorithm for energy and daylight simulations. *Proceedings: IECON 2018 - 44th Annual Conference of the IEEE Industrial Electronics Society*, *1*, 789–794. https://doi.org/10.1109/IECON.2018.8591835

Rea, M. S. (1984). Window blind occlusion: a pilot study. *Building and Environment*, *19*(2), 133–137. https://doi.org/10.1016/0360-1323(84)90038-6

Reinhart C. F., & K., V. (2003). Monitoring manual control of electric lighting and blinds Reinhart, C.F.; Voss, K. NRCC-45701. *Lighting Research and Technology*, *35*(3), 243–260.

Sanati, L., & Utzinger, M. (2013). The effect of window shading design on occupant use of blinds and electric lighting. *Building and Environment*, *64*, 67–76. https://doi.org/10.1016/j.buildenv.2013.02.013

Shen, E., Hu, J., & Patel, M. (2014). Energy and visual comfort analysis of lighting and daylight control strategies. *Building and Environment*, *78*, 155–170. https://doi.org/10.1016/j.buildenv.2014.04.028

Shen, H., & Tzempelikos, A. (2012). Daylighting and energy analysis of private offices with automated interior roller shades. *Solar Energy*, *86*(2), 681–704. https://doi.org/10.1016/j.solener.2011.11.016

Shishegar, N., & Boubekri, M. (2016). Natural Light and Productivity: Analyzing the Impacts of Daylighting on Students' and Workers' Health and Alertness. *International Journal of Advances in Chemical Engineering and Biological Sciences*, *3*(1). https://doi.org/10.15242/ijacebs.ae0416104

Subramaniam, S. (2017). *Daylighting Simulations with Radiance using Matrix-based Methods*. *October*, 145.

Tabadkani, A., Roetzel, A., Li, H. X., & Tsangrassoulis, A. (2020). A review of automatic

control strategies based on simulations for adaptive facades. *Building and Environment*, *175*(January), 106801. https://doi.org/10.1016/j.buildenv.2020.106801

Tzempelikos, Athanasios, & Ph, D. (n.d.). *An Experimental and Simulation Study of Lighting Performance in Offices with Automated Roller Shades*.

Tzempelikos, Athanasios, & Shen, H. (2013). Comparative control strategies for roller shades with respect to daylighting and energy performance. *Building and Environment*, *67*, 179–192. https://doi.org/10.1016/j.buildenv.2013.05.016

Tzempelikos, Athanassios, & Athienitis, A. K. (2007). *The impact of shading design and control on building cooling and lighting demand*. *81*, 369–382. https://doi.org/10.1016/j.solener.2006.06.015

Vasquez, N. G., Rupp, R. F., Andersen, R. K., & Toftum, J. (2022). Occupants' responses to window views, daylighting and lighting in buildings: A critical review. *Building and Environment*, *219*(February), 109172. https://doi.org/10.1016/j.buildenv.2022.109172

Wankanapon, P., & Mistrick, R. G. (n.d.). *Roller Shades and Automatic Lighting Control with Solar Radiation Control Strategies*. 35–42.

Xiong, J., & Tzempelikos, A. (2016). Model-based shading and lighting controls considering visual comfort and energy use. *Solar Energy*, *134*, 416–428. https://doi.org/10.1016/j.solener.2016.04.026

EnergyPlus weather data, Available: https://energyplus.net/weather-region/north_and_central_america_wmo_region_4/USA

Wilcox, Stephen, and William Marion. User's manual for tmy3 data sets (revised). No. NREL/TP-581-43156. National Renewable Energy Lab.(NREL), Golden, CO (United States), 2008.

Curcija, Dragan Charlie, et al. Berkeley Lab WINDOW. No. BERKELEY LAB WINDOW. Lawrence Berkeley National Lab.(LBNL), Berkeley, CA (United States), 2015. Available : https://windows.lbl.gov/software/window

DOE (U.S. Department of Energy). 2020. Commercial Prototype Buildings. Accessed August 1, 2020. https://www.energycodes.gov/development/commercial/prototype_models

Lawrence Berkeley National Laboratory "Building Performance Database," 2019. Available: https://bpd.lbl.gov/.

Shafavi, Nastaran Seyed, et al. "Occupants visual comfort assessments: A review of field studies and lab experiments." Solar energy 208 (2020): 249-274.

Ladybug tools, Ladybug and Honeybee, Version 1.1.0 Available: https://www.ladybug.tools/

RADIANCE, Version 5.4 Available : https://www.radiance-online.org/

EnergyPlus, Version 8.9.0 Available : https://energyplus.net/

Rhino 3D, Version 6.0 : https://www.rhino3d.com/

U.S. EIA 2018 Commercial Buildings Energy Consumption Survey. Available: https://www.eia.gov/consumption/commercial/data/2018/

APPENDIX 2-A: IGS CONTROLS

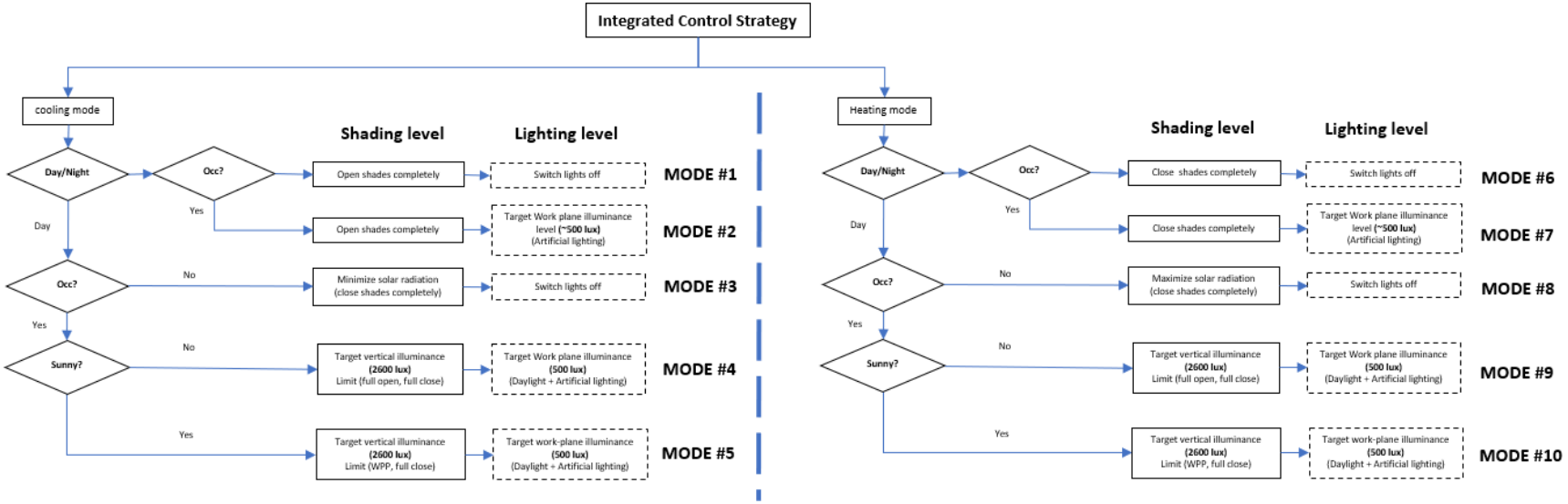

Figure 2-A.1 Control modes for Integrated Control Strategy (IGS)

APPENDIX 2-B: VISUAL COMFORT RESULTS

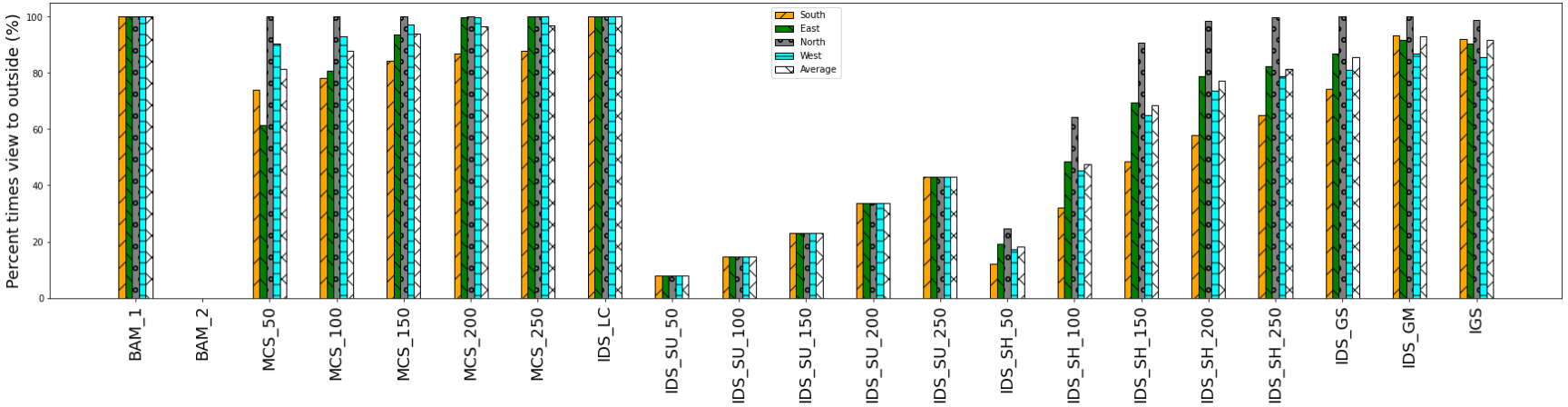

Figure 2-B.1 Annual percent of times view to the outside between (8 am to 5 pm) for all control strategies by zone orientation

Table 2-B.1 Annual percent of times view to the outside between (8 am to 5 pm) for all control strategies by zone orientation (values)

	BAM_1	BAM_2	MCS_50	MCS_100	MCS_150	MCS_200	MCS_250	IDS_LC	IDS_SU_50	IDS_SU_100	IDS_SU_150	IDS_SU_200	IDS_SU_250	IDS_SH_50	IDS_SH_100	IDS_SH_150	IDS_SH_200	IDS_SH_250	IDS_GS	IDS_GM	IGS
South	100.0	0.0	74.05 (-25.95)	78.0 (-22.0)	84.08 (-15.92)	86.79 (-13.21)	87.73 (-12.27)	100.0 (0.0)	7.89 (-92.11)	14.55 (-85.45)	23.07 (-76.93)	33.81 (-66.19)	43.1 (-56.9)	12.08 (-87.92)	32.03 (-67.97)	48.47 (-51.53)	57.78 (-42.22)	65.04 (-34.96)	74.25 (-25.75)	93.1 (-6.9)	92.05 (-7.95)
East	100.0	0.0	61.37 (-38.63)	80.82 (-19.18)	93.7 (-6.3)	99.73 (-0.27)	100.0 (0.0)	100.0 (0.0)	7.89 (-92.11)	14.55 (-85.45)	23.07 (-76.93)	33.81 (-66.19)	43.1 (-56.9)	19.12 (-80.88)	48.47 (-51.53)	69.59 (-30.41)	78.85 (-21.15)	82.33 (-17.67)	86.9 (-13.1)	91.62 (-8.38)	90.38 (-9.62)
North	100.0	0.0	100.0 (0.0)	100.0 (0.0)	100.0 (0.0)	100.0 (0.0)	100.0 (0.0)	100.0 (0.0)	7.89 (-92.11)	14.55 (-85.45)	23.07 (-76.93)	33.81 (-66.19)	43.1 (-56.9)	24.77 (-75.23)	64.3 (-35.7)	90.55 (-9.45)	98.41 (-1.59)	99.84 (-0.16)	99.89 (-0.11)	100.0 (0.0)	98.68 (-1.32)
West	100.0	0.0	90.49 (-9.51)	92.9 (-7.1)	97.18 (-2.82)	99.56 (-0.44)	100.0 (0.0)	100.0 (0.0)	7.89 (-92.11)	14.55 (-85.45)	23.07 (-76.93)	33.81 (-66.19)	43.1 (-56.9)	17.18 (-82.82)	45.26 (-54.74)	64.93 (-35.07)	73.7 (-26.3)	78.66 (-21.34)	81.1 (-18.9)	86.96 (-13.04)	85.45 (-14.55)
Average	100.0	0.0	81.48 (-18.52)	87.93 (-12.07)	93.74 (-6.26)	96.52 (-3.48)	96.93 (-3.07)	100.0 (0.0)	7.89 (-92.11)	14.55 (-85.45)	23.07 (-76.93)	33.81 (-66.19)	43.1 (-56.9)	18.29 (-81.71)	47.51 (-52.49)	68.38 (-31.62)	77.18 (-22.82)	81.47 (-18.53)	85.53 (-14.47)	92.92 (-7.08)	91.64 (-8.36)

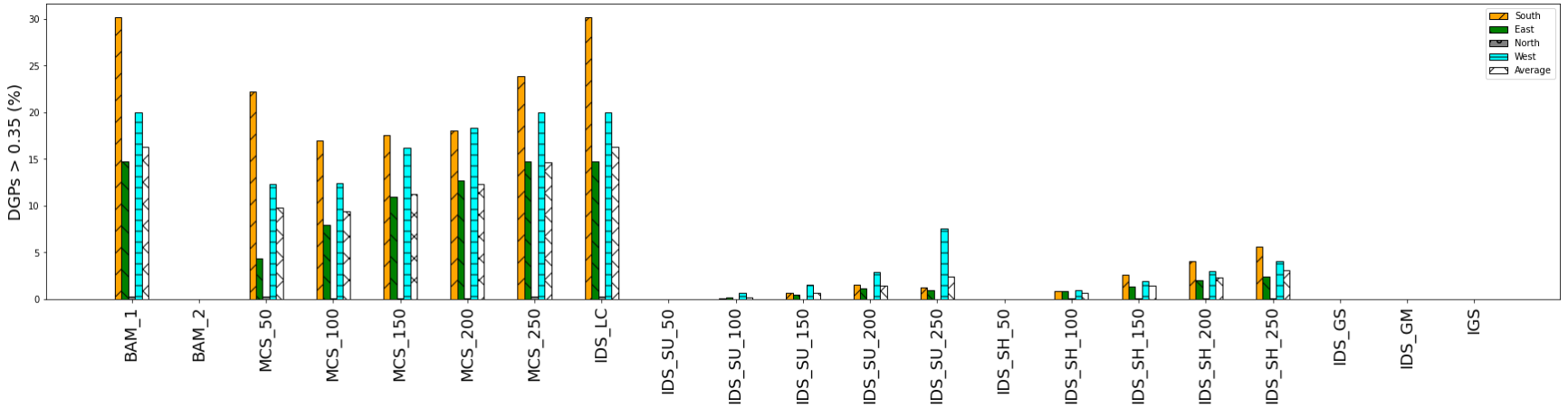

Figure 2-B.2 Annual percent of times glare (DGPs >0.35) between (8 am to 5 pm) for all control strategies by zone orientation

Table 2-B.2 Annual percent of times glare (DGPs >0.35) between (8 am to 5 pm) for all control strategies by zone orientation (values)

	BAM_1	BAM_2	MCS_50	MCS_100	MCS_150	MCS_200	MCS_250	IDS_LC	IDS_SU_50	IDS_SU_100	IDS_SU_150	IDS_SU_200	IDS_SU_250	IDS_SH_50	IDS_SH_100	IDS_SH_150	IDS_SH_200	IDS_SH_250	IDS_GS	IDS_GM	IGS
South	30.16	0.0	22.22 (-26.34)	16.99 (-43.69)	17.59 (-41.69)	18.03 (-40.24)	23.84 (-20.98)	30.16 (0.0)	0.0 (-100.0)	0.08 (-99.73)	0.66 (-97.82)	1.56 (-94.82)	1.26 (-95.82)	0.0 (-100.0)	0.85 (-97.18)	2.58 (-91.46)	4.05 (-86.56)	5.59 (-81.47)	0.0 (-100.0)	0.0 (-100.0)	0.0 (-100.0)
East	14.71	0.0	4.33 (-70.58)	7.92 (-46.18)	10.93 (-25.7)	12.66 (-13.97)	14.71 (0.0)	14.71 (0.0)	0.0 (-100.0)	0.1 (-99.07)	0.47 (-96.83)	1.15 (-92.18)	0.96 (-93.48)	0.0 (-100.0)	0.79 (-94.6)	1.34 (-90.88)	2.0 (-86.41)	2.44 (-83.43)	0.0 (-100.0)	0.0 (-100.0)	0.0 (-100.0)
North	0.22	0.0	0.22 (0.0)	0.08 (-62.5)	0.08 (-62.5)	0.08 (-62.5)	0.22 (0.0)	0.22 (0.0)	0.0 (-100.0)	0.0 (-100.0)	0.0 (-100.0)	0.0 (-100.0)	0.0 (-100.0)	0.0 (-100.0)	0.03 (-87.5)	0.03 (-87.5)	0.05 (-75.0)	0.08 (-62.5)	0.0 (-100.0)	0.0 (-100.0)	0.0 (-100.0)
West	19.95	0.0	12.33 (-38.19)	12.44 (-37.64)	16.16 (-18.96)	18.33 (-8.1)	19.95 (0.0)	19.95 (0.0)	0.0 (-100.0)	0.6 (-96.98)	1.48 (-92.58)	2.85 (-85.71)	7.53 (-62.23)	0.0 (-100.0)	0.93 (-95.33)	1.95 (-90.25)	2.96 (-85.16)	4.03 (-79.81)	0.0 (-100.0)	0.0 (-100.0)	0.0 (-100.0)
Average	16.26	0.0	9.77 (-39.89)	9.36 (-42.46)	11.19 (-31.17)	12.27 (-24.52)	14.68 (-9.73)	16.26 (0.0)	0.0 (-100.0)	0.21 (-98.74)	0.65 (-96.0)	1.39 (-91.45)	2.44 (-85.0)	0.0 (-100.0)	0.65 (-96.0)	1.47 (-90.94)	2.27 (-86.06)	3.03 (-81.34)	0.0 (-100.0)	0.0 (-100.0)	0.0 (-100.0)

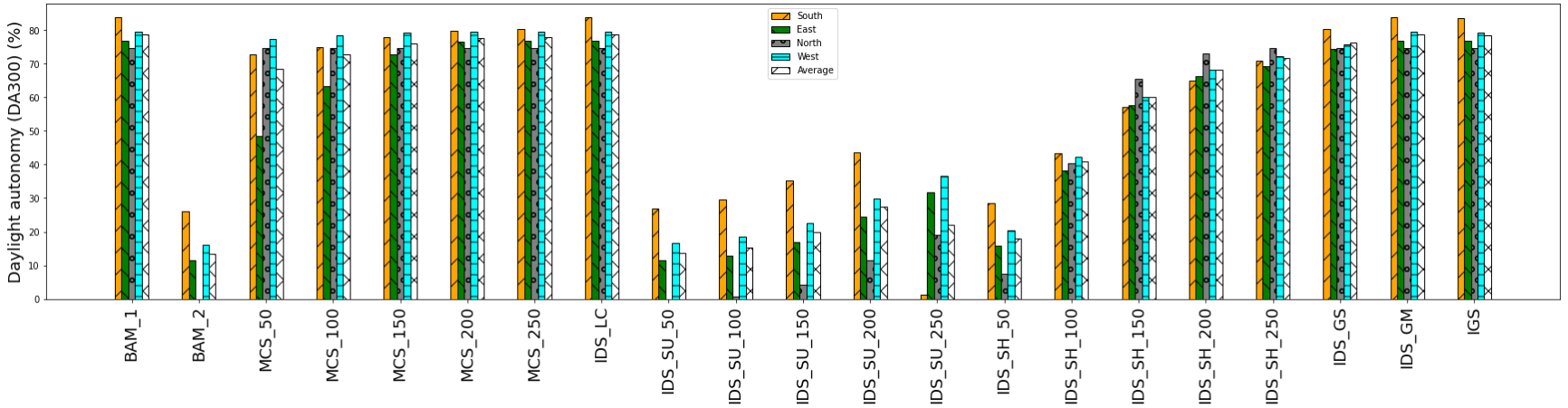

Figure 2-B.3 Daylight Autonomy (DA) between (8 am to 5 pm) for all control strategies by zone orientation

Table 2-B.3 Daylight Autonomy (DA) between (8 am to 5 pm) for all control strategies by zone orientation (values)

	BAM_1	BAM_2	MCS_50	MCS_100	MCS_150	MCS_200	MCS_250	IDS_LC	IDS_SU_50	IDS_SU_100	IDS_SU_150	IDS_SU_200	IDS_SU_250	IDS_SH_50	IDS_SH_100	IDS_SH_150	IDS_SH_200	IDS_SH_250	IDS_GS	IDS_GM	IGS
South	83.81	26.16	72.77 (-13.17)	74.9 (-10.62)	77.97 (-6.96)	79.78 (-4.81)	80.27 (-4.22)	83.81 (0.0)	26.96 (-67.83)	29.67 (-64.6)	35.12 (-58.09)	43.62 (-47.96)	1.26 (-98.5)	28.63 (-65.84)	43.32 (-48.32)	57.12 (-31.84)	65.07 (-22.36)	70.88 (-15.43)	80.27 (-4.22)	83.81 (0.0)	83.62 (-0.23)
East	76.74	11.45	48.52 (-36.77)	63.29 (-17.53)	72.63 (-5.36)	76.58 (-0.21)	76.74 (0.0)	76.74 (0.0)	11.59 (-84.9)	12.9 (-83.18)	17.01 (-77.83)	24.38 (-68.23)	31.64 (-58.76)	15.7 (-79.54)	38.14 (-50.3)	57.7 (-24.81)	66.33 (-13.57)	69.37 (-9.6)	74.27 (-3.21)	76.74 (0.0)	76.71 (-0.04)
North	74.71	0.0	74.71 (0.0)	74.71 (0.0)	74.71 (0.0)	74.71 (0.0)	74.71 (0.0)	74.71 (0.0)	0.0 (-100.0)	0.66 (-99.12)	4.33 (-94.21)	11.48 (-84.64)	19.07 (-74.48)	7.37 (-90.14)	40.33 (-46.02)	65.42 (-12.43)	73.12 (-2.13)	74.55 (-0.22)	74.6 (-0.15)	74.71 (0.0)	74.71 (0.0)
West	79.42	16.16	77.48 (-2.45)	78.44 (-1.24)	79.18 (-0.31)	79.4 (-0.03)	79.42 (0.0)	79.42 (0.0)	16.58 (-79.13)	18.41 (-76.82)	22.6 (-71.54)	29.73 (-62.57)	36.52 (-54.02)	20.3 (-74.44)	42.14 (-46.95)	60.14 (-24.28)	68.08 (-14.28)	72.14 (-9.18)	75.62 (-4.79)	79.42 (0.0)	79.15 (-0.34)
Average	78.67	13.45	68.37 (-13.09)	72.84 (-7.42)	76.12 (-3.24)	77.62 (-1.34)	77.79 (-1.12)	78.67 (0.0)	13.78 (-82.48)	15.41 (-80.41)	19.77 (-74.87)	27.3 (-65.3)	22.12 (-71.88)	18.0 (-77.12)	40.98 (-47.91)	60.1 (-23.61)	68.15 (-13.37)	71.73 (-8.82)	76.19 (-3.15)	78.67 (0.0)	78.55 (-0.16)

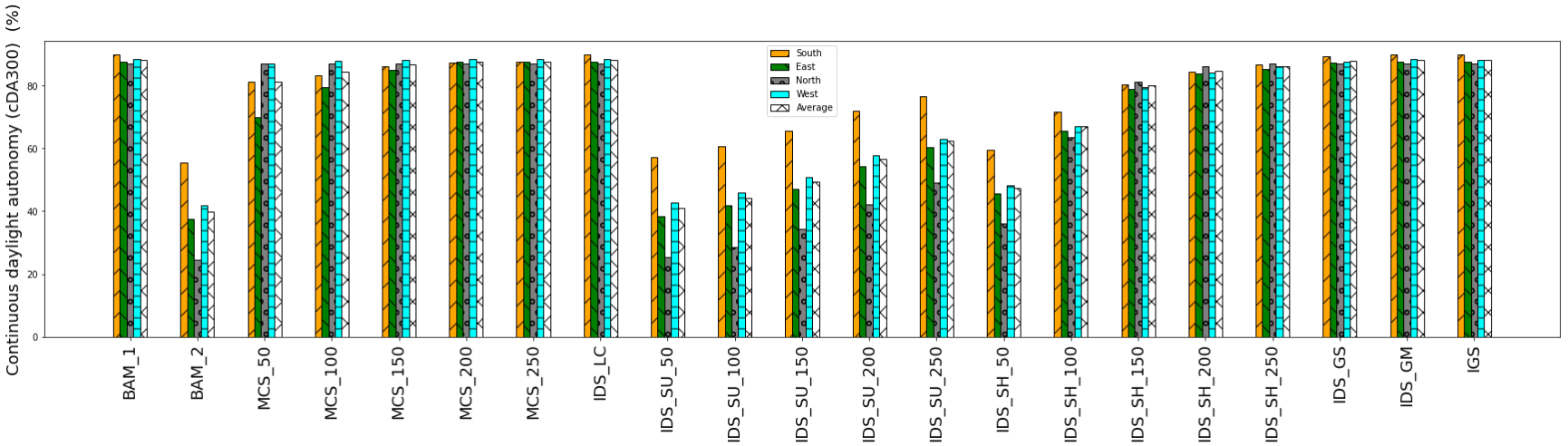

Figure 2-B.4 Continuous Daylight Autonomy (cDA) between (8 am to 5 pm) for all control strategies by zone orientation

Table 2-B.4 Continuous Daylight Autonomy (cDA) between (8 am to 5 pm) for all control strategies by zone orientation (values)

	BAM_1	BAM_2	MCS_50	MCS_100	MCS_150	MCS_200	MCS_250	IDS_LC	IDS_SU_50	IDS_SU_100	IDS_SU_150	IDS_SU_200	IDS_SU_250	IDS_SH_50	IDS_SH_100	IDS_SH_150	IDS_SH_200	IDS_SH_250	IDS_GS	IDS_GM	IGS
South	89.9	55.57	81.14 (-9.75)	85.32 (-2.88)	86.32 (-2.88)	87.32 (-2.88)	87.68 (-2.48)	89.9 (0.0)	57.23 (-36.34)	60.56 (-32.64)	65.54 (-27.1)	71.91 (-20.01)	76.66 (-14.73)	59.53 (-33.78)	71.75 (-20.19)	80.4 (-10.57)	84.44 (-6.07)	86.7 (-3.57)	89.47 (-0.48)	89.9 (0.0)	89.88 (-0.02)
East	87.73	37.67	70.04 (-20.17)	79.37 (-9.53)	85.04 (-3.07)	87.61 (-0.14)	87.73 (0.0)	87.73 (0.0)	38.53 (-56.09)	41.81 (-52.34)	47.2 (-46.21)	54.45 (-37.93)	60.53 (-31.01)	45.6 (-48.02)	65.47 (-25.38)	78.81 (-10.17)	83.74 (-4.56)	85.19 (-2.9)	87.28 (-0.52)	87.73 (0.0)	87.65 (-0.1)
North	87.08	24.48	87.08 (0.0)	87.08 (0.0)	87.08 (0.0)	87.08 (0.0)	87.08 (0.0)	87.08 (0.0)	25.26 (-70.99)	28.51 (-67.26)	34.24 (-60.68)	42.22 (-51.52)	49.04 (-43.69)	36.01 (-58.64)	63.67 (-26.89)	81.19 (-6.76)	86.16 (-1.05)	86.99 (-0.1)	87.05 (-0.04)	87.08 (0.0)	87.03 (-0.06)
West	88.35	41.81	86.97 (-1.56)	87.81 (-0.61)	88.21 (-0.16)	88.35 (-0.0)	88.35 (0.0)	88.35 (0.0)	42.86 (-51.49)	45.99 (-47.95)	50.95 (-42.33)	57.68 (-34.72)	63.05 (-28.64)	48.24 (-45.4)	67.15 (-24.0)	79.47 (-10.05)	84.26 (-4.63)	86.14 (-2.5)	87.63 (-0.81)	88.35 (0.0)	88.2 (-0.17)
Average	88.27	39.88	81.31 (-7.88)	84.36 (-4.42)	86.6 (-1.89)	87.59 (-0.77)	87.71 (-0.63)	88.27 (0.0)	40.97 (-53.58)	44.22 (-49.91)	49.48 (-43.94)	56.57 (-35.92)	62.32 (-29.4)	47.35 (-46.36)	67.01 (-24.08)	79.97 (-9.4)	84.65 (-4.1)	86.25 (-2.28)	87.86 (-0.46)	88.27 (0.0)	88.19 (-0.09)

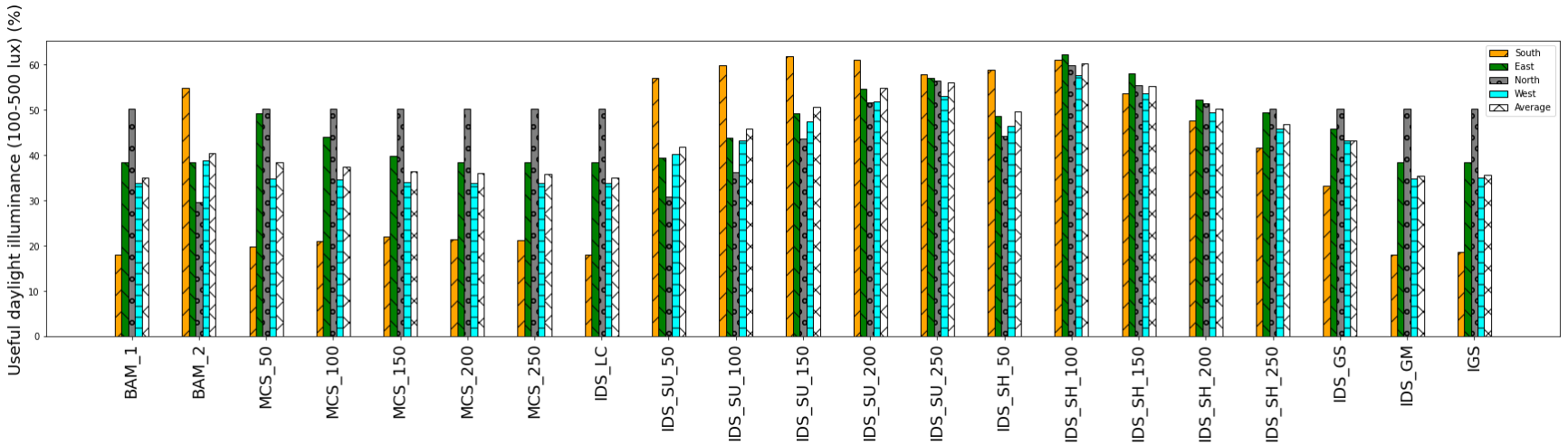

Figure 2-B.5 Useful Daylight Illuminance ($UDI_{100\text{-}500\ lux}$) between (8 am to 5 pm) for all control strategies by zone orientation

Table 2-B.5 Useful Daylight Illuminance ($UDI_{100\text{-}500\ lux}$) between (8 am to 5 pm) for all control strategies by zone orientation (values)

	BAM_1	BAM_2	MCS_50	MCS_100	MCS_150	MCS_200	MCS_250	IDS_LC	IDS_SU_50	IDS_SU_100	IDS_SU_150	IDS_SU_200	IDS_SU_250	IDS_SH_50	IDS_SH_100	IDS_SH_150	IDS_SH_200	IDS_SH_250	IDS_GS	IDS_GM	IGS
South	18.03	54.88	19.73 (9.42)	21.07 (16.87)	21.92 (21.58)	21.45 (19.0)	21.21 (17.63)	18.03 (0.0)	56.96 (215.96)	59.84 (231.91)	61.84 (243.01)	60.96 (238.15)	57.92 (221.28)	58.85 (226.44)	61.04 (238.6)	53.73 (198.02)	47.53 (163.68)	41.67 (131.16)	33.23 (84.35)	18.03 (0.0)	18.63 (3.34)
East	38.38	38.36	49.15 (28.05)	43.97 (14.56)	39.78 (3.64)	38.36 (-0.07)	38.38 (0.0)	38.38 (0.0)	39.42 (2.71)	43.84 (14.2)	49.32 (28.48)	54.71 (42.54)	57.1 (48.75)	48.55 (26.48)	62.25 (62.17)	58.03 (51.18)	52.25 (36.12)	49.4 (28.69)	45.89 (19.56)	38.47 (0.21)	38.41 (0.07)
North	50.14	29.59	50.14 (0.0)	50.14 (0.0)	50.14 (0.0)	50.14 (0.0)	50.14 (0.0)	50.14 (0.0)	30.77 (-38.63)	36.14 (-27.92)	43.62 (-13.01)	51.64 (3.01)	56.44 (12.57)	44.27 (-11.69)	59.92 (19.51)	55.42 (10.55)	51.53 (2.79)	50.3 (0.33)	50.25 (0.22)	50.14 (0.0)	50.14 (0.0)
West	33.73	38.9	34.77 (3.09)	34.63 (2.68)	34.05 (0.97)	33.75 (0.08)	33.73 (0.0)	33.73 (0.0)	40.14 (19.01)	43.32 (28.43)	47.45 (40.7)	51.78 (53.53)	53.1 (57.43)	46.52 (37.94)	57.64 (70.92)	53.67 (59.14)	49.45 (46.63)	45.78 (35.74)	43.26 (28.27)	34.88 (3.41)	35.01 (3.82)
Average	35.07	40.43	38.45 (9.63)	37.45 (6.8)	36.47 (4.0)	35.92 (2.44)	35.86 (2.27)	35.07 (0.0)	41.82 (19.26)	45.78 (30.55)	50.55 (44.16)	54.77 (56.19)	56.14 (60.08)	49.55 (41.29)	60.21 (71.7)	55.21 (57.44)	50.19 (43.13)	46.79 (33.42)	43.16 (23.07)	35.38 (0.88)	35.55 (1.37)

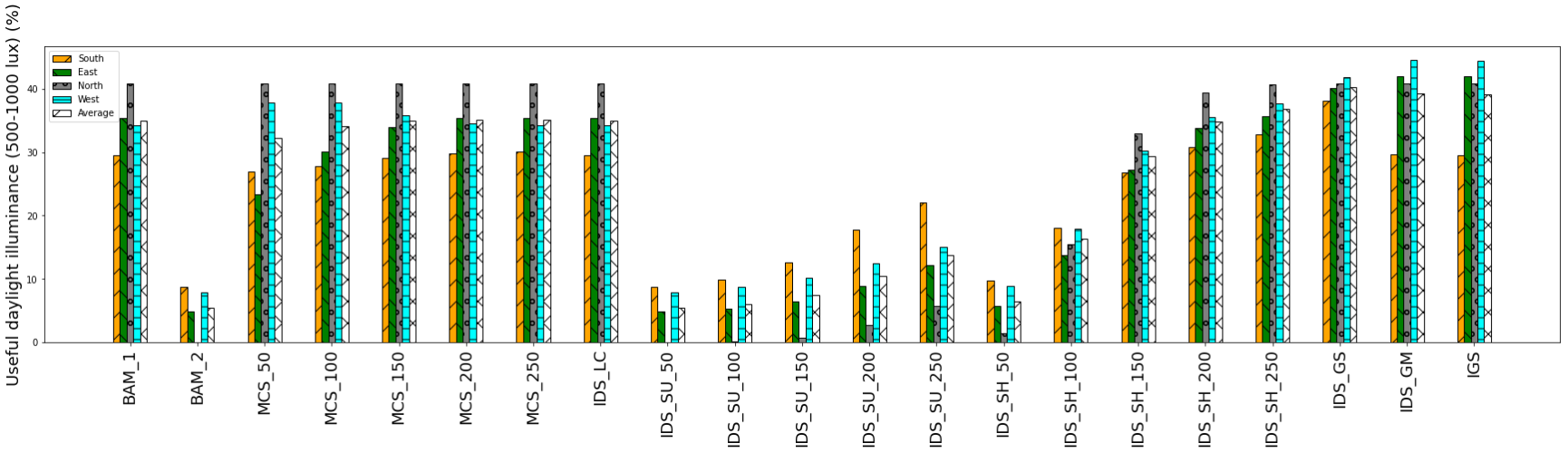

Figure 2-B.6 Useful Daylight Illuminance ($UDI_{500\text{-}1000\ lux}$) between (8 am to 5 pm) for all control strategies by zone orientation

Table 2-B.6 Useful Daylight Illuminance ($UDI_{500\text{-}1000\ lux}$) between (8 am to 5 pm) for all control strategies by zone orientation (values)

	BAM_1	BAM_2	MCS_50	MCS_100	MCS_150	MCS_200	MCS_250	IDS_LC	IDS_SU_50	IDS_SU_100	IDS_SU_150	IDS_SU_200	IDS_SU_250	IDS_SH_50	IDS_SH_100	IDS_SH_150	IDS_SH_200	IDS_SH_250	IDS_GS	IDS_GM	IGS
South	29.53	8.68	26.9 (-8.91)	27.73 (-6.12)	29.01 (-1.76)	29.86 (1.11)	30.03 (1.67)	29.53 (0.0)	8.74 (-70.41)	9.89 (-66.51)	12.6 (-57.33)	17.75 (-39.89)	22.0 (-25.51)	9.67 (-67.25)	18.03 (-38.96)	26.74 (-9.46)	30.77 (4.17)	32.88 (11.32)	38.08 (28.94)	29.73 (0.65)	29.48 (-0.19)
East	35.34	4.82	23.32 (-34.03)	30.03 (-15.04)	33.97 (-3.88)	35.34 (0.0)	35.34 (0.0)	35.34 (0.0)	4.88 (-86.2)	5.23 (-85.19)	6.41 (-81.86)	8.88 (-74.88)	12.16 (-65.58)	5.7 (-83.88)	13.73 (-61.16)	27.29 (-22.79)	33.78 (-4.42)	35.73 (1.09)	40.08 (13.41)	41.95 (18.68)	41.95 (18.68)
North	40.9	0.0	40.9 (0.0)	40.9 (0.0)	40.9 (0.0)	40.9 (0.0)	40.9 (0.0)	40.9 (0.0)	0.0 (-100.0)	0.03 (-99.93)	0.63 (-98.46)	2.63 (-93.57)	5.7 (-86.07)	1.45 (-96.45)	15.45 (-62.22)	33.01 (-19.29)	39.42 (-3.62)	40.74 (-0.4)	40.9 (0.0)	40.9 (0.0)	40.9 (0.0)
West	34.27	7.84	37.84 (10.39)	37.89 (10.55)	35.86 (4.64)	34.58 (0.88)	34.27 (0.0)	34.27 (0.0)	7.89 (-76.98)	8.74 (-74.5)	10.19 (-70.26)	12.49 (-63.55)	15.04 (-56.12)	8.88 (-74.1)	17.89 (-47.8)	30.16 (-11.99)	35.56 (3.76)	37.73 (10.07)	41.86 (22.14)	44.58 (30.06)	44.44 (29.66)
Average	35.01	5.34	32.24 (-7.92)	34.14 (-2.5)	34.94 (-0.22)	35.17 (0.45)	35.14 (0.35)	35.01 (0.0)	5.38 (-84.64)	5.97 (-82.94)	7.46 (-78.7)	10.44 (-70.19)	13.73 (-60.8)	6.42 (-81.65)	16.27 (-53.52)	29.3 (-16.31)	34.88 (-0.37)	36.77 (5.01)	40.23 (14.91)	39.29 (12.21)	39.19 (11.93)

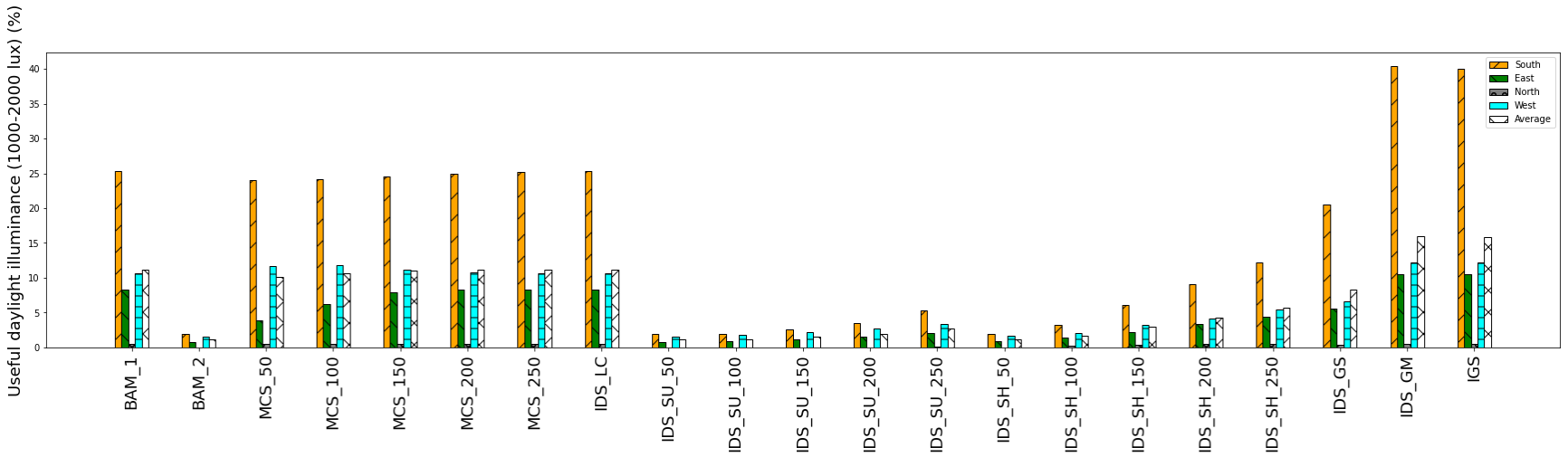

Figure 2-B.7 Useful Daylight Illuminance ($UDI_{1000\text{-}2000\ lux}$) between (8 am to 5 pm) for all control strategies by zone orientation

Table 2-B.7 Useful Daylight Illuminance ($UDI_{1000\text{-}2000\ lux}$) between (8 am to 5 pm) for all control strategies by zone orientation (values)

	BAM_1	BAM_2	MCS_50	MCS_100	MCS_150	MCS_200	MCS_250	IDS_LC	IDS_SU_50	IDS_SU_100	IDS_SU_150	IDS_SU_200	IDS_SU_250	IDS_SH_50	IDS_SH_100	IDS_SH_150	IDS_SH_200	IDS_SH_250	IDS_GS	IDS_GM	IGS
South	25.34	1.95	24.08 (-4.97)	24.14 (-4.76)	24.58 (-3.03)	24.99 (-1.41)	25.18 (-0.65)	25.34 (0.0)	1.95 (-92.32)	1.97 (-92.22)	2.52 (-90.05)	3.45 (-86.38)	5.34 (-78.92)	1.97 (-92.22)	3.18 (-87.46)	6.11 (-75.89)	9.07 (-64.22)	12.14 (-52.11)	20.49 (-19.14)	40.41 (59.46)	40.05 (58.05)
East	8.33	0.79	3.92 (-52.96)	6.19 (-25.66)	7.89 (-5.26)	8.33 (0.0)	8.33 (0.0)	8.33 (0.0)	0.79 (-90.46)	0.93 (-88.82)	1.1 (-86.84)	1.56 (-81.25)	2.05 (-75.33)	0.82 (-90.13)	1.4 (-83.22)	2.14 (-74.34)	3.32 (-60.2)	4.38 (-47.37)	5.53 (-33.55)	10.55 (26.64)	10.55 (26.64)
North	0.52	0.0	0.52 (0.0)	0.52 (0.0)	0.52 (0.0)	0.52 (0.0)	0.52 (0.0)	0.52 (0.0)	0.0 (-100.0)	0.0 (-100.0)	0.0 (-100.0)	0.0 (-100.0)	0.05 (-89.47)	0.0 (-100.0)	0.16 (-68.42)	0.38 (-26.32)	0.44 (-15.79)	0.52 (0.0)	0.41 (-21.05)	0.52 (0.0)	0.52 (0.0)
West	10.63	1.56	11.64 (9.54)	11.75 (10.57)	11.15 (4.9)	10.74 (1.03)	10.63 (0.0)	10.63 (0.0)	1.56 (-85.31)	1.81 (-82.99)	2.22 (-79.12)	2.71 (-74.48)	3.4 (-68.04)	1.64 (-84.54)	2.05 (-80.67)	3.15 (-70.36)	4.14 (-61.08)	5.45 (-48.71)	6.55 (-38.4)	12.22 (14.95)	12.16 (14.43)
Average	11.21	1.08	10.04 (-10.39)	10.65 (-4.95)	11.03 (-1.53)	11.14 (-0.55)	11.16 (-0.37)	11.21 (0.0)	1.08 (-90.4)	1.18 (-89.49)	1.46 (-86.98)	1.93 (-82.76)	2.71 (-75.79)	1.11 (-90.1)	1.7 (-84.84)	2.95 (-73.72)	4.24 (-62.16)	5.62 (-49.82)	8.25 (-26.41)	15.92 (42.11)	15.82 (41.2)

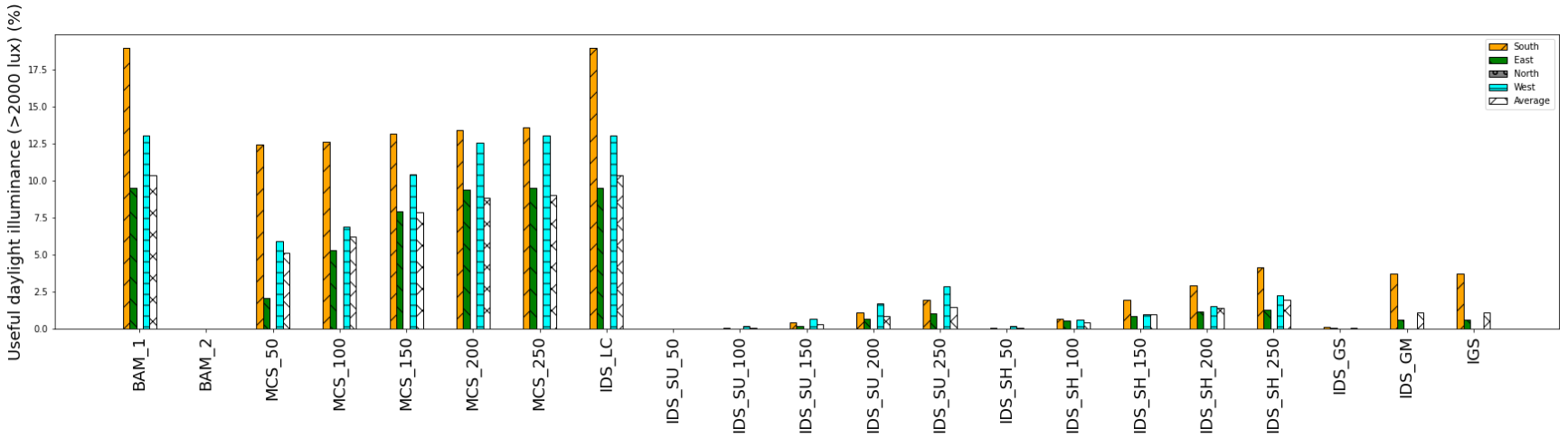

Figure 2-B.8 Useful Daylight Illuminance ($UDI_{>2000\ lux}$) between (8 am to 5 pm) for all control strategies by zone orientation

Table 2-B.8 Useful Daylight Illuminance ($UDI_{>2000\ lux}$) between (8 am to 5 pm) for all control strategies by zone orientation (values)

	BAM_1	BAM_2	MCS_50	MCS_100	MCS_150	MCS_200	MCS_250	IDS_LC	IDS_SU_50	IDS_SU_100	IDS_SU_150	IDS_SU_200	IDS_SU_250	IDS_SH_50	IDS_SH_100	IDS_SH_150	IDS_SH_200	IDS_SH_250	IDS_GS	IDS_GM	IGS
South	18.96	0.0	12.44 (-34.39)	12.63 (-33.38)	13.15 (-30.64)	13.42 (-29.19)	13.59 (-28.32)	18.96 (0.0)	0.0 (-100.0)	0.05 (-99.71)	0.41 (-97.83)	1.1 (-94.22)	1.92 (-89.88)	0.05 (-99.71)	0.63 (-96.68)	1.92 (-89.88)	2.93 (-84.54)	4.11 (-78.32)	0.08 (-99.57)	3.73 (-80.35)	3.73 (-80.35)
East	9.48	0.0	2.08 (-78.03)	5.29 (-44.22)	7.89 (-16.76)	9.4 (-0.87)	9.48 (0.0)	9.48 (0.0)	0.0 (-100.0)	0.0 (-100.0)	0.19 (-97.98)	0.63 (-93.35)	1.04 (-89.02)	0.0 (-100.0)	0.52 (-94.51)	0.85 (-91.04)	1.12 (-88.15)	1.26 (-86.71)	0.05 (-99.42)	0.6 (-93.64)	0.6 (-93.64)
North	0.0	0.0	0.0 (nan)	0.0 (nan)	0.0 (nan)	0.0 (nan)	0.0 (nan)	0.0 (nan)	0.0 (nan)	0.0 (nan)	0.0 (nan)	0.0 (nan)	0.0 (nan)	0.0 (nan)	0.0 (nan)	0.0 (nan)	0.0 (nan)	0.0 (nan)	0.0 (nan)	0.0 (nan)	0.0 (nan)
West	13.01	0.0	5.92 (-54.53)	6.88 (-47.16)	10.44 (-19.79)	12.58 (-3.37)	13.01 (0.0)	13.01 (0.0)	0.0 (-100.0)	0.14 (-98.95)	0.66 (-94.95)	1.67 (-87.16)	2.82 (-78.32)	0.14 (-98.95)	0.58 (-95.58)	0.96 (-92.63)	1.53 (-88.21)	2.25 (-82.74)	0.0 (-100.0)	0.0 (-100.0)	0.0 (-100.0)
Average	10.36	0.0	5.11 (-50.69)	6.2 (-40.19)	7.87 (-24.06)	8.85 (-14.61)	9.02 (-12.95)	10.36 (0.0)	0.0 (-100.0)	0.05 (-99.54)	0.32 (-96.96)	0.85 (-91.8)	1.45 (-86.05)	0.05 (-99.54)	0.43 (-95.84)	0.93 (-91.01)	1.4 (-86.52)	1.9 (-81.63)	0.03 (-99.67)	1.08 (-89.56)	1.08 (-89.56)

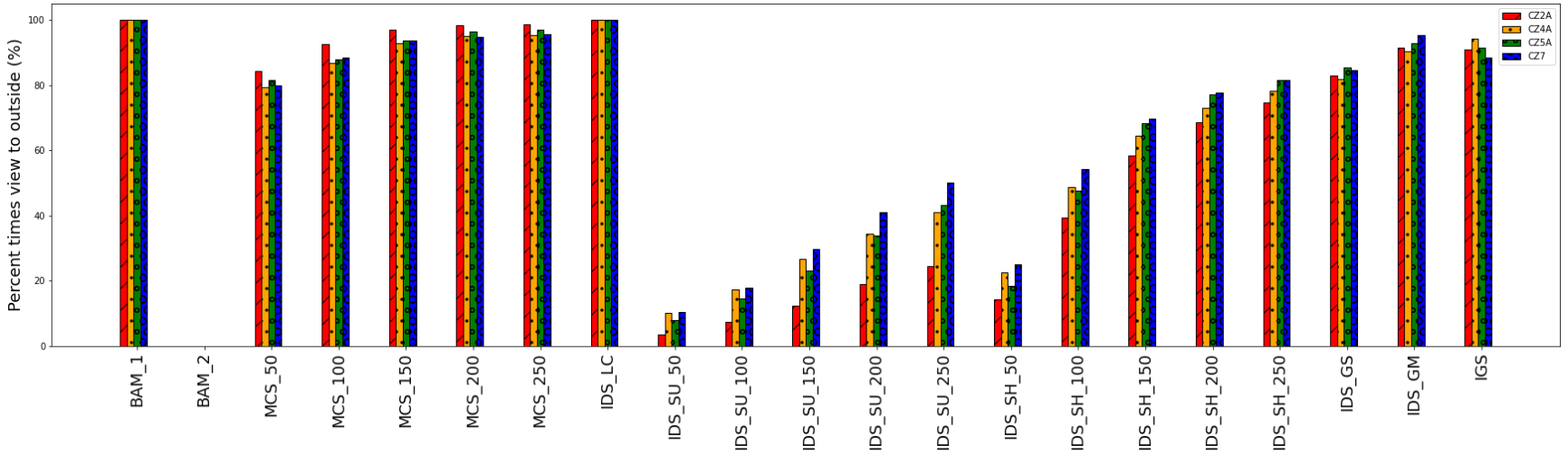

Figure 2-B.9 Annual percent of times view to the outside between (8 am to 5 pm) for all control strategies by climate zones

Table 2-B.9 Annual percent of times view to the outside between (8 am to 5 pm) for all control strategies by climate zones (values)

	BAM_1	BAM_2	MCS_50	MCS_100	MCS_150	MCS_200	MCS_250	IDS_LC	IDS_SU_50	IDS_SU_100	IDS_SU_150	IDS_SU_200	IDS_SU_250	IDS_SH_50	IDS_SH_100	IDS_SH_150	IDS_SH_200	IDS_SH_250	IDS_GS	IDS_GM	IGS
CZ2A	100.0	0.0	84.41 (-15.59)	92.65 (-7.35)	97.01 (-2.99)	98.53 (-1.47)	98.71 (-1.29)	100.0 (0.0)	3.56 (-96.44)	7.26 (-92.74)	12.36 (-87.64)	18.96 (-81.04)	24.41 (-75.59)	14.29 (-85.71)	39.49 (-60.51)	58.51 (-41.49)	68.73 (-31.27)	74.76 (-25.24)	83.03 (-16.97)	91.66 (-8.34)	91.1 (-8.9)
CZ4A	100.0	0.0	79.47 (-20.53)	86.88 (-13.12)	93.01 (-6.99)	95.05 (-4.95)	95.49 (-4.51)	100.0 (0.0)	10.16 (-89.84)	17.23 (-82.77)	26.68 (-73.32)	34.49 (-65.51)	41.07 (-58.93)	22.51 (-77.49)	48.65 (-51.35)	64.59 (-35.41)	73.05 (-26.95)	78.41 (-21.59)	81.8 (-18.2)	90.52 (-9.48)	94.3 (-5.7)
CZ5A	100.0	0.0	81.48 (-18.52)	87.93 (-12.07)	93.74 (-6.26)	96.52 (-3.48)	96.93 (-3.07)	100.0 (0.0)	7.89 (-92.11)	14.55 (-85.45)	23.07 (-76.93)	33.81 (-66.19)	43.1 (-56.9)	18.29 (-81.71)	47.51 (-52.49)	68.38 (-31.62)	77.18 (-22.82)	81.47 (-18.53)	85.53 (-14.47)	92.92 (-7.08)	91.64 (-8.36)
CZ7	100.0	0.0	79.95 (-20.05)	88.53 (-11.47)	93.85 (-6.15)	94.92 (-5.08)	95.64 (-4.36)	100.0 (0.0)	10.49 (-89.51)	17.78 (-82.22)	29.7 (-70.3)	41.15 (-58.85)	50.0 (-50.0)	25.03 (-74.97)	54.21 (-45.79)	69.79 (-30.21)	77.64 (-22.36)	81.64 (-18.36)	84.63 (-15.37)	95.26 (-4.74)	88.61 (-11.39)

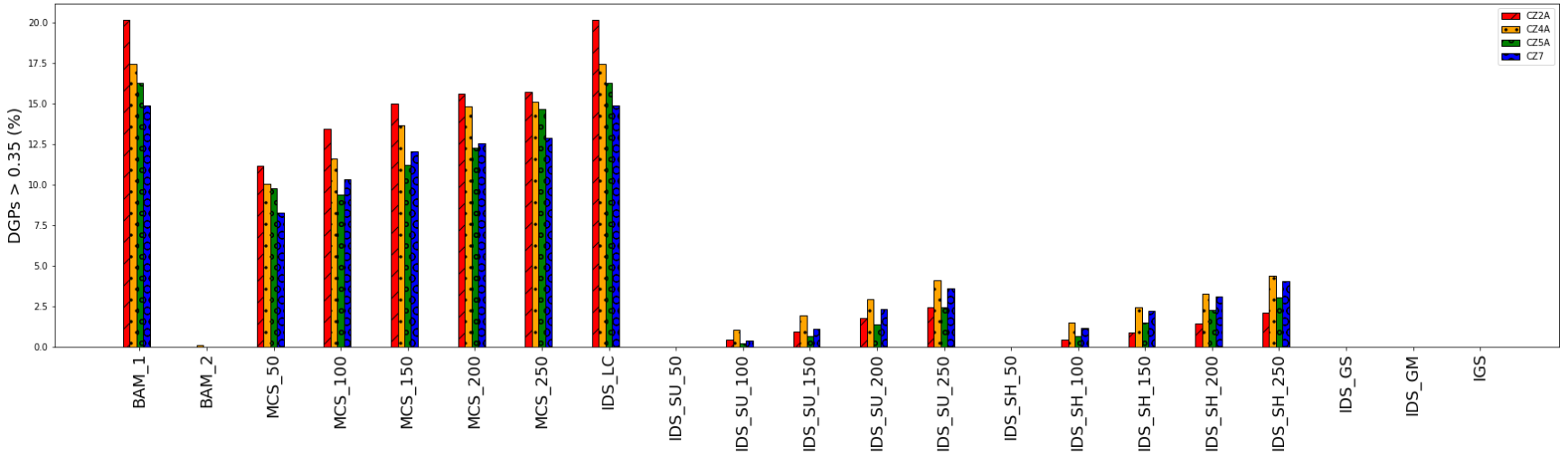

Figure 2-B.10 Annual percent of times glare (DGPs >0.35) between (8 am to 5 pm) for all control strategies by climate zones

Table 2-B.10 Annual percent of times glare (DGPs >0.35) between (8 am to 5 pm) for all control strategies by climate zones (values)

	BAM_1	BAM_2	MCS_50	MCS_100	MCS_150	MCS_200	MCS_250	IDS_LC	IDS_SU_50	IDS_SU_100	IDS_SU_150	IDS_SU_200	IDS_SU_250	IDS_SH_50	IDS_SH_100	IDS_SH_150	IDS_SH_200	IDS_SH_250	IDS_GS	IDS_GM	IGS
CZ2A	20.14	0.0	11.13 (-44.73)	13.42 (-33.33)	15.01 (-25.48)	15.62 (-22.45)	15.73 (-21.87)	20.14 (0.0)	0.0 (-100.0)	0.42 (-97.89)	0.91 (-95.48)	1.74 (-91.36)	2.44 (-87.89)	0.0 (-100.0)	0.44 (-97.82)	0.88 (-95.65)	1.41 (-92.99)	2.07 (-89.73)	0.0 (-100.0)	0.0 (-100.0)	0.0 (-100.0)
CZ4A	17.42	0.09	10.06 (-42.23)	11.59 (-33.46)	13.68 (-21.47)	14.81 (-14.98)	15.12 (-13.21)	17.42 (0.0)	0.0 (-100.0)	1.01 (-94.18)	1.91 (-89.03)	2.95 (-83.05)	4.08 (-76.6)	0.0 (-100.0)	1.48 (-91.51)	2.4 (-86.2)	3.29 (-81.12)	4.4 (-74.75)	0.0 (-100.0)	0.0 (-100.0)	0.0 (-100.0)
CZ5A	16.26	0.0	9.77 (-39.89)	9.36 (-42.46)	11.19 (-31.17)	12.27 (-24.52)	14.68 (-9.73)	16.26 (0.0)	0.0 (-100.0)	0.21 (-98.74)	0.65 (-96.0)	1.39 (-91.45)	2.44 (-85.0)	0.0 (-100.0)	0.65 (-96.0)	1.47 (-90.94)	2.27 (-86.06)	3.03 (-81.34)	0.0 (-100.0)	0.0 (-100.0)	0.0 (-100.0)
CZ7	14.88	0.0	8.27 (-44.45)	10.34 (-30.56)	12.05 (-19.01)	12.56 (-15.6)	12.86 (-13.62)	14.88 (0.0)	0.0 (-100.0)	0.37 (-97.51)	1.1 (-92.64)	2.34 (-84.26)	3.61 (-75.75)	0.0 (-100.0)	1.16 (-92.18)	2.18 (-85.37)	3.12 (-79.06)	4.05 (-72.76)	0.0 (-100.0)	0.0 (-100.0)	0.0 (-100.0)

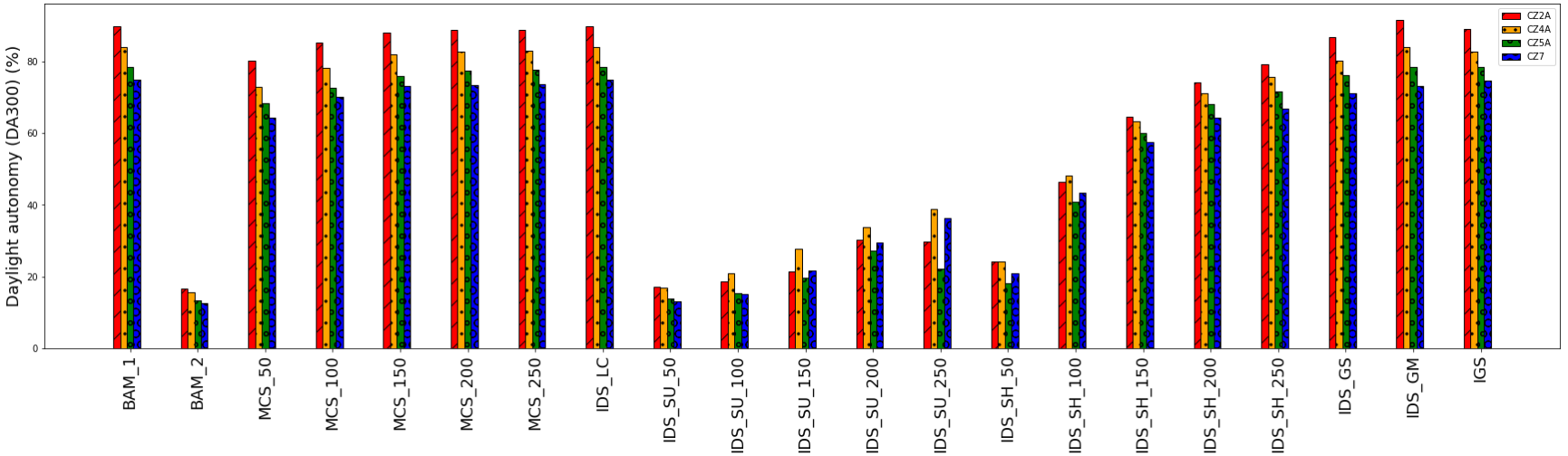

Figure 2-B.11 Daylight Autonomy (DA) between (8 am to 5 pm) for all control strategies by climate zones

Table 2-B.11 Daylight Autonomy (DA) between (8 am to 5 pm) for all control strategies by climate zones (values)

	BAM_1	BAM_2	MCS_50	MCS_100	MCS_150	MCS_200	MCS_250	IDS_LC	IDS_SU_50	IDS_SU_100	IDS_SU_150	IDS_SU_200	IDS_SU_250	IDS_SH_50	IDS_SH_100	IDS_SH_150	IDS_SH_200	IDS_SH_250	IDS_GS	IDS_GM	IGS
CZ2A	89.84	16.53	80.23 (-10.69)	85.47 (-4.86)	88.05 (-1.98)	88.93 (-1.01)	88.99 (-0.95)	89.84 (0.0)	17.21 (-80.84)	18.64 (-79.25)	21.39 (-76.19)	30.15 (-66.44)	29.71 (-66.93)	24.17 (-73.09)	46.51 (-48.23)	64.66 (-28.03)	74.18 (-17.42)	79.42 (-11.6)	86.86 (-3.31)	91.64 (2.01)	89.25 (-0.65)
CZ4A	84.12	15.7	72.95 (-13.29)	78.37 (-6.84)	82.17 (-2.32)	82.99 (-1.35)	83.09 (-1.23)	84.12 (0.0)	16.97 (-79.83)	20.89 (-75.17)	27.8 (-66.95)	33.88 (-59.73)	38.9 (-53.75)	24.11 (-71.34)	48.13 (-42.79)	63.36 (-24.68)	71.22 (-15.34)	75.73 (-9.98)	80.3 (-4.54)	84.1 (-0.02)	82.89 (-1.47)
CZ5A	78.67	13.45	68.37 (-13.09)	72.84 (-7.42)	76.12 (-3.24)	77.62 (-1.34)	77.79 (-1.12)	78.67 (0.0)	13.78 (-82.48)	15.41 (-80.41)	19.77 (-74.87)	27.3 (-65.3)	22.12 (-71.88)	18.0 (-77.12)	40.98 (-47.91)	60.1 (-23.61)	68.15 (-13.37)	71.73 (-8.82)	76.19 (-3.15)	78.67 (0.0)	78.55 (-0.16)
CZ7	75.03	12.56	64.29 (-14.31)	70.2 (-6.44)	73.14 (-2.52)	73.5 (-2.04)	73.77 (-1.68)	75.03 (0.0)	13.03 (-82.63)	15.21 (-79.73)	21.75 (-71.01)	29.62 (-60.52)	36.42 (-51.45)	20.92 (-72.12)	43.34 (-42.23)	57.46 (-23.42)	64.37 (-14.2)	67.0 (-10.7)	71.18 (-5.12)	73.21 (-2.43)	74.82 (-0.27)

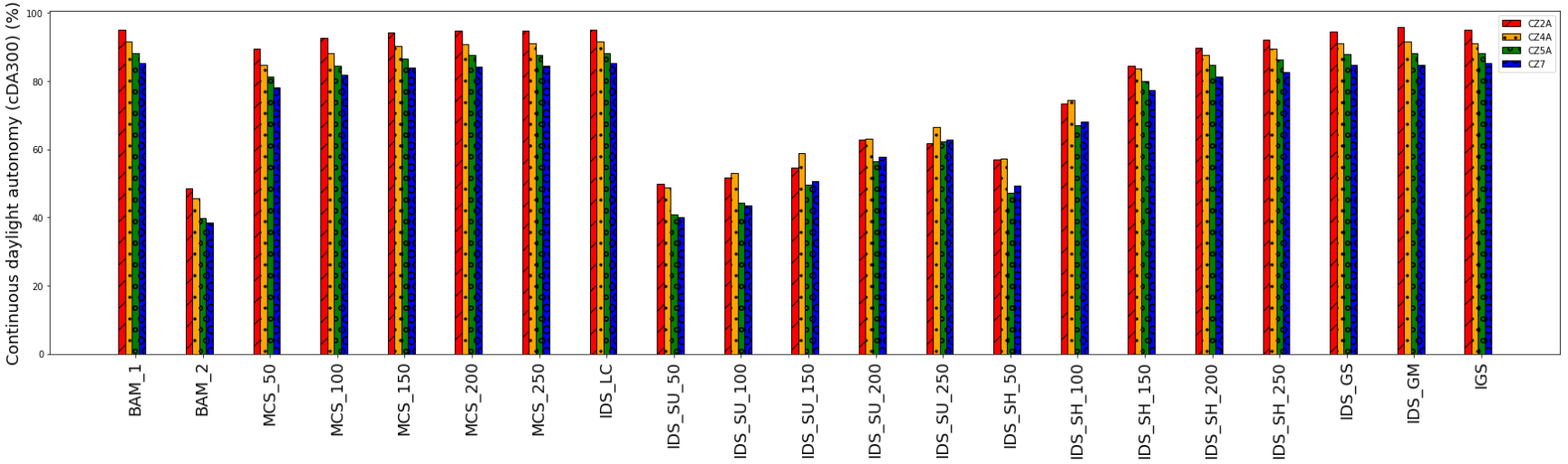

Figure 2-B.12 Continuous Daylight Autonomy (cDA) between (8 am to 5 pm) for all control strategies by zone orientation

Table 2-B.12 Continuous Daylight Autonomy (cDA) between (8 am to 5 pm) for all control strategies by zone orientation (values)

	BAM_1	BAM_2	MCS_50	MCS_100	MCS_150	MCS_200	MCS_250	IDS_LC	IDS_SU_50	IDS_SU_100	IDS_SU_150	IDS_SU_200	IDS_SU_250	IDS_SH_50	IDS_SH_100	IDS_SH_150	IDS_SH_200	IDS_SH_250	IDS_GS	IDS_GM	IGS
CZ2A	95.07	48.46	89.47 (-5.89)	92.64 (-2.56)	94.15 (-0.98)	94.67 (-0.43)	94.7 (-0.39)	95.07 (0.0)	49.83 (-47.59)	51.82 (-45.5)	54.74 (-42.43)	62.9 (-33.84)	61.64 (-35.16)	57.01 (-40.03)	73.47 (-22.72)	84.54 (-11.08)	89.67 (-5.68)	92.04 (-3.19)	94.58 (-0.52)	95.77 (0.73)	94.92 (-0.16)
CZ4A	91.65	45.7	84.81 (-7.46)	88.12 (-3.85)	90.37 (-1.39)	90.91 (-0.8)	90.97 (-0.74)	91.65 (0.0)	48.7 (-46.86)	53.0 (-42.17)	58.78 (-35.87)	63.14 (-31.1)	66.61 (-27.32)	57.33 (-37.45)	74.56 (-18.65)	83.68 (-8.69)	87.77 (-4.23)	89.58 (-2.25)	90.97 (-0.74)	91.65 (-0.0)	91.2 (-0.49)
CZ5A	88.27	39.88	81.31 (-7.88)	84.36 (-4.42)	86.6 (-1.89)	87.59 (-0.77)	87.71 (-0.63)	88.27 (0.0)	40.97 (-53.58)	44.22 (-49.91)	49.48 (-43.94)	56.57 (-35.92)	62.32 (-29.4)	47.35 (-46.36)	67.01 (-24.08)	79.97 (-9.4)	84.65 (-4.1)	86.25 (-2.28)	87.86 (-0.46)	88.27 (0.0)	88.19 (-0.09)
CZ7	85.33	38.59	78.08 (-8.5)	81.9 (-4.02)	84.0 (-1.56)	84.3 (-1.21)	84.5 (-0.98)	85.33 (0.0)	40.11 (-53.0)	43.61 (-48.9)	50.71 (-40.58)	57.67 (-32.42)	62.79 (-26.41)	49.44 (-42.06)	68.17 (-20.11)	77.4 (-9.3)	81.27 (-4.76)	82.65 (-3.15)	84.61 (-0.84)	84.76 (-0.67)	85.23 (-0.12)

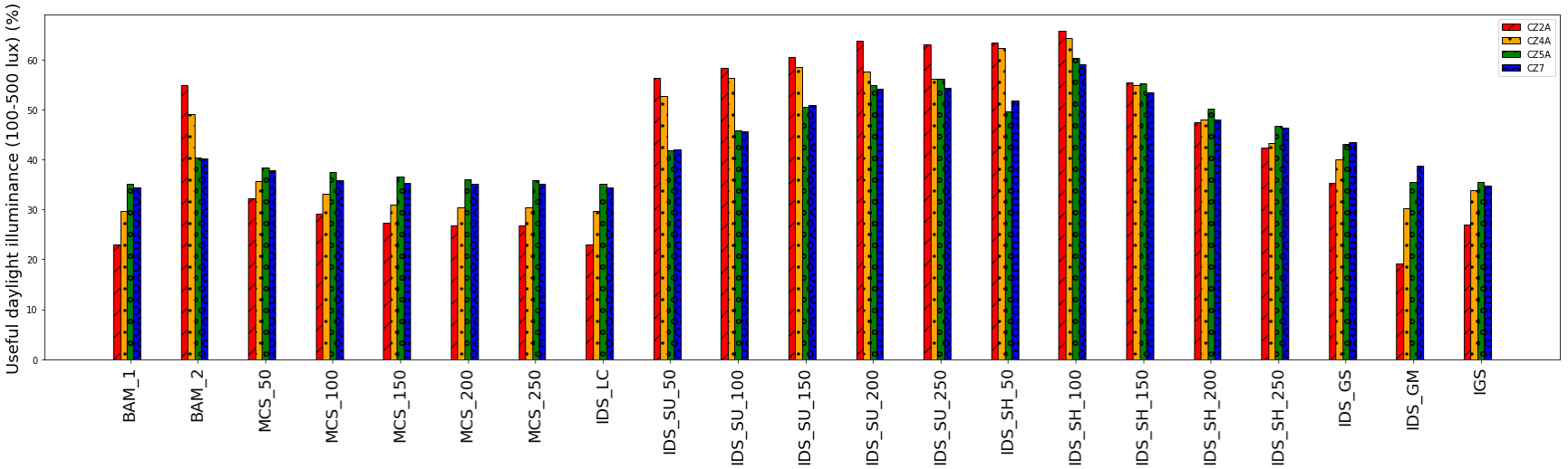

Figure 2-B.13 Useful Daylight Illuminance ($UDI_{100\text{-}500\ lux}$) between (8 am to 5 pm) for all control strategies by climate zones

Table 2-B.13 Useful Daylight Illuminance ($UDI_{100\text{-}500\ lux}$) between (8 am to 5 pm) for all control strategies by climate zones (values)

	BAM_1	BAM_2	MCS_50	MCS_100	MCS_150	MCS_200	MCS_250	IDS_LC	IDS_SU_50	IDS_SU_100	IDS_SU_150	IDS_SU_200	IDS_SU_250	IDS_SH_50	IDS_SH_100	IDS_SH_150	IDS_SH_200	IDS_SH_250	IDS_GS	IDS_GM	IGS
CZ2A	22.94	54.82	32.14 (40.13)	29.18 (27.23)	27.32 (19.11)	26.77 (16.72)	26.73 (16.51)	22.94 (0.0)	56.32 (145.51)	58.27 (154.02)	60.54 (163.93)	63.78 (178.05)	63.0 (174.65)	63.36 (176.23)	65.68 (186.35)	55.34 (141.27)	47.34 (106.39)	42.41 (84.89)	35.34 (54.08)	19.08 (-16.81)	26.97 (17.56)
CZ4A	29.72	49.09	35.68 (20.05)	33.09 (11.34)	31.01 (4.36)	30.47 (2.54)	30.36 (2.17)	29.72 (0.0)	52.62 (77.05)	56.26 (89.31)	58.45 (96.68)	57.53 (93.59)	56.14 (88.89)	62.3 (109.63)	64.25 (116.18)	54.88 (84.67)	48.05 (61.7)	43.31 (45.72)	39.99 (34.55)	30.26 (1.82)	33.75 (13.55)
CZ5A	35.07	40.43	38.45 (9.63)	37.45 (6.8)	36.47 (4.0)	35.92 (2.44)	35.86 (2.27)	35.07 (0.0)	41.82 (19.26)	45.78 (30.55)	50.55 (44.16)	54.77 (56.19)	56.14 (60.08)	49.55 (41.29)	60.21 (71.7)	55.21 (57.44)	50.19 (43.13)	46.79 (33.42)	43.16 (23.07)	35.38 (0.88)	35.55 (1.37)
CZ7	34.34	40.23	37.88 (10.29)	35.79 (4.21)	35.25 (2.63)	35.19 (2.47)	35.14 (2.31)	34.34 (0.0)	41.95 (22.14)	45.66 (32.97)	50.88 (48.17)	54.05 (57.38)	54.23 (57.9)	51.76 (50.72)	58.96 (71.68)	53.4 (55.5)	47.99 (39.73)	46.27 (34.74)	43.39 (26.35)	38.78 (12.92)	34.77 (1.24)

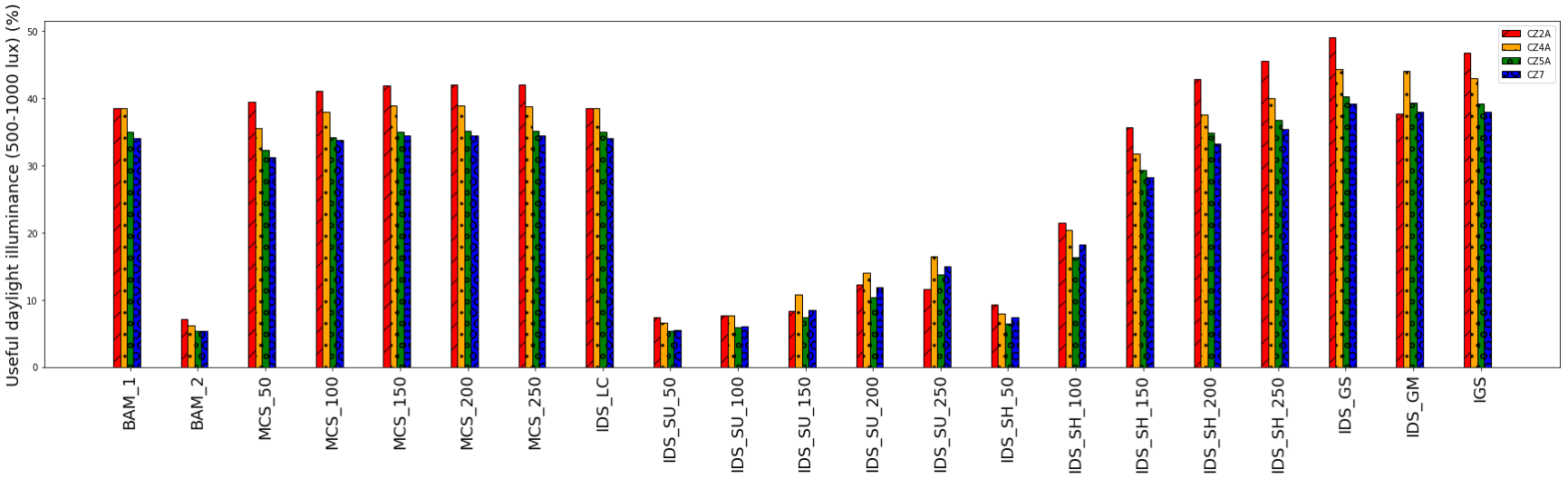

Figure 2-B.14 Useful Daylight Illuminance ($UDI_{500\text{-}1000\ lux}$) between (8 am to 5 pm) for all control strategies by climate zones

Table 2-B.14 Useful Daylight Illuminance ($UDI_{500\text{-}1000\ lux}$) between (8 am to 5 pm) for all control strategies by climate zones (values)

	BAM_1	BAM_2	MCS_50	MCS_100	MCS_150	MCS_200	MCS_250	IDS_LC	IDS_SU_50	IDS_SU_100	IDS_SU_150	IDS_SU_200	IDS_SU_250	IDS_SH_50	IDS_SH_100	IDS_SH_150	IDS_SH_200	IDS_SH_250	IDS_GS	IDS_GM	IGS
CZ2A	38.46	7.15	39.43 (2.53)	41.14 (6.96)	41.87 (8.87)	42.03 (9.3)	41.99 (9.19)	38.46 (0.0)	7.4 (-80.77)	7.69 (-80.0)	8.41 (-78.13)	12.25 (-68.16)	11.64 (-69.74)	9.29 (-75.85)	21.49 (-44.11)	35.62 (-7.37)	42.84 (11.4)	45.51 (18.34)	49.04 (27.52)	37.73 (-1.91)	46.84 (21.78)
CZ4A	38.46	6.21	35.55 (-7.57)	37.92 (-1.39)	38.99 (1.39)	38.95 (1.28)	38.82 (0.93)	38.46 (0.0)	6.6 (-82.85)	7.71 (-79.95)	10.73 (-72.11)	14.05 (-63.46)	16.43 (-57.28)	7.92 (-79.41)	20.4 (-46.96)	31.73 (-17.49)	37.53 (-2.4)	39.97 (3.94)	44.38 (15.39)	44.09 (14.64)	42.94 (11.65)
CZ5A	35.01	5.34	32.24 (-7.92)	34.14 (-2.5)	34.94 (-0.22)	35.17 (0.45)	35.14 (0.35)	35.01 (0.0)	5.38 (-84.64)	5.97 (-82.94)	7.46 (-78.7)	10.44 (-70.19)	13.73 (-60.8)	6.42 (-81.65)	16.27 (-53.52)	29.3 (-16.31)	34.88 (-0.37)	36.77 (5.01)	40.23 (14.91)	39.29 (12.21)	39.19 (11.93)
CZ7	34.11	5.33	31.23 (-8.45)	33.82 (-0.86)	34.52 (1.2)	34.41 (0.88)	34.4 (0.86)	34.11 (0.0)	5.49 (-83.9)	6.1 (-82.11)	8.53 (-75.0)	11.9 (-65.1)	15.04 (-55.9)	7.44 (-78.19)	18.24 (-46.53)	28.26 (-17.15)	33.2 (-2.67)	35.45 (3.94)	39.18 (14.88)	37.97 (11.31)	37.99 (11.39)

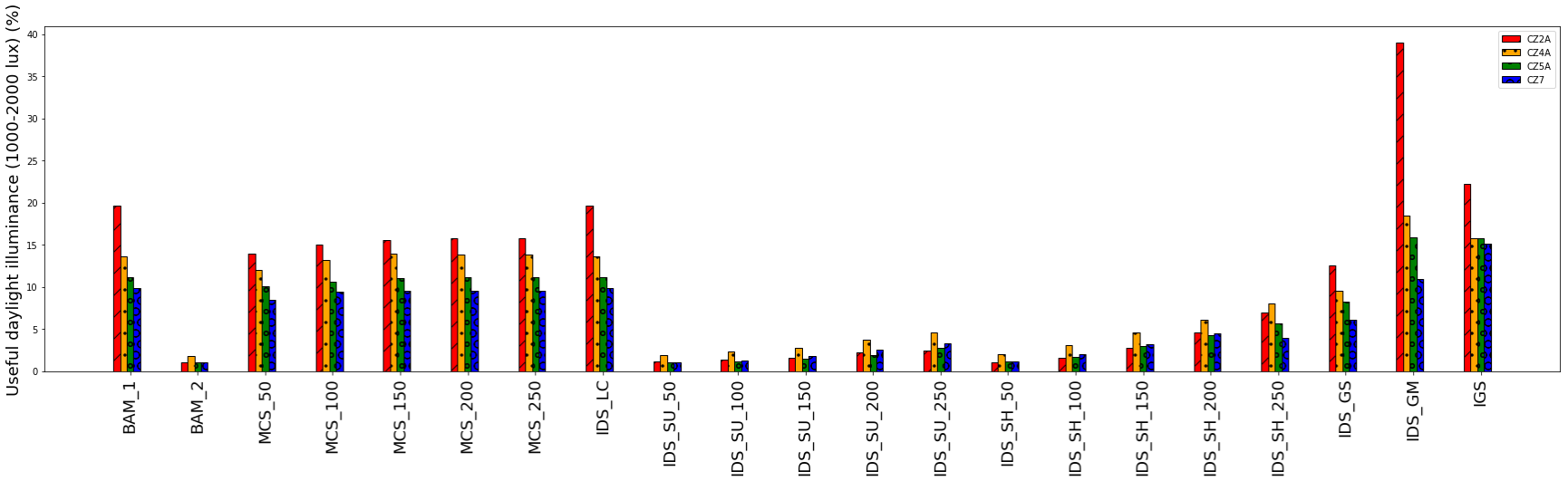

Figure 2-B.15 Useful Daylight Illuminance ($UDI_{1000\text{-}2000\ lux}$) between (8 am to 5 pm) for all control strategies by climate zones

Table 2-B.15 Useful Daylight Illuminance ($UDI_{1000\text{-}2000\ lux}$) between (8 am to 5 pm) for all control strategies by climate zones (values)

	BAM_1	BAM_2	MCS_50	MCS_100	MCS_150	MCS_200	MCS_250	IDS_LC	IDS_SU_50	IDS_SU_100	IDS_SU_150	IDS_SU_200	IDS_SU_250	IDS_SH_50	IDS_SH_100	IDS_SH_150	IDS_SH_200	IDS_SH_250	IDS_GS	IDS_GM	IGS
CZ2A	19.62	1.01	13.92 (-29.02)	15.05 (-23.25)	15.6 (-20.46)	15.78 (-19.55)	15.8 (-19.45)	19.62 (0.0)	1.1 (-94.38)	1.34 (-93.19)	1.6 (-91.83)	2.21 (-88.76)	2.48 (-87.36)	1.08 (-94.52)	1.59 (-91.9)	2.79 (-85.79)	4.58 (-76.68)	6.93 (-64.66)	12.55 (-36.03)	39.0 (98.81)	22.19 (13.13)
CZ4A	13.68	1.77	12.01 (-12.21)	13.23 (-3.3)	13.91 (1.65)	13.85 (1.2)	13.88 (1.4)	13.68 (0.0)	1.92 (-85.94)	2.28 (-83.33)	2.78 (-79.68)	3.68 (-73.12)	4.64 (-66.07)	1.99 (-85.49)	3.05 (-77.68)	4.63 (-66.17)	6.11 (-55.36)	8.06 (-41.09)	9.54 (-30.28)	18.46 (34.88)	15.76 (15.17)
CZ5A	11.21	1.08	10.04 (-10.39)	10.65 (-4.95)	11.03 (-1.53)	11.14 (-0.55)	11.16 (-0.37)	11.21 (0.0)	1.08 (-90.4)	1.18 (-89.49)	1.46 (-86.98)	1.93 (-82.76)	2.71 (-75.79)	1.11 (-90.1)	1.7 (-84.84)	2.95 (-73.72)	4.24 (-62.16)	5.62 (-49.82)	8.25 (-26.41)	15.92 (42.11)	15.82 (41.2)
CZ7	9.85	1.03	8.47 (-14.05)	9.38 (-4.73)	9.58 (-2.71)	9.55 (-3.06)	9.58 (-2.78)	9.85 (0.0)	1.08 (-89.01)	1.27 (-87.13)	1.78 (-81.92)	2.53 (-74.27)	3.28 (-66.69)	1.14 (-88.46)	2.03 (-79.42)	3.23 (-67.18)	4.44 (-54.94)	3.95 (-59.94)	6.11 (-37.97)	10.9 (10.64)	15.14 (53.69)

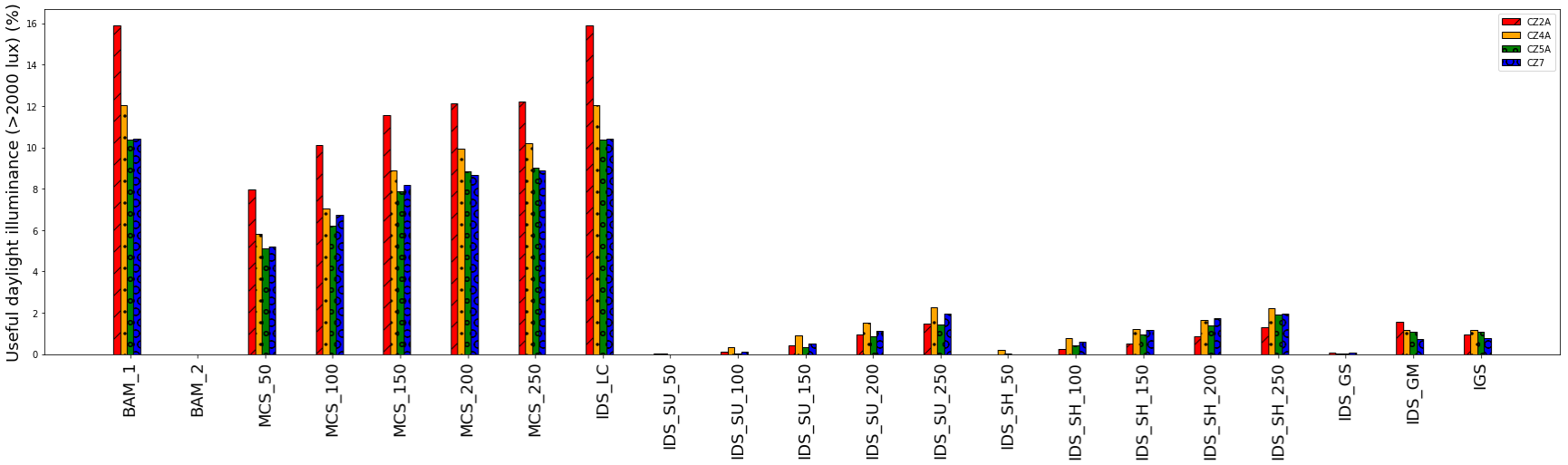

Figure 2-B.16 Useful Daylight Illuminance ($UDI_{>2000\ lux}$) between (8 am to 5 pm) for all control strategies by climate zones

Table 2-B.16 Useful Daylight Illuminance ($UDI_{>2000\ lux}$) between (8 am to 5 pm) for all control strategies by climate zones (values)

	BAM_1	BAM_2	MCS_50	MCS_100	MCS_150	MCS_200	MCS_250	IDS_LC	IDS_SU_50	IDS_SU_100	IDS_SU_150	IDS_SU_200	IDS_SU_250	IDS_SH_50	IDS_SH_100	IDS_SH_150	IDS_SH_200	IDS_SH_250	IDS_GS	IDS_GM	IGS
CZ2A	15.89	0.0	7.96 (-49.91)	10.12 (-36.34)	11.58 (-27.16)	12.12 (-23.75)	12.21 (-23.15)	15.89 (0.0)	0.01 (-99.91)	0.14 (-99.14)	0.4 (-97.46)	0.93 (-94.14)	1.49 (-90.65)	0.0 (-100.0)	0.26 (-98.36)	0.53 (-96.68)	0.84 (-94.7)	1.29 (-91.85)	0.07 (-99.57)	1.58 (-90.04)	0.97 (-93.92)
CZ4A	12.05	0.0	5.84 (-51.59)	7.06 (-41.42)	8.88 (-26.31)	9.95 (-17.5)	10.2 (-15.4)	12.05 (0.0)	0.01 (-99.89)	0.32 (-97.39)	0.89 (-92.61)	1.51 (-87.5)	2.25 (-81.36)	0.19 (-98.41)	0.76 (-93.69)	1.23 (-89.83)	1.65 (-86.31)	2.21 (-81.7)	0.04 (-99.66)	1.15 (-90.45)	1.15 (-90.45)
CZ5A	10.36	0.0	5.11 (-50.69)	6.2 (-40.19)	7.87 (-24.06)	8.85 (-14.61)	9.02 (-12.95)	10.36 (0.0)	0.0 (-100.0)	0.05 (-99.54)	0.32 (-96.96)	0.85 (-91.8)	1.45 (-86.05)	0.05 (-99.54)	0.43 (-95.84)	0.93 (-91.01)	1.4 (-86.52)	1.9 (-81.63)	0.03 (-99.67)	1.08 (-89.56)	1.08 (-89.56)
CZ7	10.43	0.0	5.22 (-49.97)	6.73 (-35.52)	8.2 (-21.41)	8.66 (-16.94)	8.89 (-14.77)	10.43 (0.0)	0.0 (-100.0)	0.12 (-98.88)	0.52 (-95.01)	1.14 (-89.03)	1.97 (-81.09)	0.0 (-100.0)	0.61 (-94.16)	1.17 (-88.77)	1.73 (-83.45)	1.96 (-81.22)	0.05 (-99.47)	0.75 (-92.84)	0.77 (-92.58)

APPENDIX 2-C: ENERGY USE RESULTS

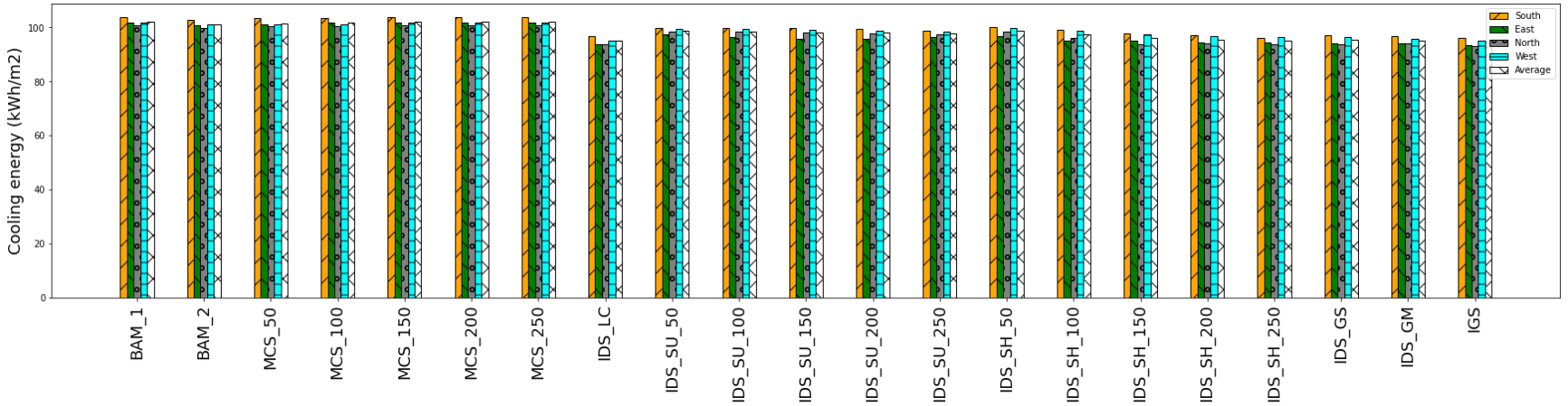

Figure 2-C.1 Comparison of annual cooling EUI by zone orientation

Table 2-C.1 Comparison of annual cooling EUI by zone orientation (values)

	BAM_1	BAM_2	MCS_50	MCS_100	MCS_150	MCS_200	MCS_250	IDS_LC	IDS_SU_50	IDS_SU_100	IDS_SU_150	IDS_SU_200	IDS_SU_250	IDS_SH_50	IDS_SH_100	IDS_SH_150	IDS_SH_200	IDS_SH_250	IDS_GS	IDS_GM	IGS
South	103.61	102.65	103.3 (-0.3)	103.38 (-0.22)	103.54 (-0.07)	103.61 (0.0)	103.61 (0.0)	96.78 (-6.59)	99.78 (-3.7)	99.67 (-3.8)	99.48 (-3.99)	99.17 (-4.29)	98.58 (-4.85)	99.92 (-3.56)	99.05 (-4.4)	97.7 (-5.7)	96.87 (-6.51)	95.93 (-7.41)	97.01 (-6.37)	96.6 (-6.77)	96.02 (-7.33)
East	101.64	100.59	100.8 (-0.83)	101.57 (-0.07)	101.58 (-0.06)	101.62 (-0.02)	101.63 (-0.01)	93.65 (-7.86)	97.33 (-4.24)	96.45 (-5.11)	95.74 (-5.8)	95.58 (-5.96)	96.26 (-5.29)	96.76 (-4.8)	94.91 (-6.62)	95.07 (-6.46)	94.35 (-7.17)	94.19 (-7.33)	94.03 (-7.49)	93.88 (-7.63)	93.32 (-8.19)
North	100.65	99.56	100.3 (-0.35)	100.41 (-0.24)	100.58 (-0.07)	100.64 (-0.01)	100.65 (0.0)	93.75 (-6.86)	98.33 (-2.31)	98.25 (-2.38)	98.07 (-2.56)	97.76 (-2.87)	97.14 (-3.49)	98.34 (-2.3)	95.96 (-4.66)	93.51 (-7.09)	93.91 (-6.7)	93.68 (-6.92)	93.7 (-6.91)	93.79 (-6.82)	92.95 (-7.65)
West	101.67	101.11	100.97 (-0.69)	100.94 (-0.72)	101.79 (0.12)	101.68 (0.01)	101.67 (0.0)	95.1 (-6.46)	99.3 (-2.33)	99.16 (-2.47)	98.99 (-2.64)	98.77 (-2.85)	98.33 (-3.29)	99.64 (-2.0)	98.6 (-3.02)	97.19 (-4.41)	96.6 (-4.99)	96.2 (-5.38)	96.23 (-5.35)	95.47 (-6.1)	94.98 (-6.58)
Average	101.89	100.98	101.34 (-0.54)	101.58 (-0.31)	101.87 (-0.02)	101.89 (-0.0)	101.89 (-0.0)	94.82 (-6.94)	98.68 (-3.15)	98.38 (-3.44)	98.07 (-3.75)	97.82 (-4.0)	97.58 (-4.23)	98.66 (-3.17)	97.13 (-4.67)	95.87 (-5.91)	95.43 (-6.34)	95.0 (-6.76)	95.24 (-6.53)	94.94 (-6.83)	94.32 (-7.43)

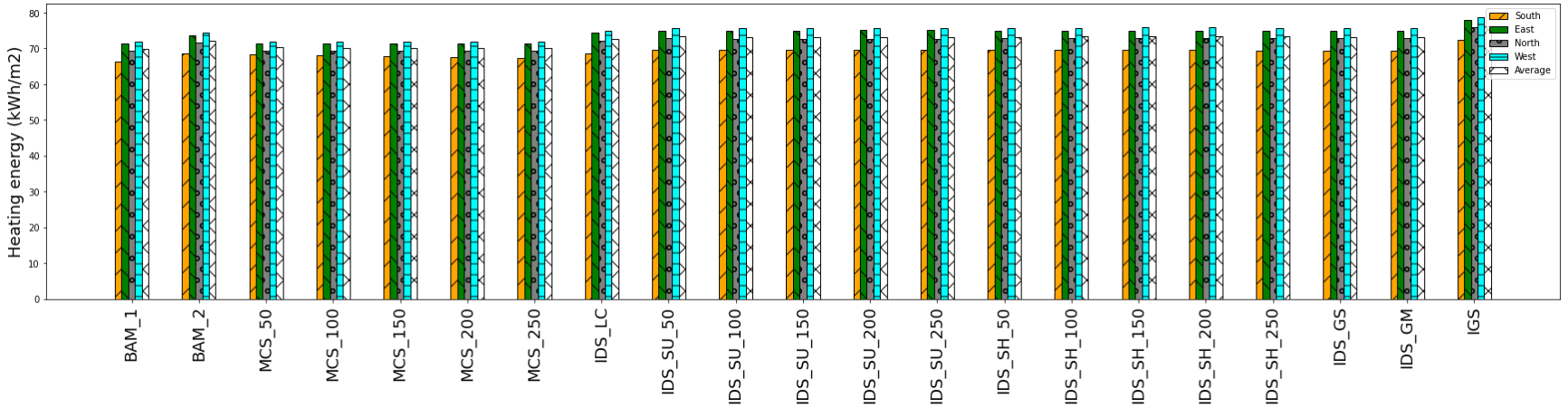

Figure 2-C.2 Comparison of annual heating EUI by zone orientation

Table 2-C.2 Comparison of annual heating EUI by zone orientation (values)

	BAM_1	BAM_2	MCS_50	MCS_100	MCS_150	MCS_200	MCS_250	IDS_LC	IDS_SU_50	IDS_SU_100	IDS_SU_150	IDS_SU_200	IDS_SU_250	IDS_SH_50	IDS_SH_100	IDS_SH_150	IDS_SH_200	IDS_SH_250	IDS_GS	IDS_GM	IGS
South	66.3	68.52	68.26 (2.96)	68.11 (2.73)	67.75 (2.19)	67.52 (1.84)	67.42 (1.69)	68.67 (3.57)	69.63 (5.02)	69.58 (4.95)	69.55 (4.9)	69.52 (4.86)	69.5 (4.83)	69.48 (4.8)	69.47 (4.78)	69.47 (4.78)	69.48 (4.8)	69.46 (4.77)	69.46 (4.77)	69.38 (4.65)	72.27 (9.0)
East	71.44	73.63	71.41 (-0.04)	71.4 (-0.06)	71.44 (0.0)	71.43 (-0.01)	71.44 (0.0)	74.3 (4.0)	74.97 (4.94)	75.0 (4.98)	75.03 (5.03)	75.04 (5.04)	75.06 (5.07)	74.88 (4.82)	74.93 (4.89)	74.99 (4.97)	74.99 (4.97)	75.0 (4.98)	75.0 (4.98)	74.99 (4.97)	77.95 (9.11)
North	69.42	71.66	69.36 (-0.09)	69.38 (-0.06)	69.4 (-0.03)	69.42 (0.0)	69.42 (0.0)	72.21 (4.02)	72.79 (4.85)	72.75 (4.8)	72.73 (4.77)	72.73 (4.77)	72.73 (4.77)	72.8 (4.87)	72.91 (5.03)	72.94 (5.07)	72.95 (5.08)	72.93 (5.06)	72.87 (4.97)	72.84 (4.93)	75.92 (9.36)
West	71.8	74.38	71.95 (0.21)	71.83 (0.04)	71.8 (0.0)	71.75 (-0.07)	71.75 (-0.07)	74.84 (4.23)	75.79 (5.56)	75.72 (5.46)	75.67 (5.39)	75.64 (5.35)	75.6 (5.29)	75.68 (5.4)	75.78 (5.54)	75.81 (5.58)	75.82 (5.6)	75.79 (5.56)	75.71 (5.45)	75.63 (5.33)	78.7 (9.61)
Average	69.74	72.05	70.24 (0.72)	70.18 (0.63)	70.1 (0.51)	70.03 (0.42)	70.01 (0.38)	72.5 (3.96)	73.3 (5.1)	73.26 (5.05)	73.24 (5.03)	73.23 (5.01)	73.22 (4.99)	73.21 (4.98)	73.27 (5.07)	73.3 (5.11)	73.31 (5.12)	73.3 (5.1)	73.26 (5.05)	73.21 (4.98)	76.21 (9.28)

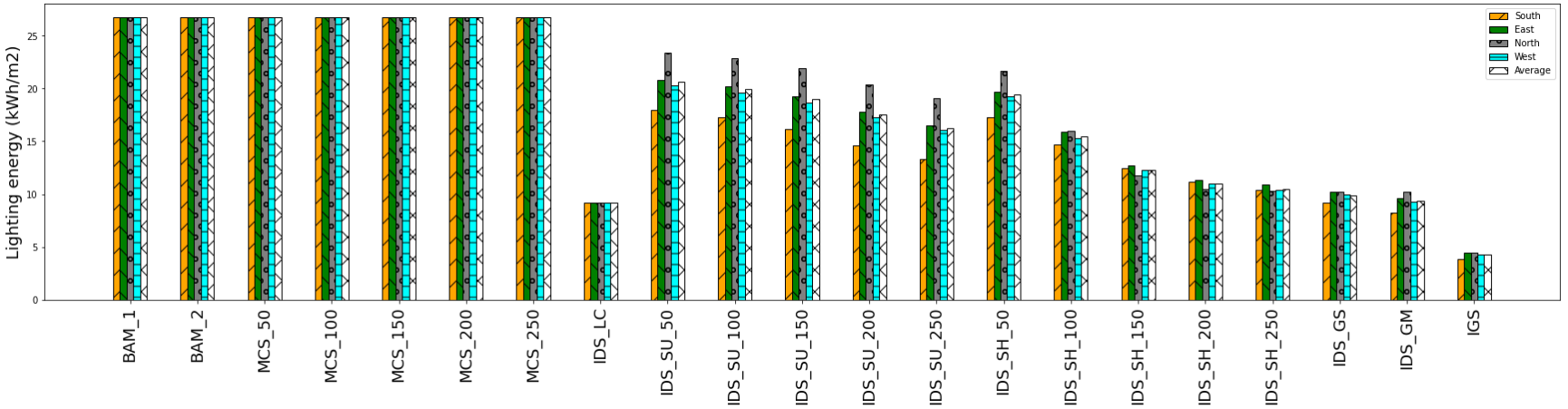

Figure 2-C.3 Comparison of annual lighting EUI by zone orientation

Table 2-C.3 Comparison of annual lighting EUI by zone orientation (values)

	BAM_1	BAM_2	MCS_50	MCS_100	MCS_150	MCS_200	MCS_250	IDS_LC	IDS_SU_50	IDS_SU_100	IDS_SU_150	IDS_SU_200	IDS_SU_250	IDS_SH_50	IDS_SH_100	IDS_SH_150	IDS_SH_200	IDS_SH_250	IDS_GS	IDS_GM	IGS
South	26.75	26.75	26.75 (0.0)	26.75 (0.0)	26.75 (0.0)	26.75 (0.0)	26.75 (0.0)	9.2 (-65.61)	17.97 (-32.82)	17.27 (-35.44)	16.19 (-39.48)	14.63 (-45.31)	13.36 (-50.06)	17.3 (-35.33)	14.68 (-45.12)	12.43 (-53.53)	11.2 (-58.13)	10.39 (-61.16)	9.15 (-65.79)	8.27 (-69.08)	3.89 (-85.46)
East	26.75	26.75	26.75 (0.0)	26.75 (0.0)	26.75 (0.0)	26.75 (0.0)	26.75 (0.0)	9.2 (-65.61)	20.83 (-22.13)	20.23 (-24.37)	19.25 (-28.04)	17.79 (-33.5)	16.54 (-38.17)	19.68 (-26.43)	15.91 (-40.52)	12.72 (-52.45)	11.36 (-57.53)	10.89 (-59.29)	10.21 (-61.83)	9.63 (-64.0)	4.41 (-83.51)
North	26.75	26.75	26.75 (0.0)	26.75 (0.0)	26.75 (0.0)	26.75 (0.0)	26.75 (0.0)	9.2 (-65.61)	23.41 (-12.49)	22.85 (-14.58)	21.89 (-18.17)	20.41 (-23.7)	19.09 (-28.64)	21.64 (-19.1)	16.02 (-40.11)	11.81 (-55.85)	10.5 (-60.75)	10.27 (-61.61)	10.25 (-61.68)	10.23 (-61.76)	4.48 (-83.25)
West	26.75	26.75	26.75 (0.0)	26.75 (0.0)	26.75 (0.0)	26.75 (0.0)	26.75 (0.0)	9.2 (-65.61)	20.26 (-24.26)	19.58 (-26.8)	18.63 (-30.36)	17.26 (-35.48)	16.09 (-39.85)	19.28 (-27.93)	15.28 (-42.88)	12.32 (-53.94)	10.98 (-58.95)	10.38 (-61.2)	9.96 (-62.77)	9.25 (-65.42)	4.26 (-84.07)
Average	26.75	26.75	26.75 (0.0)	26.75 (0.0)	26.75 (0.0)	26.75 (0.0)	26.75 (0.0)	9.2 (-65.61)	20.62 (-22.93)	19.98 (-25.3)	18.99 (-29.01)	17.52 (-34.5)	16.27 (-39.18)	19.48 (-27.2)	15.47 (-42.16)	12.32 (-53.94)	11.01 (-58.84)	10.48 (-60.81)	9.89 (-63.02)	9.34 (-65.07)	4.26 (-84.07)

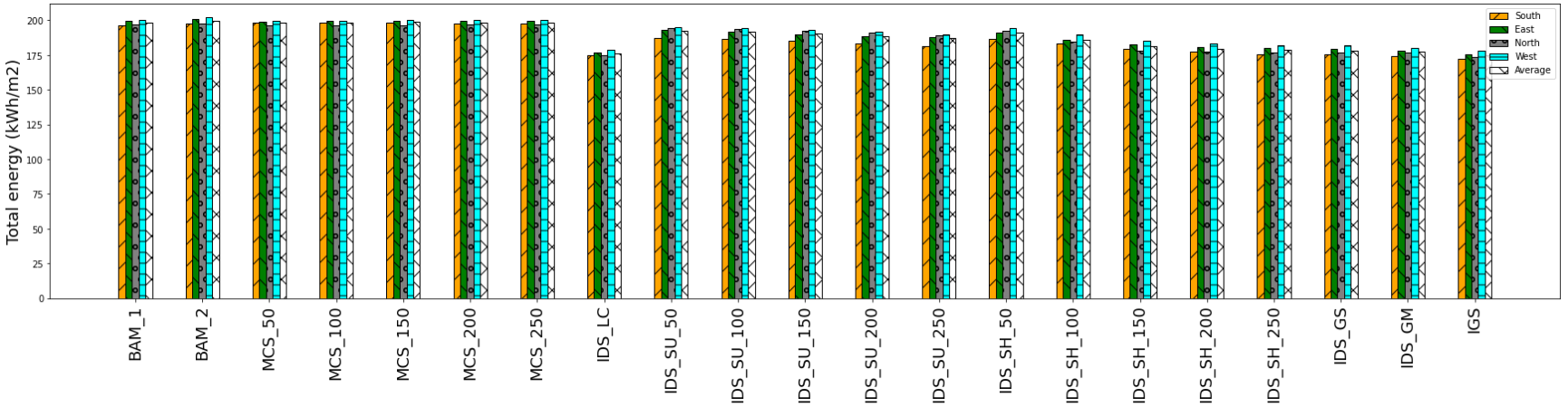

Figure 2-C.4 Comparison of annual total EUI by zone orientation

Table 2-C.4 Comparison of annual total EUI by zone orientation (values)

	BAM_1	BAM_2	MCS_50	MCS_100	MCS_150	MCS_200	MCS_250	IDS_LC	IDS_SU_50	IDS_SU_100	IDS_SU_150	IDS_SU_200	IDS_SU_250	IDS_SH_50	IDS_SH_100	IDS_SH_150	IDS_SH_200	IDS_SH_250	IDS_GS	IDS_GM	IGS
South	196.66	197.92	198.31 (0.84)	198.24 (0.8)	198.04 (0.7)	197.88 (0.62)	197.78 (0.57)	174.65 (-11.19)	187.38 (-4.72)	186.52 (-5.16)	185.22 (-5.82)	183.32 (-6.78)	181.44 (-7.74)	186.7 (-5.06)	183.2 (-6.84)	179.6 (-8.67)	177.55 (-9.72)	175.78 (-10.62)	175.62 (-10.7)	174.25 (-11.4)	172.18 (-12.45)
East	199.83	200.97	198.96 (-0.44)	199.72 (-0.06)	199.77 (-0.03)	199.8 (-0.02)	199.82 (-0.01)	177.15 (-11.35)	193.13 (-3.35)	191.68 (-4.08)	190.02 (-4.91)	188.41 (-5.71)	187.86 (-5.99)	191.32 (-4.26)	185.75 (-7.05)	182.78 (-8.53)	180.7 (-9.57)	180.08 (-9.88)	179.24 (-10.3)	178.5 (-10.67)	175.68 (-12.09)
North	196.82	197.97	196.41 (-0.21)	196.54 (-0.14)	196.73 (-0.05)	196.81 (-0.01)	196.82 (0.0)	175.16 (-11.0)	194.53 (-1.16)	193.85 (-1.51)	192.69 (-2.1)	190.9 (-3.01)	188.96 (-3.99)	192.78 (-2.05)	184.89 (-6.06)	178.26 (-9.43)	177.36 (-9.89)	176.88 (-10.13)	176.82 (-10.16)	176.86 (-10.14)	173.35 (-11.92)
West	200.22	202.24	199.67 (-0.27)	199.52 (-0.35)	200.34 (0.06)	200.18 (-0.02)	200.17 (-0.02)	179.14 (-10.53)	195.35 (-2.43)	194.46 (-2.88)	193.29 (-3.46)	191.67 (-4.27)	190.02 (-5.09)	194.6 (-2.81)	189.66 (-5.27)	185.32 (-7.44)	183.4 (-8.4)	182.37 (-8.92)	181.9 (-9.15)	180.35 (-9.92)	177.94 (-11.13)
Average	198.38	199.77	198.34 (-0.02)	198.5 (0.06)	198.72 (0.17)	198.67 (0.14)	198.65 (0.13)	176.52 (-11.02)	192.6 (-2.92)	191.63 (-3.41)	190.3 (-4.07)	188.58 (-4.94)	187.07 (-5.7)	191.35 (-3.54)	185.88 (-6.3)	181.49 (-8.52)	179.75 (-9.39)	178.78 (-9.88)	178.4 (-10.08)	177.49 (-10.53)	174.79 (-11.89)

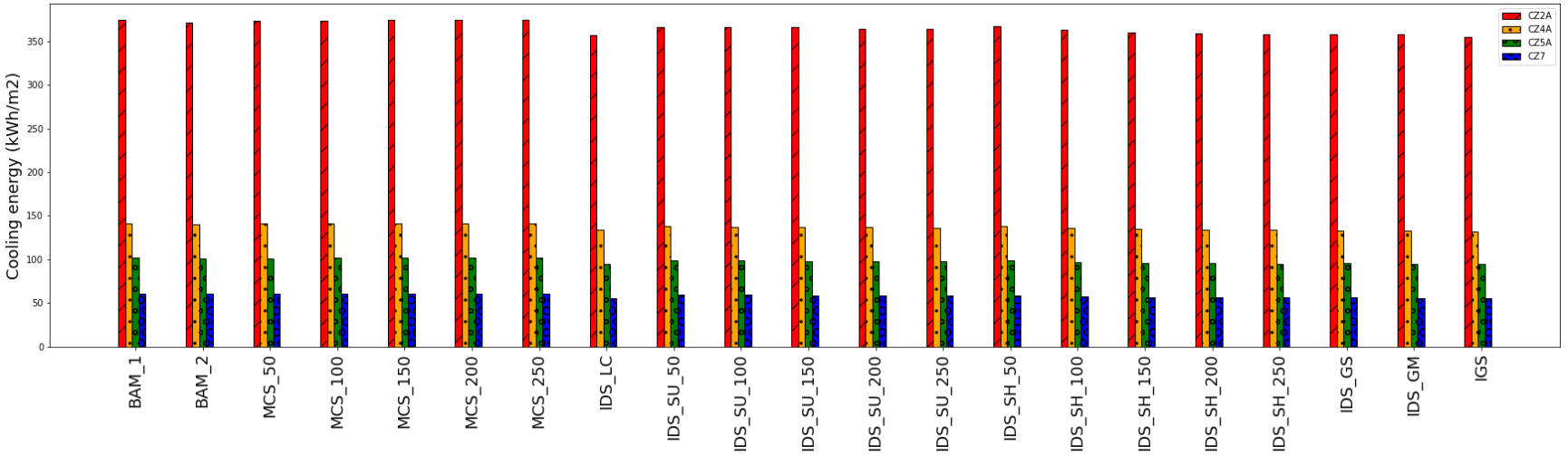

Figure 2-C.5 Comparison of annual cooling EUI by climate zone

Table 2-C.5 Comparison of annual cooling EUI by climate zone (values)

	BAM_1	BAM_2	MCS_50	MCS_100	MCS_150	MCS_200	MCS_250	IDS_LC	IDS_SU_50	IDS_SU_100	IDS_SU_150	IDS_SU_200	IDS_SU_250	IDS_SH_50	IDS_SH_100	IDS_SH_150	IDS_SH_200	IDS_SH_250	IDS_GS	IDS_GM	IGS
CZ2A	374.27	371.71	373.16 (-0.3)	373.43 (-0.23)	374.2 (-0.02)	374.23 (-0.01)	374.24 (-0.01)	357.22 (-4.55)	366.72 (-2.02)	366.45 (-2.09)	366.0 (-2.21)	364.73 (-2.55)	363.99 (-2.75)	366.88 (-1.98)	362.81 (-3.06)	359.75 (-3.88)	359.02 (-4.07)	358.32 (-4.26)	357.99 (-4.35)	357.63 (-4.45)	355.23 (-5.09)
CZ4A	141.55	140.15	140.82 (-0.52)	141.33 (-0.16)	141.45 (-0.07)	141.5 (-0.04)	141.5 (-0.04)	134.27 (-5.15)	137.68 (-2.74)	137.26 (-3.03)	136.89 (-3.3)	136.54 (-3.54)	136.26 (-3.74)	137.66 (-2.75)	135.98 (-3.94)	134.59 (-4.92)	133.68 (-5.56)	133.48 (-5.7)	133.23 (-5.88)	133.16 (-5.93)	132.16 (-6.64)
CZ5A	101.89	100.98	101.34 (-0.54)	101.58 (-0.31)	101.87 (-0.02)	101.89 (-0.0)	101.89 (-0.0)	94.82 (-6.94)	98.68 (-3.15)	98.38 (-3.44)	98.07 (-3.75)	97.82 (-4.0)	97.58 (-4.23)	98.66 (-3.17)	97.13 (-4.67)	95.87 (-5.91)	95.43 (-6.34)	95.0 (-6.76)	95.24 (-6.53)	94.94 (-6.83)	94.32 (-7.43)
CZ7	61.01	60.34	60.56 (-0.73)	60.69 (-0.52)	61.02 (0.02)	61.01 (-0.0)	61.0 (-0.01)	55.7 (-8.7)	59.19 (-2.98)	59.06 (-3.19)	58.7 (-3.78)	58.73 (-3.73)	58.48 (-4.14)	58.74 (-3.71)	57.6 (-5.58)	56.72 (-7.04)	56.3 (-7.71)	56.01 (-8.19)	56.02 (-8.18)	55.93 (-8.33)	55.66 (-8.77)

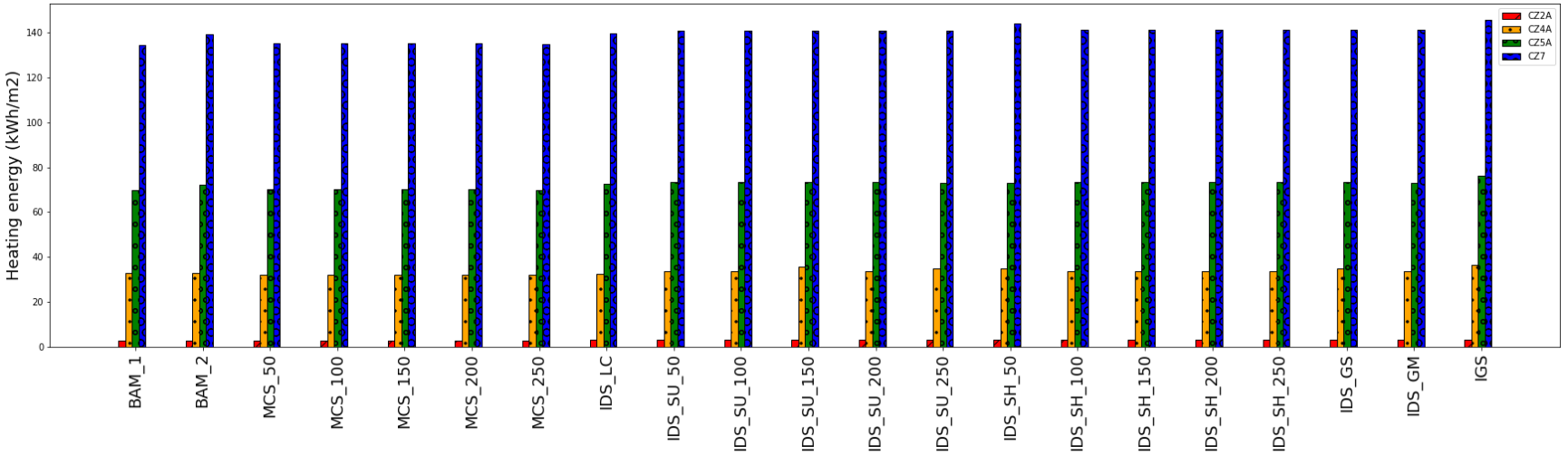

Figure 2-C.6 Comparison of annual heating EUI by climate zone

Table 2-C.6 Comparison of annual heating EUI by climate zone (values)

	BAM_1	BAM_2	MCS_50	MCS_100	MCS_150	MCS_200	MCS_250	IDS_LC	IDS_SU_50	IDS_SU_100	IDS_SU_150	IDS_SU_200	IDS_SU_250	IDS_SH_50	IDS_SH_100	IDS_SH_150	IDS_SH_200	IDS_SH_250	IDS_GS	IDS_GM	IGS
CZ2A	2.76	2.84	2.78 (0.36)	2.77 (0.27)	2.77 (0.27)	2.77 (0.27)	2.77 (0.27)	2.9 (5.06)	2.96 (7.05)	2.96 (6.96)	2.95 (6.78)	2.95 (6.6)	2.95 (6.6)	2.95 (6.69)	2.94 (6.51)	2.94 (6.51)	2.94 (6.51)	2.94 (6.51)	2.94 (6.42)	2.94 (6.15)	3.18 (14.83)
CZ4A	32.97	32.8	31.96 (-3.06)	31.95 (-3.1)	31.95 (-3.11)	31.95 (-3.11)	31.94 (-3.14)	32.39 (-1.77)	33.74 (2.33)	33.72 (2.26)	35.55 (7.81)	33.71 (2.25)	34.9 (5.86)	34.88 (5.78)	33.71 (2.24)	33.72 (2.25)	33.71 (2.24)	33.7 (2.21)	34.86 (5.72)	33.62 (1.98)	36.51 (10.74)
CZ5A	69.74	72.05	70.24 (0.72)	70.18 (0.63)	70.1 (0.51)	70.03 (0.42)	70.01 (0.38)	72.5 (3.96)	73.3 (5.1)	73.26 (5.05)	73.24 (5.03)	73.23 (5.01)	73.22 (4.99)	73.21 (4.98)	73.27 (5.07)	73.3 (5.11)	73.31 (5.12)	73.3 (5.1)	73.26 (5.05)	73.21 (4.98)	76.21 (9.28)
CZ7	134.5	139.22	135.51 (0.75)	135.37 (0.65)	135.22 (0.54)	135.16 (0.5)	135.08 (0.44)	139.81 (3.95)	140.88 (4.74)	140.82 (4.7)	140.86 (4.73)	140.91 (4.77)	140.98 (4.82)	144.2 (7.22)	141.26 (5.03)	141.33 (5.08)	141.32 (5.07)	141.31 (5.07)	141.28 (5.05)	141.24 (5.02)	145.68 (8.31)

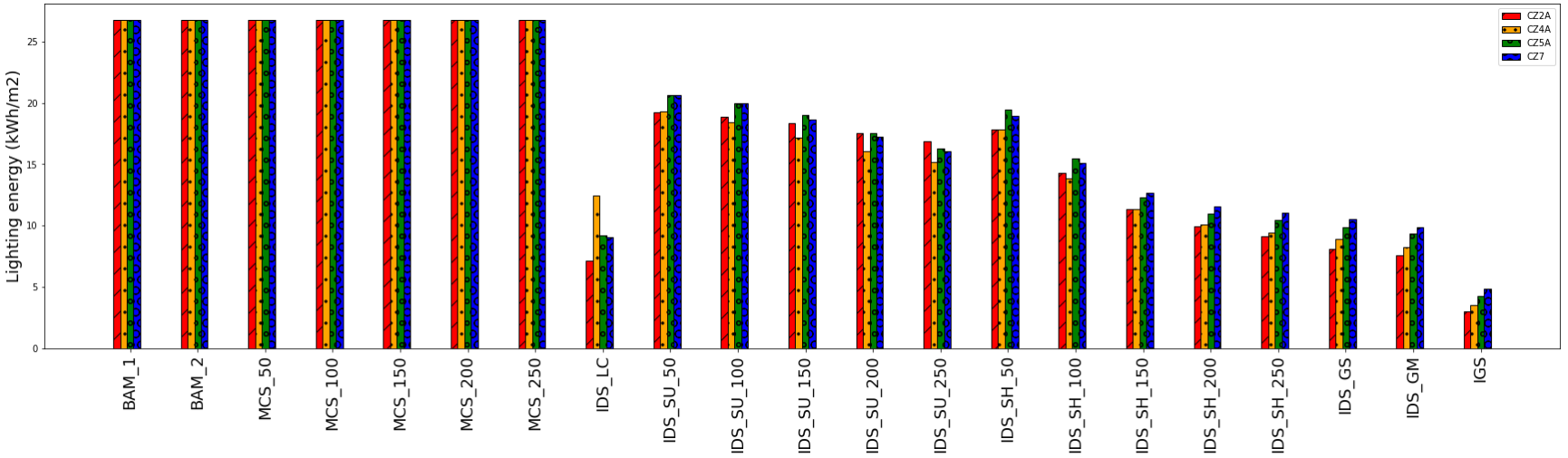

Figure 2-C.7 Comparison of annual lighting EUI by climate zone

Table 2-C.7 Comparison of annual lighting EUI by climate zone (values)

	BAM_1	BAM_2	MCS_50	MCS_100	MCS_150	MCS_200	MCS_250	IDS_LC	IDS_SU_50	IDS_SU_100	IDS_SU_150	IDS_SU_200	IDS_SU_250	IDS_SH_50	IDS_SH_100	IDS_SH_150	IDS_SH_200	IDS_SH_250	IDS_GS	IDS_GM	IGS
CZ2A	26.75	26.75	26.75 (0.0)	26.75 (0.0)	26.75 (0.0)	26.75 (0.0)	26.75 (0.0)	7.16 (-73.23)	19.27 (-27.97)	18.85 (-29.54)	18.37 (-31.34)	17.56 (-34.37)	16.88 (-36.9)	17.88 (-33.18)	14.26 (-46.68)	11.37 (-57.5)	9.93 (-62.88)	9.16 (-65.75)	8.12 (-69.64)	7.55 (-71.79)	3.04 (-88.65)
CZ4A	26.75	26.75	26.75 (0.0)	26.75 (0.0)	26.75 (0.0)	26.75 (0.0)	26.75 (0.0)	12.45 (-53.46)	19.33 (-27.73)	18.44 (-31.07)	17.16 (-35.87)	16.06 (-39.98)	15.21 (-43.14)	17.87 (-33.21)	13.84 (-48.28)	11.33 (-57.64)	10.11 (-62.2)	9.46 (-64.64)	8.94 (-66.6)	8.24 (-69.19)	3.52 (-86.84)
CZ5A	26.75	26.75	26.75 (0.0)	26.75 (0.0)	26.75 (0.0)	26.75 (0.0)	26.75 (0.0)	9.2 (-65.61)	20.62 (-22.93)	19.98 (-25.3)	18.99 (-29.01)	17.52 (-34.5)	16.27 (-39.18)	19.48 (-27.2)	15.47 (-42.16)	12.32 (-53.94)	11.01 (-58.84)	10.48 (-60.81)	9.89 (-63.02)	9.34 (-65.07)	4.26 (-84.07)
CZ7	26.75	26.75	26.75 (0.0)	26.75 (0.0)	26.75 (0.0)	26.75 (0.0)	26.75 (0.0)	9.03 (-66.24)	20.61 (-22.95)	19.95 (-25.4)	18.62 (-30.39)	17.26 (-35.49)	16.05 (-39.99)	18.93 (-29.21)	15.11 (-43.52)	12.7 (-52.51)	11.59 (-56.68)	11.04 (-58.72)	10.56 (-60.54)	9.88 (-63.08)	4.82 (-81.97)

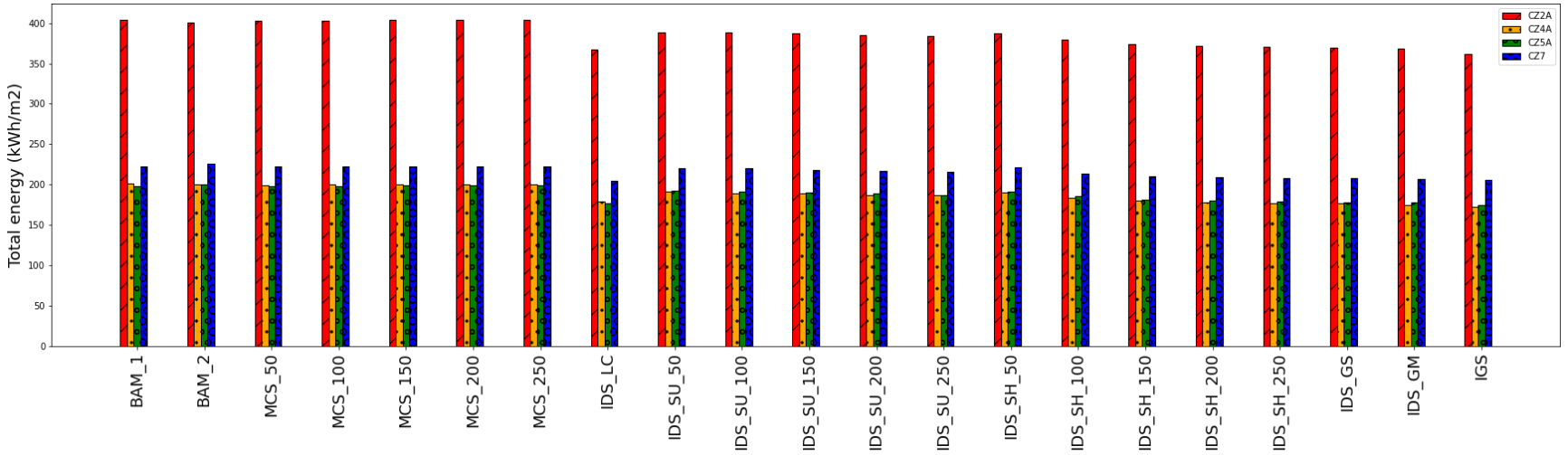

Figure 2-C.8 Comparison of annual total EUI by climate zone

Table 2-C.8 Comparison of annual total EUI by climate zone (values)

	BAM_1	BAM_2	MCS_50	MCS_100	MCS_150	MCS_200	MCS_250	IDS_LC	IDS_SU_50	IDS_SU_100	IDS_SU_150	IDS_SU_200	IDS_SU_250	IDS_SH_50	IDS_SH_100	IDS_SH_150	IDS_SH_200	IDS_SH_250	IDS_GS	IDS_GM	IGS
CZ2A	403.78	401.3	402.69 (-0.27)	402.95 (-0.21)	403.72 (-0.02)	403.75 (-0.01)	403.76 (-0.01)	367.29 (-9.04)	388.94 (-3.68)	388.25 (-3.85)	387.32 (-4.08)	385.23 (-4.59)	383.82 (-4.95)	387.7 (-3.98)	380.02 (-5.89)	374.06 (-7.36)	371.9 (-7.9)	370.42 (-8.26)	369.05 (-8.6)	368.12 (-8.83)	361.44 (-10.49)
CZ4A	201.28	199.7	199.53 (-0.87)	200.03 (-0.62)	200.15 (-0.56)	200.2 (-0.53)	200.19 (-0.54)	179.1 (-11.02)	190.75 (-5.23)	189.42 (-5.89)	189.59 (-5.81)	186.31 (-7.44)	186.38 (-7.4)	190.4 (-5.4)	183.52 (-8.82)	179.64 (-10.75)	177.5 (-11.81)	176.64 (-12.24)	177.03 (-12.05)	175.03 (-13.04)	172.19 (-14.45)
CZ5A	198.38	199.77	198.34 (-0.02)	198.5 (0.06)	198.72 (0.17)	198.67 (0.14)	198.65 (0.13)	176.52 (-11.02)	192.6 (-2.92)	191.63 (-3.41)	190.3 (-4.07)	188.58 (-4.94)	187.07 (-5.7)	191.35 (-3.54)	185.88 (-6.3)	181.49 (-8.52)	179.75 (-9.39)	178.78 (-9.88)	178.4 (-10.08)	177.49 (-10.53)	174.79 (-11.89)
CZ7	222.25	226.31	222.82 (0.25)	222.81 (0.25)	222.98 (0.33)	222.92 (0.3)	222.84 (0.26)	204.54 (-7.97)	220.68 (-0.71)	219.83 (-1.09)	218.18 (-1.83)	216.9 (-2.41)	215.51 (-3.03)	221.88 (-0.17)	213.96 (-3.73)	210.74 (-5.18)	209.21 (-5.87)	208.37 (-6.25)	207.86 (-6.48)	207.05 (-6.84)	206.16 (-7.24)

CHAPTER 3 – SENSITIVITY ANALYSIS USING PARAMATRIC MODELS

to be submitted (Journal Energy)

ABSTRACT

Window shades can control solar both the radiation and daylight entering the space, whereas lighting energy can minimize based on available daylight. Thus, shading and lighting controls can save energy while improving occupants' visual comfort simultaneously. The energy consumption and the visual comfort, however, depend on multiple variables such as different room sizes, zone orientation, building location, as well as a variety of other variables such as window configurations, sizes, and shading materials. Past studies have used parametric/optimization methods to find the ideal combination of these variables to optimize both Energy Use Intensity (EUI) and the available daylight using visual comfort metrics such as UDI (Useful Daylight Illuminance). However, these optimization and parametric studies do not factor in metrics such as glare, view outside and thermal comfort for an optimal solution. This study aims to optimize various variables such as WWR for all four orientations, shade material properties such as openness factor, and the length of the building overhang depth to estimate best-case scenarios for UDI, EUI, glare, and view to the outside, and thermal comfort using PMV (Predicted Mean Vote). The control strategy used for this study is based on glare that restricts the glare under DGP < 0.35 using roller shades controlled at (3) positions (Fully closed, 50% closed, and fully open). The study also aims to find the best-case solution for nine (9) different building aspect ratios. The study uses Rhino/Grasshopper interface with Honeybee and Ladybug to develop a daylighting model (RADIANCE) and an energy model (EnergyPlus). The study concludes that the best solution for two (2) variable combinations such as with one of the variables involving EUI (such as EUI and UDI, EUI and View, EUI, and PMV) the solution) is predominantly a low 1% openness factor for shade openness factor combined with high WWR values (such as 75 % and 50%) for the South

and West facing direction. The other set of optimum solutions involves a high shade openness factor (5% and 10 %) openness factor for shade openness factor combined with low WWR values (such as 25 % and 50%). For the north-facing direction, the optimum values for results do not show any particular pattern. For the variable shade overhang depth, no overhangs are slightly preferable for square buildings whereas overhangs with 1 meter depth are preferable for more rectangular buildings. However, the difference is very small.

Keywords: Lighting and shading control, sensitivity analysis, Parametric model, building form

3.1 INTRODUCTION

Windows allow solar radiation and natural light to enter the building. Incoming solar radiation can significantly increase or reduce a building's energy consumption based on whether this occurs in a cooling, or a heating dominated season. Window also allows daylight into the space, where low levels of daylight can increase the lighting energy consumption whereas too much daylight can cause visual discomfort. Further, windows provide occupants with natural light, a view to the outside, and enhance productivity (Edwards & Torcellini, 2002) (Shishegar & Boubekri, 2016) and provide a sense of well-being which is important considering people spend approximately 90% of their time indoors (Mitra et al., 2022).

Further in most buildings, the shading devices are operated manually by occupants. In such scenarios, studies suggest that they are not used effectively (Rea, 1984) [to] manage the incoming solar radiation and daylight. With automated shading and lighting controls, this responsibility can be transferred from the occupant to an effective lighting and shading controls that can balance excessive daylight or glare, providing a view for occupants to the exterior, and limiting artificial lighting and HVAC (heating, ventilation, and air conditioning) energy use is needed.

Recent review studies have extensively summarized daylighting and glare values metrics (Vasquez et al., 2022)(Carlucci et al., 2015)(Sadeghi et al., 2016)(Da Silva et al., 2012) that are used for lighting and shading control strategies. These metrics are used both as input variable thresholds for shading and lighting levels and/or to evaluate the performance of a control strategy. Commonly used daylighting metrics include Daylighting Factor (DF), Daylight Autonomy (DA), Continuous Daylight Autonomy (cDA), Useful Daylight Illuminance (UDI), and Spatial Daylight Autonomy (sDA) and Annual Sunlight Exposure (ASE). For estimating glare, researchers have used Daylight Glare Index (DGI), Unified Glare Rating (UGR), Daylight Glare Probability (DGP), Simplified Daylight Glare Probability (DGPs) and Predicted Glare Sensation Vote (PGSV).

Studies have used automated shading and lighting control strategies with the common ones using either visual comfort metrics or the amount of solar radiation entering space. Past studies that use the common visual comfort metrics include glare indices (Xiong and Tzempelikos, 2016 ; Da Silva et al., 2012 ; Shen et al., 2014 ; de Vries et al., 2021; Kunwar and Bhandari, 2020 ; Bian et al., 2020), vertical illuminance inside the building (Bian et al., 2020; de Vries et al., 2021; Kunwar & Bhandari, 2020; Shen 2012; Xiong and Tzempelikos, 2016). For solar radiation-based control, a solar radiation threshold is used to control the radiation entering the space (Tzempelikos and Athienitis, 2007; Wankanapon and Mistrick ,2011; Shen 2012; Shen and Tzempelikos, 2012; A. Atzeri et al., 2018). Usually, this value ranges from 20 W/m^2 to 400 W/m^2. In addition to using visual comfort criterion or solar radiation entering the space, some studies have also used factors such as occupant behavior (Bourgeois et al., 2006)(Athanassios Tzempelikos & Athienitis, 2007)(Da Silva et al., 2012)(E. Shen et al., 2014), sun tracking (de Vries et al., 2021; E. Shen et al., 2014), indoor temperature (Karlsen et al., 2016), HVAC state (heating/cooling mode) and

different controls for day and night (E. Shen et al., 2014) to develop integrated shading and lighting controls.

The general conclusion from these lighting and shading control strategy review studies is that simple automated shade control using glare metrics works best for both visual comfort and energy use reduction as compared to any other control strategy. Thus, this study plans to use a glare-based control strategy using a metric called DGPs (Simplified Daylight Glare Probability). DGPs is a simple empirical relation between vertical illuminance at the eye level of the occupants and glare and can be used as the simplified version of DGP. As per (Weinold 2007), a DGPs value of 0.35 and higher can cause visual discomfort for occupants and is considered as the upper threshold for glare. This glare value corresponds to a vertical illuminance threshold of approximately value of 2600 lux.

However, even when using a particular automated lighting and shading different control strategy. There are many variables that can influence the results of these daylight and energy modeling studies. These variables include building location (Bourgeois et al., 2006)(E. Shen et al., 2014)(Karlsen et al., 2016)(Do and Chan, 2020)(Kunwar & Bhandari, 2020), zone orientation (Wankanapon & Mistrick, 2011)(Shen 2012)(H. Shen & Tzempelikos, 2012)(Da Silva et al., 2012)(Kunwar et al.)(Kunwar & Bhandari, 2020)(A. M. Atzeri et al., 2018)(Do and Chan, 2020), Window-to-Wall Ratio (WWR) (E. S. Lee & Selkowitz, 2006)(Wankanapon & Mistrick, 2011)(H. Shen & Tzempelikos, 2012)(Da Silva et al., 2012)(E. Shen et al., 2014)(A. M. Atzeri et al., 2018), sensor distance from the window or sensor orientation (E. S. Lee & Selkowitz, 2006)(Wankanapon & Mistrick, 2011)(Konstantzos et al., 2015)(H. Shen & Tzempelikos, 2012)(Kunwar et al., 2019)(Bian et al., 2020), shade material types and properties (Wankanapon & Mistrick, 2011)(Shen 2012)(H. Shen & Tzempelikos, 2012)(E. Shen et al., 2014)(Karlsen et al., 2016)(A.

M. Atzeri et al., 2018), window/glazing configuration (E. S. Lee & Selkowitz, 2006)(Da Silva et al., 2012)(A. M. Atzeri et al., 2018)(Do and Chan, 2020) for evaluated control strategies

Although the studies stated above provide sensitivity analysis for input variables. Parametric models can be used to see the influence of all the variables at once as opposed to sensitivity analysis where a particular variable is changed while all others are fixed. Another approach is to use optimization models which rank the input variable for a particular objective function. Table 3-1 shows a review of past literature for parametric or optimization studies that include daylighting components. Therefore, studies with just daylight modeling are selected or studies with both daylight and energy modeling are chosen for review. All the studies with just energy modeling are excluded. Various parameters such as simulation tools used, optimization method if used, input variables for optimization/parametric model, type of shading system and output metrics used for selection of the best model are shown for each study in Table 3-1.

Table 3-1 Review of Parametric/Optimization studies with daylight simulation

Reference	Location	Simulation type	Simulation Tools used	Optimization tool/Parametric model	Input variables	Shading system type	Output metrics
(Toutou et al., 2018)	Helwan, Egypt	Daylight + Energy	RADIANCE and EnergyPlus using (Ladybug and Honeybee tools)	Optimization using Octopus (plugin for grasshopper)	- WWR South - WWR East - Window material - Wall construction - Shading depth - Shading width - Shade angle	- Horizontal Louvers shades	- Useful Daylight Illuminance (UDI) - Energy Use Intensity (EUI)
(Wagdy & Fathy, 2015)	Cairo, Egypt.	Daylight	Diva-for-Rhino	Parametric model	- WWR South - Louvers count, - Louvers tilt angle, - Screen depth ratio, - Screen reflectivity	- Horizontal Louvers shades	- Spatial Daylight Autonomy (sDA300/50%) - Annual Sunlight Exposure (ASE1000/250h) - Daylight Availability (DA) - DGPs (Glare)
(Krarti et al., 2005)	Atlanta Chicago Denver Phoenix	Daylight + Energy	DOE-2	Parametric model	- Building geometries - Glazing properties - WWR - Building Location	- No shades	- Percent lighting energy reduction
(Eltaweel & Yuehong, 2017)	New Cairo	Daylight	RADIANCE and DAYSIM	Parametric model	- Slat geometry - Glazing type	- Horizontal slats + Electrochromic glazing	- Percent area with illuminance range of 300–500 lx
(Hegazy et al., 2013)	Cairo, Egypt	Daylight + Energy	Diva-for-Rhino and Design Builder	Parametric model	- WWR - Glazing properties - Shade types	- Tinted glazing - Perforated screen - Combined shading (overhang+ side fins) - Combined shading + Blinds - Combined shading + Tinted glazing - Blinds + tinted glazing	- Daylight Autonomy (DA) - Useful Daylight Illuminance (UDI) - Energy Use Intensity (EUI)
(M. ElBatran & Ismaeel, 2021)	Cairo, Egypt	Daylight	Diva-for-Rhino	Parametric model	- Screen perforation % - Screen depth - Screen Gap width	- Perforated screen	- Spatial Daylight Autonomy (sDA300/50%) - Annual Sunlight Exposure (ASE1000/250h)
(K. S. Lee et al., 2016)	-	Daylight	Diva-for-Rhino	Optimization using Galapagos	- Louvers shades - Louvers angle - Louver depth - WWR south	- Horizontal Louvers - Vertical Louvers - Delaunay pattern screen - Voronoi pattern screen	-Daylight Factor (DA)
(Nasrollahi & Shokry, 2020)	Kermanshah, Iran	Daylight + Energy	Relux	Parametric model	- WWR - Surface's Reflectivity	- External Awning (overhangs)	-Daylight Factor -Energy Consumption
(Reffat & Ahmad, 2020)	Cairo, Egypt	Daylight + Energy	IES-VE	Parametric model	- Building rotation	- Light shelf - Horizontal Louvers - Horizontal sun-breaker - Vertical sun-breaker	- Total energy consumption - CIE glare index - Useful Daylight Illuminance (UDI)
(Konis et al., 2016)	Helsinki New York Los Angeles Mexico City	Daylight + Energy	RADIANCE and EnergyPlus	Optimization using Octopus	- Building form - Shades from surrounding buildings	- No shades	- Useful Daylight Illuminance (UDI) - Energy Use Intensity (EUI)

Table 3-1 (cont'd)

(González & Fiorito, 2015)	Sydney	Daylight + Energy	Diva-for-Rhino	Optimization using Galapagos	- Shade depth - Shade angle - Shade width	- Horizontal Louvers	-Daylight Autonomy (DA) -Useful Daylight Illuminance (UDI). -Total Energy Savings. -Total CO2 emissions
(Bakmohammadi & Noorzai, 2020)	Tehran-Mehrabad	Daylight + Energy	Honeybee and Ladybug	Optimization using Octopus	- Building orientation - Wall angle - WWR - Glazing material	- No shades	- Useful Daylight Illuminance (UDI) - Daylight Autonomy (DA) - Energy Use Intensity (EUI) - Occupant Thermal Comfort (CRT)
(Fang & Cho, 2019)	Miami Atlanta Chicago	Daylight + Energy	RADIANCE and EnergyPlus	Optimization using Octopus	- Building depth - Roof ridge location - Skylight width (m) - Skylight length (m) - Skylight location (m) - Skylight orientation - WWR – South - WWR – North	- Horizontal Louvers	- Useful Daylight Illuminance (UDI) - Energy Use Intensity (EUI)
(Kirimtat et al., 2019)		Daylight + Energy	RADIANCE and EnergyPlus	genetic algorithm (NSGA II) and (JcGA-DE)	- Distance from glazing - Rotation with respect to glazing	- Fixed amorphous panels	- Total Energy Consumption (TEC) - Useful Daylight Illuminance (UDI)
(Pilechiha et al., 2020)	Tehran.	Daylight + Energy	Ladybug and Honeybee tools	Optimization using Octopus	- WWR - Window location on wall	- No shades	-Spatial Daylight Autonomy (sDA300/50%) -Annual Sunlight Exposure (ASE1000/250h) - Useful Daylight Illuminance (UDI) - Energy Use Intensity (EUI)
(Zani et al., 2017)	Xi'an, China	Daylight + Energy	EnergyPlus	NSGA-II	- WWR, - Zone Orientation - Glazing material	- No shades	- Total Energy Consumption - Indoor thermal comfort - Work plane illuminance
(Mahdavinejad & Mohammadi, 2018)	Tehran-Iran	Daylight + Energy	Daysim and EnergyPlus	Optimization using Octopus	- Shade depth - Shade angle - Distance from facade	-Horizontal Louvers	- Heating and cooling energy - Useful Daylight Illuminance (UDI)
(Zhang et al., 2017a)	Tianjin, China	Daylight + Energy	RADIANCE and EnergyPlus	Optimization using Octopus	- Orientation - Room /corridor depth - WWR - Glazing materials - Shading types	- Venetian blinds - Roller shade	Heating + lighting energy demand, - Summer thermal discomfort (STD) - Useful Daylight Illuminance (UDI)
(Manzan & Clarich, 2017)	Trieste, Italy	Daylight + Energy	Daysim and ESP-r	modeFRONTIER (FAST), NSGA II	- Glazing Type - Blind angle - Blind depth	-Venetian blinds.	- Useful Daylight Illuminance (UDI) - Energy Use Intensity (EUI)
(Motamedi & Liedl, 2017)	San Francisco,	Daylight + Energy	RADIANCE and EnergyPlus	- Optimization (gradient descent) Exhaustive search (parametric analysis) in	- Optimize Skylight Floor Area Ratio (SFR)	- No shades	- Spatial Daylight Autonomy (sDA300/50%) - Useful Daylight Illuminance (UDI) - Source energy

The building shape or form factor is another variable that affects both the energy use and amount of daylight available in the building significantly. For instance, when comparing a long rectangular building with a square shaped building, the long rectangular shape can provide a higher percentage of building floor with daylight as compared to the square building. However, for the same volume the rectangular building has more wall surface exposed to the outside, increasing the heat transfer due to conduction. Various studies such as (Mokrzecka, 2018) (Feng et al., 2021) (Catalina et. al. 2011) (Zhang et al., 2017b) use the term compactness which is the volume to surface area ratio. Table 3-2 shows the studies that have building form as one of the variables for sensitivity analysis. However, most of the studies evaluate the impact of building form on energy use and thermal comfort and not visual comfort. Though these studies only provide energy analysis they do a wide variety of building shapes such as square, Rectangular, T-shaped, L-shaped, C-shaped, U- shaped, H- shaped, Trapezoidal, Cross shaped and some free form shapes.

Further, studies that include both energy and daylighting analysis such as (Krarti et al., 2005) and (Fang & Cho, 2019) considered different building form factors for rectangular building. Study (Krarti et al., 2005) does not use any shades in the analysis whereas study (Fang & Cho, 2019) used horizontal louvers with skylights for it analysis. Study (Konis et al., 2016) also explores non-rectangular building form factors with no shades for its impact on EUI and UDI. This study also evaluates the impact of nine (9) different building form factors apart from all the other goals mentioned before.

Table 3-2 Review of studies involving building form

Reference	Location	Simulation type	Building form variables	Simulation Tools used	Goal of the study
(Smith, 2012)	Minneapolis Baltimore Atlanta Phoenix	Energy	(3) Building shapes and zoning patterns	DOE-2 simulation engine with Autodesk® Project Vasari	Study the change energy used due to different building shapes (non – rectangular shapes)
(Dogan et al., 2015)	Phoenix Anchorage Boston	Energy	Building forms explored - Rectangular, Courtyard type, Polyline, and Freeform	EnergyPlus using Grasshopper and Archsim	Explores energy use difference for different building shapes with internal topologies such as corridor locations, compartmentalization, and open building layout
(Gratia & De Herde, 2003)	Belgium	Daylight + Energy	Building forms explored - Square (single story), Square (multi story), Rectangular, Cross-shaped, Polyline	TAS software package for thermal analysis of buildings	Categorize building form based on compactness (Volume to surface areas ratio)
(Mokrzecka, 2018)	(Köppen climate classification Dfb and Cfb)	Energy	Explores 40 different building shapes involving. - Square, Rectangle, L-shaped, C-shaped and U-shape	Sketchup and Sefaira	Investigate the impact variables such as building shape and orientation on its heating energy use and indoor comfort
(Feng et al., 2021)	Fort Collins, Colorado	Energy	Building shapes explored -Rectangular, T-shaped, L-shaped, C-shaped, U-shaped, H- shaped, Trapezoidal, Cross shaped	whole-building energy simulation, RIUSKA is used	Optimization of energy consumption in residential buildings
(Catalina et. al. 2011)	Lyon and nice	Daylight + Energy	Building shapes explored -Rectangular, T-shaped, and stepped 2 story building model	Empirical relation for energy model and Dialux for daylighting model	Estimate energy consumption for different building shapes, glazing areas and locations using energy and daylighting model
(Zhang et al., 2017b)	(8) cities in cold climate in China	Energy simulation	Building shapes explored Rectangular, L-shaped, C-shaped, H- shaped H- shaped with atrium, Block shaded/courtyard	DesignBuilder.	Impact of variable such as building shape, window to wall ratio, room depth, and orientation on the energy use and thermal comfort in school buildings
(Krarti et al., 2005)	Atlanta Chicago Denver Phoenix	Daylight + Energy	Rectangular building with 4 different aspect ratios	DOE-2	Explored the impact of building geometry, window opening size, and glazing type and location using on daylighting and energy use
(Konis et al., 2016)	Helsinki New York Los Angeles Mexico City	Daylight + Energy	non-rectangular building form factors	RADIANCE and EnergyPlus	
(Fang & Cho, 2019)	Miami Atlanta Chicago	Daylight + Energy	Rectangular building with different aspect ratios	RADIANCE and EnergyPlus	Explored the impact of building aspect ration, WWR, and skylight size on daylighting and energy use with an optimization model

3.2 Research gap and goals

Various studies have explored using parametric/optimization models to estimate what set of input variables can be used to optimize respective output metrics. The studies using parametric/optimization models with shading system as roller shades is limited (M. ElBatran & Ismaeel, 2021) (Hegazy et al., 2013) (Zhang et al., 2017a) . Most literature studies focus on using

horizontal and vertical louvers. Although studies involving controls based on roller shades provide sensitivity analysis to input variables. A parametric model can be used to estimate the influence of all the variables at once as opposed to sensitivity analysis, where a particular variable is changed while all others are fixed.

Further, studies using a parametric model for a roller that switches between different shade positions based on a control strategy are rare. This study uses roller shades with three shade positions (fully open, 50 percent closed, and fully closed). Further, this study uses a daylighting model that controls shade in all four orientations independently for each timestep. Literature reviews for parametric/optimization studies for daylighting models usually use only two output metrics, Energy Use Intensity (EUI), and one daylighting metric, usually Useful Daylight Illuminance (UDI) or Daylight Autonomy (DA). A few studies have also used Spatial Daylight Autonomy (sDA) and Annual Sunlight Exposure (ASE) as the output metrics for visual comfort. This study uses a glare-based daylighting control strategy (shades are lowered if DGPs>0.35) with multiple output metrics such as Energy Use Intensity (EUI), Useful Daylight Illuminance (UDI), view to the outside, and percent improvement in thermal comfort.

The office building is the most common type of commercial building in the United States (U.S. EIA 2018). In addition, over 50% of the commercial buildings are smaller than 5500 sq. ft. (U.S. EIA 2018) and can thus be categorized as small office buildings. Thus, this model uses a single-floor small office building with a total area of 5500 sq. ft (510 m^2). The model uses the US DOE commercial Prototype building model (U.S. DOE 2020) for various building schedules, setpoints, and building loads such as equipment, lighting, and ventilation load. The latest energy code standard ASHRAE 90.1- 2019 is used for the building envelope properties as it is assumed that all

the new buildings that will be constructed will follow the strictest energy code for a conservative estimate of energy savings.

Thus, an energy and daylighting model is developed using six (6) input variables such as WWR for all four orientations, shade material openness factor, and the length overhang depth to evaluate the best-case scenarios for UDI, EUI, view to the outside, and improvement and thermal comfort. This process is repeated for nine (9) different building form factors to estimate the variation in results as the building form factor is changed. To determine the incremental change of each parametric run over a certain baseline case, the default DOE small office building model is used with AHSRAE 90.1 - 2019 building, schedules, setpoints, building loads and building envelope properties with the same form factor and WWR as the parametric run. The baseline case does not have any window overhangs or shades with no lighting and shading controls.

The remainder of this research is organized as follows, Section 3 discusses the validation of a daylighting model for a test building in Ankeny, Iowa. Section 4 discusses the steps for building daylighting and energy model development for the parametric run. Section 5 discusses the results of the validation model whereas Section 6 shows best-case results for the parametric model run. Section 7 includes the discussion and the limitations of the study and finally, section 8 concludes the findings for this study.

3.3 Daylight model validation

3.3.1 Test Setup and measured data

The study aims to find the best-case scenario for input variables such as WWR by orientation, window shade properties, and length of window overhangs for a rectangular building for different form factors while optimizing visual comfort and energy use. However, before building the optimization model, a real building was used to validate various variables considered fixed for the

optimization, such as wall, ceiling, and floor reflectivity. The validation model also provides further confidence that the current setup used for daylighting and energy simulation using RADIANCE and EnergyPlus with Ladybug tools as the interface will provide satisfactory results during optimization without errors.

The test building is located in Ankeny, Iowa, and consists of six identical rooms, two facing each South, East, and West. Each room pair is labeled as Room A and Room B and shown in Figure 3-1(a). For this study, only Test Room A for all three directions is used for validation. The main difference between rooms A and B is the type of window glazing used. Room A uses a double plane window with 3 mm of clear glass on both sides with an air gap, whereas glazing in Room B is used as a double pane window low-E glazing on one side with an air gap that is 90 % argon and 10 % air. The window area for the test room is 6.88 m^2, which makes up approximately 48% of the exterior façade area of each room. These windows are approximately 0.91 meters above the finished floor height. Window glazing properties for Test Room A are specified in Table 3-3. The lighting system in each test room consists of four 0.6 m x 0.6 m recessed grid troffers, as shown in Figure 3-1(b). Each fixture contains three U-shaped T8 fluorescent tube lamps sized 31 W.

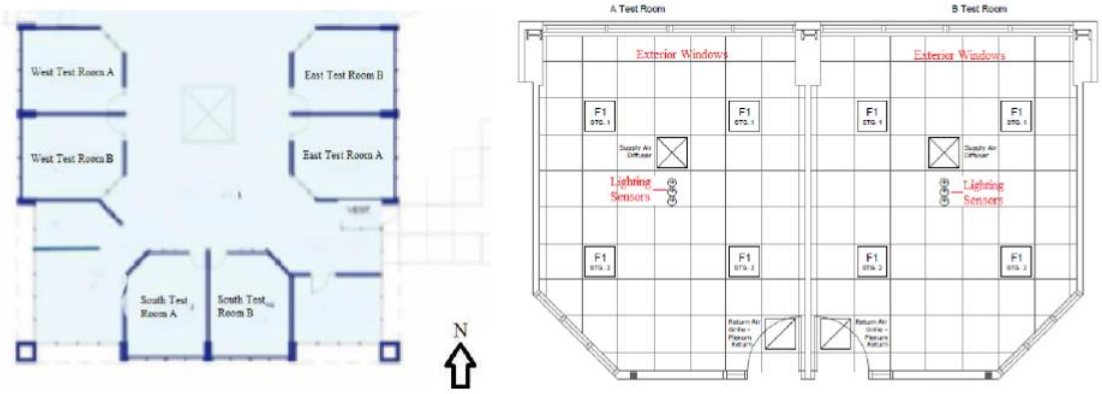

Figure 3-1 Room orientations for test facility in Ankeny, IA

Table 3-3 Description of window used in all the Test Room A (all three directions)

Type of glass	Size	U-factor	Visible Transmittance	Shading Coefficient
Double pane Clear/ Clear 3 mm glass	1.52 m x 4.63 m	3.12 W/m^{2}-K	81%	0.85

Illuminance data is collected for four sensor points (three at the work plane level and one vertical sensor at the occupant's eye level to simulate glare) inside the room, as shown in Table 3-4. Data collected by these sensors (+/- 5%) was used for model validation. A weather station was used to collect weather and solar data, including global horizontal and direct normal irradiation, ambient temperature, relative humidity, wind direction, and wind speed at the test site during illuminance data collection. The collected weather data was used to create a custom weather file for daylight simulation. The collected illuminance data and the simulated data are compared hourly for validation.

Table 3-4 Position of illuminance sensors in the test room

Sensor type	Height from floor	Distance from exterior window
Work plane illuminance	0.76 m	1 m, 2.5 m, 4 m
Vertical illuminance	1.2 m	3 m

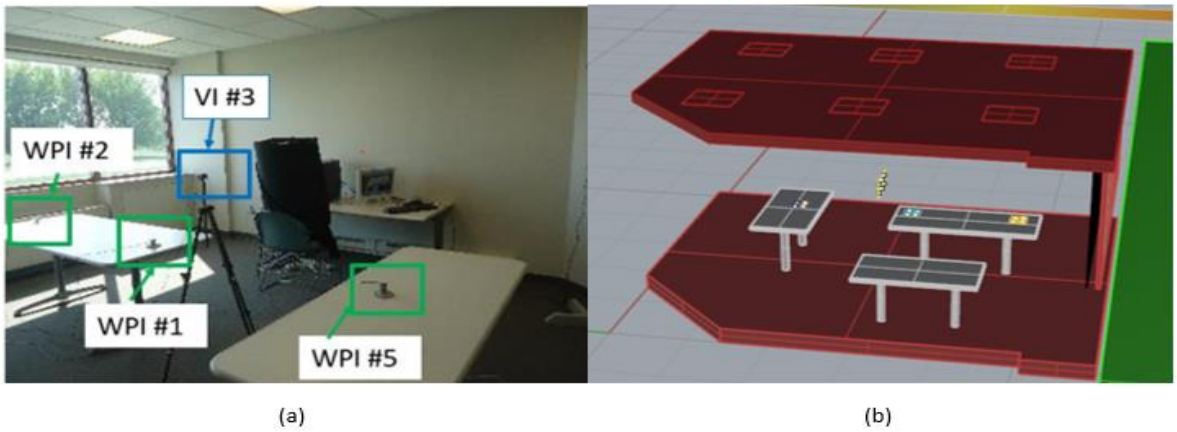

Figure 3-2 (a) Location and labels for sensors and (b) Radiance geometry for the test room

3.3.2 Validation model description

To model the daylighting, RADIANCE is used, which is a set of programs used for lighting design. This is used in a Ladybug and Honeybee v.1.1.0 (Ladybug tools) environment, a plugin for Rhino3D and Grasshopper (Rhino 3D v.6.0). The main inputs used for the daylighting model used for model validation are (i) zone geometry and reflectance values for zone surfaces such as walls, ceiling and floor) and transmittance for windows (ii) sensor locations and direction, and (iii) weather data as an input to generate illuminance. These inputs are described in detail below.

(i) The building geometry was drawn using Rhino based on the room dimensions. The zone surface reflectivity used for the model are shown in Table 3-3

(ii) The sensors were placed in the model at a distance as shown in Table 3-5 and Figure 3-2. The work plane sensors face the ceiling whereas the vertical sensor faces the window and is located at the occupant's eye level.

(iii) The weather data collected at the test Location is used to develop a weather file that is used for the daylighting simulation. The test location (Ankeny, IA) falls under ASHRAE climate CZ 5A which can be described as cool and humid.

Table 3-5 Surface reflectance values used for the daylighting model

Surface type	Surface reflectance
Walls	0.8
Ceiling	0.7
Floor	0.2
Door	0.2
Ground	0.2

The daylighting model is set to run for the whole year with a timestep of 1 hour. The Measured data and the simulation results are compared at an hourly level for the days measured data was collected. The measured and the simulated results are compared using the Metric CV-RMSE (Root Mean Squared). There is no established limit for CV- RMSE for comparing daylighting data unlike

energy consumption results using ASHRAE guideline 14. The results for all three Test Rooms are shown in the model results section.

3.4 Parametric model building and description

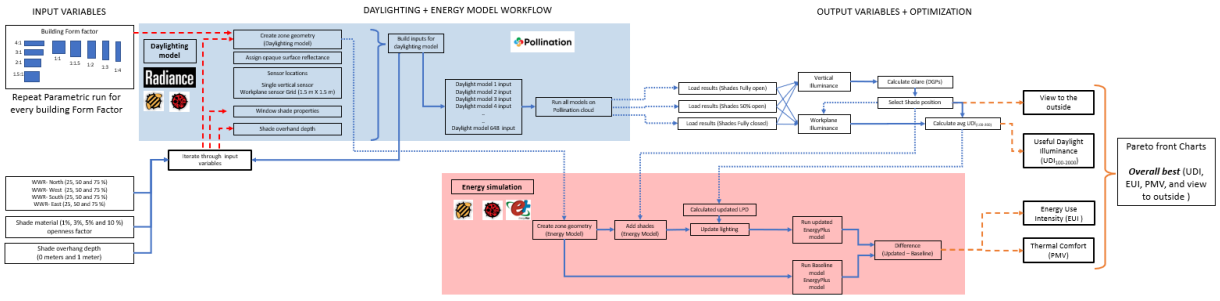

Figure 3-3: Modeling workflow for optimization

3.4.1 Input Variables

Various inputs for the model are varied to see the change to quantify the change in the output metrics. The initial variable selected is the building form factor which is used to fix the building shape. The best parametric solution is developed for each building form factor. The rest of the variables such as WWR by orientation, shade properties, and the shade overhang length are updated till an optimized solution is found for each building form factor. This process is repeated for each building form factor listed in figure 3-4 below. All the input variables are discussed in detail below.

- **Building form factor:** This is used as the variable to select an overall building aspect ratio. All the building form factors for which the optimized solution is found are shown in Figure 3-4. For building form factors (4:1, 3:1, 2:1, 1.5:1) the longer side faces the South and the North side whereas for the building form factors (1:4, 1:3, 1:2, 1:1.5) the longer side faces the East and the West direction. Building form factor (1:1) is a square building with all

sides equal. The building area for all the form factors is the same and is 511 m^2 which is the area for the US DOE small office prototype building model.

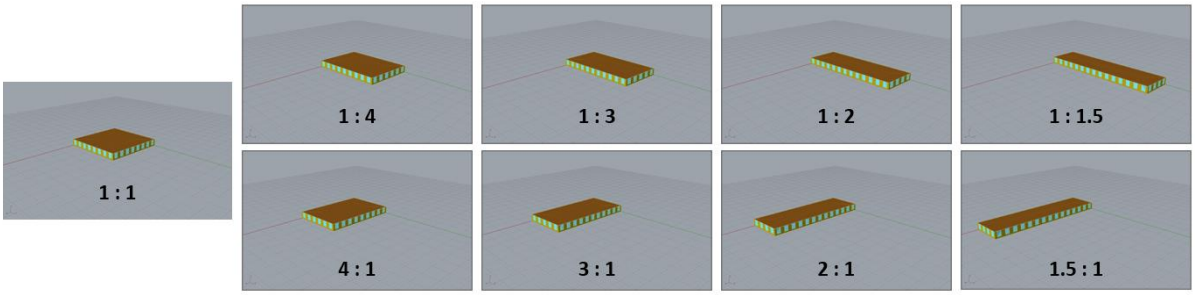

Figure 3-4: Input variable – Building form factor

- **Window to Wall Ratio (WWR):** The model used 4 different inputs for WWR ratio for the optimization as shown in figure 3-5. These include the following WWR option (25% , 50% and 75%). Figure 3-5 shows all the window WWR configurations used in the optimization. For simplicity figure 3-5 shows the same WWR for all orientation, however the model uses different WWR input variable for each orientation (South, East, North and West), that is four different variables are used for optimization namely WWR_South, WWR_North, WWR_East and WWR_West. For instance, the model can have 25% WWR for the south side, 50% WWR for the East and the West side and 75% WWR for North side during the optimization. Thus, this leads to 81 possible window combinations of the WWR variable.

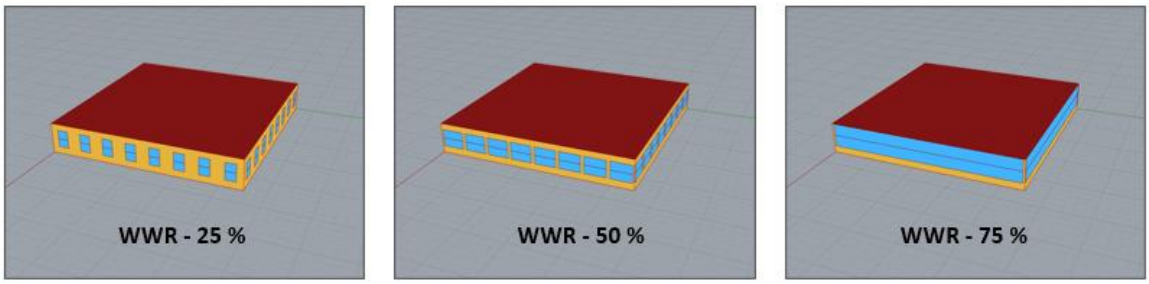

Figure 3-5: Input variables – WWR

- **Shade material:** The model used 4 different inputs for shade material based on the shade openness factor (1%, 3%, 5% and 10%). The RADIANCE 2-phase method is used for the daylighting simulation. A BSDF (Bi-directional Scattering and Distribution Function) file is used to define the shade properties. These BSDF files were generated using WINDOW LBNL v.7.7 for a window with and without roller shades.
- **Shade overhang depth:** The model used 2 different inputs for shade overhang depth for the optimization as shown in Figure 3-6. These include no shade overhangs and the other with a shade depth of 1 meter. The same shade overhang depth is used for all the orientations.

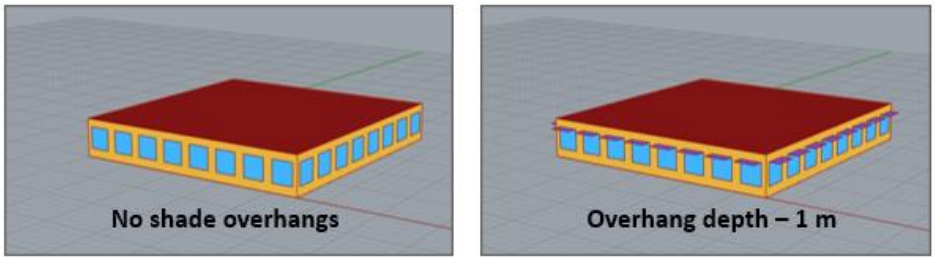

Figure 3-6: Input variable – Overhang depth

Therefore, considering all input variables, this leads to 648 daylighting models for each form factor. Further the model also considers the shades opening and closing in three positions (Full open, 50 % closed and fully closed) based on the amount of glare at the vertical sensor points. As

running daylighting simulation and be very time intensive a cloud-based computing platform called pollination is used for the daylighting simulations.

3.4.2 Daylighting model

Similar to the validation model, the daylighting model used the RADIANCE 2-Phase matrix method in a Ladybug and Honeybee v.1.1.0 (Ladybug tools) environment, which is a plugin for Rhino3D and Grasshopper (Rhino 3D v.6.0). The main steps for the daylighting used for optimization model are shown in Figure 3-3. They are as follows: (a) Develop zone geometry (b) Horizontal and vertical sensor placement (c) Run daylighting model with 3 cases with Pollination (d) Calculate glare and select shade position I Evaluate average view to the outside (f) Evaluate UDI. These steps are explained in detail below.

(d) **Develop zone geometry:** The building geometry is made using the building form factor variable, and the other variables (WWR, shade material properties, and shade overhang length) with the fixed variables such as surface reflectivity for wall, floor, and ceiling surface) discussed in the validation section.

(e) Horizonal and vertical sensors: The horizontal sensors are used to calculate the UDI and the lighting energy use, while the vertical sensor is used to calculate glare, which is used to control the shades. The horizontal sensors are placed throughout the zone in a grid (1.5 m x 1.5 m) at a height of 0.76 m, as shown in Figure 3-7. The vertical sensor is placed at a distance of 1.5 meters from the window, facing the window, and at a height of 1.2 meters (eye level).

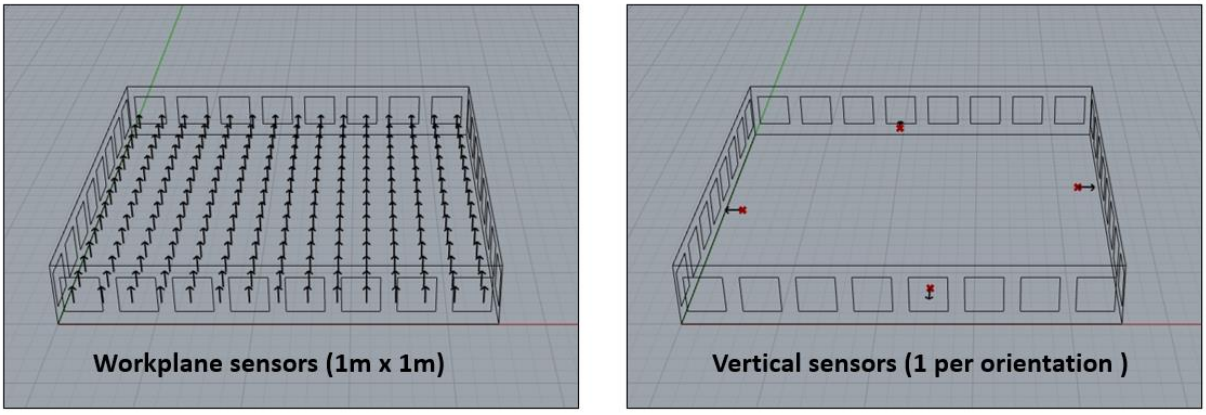

Figure 3-7: Work plane sensor grid points (0.76 meters high) and vertical sensors at eye level (1.2 meters high)

(f) **Run daylighting model (for three shade positions) on Pollination:** Based on the inputs from step (a) and step (b). Inputs for the RADIANCE simulation is generated for all 648 models. This includes all three cases with shades fully closed, shades 50% closed, and shades fully open for the entire year to mimic the lowering of shade based on available daylight. Once the RADIANCE simulation inputs are generated for all the models, these are submitted for a batch run using Pollination.

(g) **Glare calculation and shade position selection:** Once all the models are run on the pollination cloud, the results for each model are loaded sequentially, including the illuminance results for the workplace and vertical sensors. The shade position is selected between fully closed, 50% closed, and fully open based on a control strategy that uses glare for control. The glare metric used for control is DGPs (Simplified Daylight Glare Probability), an empirical relation between the glare and the vertical illuminance at eye level. The DGPs value above which glare is perceptible by the occupants is 0.35, which corresponds to 2600 lux of vertical illuminance at the eye level. Thus, using the simulated vertical illuminance value, DGPs is calculated. If the DGPs value at a particular timestep

is greater than 0.35, the shades are closed to 50%, and if the DPGs is still greater than 0.35, then the shades are fully closed.

(h) Output variable – Evaluate average view to the outside: View to the outside is calculated as the sum of values assigned to view for each timestep. For each timestep, if the shade is fully open the view is assigned a value of 1, if the shades are half closed a value of 0.5 is assigned and if the shades are fully closed the view is assigned a value of 0. These values are summed for the entire year to get a view to the outside for each orientation. The average view to the outside for the entire model is the average for all four orientations.

(i) **Output variable – Evaluate average $UDI_{100\text{-}2000}$:** The $UDI_{100\text{-}2000}$ for the entire building is the count of work plane sensors with illuminance between 100 lux and 2000 lux at each timestep for the selected shade position. The average $UDI_{100\text{-}2000}$ for the entire building is the average for all the timesteps between the hours of 8 a.m. to 5 p.m. each day of the year.

3.4.3 Energy model

The energy model used EnergyPlus (v8.9.0) for energy simulation in a Ladybug and Honeybee v.1.1.0 (Ladybug tools). The inputs from the daylighting model are used to update the shade position and the lighting levels in the energy model to generate two outputs EUI (Energy Use Intensity) and PMV (Predicted Mean Vote). The main steps for energy simulation for the optimization model are shown in Figure 3-3 and are as follows (a) Update shades in the energy model (b) Update lighting level (c) Run energy simulation and (d) Evaluate EUI and PMV

(a) Updated shades in the energy model: Based on the selected shade position from the daylighting model. One of three shaded positions (fully open, 50 % closed, and fully closed) is selected for each timestep, and an hourly schedule is developed for the shade operation. The shade position schedule is applied to the energy model.

(b) Update lighting levels: The zone is assumed to use a continuous dimming control with a setpoint of 500 lux. The lighting power is assumed to be linearly proportional to the lighting level (lux). The original LPD is reduced based on the available illuminance at the work plane sensors in the zone. If the illuminance at the sensor is greater than 500 lux, then a LPD of zero is assumed for the area associated with that sensor. For instance, if the zone has 20 sensors, each sensor is responsible for dimming lights for 1/20 of the area. If the illuminance at any sensor is between 0 and 500 lux, the LPD is reduced to provide the remaining amount of light such that the total daylight and artificial light is 500 lux.

(c) Run energy simulation: Two energy simulation models are generated to estimate results, (i) a baseline energy model, one which does not include any shading and lighting control but with the same form factor, and (ii) an updated model in which the selected shading position and LPDs are updated based on the daylighting result. Both the energy models assume ideal air loads

(d) Evaluate EUI and PMV: For both energy models, the annual EUI for the entire building is calculated as the summation of cooling, heating, and lighting loads divided by the total area for the entire building. Heating, cooling, and lighting energy are expressed in kWh/m2. Further to estimate thermal comfort, Predicted Mean vote (PMV) is used, which is a scale between -3 to + 3 where positive three (+3) denotes the room is too hot, whereas negative three (-3) denotes the room is too cold. The calculation for PMV and the variables used to calculate it are discussed in detail here [ASHRAE 55].

3.5 Validation model results

The Figures (3-8 to 3-10) below show the comparison between the test building measured data with the simulated results for all three Test Rooms for the South, West, and East zones,

respectively. CV-RMSE is used as the metric for comparison. Table 3-6 shows the period for which the data for which measured and simulated data is compared for each Test Room. For the south-facing zone, the simulated data matches well with the collected data for all four (4) sensor points. For the West and the East zone for work plane sensor (WPI_2), the simulation overestimates the illuminance values for a few hours in the evening and morning, respectively. However, the higher simulated results for a few hours can be ignored as the control strategy used for shade control in the optimization section uses glare control at the occupant's eye level (sensor VI) to choose an appropriate shade position (Fully open, 50 % closed and fully closed). The glare metric used for control is DGPs (Simplified Daylight Glare Probability), an empirical relation between the glare and the vertical illuminance at eye level. The DGPs value above which glare is perceptible by the occupants is 0.35, which corresponds to 2600 lux of vertical illuminance at the eye level. The overpredicted values occur when vertical illuminance is significantly higher than 2600 lux, so the shades will likely be fully closed during these timestamps. The simulated illuminance values for all the other sensor points (WPI_1, WPI_2, and VI) satisfactorily match the collected data for the West and the East zones.

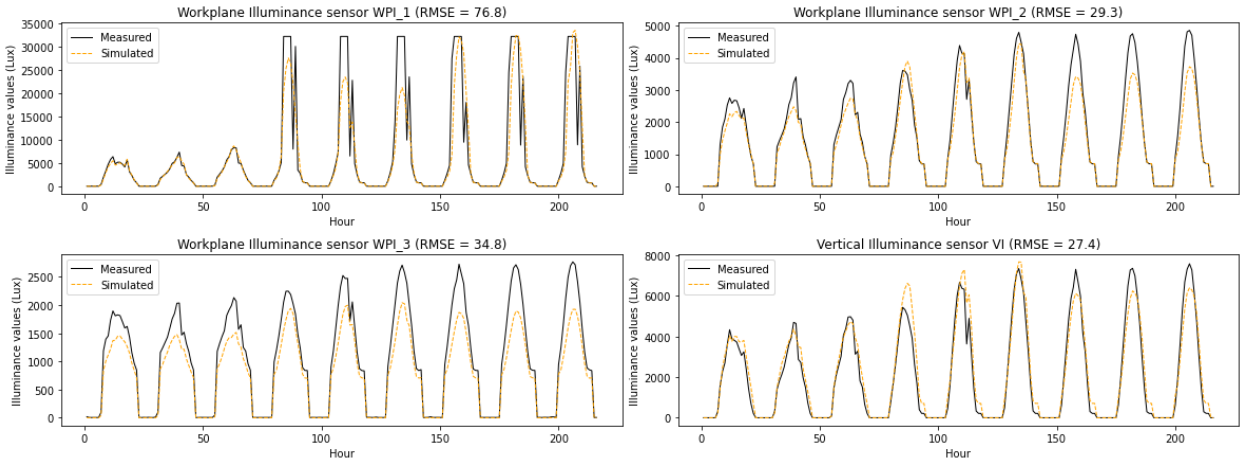

Figure 3-8 Work plane and vertical illuminance sensor validation for the South zone

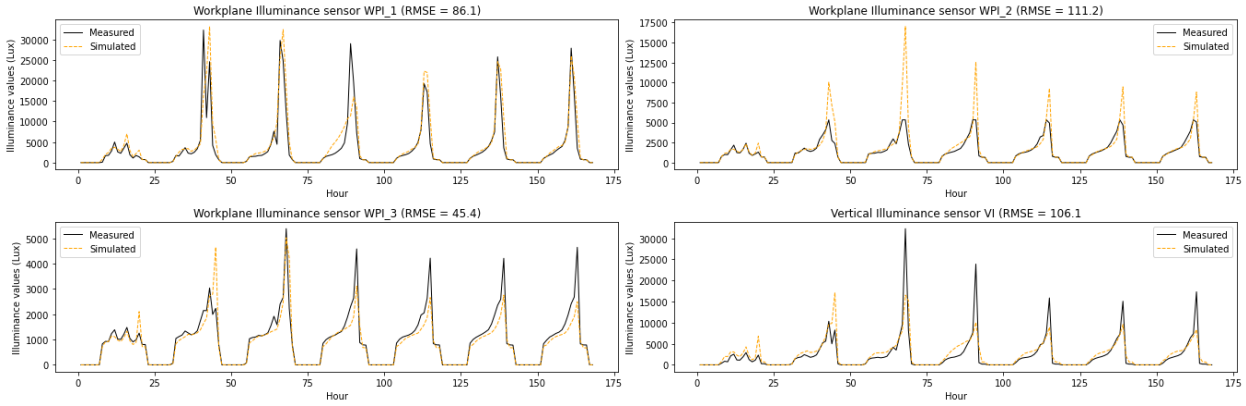

Figure 3-9 Work plane and vertical illuminance sensor validation for the West zone

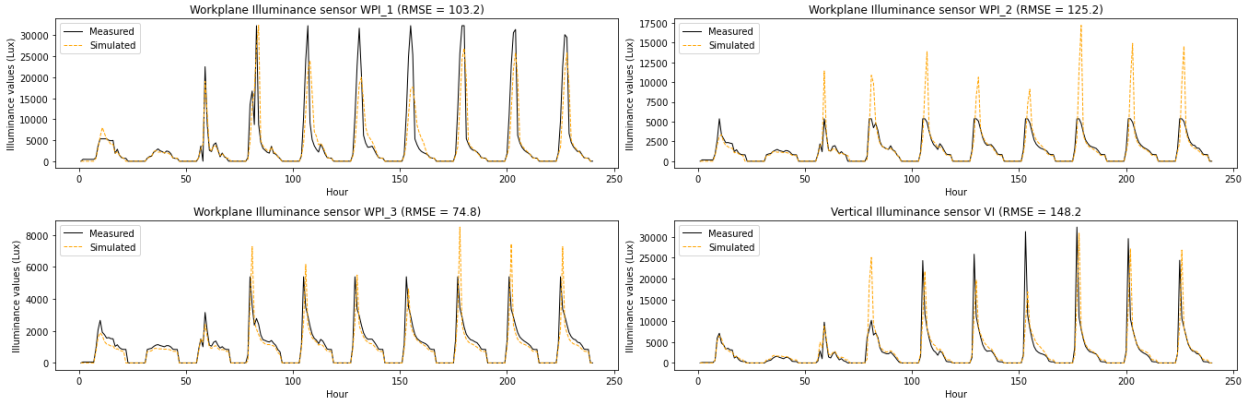

Figure 3-10 Work plane and vertical illuminance sensor validation for the East zone

Table 3-6 Validation results RMSE summary

Zones orientation	Time period (days)	WPI_1 sensor (CV-RMSE)	WPI_2 sensor (CV-RMSE)	WPI_3 sensor (CV-RMSE)	VI sensor (CV- RMSE)
South	9	76.8	29.3	34.8	27.4
East	10	103.2	125.2	74.8	148.2
West	7	86.1	121.3	45.4	106.1

3.6 Parametric simulation model results

The Figures (3-11 to 3-19) below show the scatter plot for four different metrics that are maximized in the namely percent total EUI reduction as compared to baseline, Average UDI for all four directions for times between 8 am to 5pm, time's view to the outside and percentage improvement in thermal comfort. All the black dots represent all the iterations whereas the value in green shows

the best-case solution for all four variables combined for all the 648 parametric iterations for each form factor. Each the sublot, which consists of two variables, also shows a pareto front, which is the best solution for those pair of variables. Figures (3-11 to 3-15) show these results for 5 different building form factors namely (1:1, 1.5:1, 2:1, 3:1, 4:1). For all the rectangular building form factors. The longer side faces the North – South direction. Appendix A also shows the results for form factors (1:4, 1:3, 1:2, 1:1.5) where the longer side faces the East- West direction.

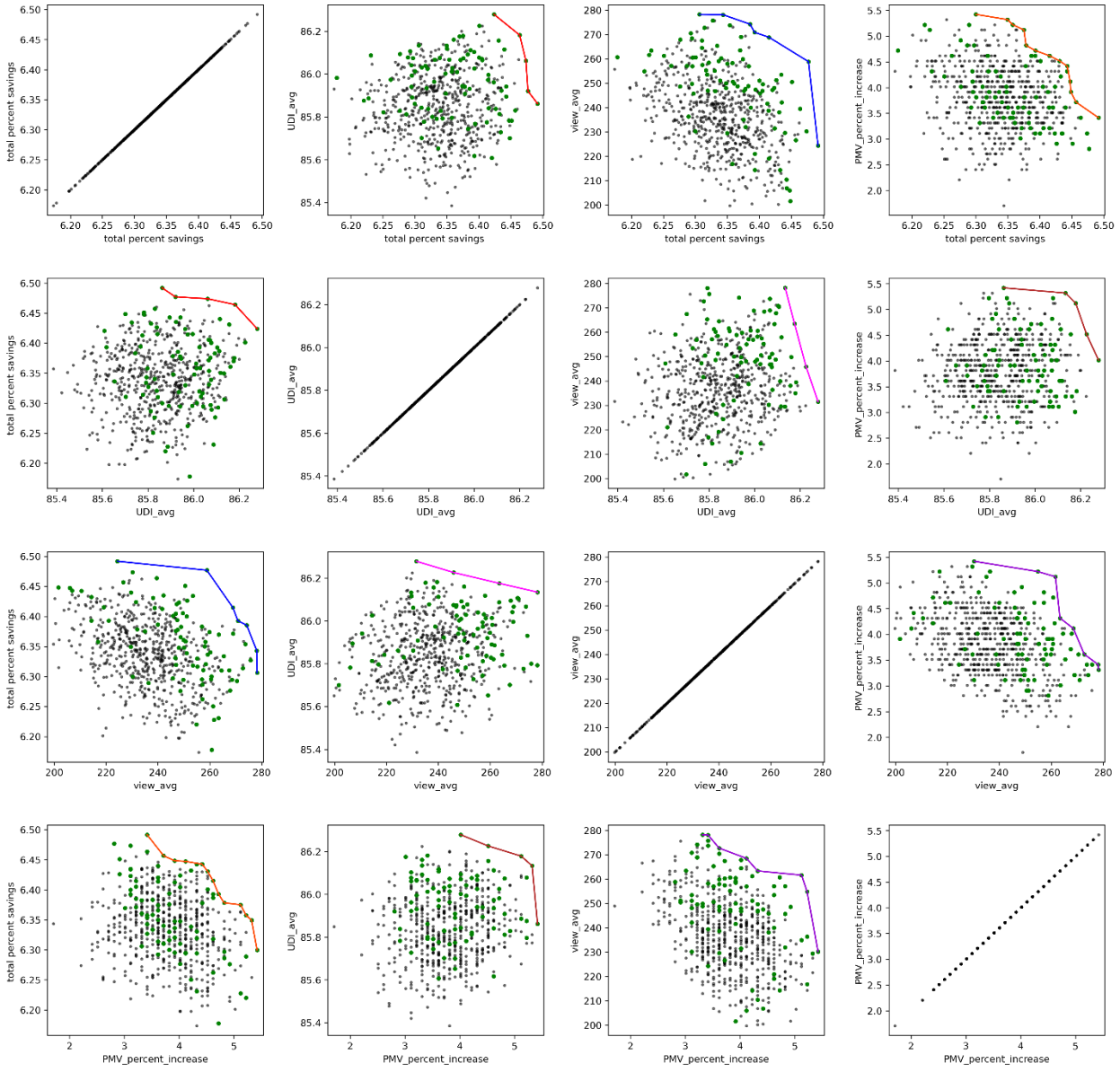

Figure 3-10 Scatter plot and parent front for form factor (1:1)

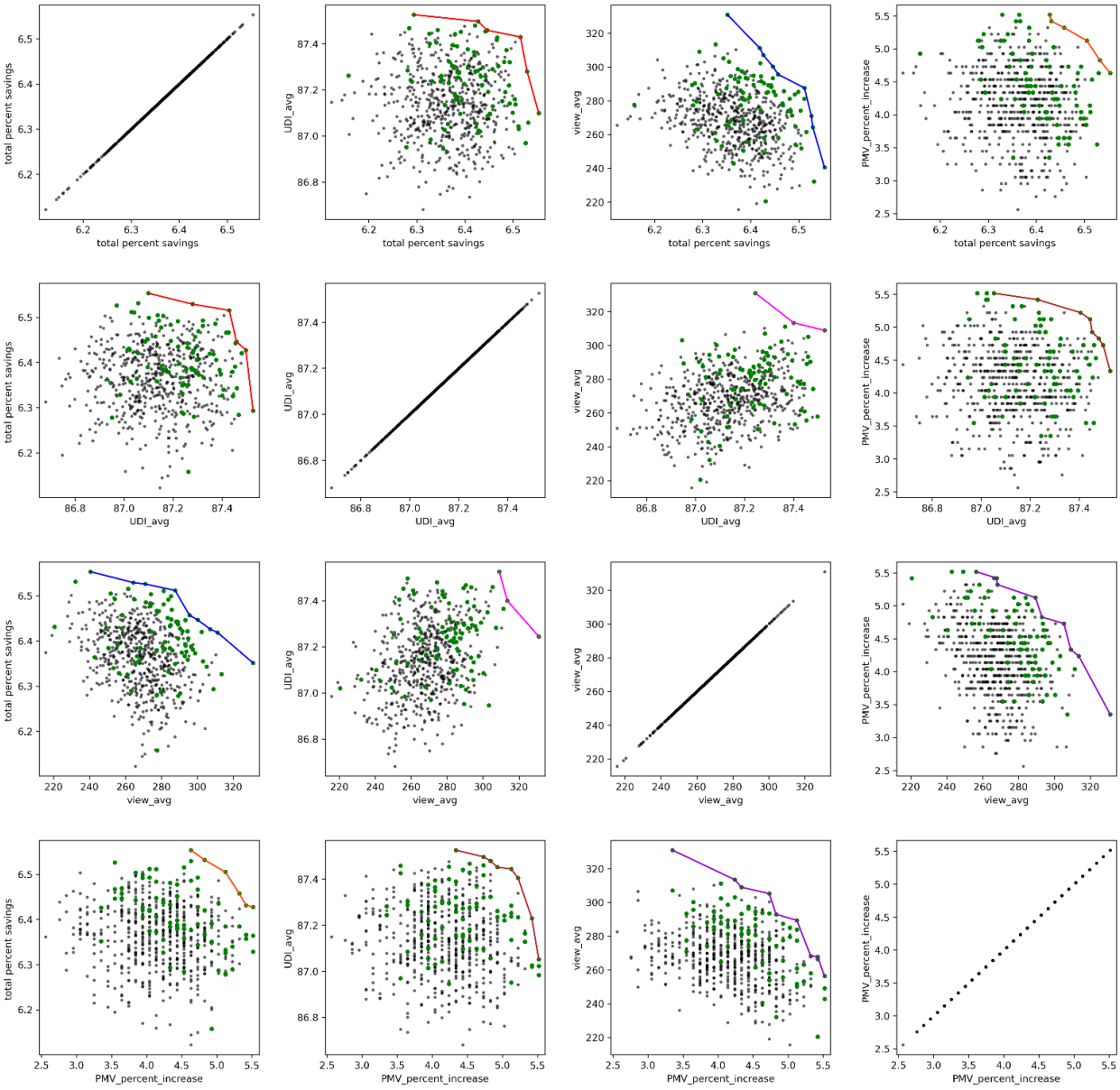

Figure 3-11 Scatter plot and parent front for form factor (1.5:1)

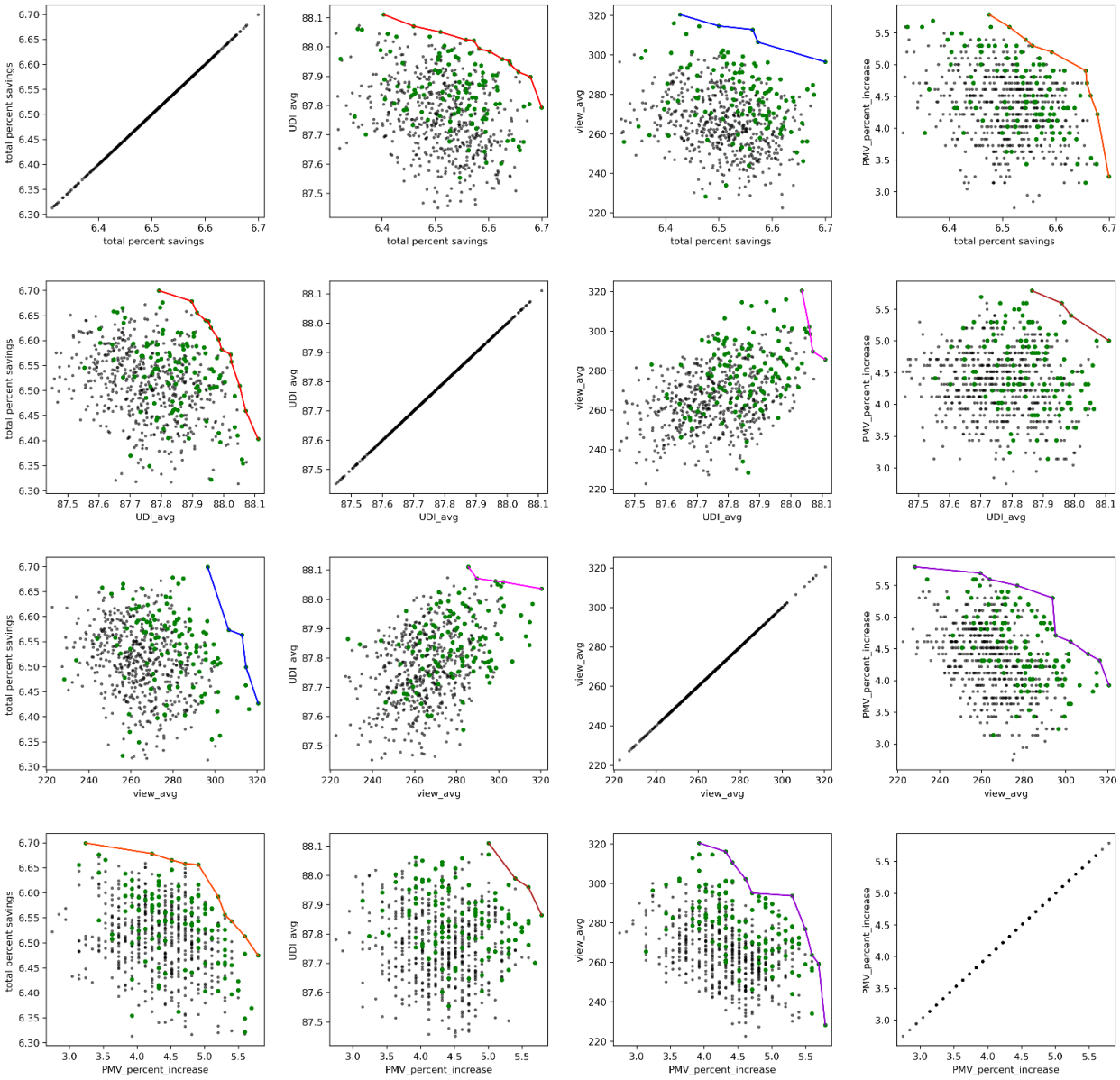

Figure 3-12 Scatter plot and parent front for form factor (2:1)

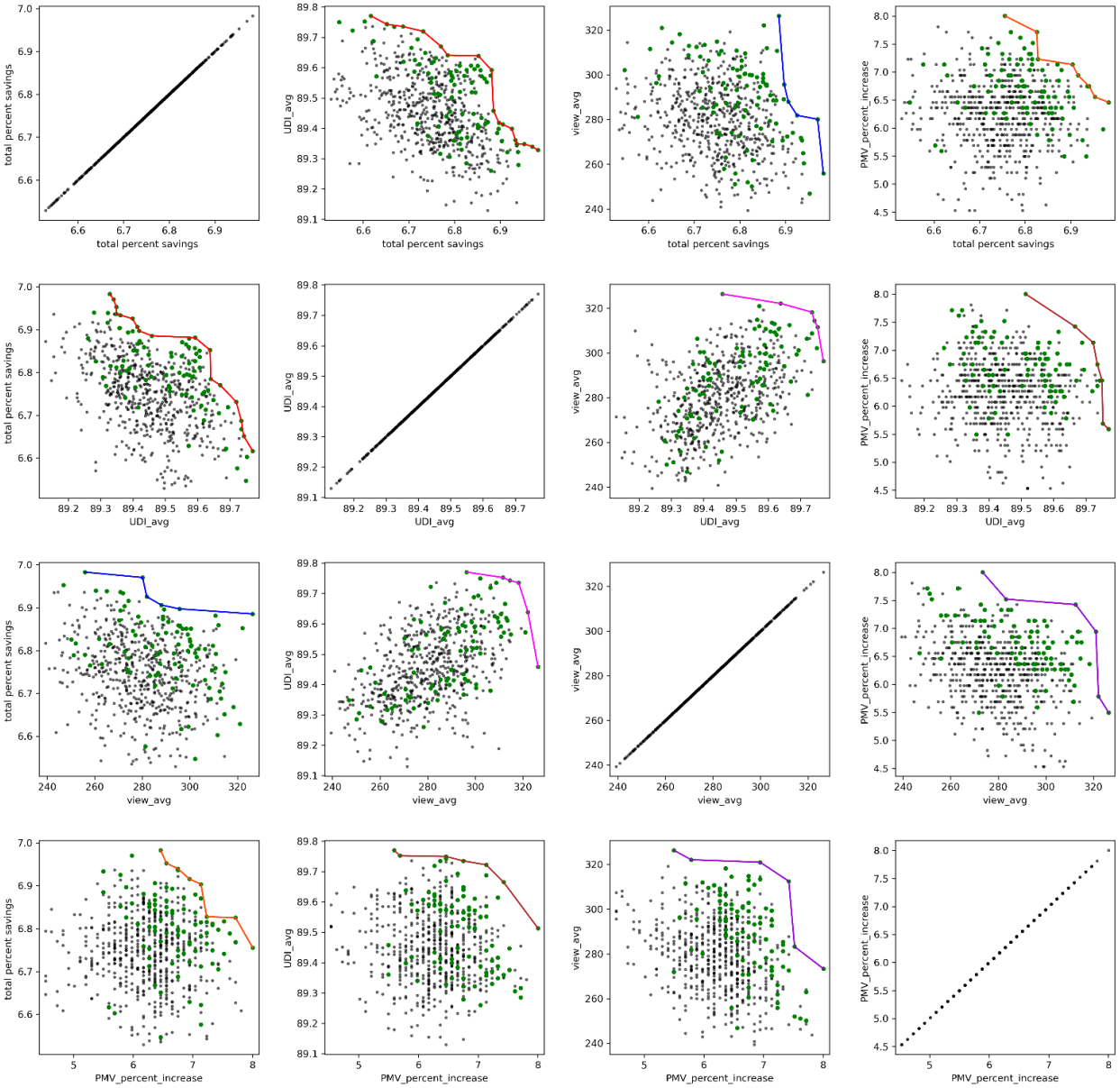

Figure 3-13 Scatter plot and parent front for form factor (3:1)

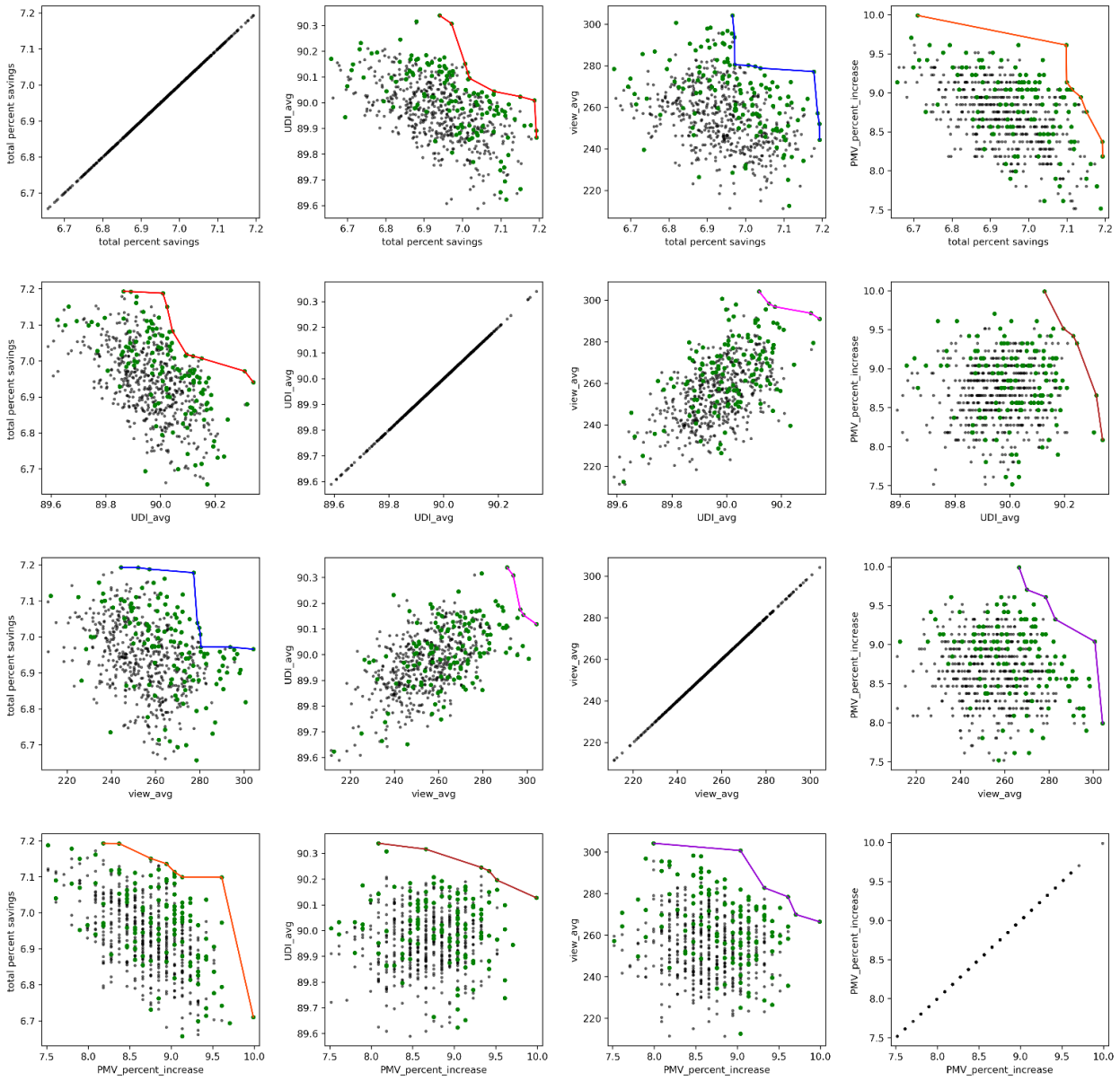

Figure 3-14 Scatter plot and parent front for form factor (4:1)

For all the points selected for the pareto front shown in Figures (3-10 to 3-14) for two (2) variable combination and Tables 3-7 to 3-12 below provide additional information on what the input variables for the best selected models far. The tables below compare the most common input variables using histograms. As the number of points making the pareto front vary for all the two (2) variable combinations and for different building form for the same variable combinations, percentage values that a particular input variable is selected is also shown with the histograms.

Tables 3-11 to 3-14 compare six two (2) variable combinations namely (i) EUI and UDI, (ii) EUI and View (iii) EUI and PMV (iv) UDI and View, (v) UDI and PMV, and (vi) View and PMV. For each of these two variable combinations the Table provides results by building form factor for five (5) different building forms namely (1:1, 1.5:1, 2:1, 3:1, 4:1). For each of the form factors the histograms are shown for all the input variables used in the study (WWR by orientation, shade openness factor and window overhang depth). Table 3-13 however, shows the similar result for four (4) variable combinations that is, all the performance metrics. The points shown in Table 3-13 correspond to all the green points shown in Figures (3-10 to 3-14). Appendix B also shows the results for form factors (1:4, 1:3, 1:2, 1:1.5) for all the two (2) variables combinations whereas Appendix D provides the results for form factors (1:4, 1:3, 1:2, 1:1.5) for four (4) variables combinations. Additionally, Appendix C also shows results for 3-variable combination for all nine (9) building form factors (1:1, 1.5:1, 2:1, 3:1, 4:1, 1:4, 1:3, 1:2 and 1:1.5).

Table 3-7 Input variable histograms for Pareto Front 2 variable combination (EUI and UDI)

Form Factor (1:1)	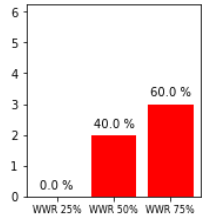	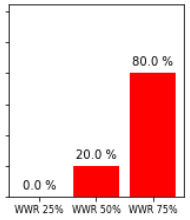	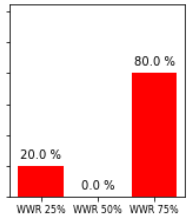	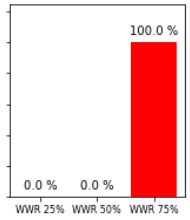	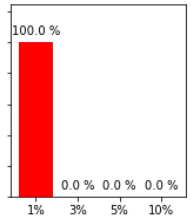	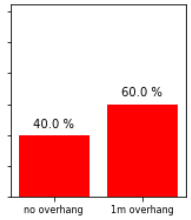
Form Factor (1.5:1)	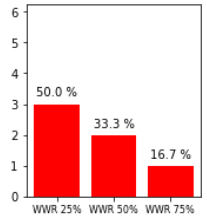	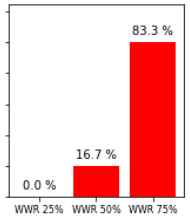	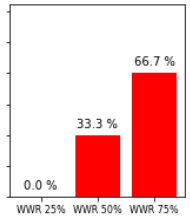	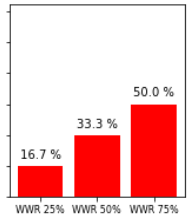	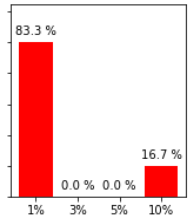	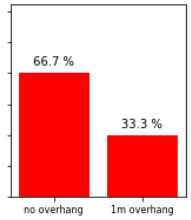
Form Factor (2:1)	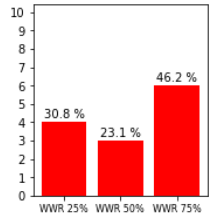	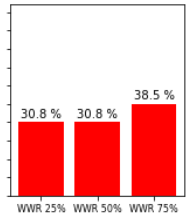	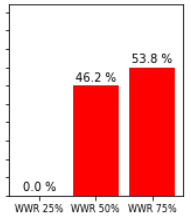	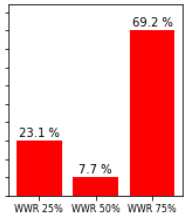	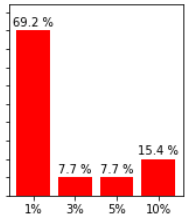	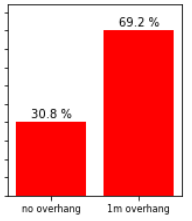
Form Factor (3:1)	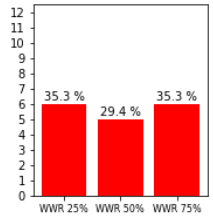	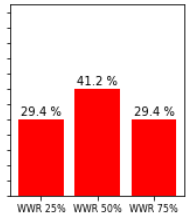	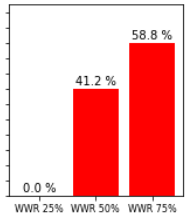	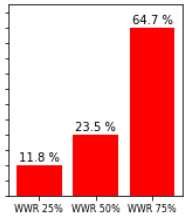	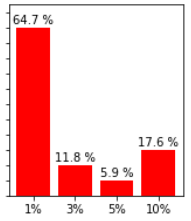	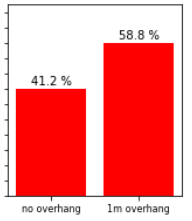
Form Factor (4:1)	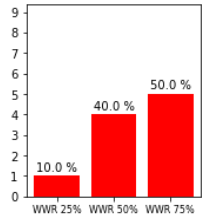	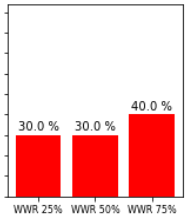	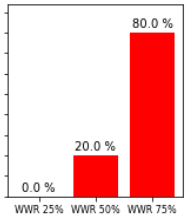	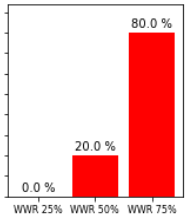	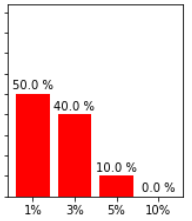	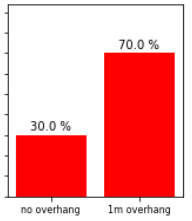

Table 3-8 Input variable histograms for Pareto Front 2 variable combination (EUI and View)

Form Factor (1:1)	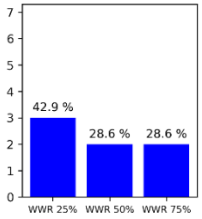	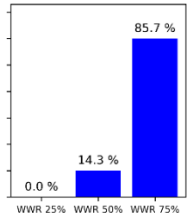	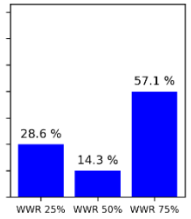	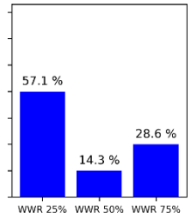	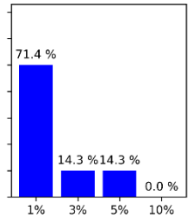	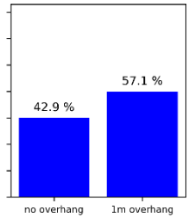
Form Factor (1.5:1)	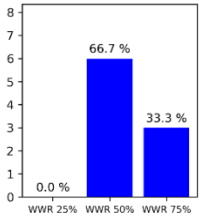	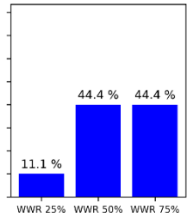	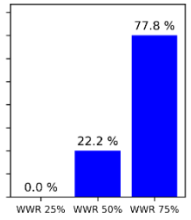	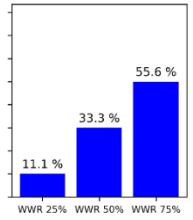	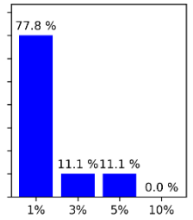	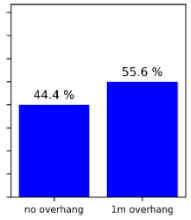
Form Factor (2:1)	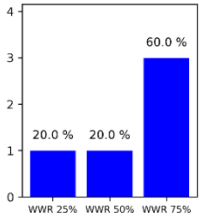	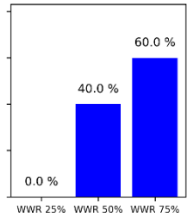	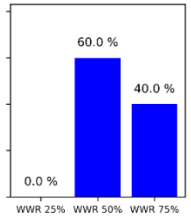	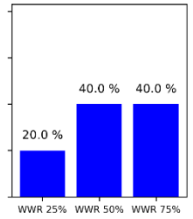	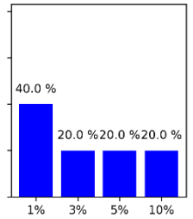	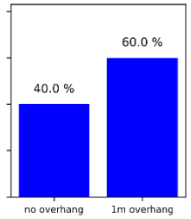
Form Factor (3:1)	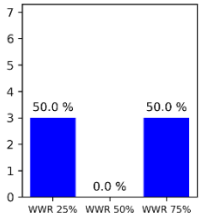	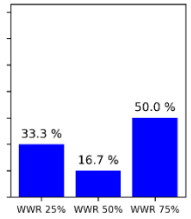	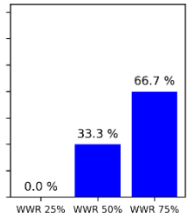	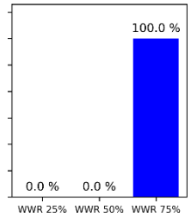	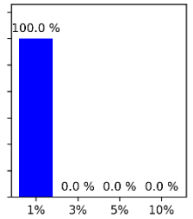	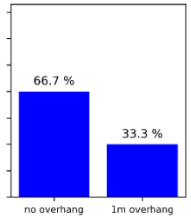
Form Factor (4:1)	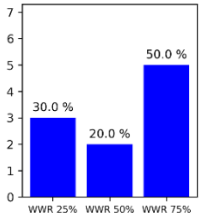	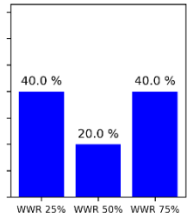	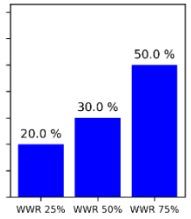	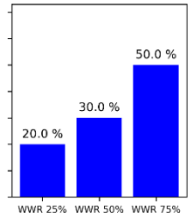	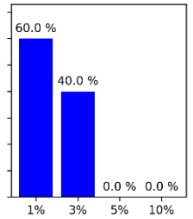	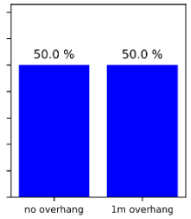

Table 3-9 Input variable histograms for Pareto Front 2 variable combination (EUI and PMV)

Form Factor (1:1)	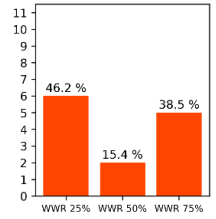	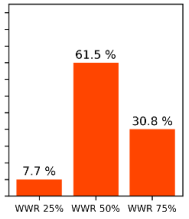	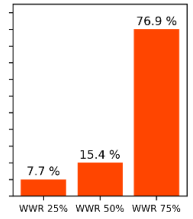	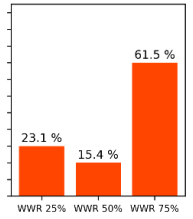	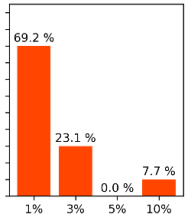	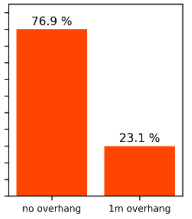
Form Factor (1.5:1)	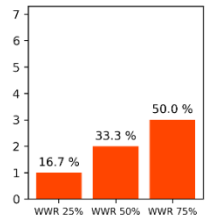	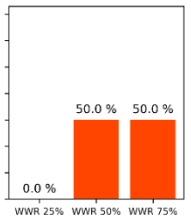	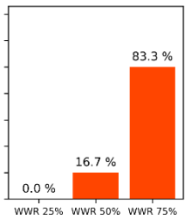	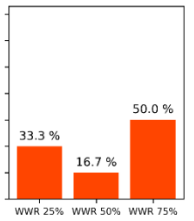	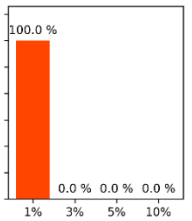	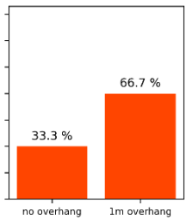
Form Factor (2:1)	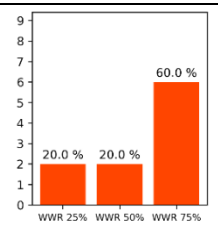	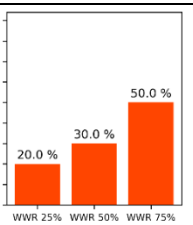	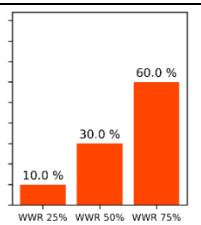	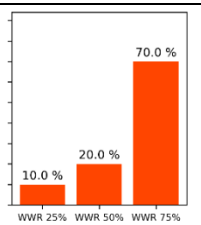	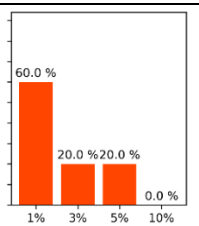	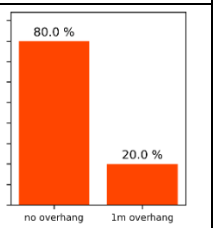
Form Factor (3:1)	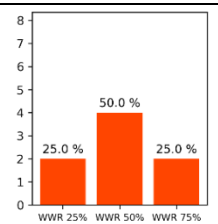	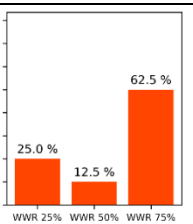	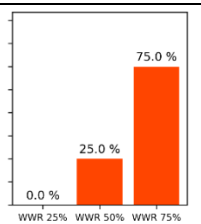	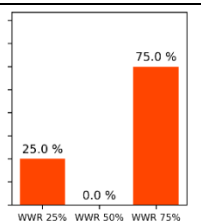	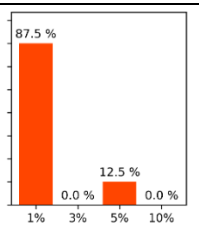	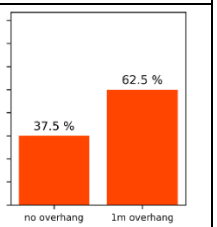
Form Factor (4:1)	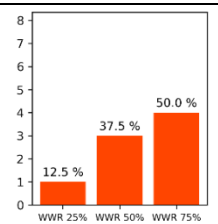	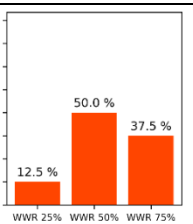	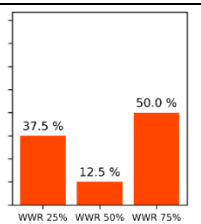	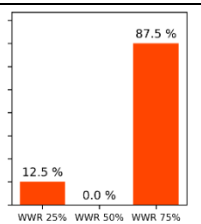	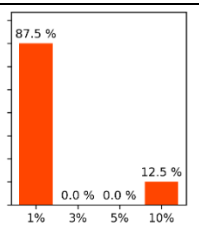	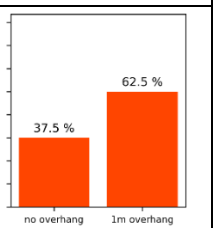

Table 3-10 Input variable histograms for Pareto Front 2 variable combination (UDI and View)

Form Factor (1:1)	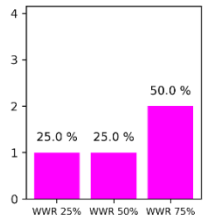	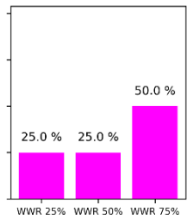	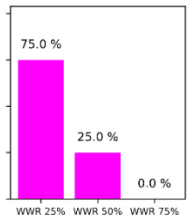	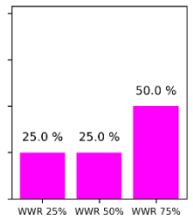	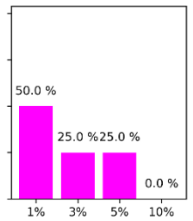	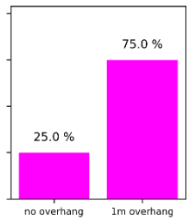
Form Factor (1.5:1)	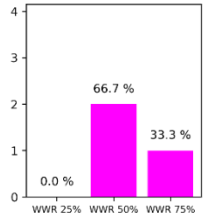	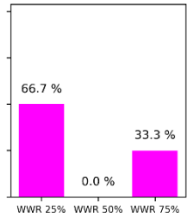	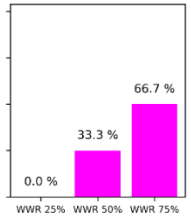	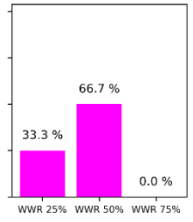	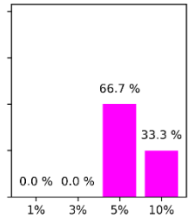	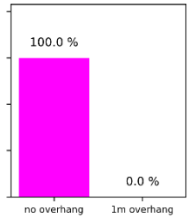
Form Factor (2:1)	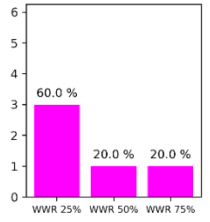	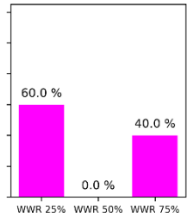	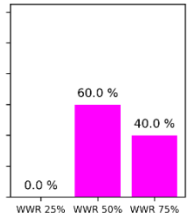	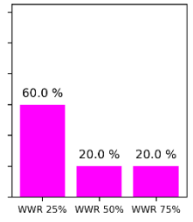	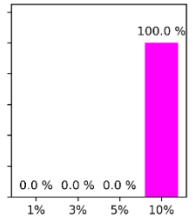	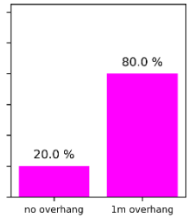
Form Factor (3:1)	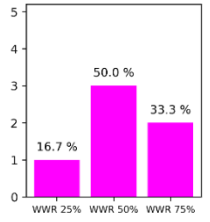	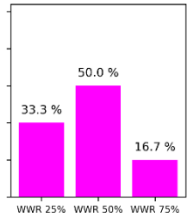	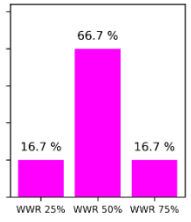	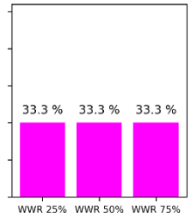	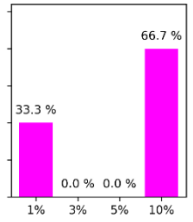	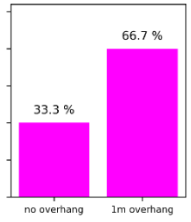
Form Factor (4:1)	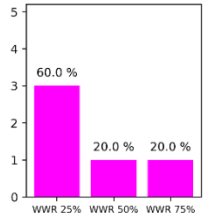	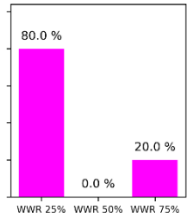	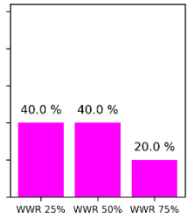	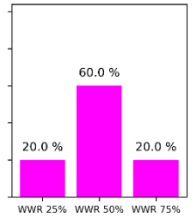	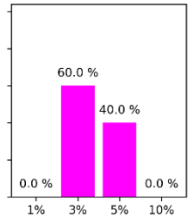	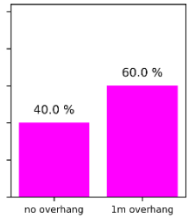

Table 3-11 Input variable histograms for Pareto Front 2 variable combination (UDI and PMV)

Form Factor (1:1)	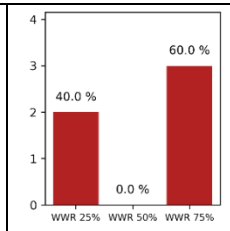	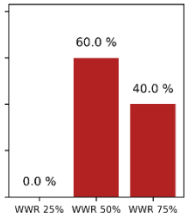	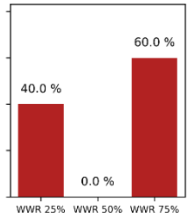	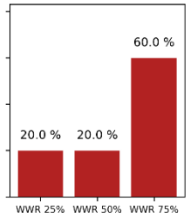	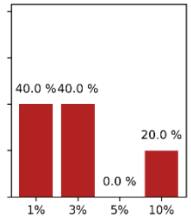	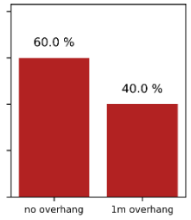
Form Factor (1.5:1)	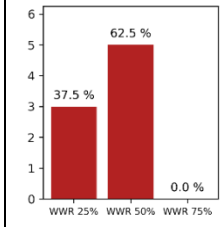	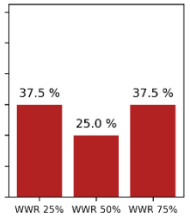	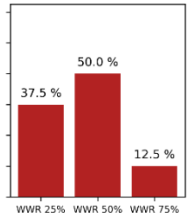	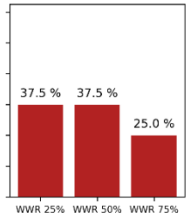	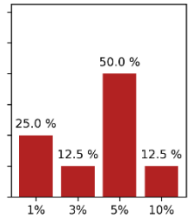	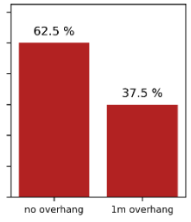
Form Factor (2:1)	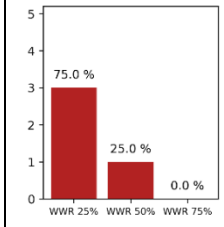	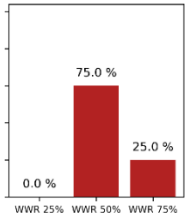	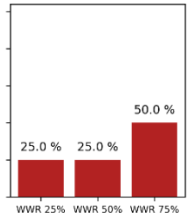	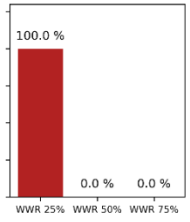	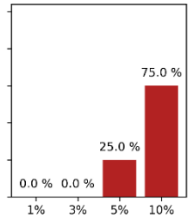	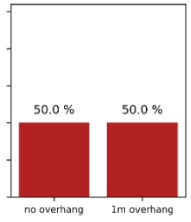
Form Factor (3:1)	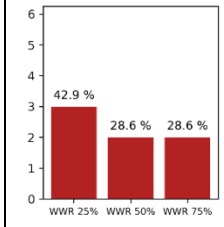	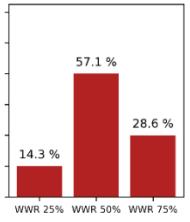	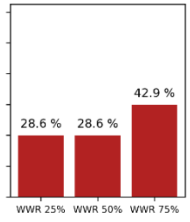	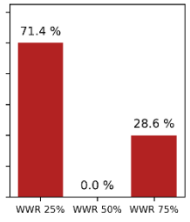	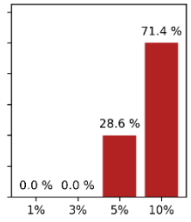	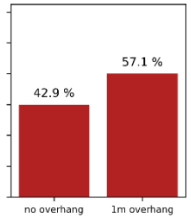
Form Factor (4:1)	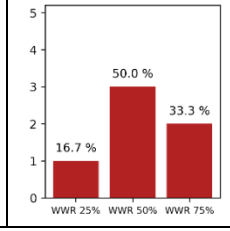	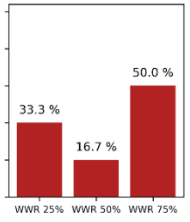	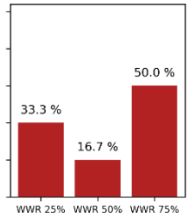	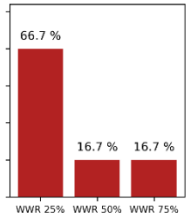	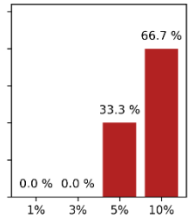	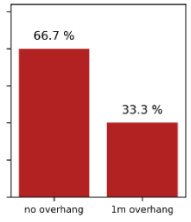

Table 3-12 Input variable histograms for Pareto Front 2 variable combination (View and PMV)

Form Factor (1:1)	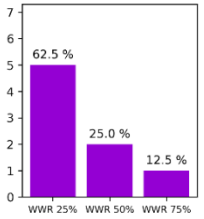	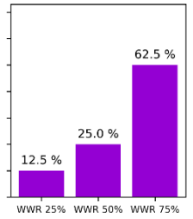	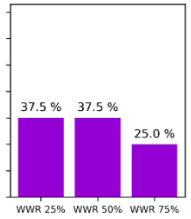	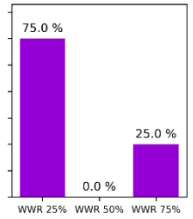	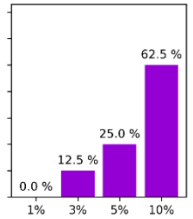	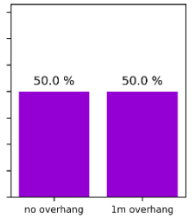
Form Factor (1.5:1)	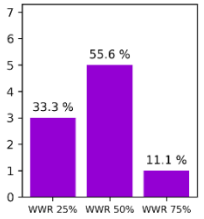	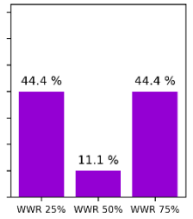	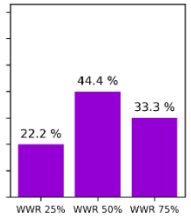	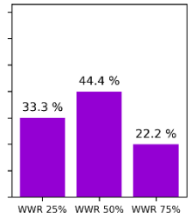	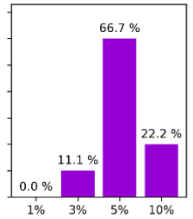	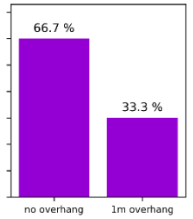
Form Factor (2:1)	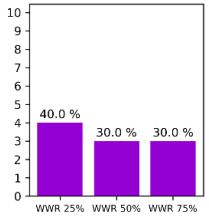	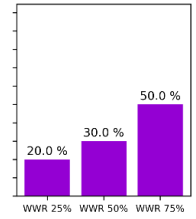	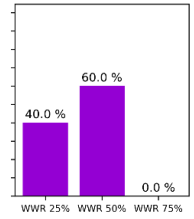	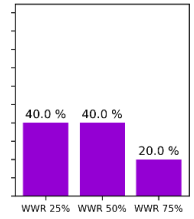	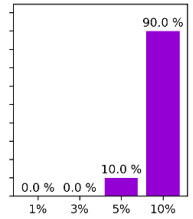	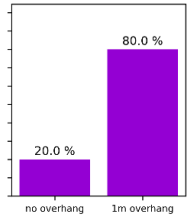
Form Factor (3:1)	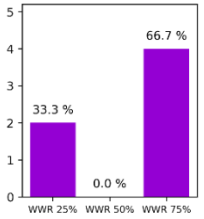	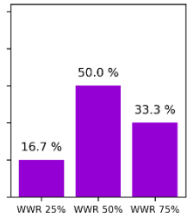	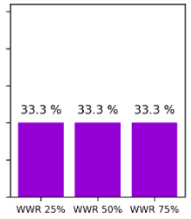	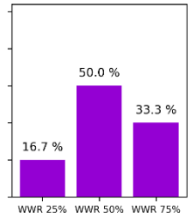	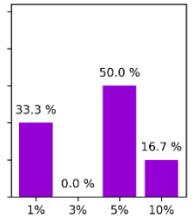	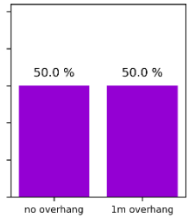
Form Factor (4:1)	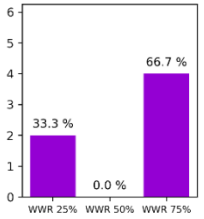	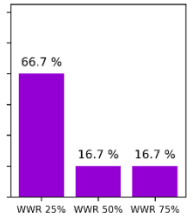	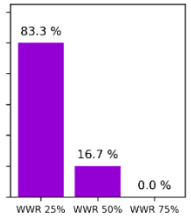	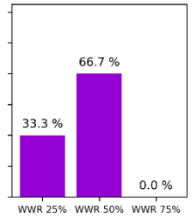	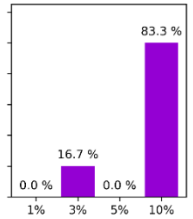	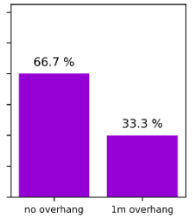

Table 3-13 Input variable histograms for Pareto Front 4 variable combination (EUI, UDI, View, and PMV)

Form Factor (1:1)	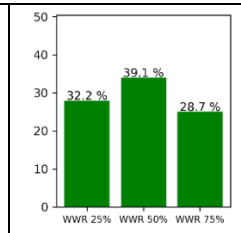	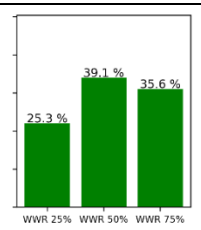	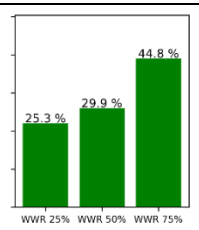	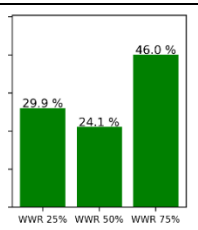	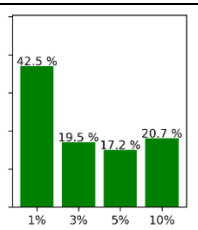	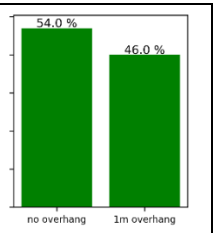
Form Factor (1.5:1)	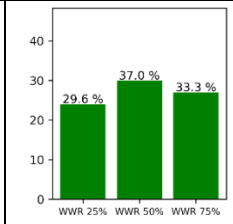	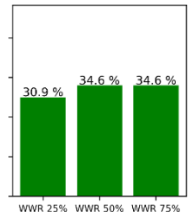	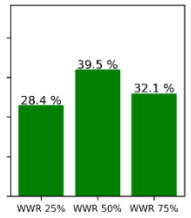	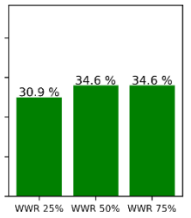	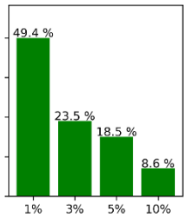	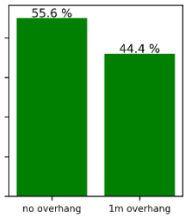
Form Factor (2:1)	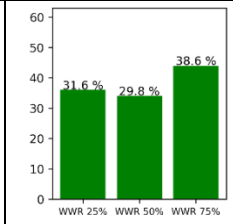	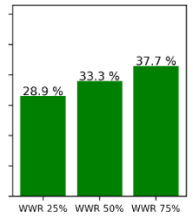	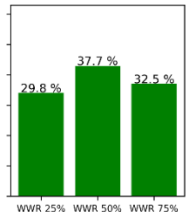	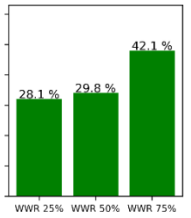	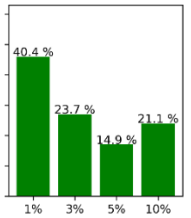	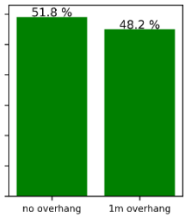
Form Factor (3:1)	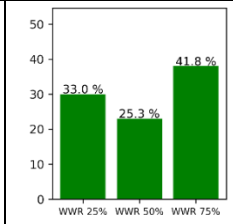	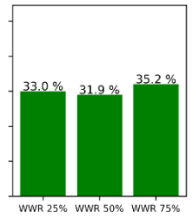	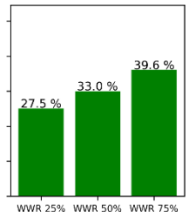	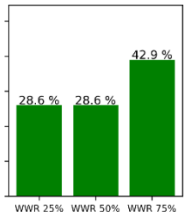	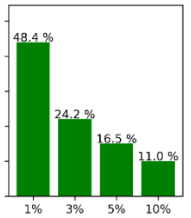	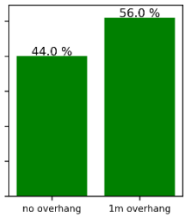
Form Factor (4:1)	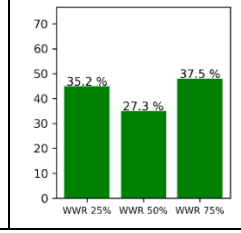	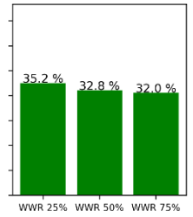	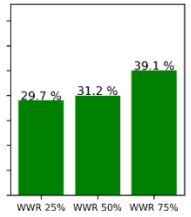	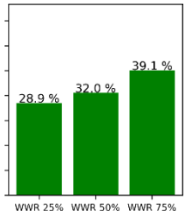	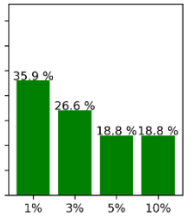	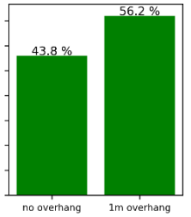

WWR by zone orientation

Three input options were used for the WWR variable are (WWR 25 %, WWR 50% and WWR 75%). The model also uses WWR variables for each orientation separately. For instance, the model can have 25% WWR for the South side, 50% WWR for the East and the West side and 75% WWR for North side as one of the iterations for the parametric run. Thus, this leads to 81 possible window combinations with just the WWR variable.

WWR North

For the North side, for most of the building form factors the optimum solution for two (2) variable combinations the results are a mix of all the WWR combinations and there are no conclusion best solutions patterns observed. The results are also inclusive when all four metrics are considered as in Table 3-13.

WWR East

The building form factor shifts from 1:1 (square-shaped building) to a building form factor of 4:1 where the East side is shorter. The optimum solution for two (2) variable combinations prefers lower WWR for two (2) variable combinations variables involving View to the outside For the other two (2) variable combinations variables involving EUI, UDI, and thermal comfort the results shift from high WWR ratio for from factor of 1:1 to an even split between all the WWR ratios for from factor of 4:1. When all the four metrics are considered as in Table 3-13, the overall solution shifts sightly high preference for higher WWR ratio for square shaped building to an even split for all the WWR for from factor of 4:1.

WWR South

For most buildings form factors for the South facing side South side. For all the five building factors, the preferred WWR for the best variable for a two (2) variable combination pareto results

involving EUI (such as EUI and UDI, EUI and View, EUI, and PMV) is predominantly higher WWR. This is coupled with the shade openness factor selected as 1% which doesn't allow much solar ration into the space. It is also highly likely that shade is closed for the south side during very timesteps with high glare causing daylight. The preferred WWR for the South side for the best variable for two (2) variable combinations involving variables other than EUI is a mix of all the possible WWR combinations. For various cases for two (2) variable combinations involving variables other than EUI, the shade openness factor preference is higher (5% and 10 % openness factor) which works well with lower WWR. When all four metrics are considered Table 3-13, the solution shifts sightly high preference for a higher WWR ratio for all the building form factors.

WWR West

For the West side, for most of the building form factors the optimum solution for two (2) variable combinations prefers higher WWR for two (2) variable combinations variables. When all four metrics are considered in Table 3-13, the overall best solution still prefers a higher WWR ratio for most building forms.

Shade openness factor

The four (4) input options used for the Shade openness factor for this variable are (1% openness, 3% openness, 5% openness, and 10 % openness. For all the five building factors, the preferred openness factor for the best variable for two combination pareto results involving EUI (such as EUI and UDI, EUI and View, EUI, and PMV) is predominantly a 1% openness factor. While the preferred openness factor for the best variable for two combination pareto results involving UDI and View (such as UDI and View, UDI and PMV, View, and PMV) is predominantly 5% and 10 % openness factor with more instances with the best solution with 10 % openness factor. When all four metrics are considered as in Table 3-13, of the solutions the best model uses a 1 % openness

factor with other 50 % of the time the best model uses a 3%, 5 %, and 10 % openness factor. The variation in result between building form factors is not significantly different.

Shade overhang depth

The two (2) input options used for the Shade overhang depth are either no shade overhang or shade overhang with a depth of 1 meter. As the variable is most suspected to impact the view and the UDI metrics more. As the view to the outside is based on the glare caused to the occupants and shade subsequently closing if the glare values (DGPs exceeding 0.35). The UDI is calculated for the bin between 100 and 2000. The results for two (2) variable combinations for the best solution selected for all the 6 combinations the results is mixed on if shade overhang should be used or not. And the results seem inconclusive. This might be possible as a 1-meter shade overhang might not be sufficient distance for a window overhang to influence the results. When all four metrics are considered as in Table 3-13, no overhangs are slightly preferable for square buildings whereas overhangs with 1 meter depth are preferable for more rectangular buildings. However, the difference is very close to 50-50. Therefore, the variation in result between building form factors is slightly different.

3.7 CONCLUSIONS

The energy consumption and the visual comfort depend on multiple variables, such as different room sizes, zone orientation, and building location, and various other variables such as window configurations, sizes, and shading materials. Past studies have used parametric/optimization methods to find the ideal combination of these variables to optimize both Energy Use Intensity (EUI) and UDI (Useful Daylight Illuminance). However, these do not consider metrics such as glare, view outside, and thermal comfort for an optimal solution. Further, studies using parametric/optimization models with shading systems as roller shades are limited, and further

roller shade studies that switch between different shade positions based on a control strategy are rare for parametric and optimization studies. This study thus aims to optimize various variables such as WWR for all four orientations, shade material properties such as openness factor, and the length of the building overhang depth to estimate best-case scenarios for UDI, EUI, glare, and view to the outside, and thermal comfort using PMV (Predicted Mean Vote). The control strategy used for this study is based on glare that restricts the glare under DGP < 0.35 using roller shades controlled at (3) positions (Fully closed, 50% closed, and fully open). The study also aims to find the best-case solution for nine (9) different building aspect ratios. The study uses Rhino/Grasshopper interface with Honeybee and Ladybug to develop a daylighting model (RADIANCE) and an energy model (EnergyPlus) for a small office building.

The study concludes that the best solution for two (2) variable combinations such as with one of the variables involving EUI (such as EUI and UDI, EUI and View, EUI, and PMV) the solution) is predominantly a low 1% openness factor for shade openness factor combined with high WWR values (such as 75 % and 50%) for the South and West facing direction. The other set of optimum solutions involves a high shade openness factor (5% and 10 %) openness factor for shade openness factor combined with low WWR values (such as 25 % and 50%). For the north-facing direction, the optimum values for results do not show any particular pattern. For the variable shade overhang depth, no overhangs are slightly preferable for square buildings whereas overhangs with 1 meter depth are preferable for more rectangular buildings. However, the difference is very close to 50-50. Therefore, the variation in result between building form factors is only slightly different.

There are some limitations to this study, as well as opportunities for future work. (a) The minimum timestep for the analysis is one hour due to the significant time taken for RADIANCE simulation for granular timesteps. Studies with more granular timesteps for daylighting and energy simulation

can highlight incremental savings by capturing fluctuating weather conditions. (b) The occupancy schedule used in the model is based on the DOE model Prototype Building model's hourly occupancy schedule. A stochastic model or a case study that accounts for occupancy at a finer timestep. (c) While using the Ladybug tool's cloud computing option allows the author to develop a large parametric model, even with cloud-based tools, it can still be very difficult to add every variable that influences the model's performance. Further, cloud-based tools currently only allow for the development of parametric models and not optimization-based models. Optimization-based algorithms with cloud-based computing can allow more variables to be incorporated into the simulation for a more fine-tuned result. (d) This study explored input variables such as WWR, shade properties, and shade overhang depth. However, other variables, such as glazing type, minimum windowsill heights, and different climate zones, can provide further insight into the impact. For future work, the author proposes to also study the impact of daylighting and its controls on different types of commercial buildings. (e) The shade depth variable can be optimized for each orientation instead of using the same shade depth for all directions (that converts one variable into four additional variables, increasing the number of simulations significantly). (f) The study only considers form factors with rectangular shapes. However, buildings with non-rectangular shapes such as U-shaped, T-shaped, H-shaped, trapezoidal, and other free-form building shapes combined with the effect of daylight and energy performance are not well studied. If such non-rectangular building shapes with multiple stories are analyzed, the shading effect of parts of the same building over other parts of the building must be carefully evaluated.

REFERENCES

Atzeri, A., Cappelletti, F., & Gasparella, A. (2014). Internal versus external shading devices performance in office buildings. *Energy Procedia*, *45*, 463–472. https://doi.org/10.1016/j.egypro.2014.01.050

Atzeri, A. M., Gasparella, A., Cappelletti, F., & Tzempelikos, A. (2018). Comfort and energy performance analysis of different glazing systems coupled with three shading control strategies. *Science and Technology for the Built Environment*, *24*(5), 545–558. https://doi.org/10.1080/23744731.2018.1449517

Bakmohammadi, P., & Noorzai, E. (2020). Optimization of the design of the primary school classrooms in terms of energy and daylight performance considering occupants' thermal and visual comfort. *Energy Reports*, *6*, 1590–1607. https://doi.org/10.1016/j.egyr.2020.06.008

Bian, Y., Dai, Q., Ma, Y., & Liu, L. (2020). Variable set points of glare control strategy for side-lit spaces: Daylight glare tolerance by time of day. *Solar Energy*, *201*(March), 268–278. https://doi.org/10.1016/j.solener.2020.03.016

Bourgeois, D., Reinhart, C., & Macdonald, I. (2006). Adding advanced behavioural models in whole building energy simulation: A study on the total energy impact of manual and automated lighting control. *Energy and Buildings*, *38*(7), 814–823. https://doi.org/10.1016/j.enbuild.2006.03.002

Carlucci, S., Causone, F., De Rosa, F., & Pagliano, L. (2015). A review of indices for assessing visual comfort with a view to their use in optimization processes to support building integrated design. *Renewable and Sustainable Energy Reviews*, *47*(7491), 1016–1033. https://doi.org/10.1016/j.rser.2015.03.062

Da Silva, P. C., Leal, V., & Andersen, M. (2012a). Influence of shading control patterns on the energy assessment of office spaces. *Energy and Buildings*, *50*, 35–48. https://doi.org/10.1016/j.enbuild.2012.03.019

Da Silva, P. C., Leal, V., & Andersen, M. (2012b). Influence of shading control patterns on the energy assessment of office spaces. *Energy and Buildings*, *50*, 35–48. https://doi.org/10.1016/j.enbuild.2012.03.019

de Vries, S. B., Loonen, R. C. G. M., & Hensen, J. L. M. (2021). Simulation-aided development of automated solar shading control strategies using performance mapping and statistical classification. *Journal of Building Performance Simulation*, *14*(6), 770–792. https://doi.org/10.1080/19401493.2021.1887355

Do, C. T., & Chan, Y. C. (2020). Evaluation of the effectiveness of a multi-sectional facade with Venetian blinds and roller shades with automated shading control strategies. *Solar Energy*, *212*(October), 241–257. https://doi.org/10.1016/j.solener.2020.11.003

Do, C. T., & Chan, Y. C. (2021). Daylighting performance analysis of a facade combining

daylight-redirecting window film and automated roller shade. *Building and Environment*, *191*(October 2020), 107596. https://doi.org/10.1016/j.buildenv.2021.107596

Dogan, T., Saratsis, E., & Reinhart, C. (2015). THE OPTIMIZATION POTENTIAL OF FLOOR-PLAN TYPOLOGIES IN EARLY DESIGN ENERGY MODELING Massachusetts Institute of Technology , Cambridge , MA 02139 , USA. *Building Simulation Conference*.

Edwards, L., & Torcellini, P. (2002). A Literature Review of the Effects of Natural Light on Building Occupants A Literature Review of the Effects of Natural Light on Building Occupants. *Contract*, *July*, 55.

Eltaweel, A., & Yuehong, S. (2017). Using integrated parametric control to achieve better daylighting uniformity in an office room: A multi-Step comparison study. *Energy and Buildings*, *152*, 137–148. https://doi.org/10.1016/j.enbuild.2017.07.033

Fang, Y., & Cho, S. (2019). Design optimization of building geometry and fenestration for daylighting and energy performance. *Solar Energy*, *191*(November 2018), 7–18. https://doi.org/10.1016/j.solener.2019.08.039

Feng, J., Luo, X., Gao, M., Abbas, A., Xu, Y. P., & Pouramini, S. (2021). Minimization of energy consumption by building shape optimization using an improved Manta-Ray Foraging Optimization algorithm. *Energy Reports*, *7*, 1068–1078. https://doi.org/10.1016/j.egyr.2021.02.028

González, J., & Fiorito, F. (2015). *Daylight Design of Office Buildings: Optimisation of External Solar Shadings by Using Combined Simulation Methods*. 560–580. https://doi.org/10.3390/buildings5020560

Goovaerts, C., Descamps, F., & Jacobs, V. A. (2017). Shading control strategy to avoid visual discomfort by using a low-cost camera: A field study of two cases. *Building and Environment*, *125*, 26–38. https://doi.org/10.1016/j.buildenv.2017.08.030

Gratia, E., & De Herde, A. (2003). Design of low energy office buildings. *Energy and Buildings*, *35*(5), 473–491. https://doi.org/10.1016/S0378-7788(02)00160-3

Hegazy, M. A., Attia, S., & Moro, J. L. (2013). Parametric analysis for daylight autonomy and energy consumption in hot climates. *Proceedings of BS 2013: 13th Conference of the International Building Performance Simulation Association*, 2232–2240.

Karlsen, L., Heiselberg, P., Bryn, I., & Johra, H. (2016). Solar shading control strategy for office buildings in cold climate. *Energy and Buildings*, *118*(0130), 316–328. https://doi.org/10.1016/j.enbuild.2016.03.014

Kirimtat, A., Krejcar, O., Ekici, B., & Fatih Tasgetiren, M. (2019). Multi-objective energy and daylight optimization of amorphous shading devices in buildings. *Solar Energy*, *185*(March), 100–111. https://doi.org/10.1016/j.solener.2019.04.048

Konis, K., Gamas, A., & Kensek, K. (2016). Passive performance and building form: An optimization framework for early-stage design support. *Solar Energy*, *125*, 161–179. https://doi.org/10.1016/j.solener.2015.12.020

Konstantzos, I., Tzempelikos, A., & Chan, Y. C. (2015). Experimental and simulation analysis of daylight glare probability inoffices with dynamic window shades. *Building and Environment*, *87*, 244–254. https://doi.org/10.1016/j.buildenv.2015.02.007

Krarti, M., Erickson, P. M., & Hillman, T. C. (2005). A simplified method to estimate energy savings of artificial lighting use from daylighting. *Building and Environment*, *40*(6), 747–754. https://doi.org/10.1016/j.buildenv.2004.08.007

Kunwar, N., & Bhandari, M. (2020). A comprehensive analysis of energy and daylighting impact of window shading systems and control strategies on commercial buildings in the United States. *Energies*, *13*(9). https://doi.org/10.3390/en13092401

Kunwar, N., Cetin, K. S., Passe, U., Zhou, X., & Li, Y. (2019a). Full-scale experimental testing of integrated dynamically-operated roller shades and lighting in perimeter office spaces. *Solar Energy*, *186*(March), 17–28. https://doi.org/10.1016/j.solener.2019.04.069

Kunwar, N., Cetin, K. S., Passe, U., Zhou, X., & Li, Y. (2019b). Full-scale experimental testing of integrated dynamically-operated roller shades and lighting in perimeter office spaces. *Solar Energy*, *186*(February), 17–28. https://doi.org/10.1016/j.solener.2019.04.069

Lee, E. S., & Selkowitz, S. E. (2006). The New York Times Headquarters daylighting mockup: Monitored performance of the daylighting control system. *Energy and Buildings*, *38*(7), 914–929. https://doi.org/10.1016/j.enbuild.2006.03.019

Lee, K. S., Han, K. J., & Lee, J. W. (2016). Feasibility study on parametric optimization of daylighting in building shading design. *Sustainability (Switzerland)*, *8*(12), 1–16. https://doi.org/10.3390/su8121220

M. ElBatran, R., & Ismaeel, W. S. E. (2021). Applying a parametric design approach for optimizing daylighting and visual comfort in office buildings. *Ain Shams Engineering Journal*, *12*(3), 3275–3284. https://doi.org/10.1016/j.asej.2021.02.014

Mahdavinejad, M., & Mohammadi, S. (2018). Parametric optimization of daylight and thermal performance through louvers in hot and dry climate of Tehran. *Journal of Fundamental and Applied Sciences*, *8*(3), 1221. https://doi.org/10.4314/jfas.v8i3.32

Manzan, M., & Clarich, A. (2017). FAST energy and daylight optimization of an office with fixed and movable shading devices. *Building and Environment*, *113*, 175–184. https://doi.org/10.1016/j.buildenv.2016.09.035

Mitra, D., Chu, Y., & Cetin, K. (2022). COVID-19 impacts on residential occupancy schedules and activities in U . S . Homes in 2020 using ATUS. *Applied Energy*, *324*(August), 119765. https://doi.org/10.1016/j.apenergy.2022.119765

Mokrzecka, M. (2018). Influence of building shape and orientation on heating demand: Simulations for student dormitories in temperate climate conditions. *E3S Web of Conferences*, *44*, 1–8. https://doi.org/10.1051/e3sconf/20184400117

Motamedi, S., & Liedl, P. (2017). Integrative algorithm to optimize skylights considering fully impacts of daylight on energy. *Energy and Buildings*, *138*, 655–665. https://doi.org/10.1016/j.enbuild.2016.12.045

Nasrollahi, N., & Shokry, E. (2020). Parametric analysis of architectural elements on daylight, visual comfort, and electrical energy performance in the study spaces. *Journal of Daylighting*, *7*(1), 57–72. https://doi.org/10.15627/jd.2020.5

Pilechiha, P., Mahdavinejad, M., Pour Rahimian, F., Carnemolla, P., & Seyedzadeh, S. (2020). Multi-objective optimisation framework for designing office windows: quality of view, daylight and energy efficiency. *Applied Energy*, *261*(July 2019), 114356. https://doi.org/10.1016/j.apenergy.2019.114356

Rea, M. S. (1984). Window blind occlusion: a pilot study. *Building and Environment*, *19*(2), 133–137. https://doi.org/10.1016/0360-1323(84)90038-6

Reffat, R. M., & Ahmad, R. M. (2020). Determination of optimal energy-efficient integrated daylighting systems into building windows. *Solar Energy*, *209*(September), 258–277. https://doi.org/10.1016/j.solener.2020.08.086

Sadeghi, S. A., Karava, P., Konstantzos, I., & Tzempelikos, A. (2016). Occupant interactions with shading and lighting systems using different control interfaces: A pilot field study. *Building and Environment*, *97*, 177–195. https://doi.org/10.1016/j.buildenv.2015.12.008

Shen, E., Hu, J., & Patel, M. (2014). Energy and visual comfort analysis of lighting and daylight control strategies. *Building and Environment*, *78*, 155–170. https://doi.org/10.1016/j.buildenv.2014.04.028

Shen, H., & Tzempelikos, A. (2012). Daylighting and energy analysis of private offices with automated interior roller shades. *Solar Energy*, *86*(2), 681–704. https://doi.org/10.1016/j.solener.2011.11.016

Shishegar, N., & Boubekri, M. (2016). Natural Light and Productivity: Analyzing the Impacts of Daylighting on Students' and Workers' Health and Alertness. *International Journal of Advances in Chemical Engineering and Biological Sciences*, *3*(1). https://doi.org/10.15242/ijacebs.ae0416104

Smith, L. (2012). Beyond the shoebox: Thermal zoning approaches for complex building shapes. *ASHRAE Transactions*, *118*(PART 2), 141–148.

Toutou, A., Fikry, M., & Mohamed, W. (2018). The parametric based optimization framework daylighting and energy performance in residential buildings in hot arid zone. *Alexandria Engineering Journal*, *57*(4), 3595–3608. https://doi.org/10.1016/j.aej.2018.04.006

Tzempelikos, Athanasios, & Ph, D. (n.d.). *An Experimental and Simulation Study of Lighting Performance in Offices with Automated Roller Shades*.

Tzempelikos, Athanassios, & Athienitis, A. K. (2007). *The impact of shading design and control on building cooling and lighting demand*. *81*, 369–382. https://doi.org/10.1016/j.solener.2006.06.015

Vasquez, N. G., Rupp, R. F., Andersen, R. K., & Toftum, J. (2022). Occupants' responses to window views, daylighting and lighting in buildings: A critical review. *Building and Environment*, *219*(February), 109172. https://doi.org/10.1016/j.buildenv.2022.109172

Wagdy, A., & Fathy, F. (2015). A parametric approach for achieving optimum daylighting performance through solar screens in desert climates. *Journal of Building Engineering*, *3*, 155–170. https://doi.org/10.1016/j.jobe.2015.07.007

Wankanapon, P., & Mistrick, R. G. (n.d.). *Roller Shades and Automatic Lighting Control with Solar Radiation Control Strategies*. 35–42.

Xiong, J., & Tzempelikos, A. (2016). Model-based shading and lighting controls considering visual comfort and energy use. *Solar Energy*, *134*, 416–428. https://doi.org/10.1016/j.solener.2016.04.026

Zani, A., Andaloro, M., Deblasio, L., Ruttico, P., & Mainini, A. G. (2017). Computational Design and Parametric Optimization Approach with Genetic Algorithms of an Innovative Concrete Shading Device System. *Procedia Engineering*, *180*, 1473–1483. https://doi.org/10.1016/j.proeng.2017.04.310

Zhang, A., Bokel, R., van den Dobbelsteen, A., Sun, Y., Huang, Q., & Zhang, Q. (2017a). Optimization of thermal and daylight performance of school buildings based on a multi-objective genetic algorithm in the cold climate of China. *Energy and Buildings*, *139*, 371–384. https://doi.org/10.1016/j.enbuild.2017.01.048

Zhang, A., Bokel, R., van den Dobbelsteen, A., Sun, Y., Huang, Q., & Zhang, Q. (2017b). The effect of geometry parameters on energy and thermal performance of school buildings in cold climates of China. *Sustainability (Switzerland)*, *9*(10). https://doi.org/10.3390/su9101708

APPENDIX 3-A: TWO VARIABLE SCATTER PLOTS

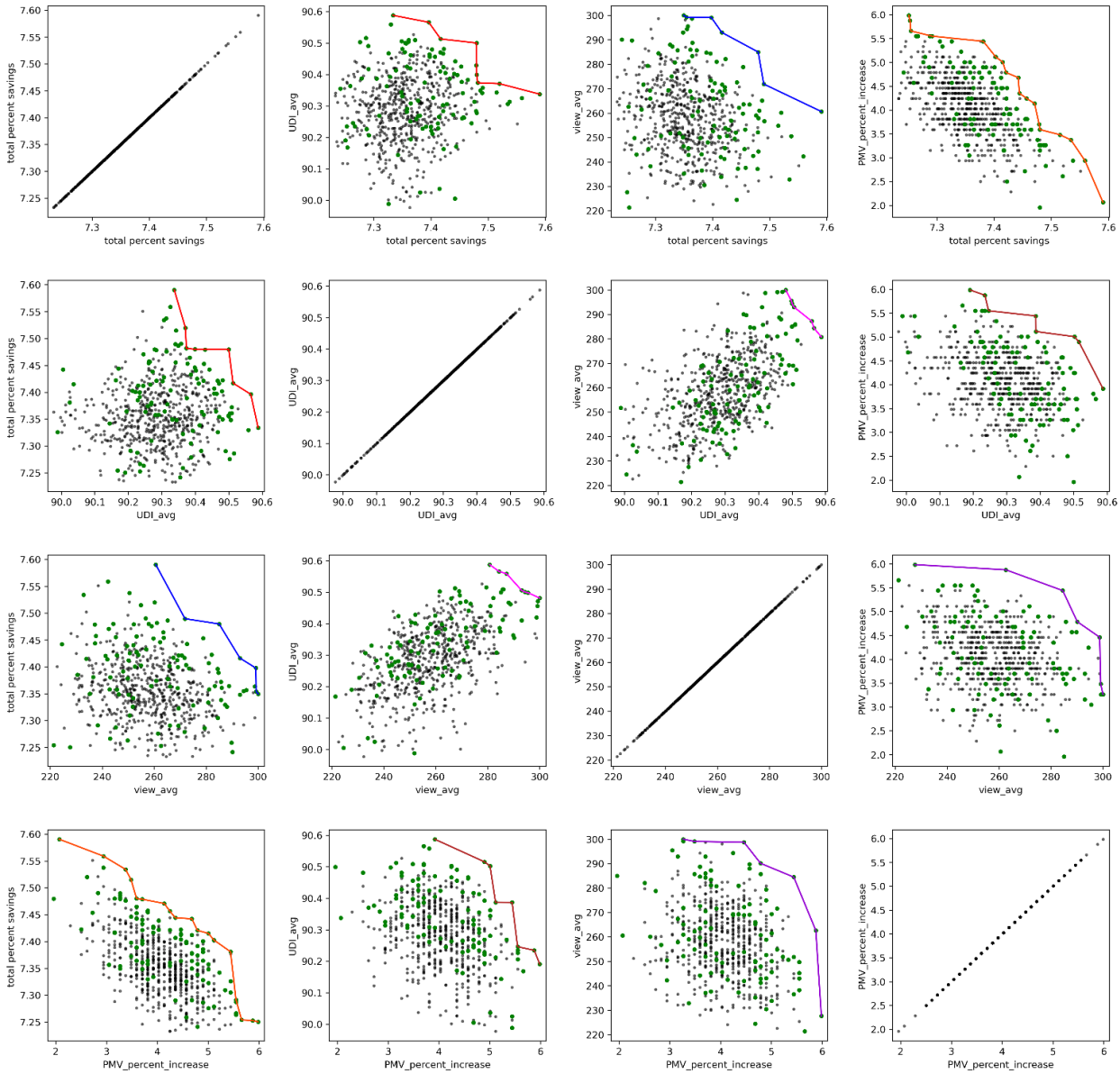

Figure 3-A.1 Scatter plot and parent front for form factor (1:4)

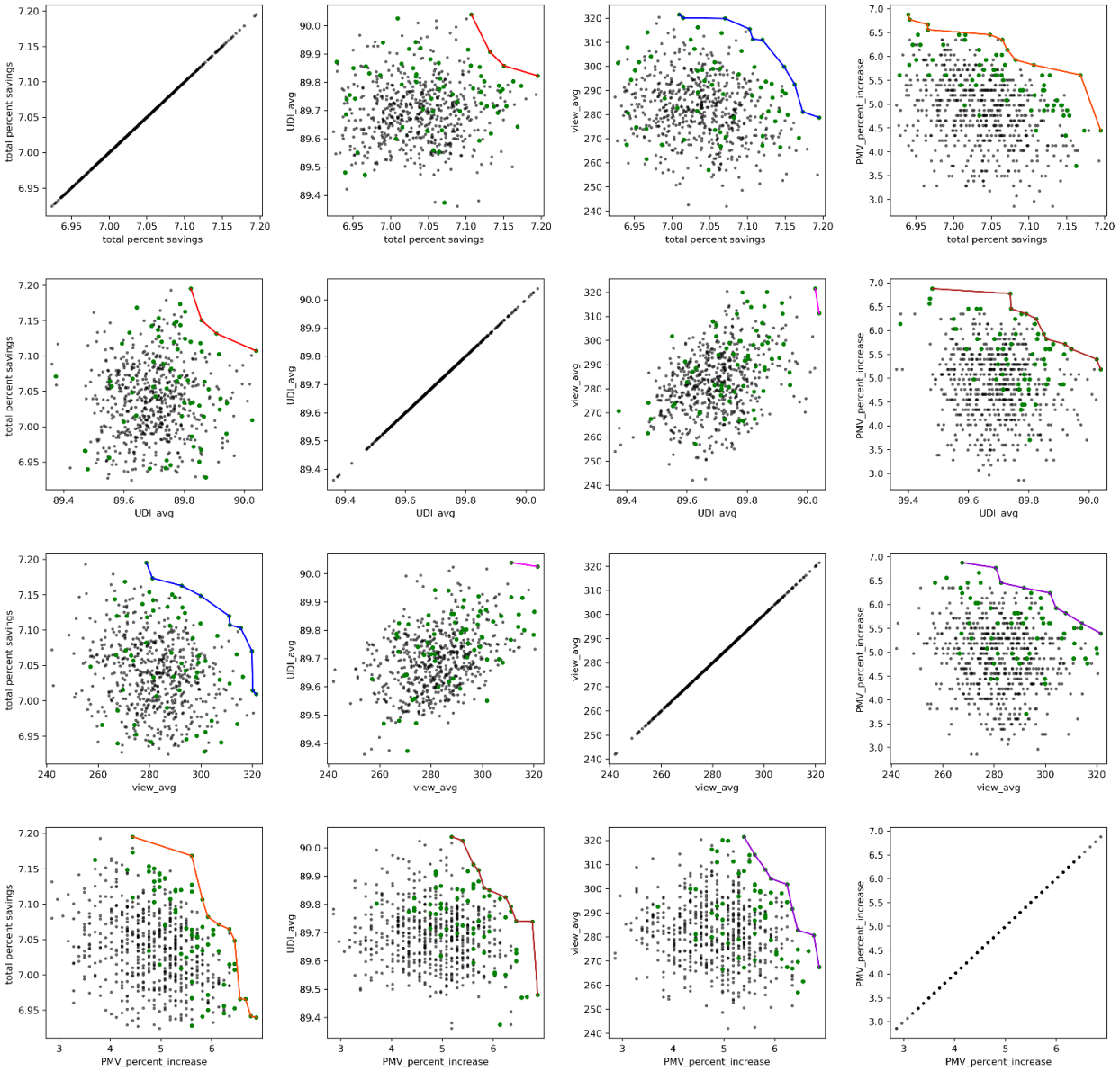

Figure 3-A.2 Scatter plot and parent front for form factor (1:3)

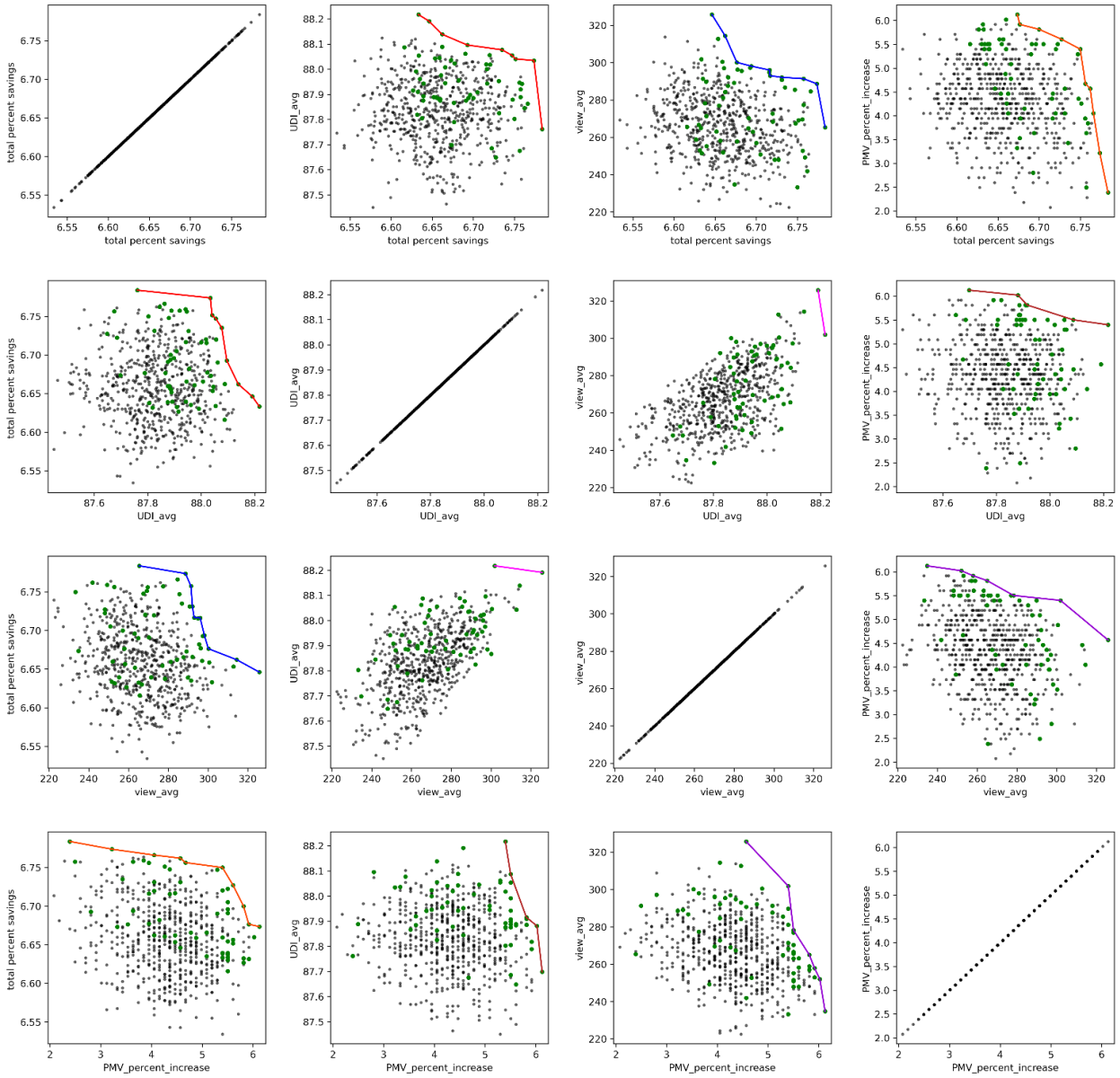

Figure 3-A.3 Scatter plot and parent front for form factor (1:2)

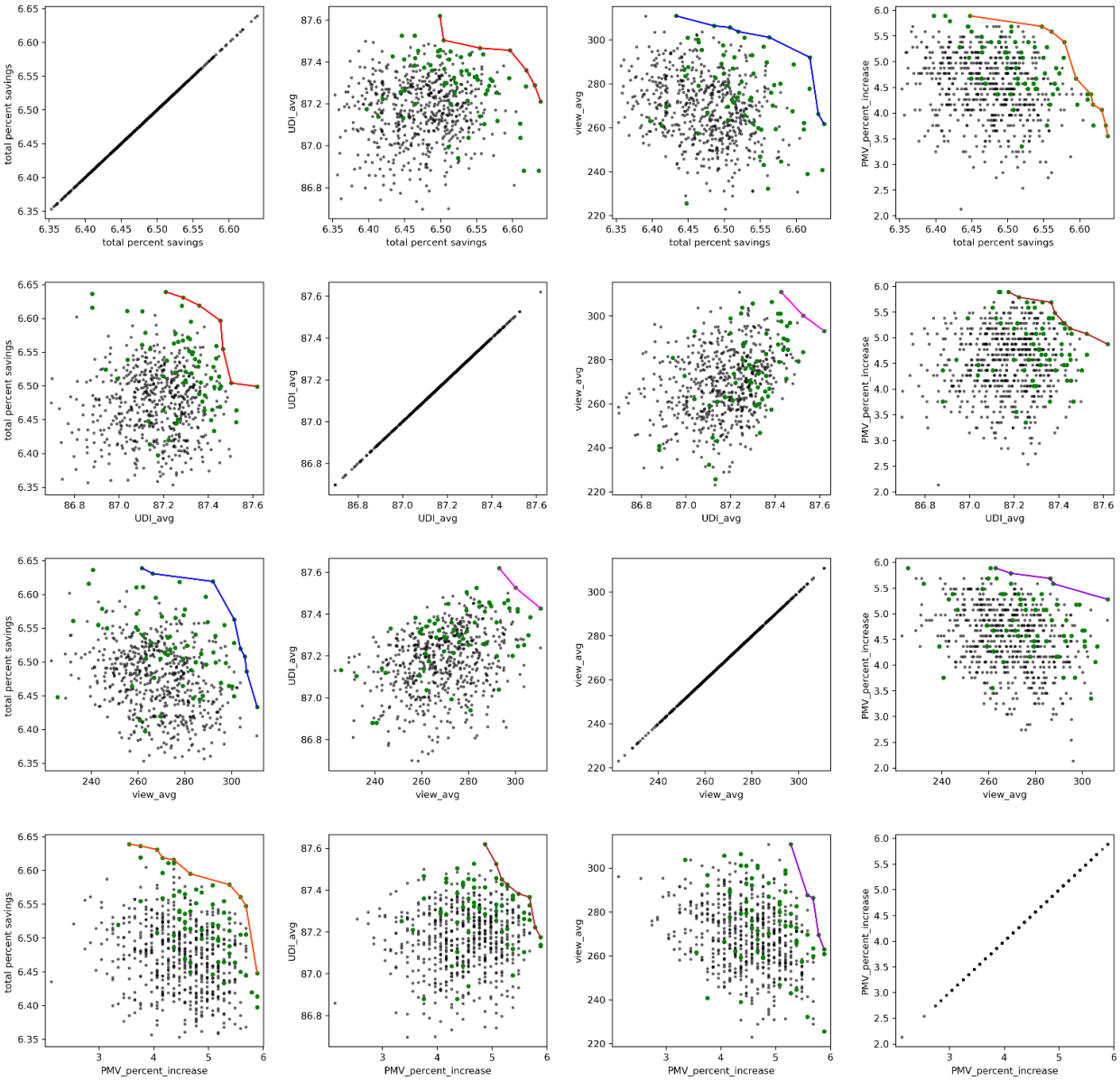

Figure 3-A.4 Scatter plot and parent front for form factor (1:1.5)

APPENDIX 3-B: TWO VARIABLE PARETO RESULTS

Table 3-B.1 Input variable histograms for Pareto Front 2 variable combination (EUI and UDI)

Form Factor (1:4)	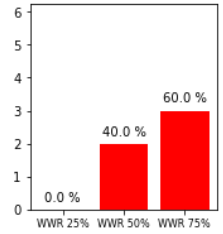	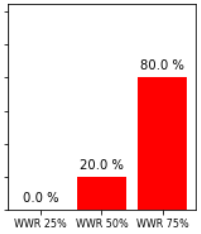	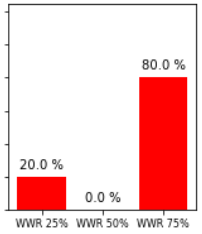	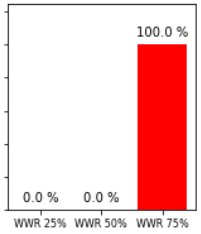	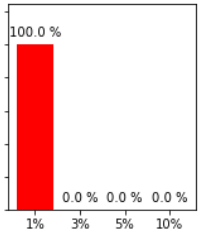	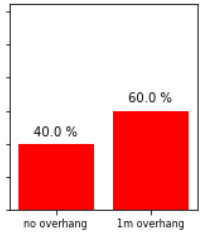
Form Factor (1:3)	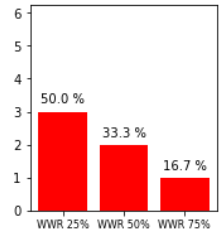	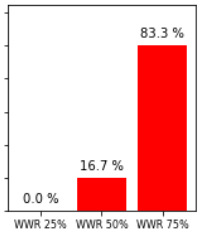	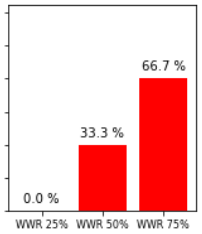	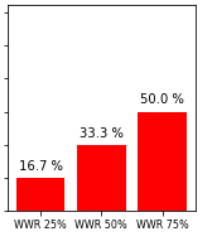	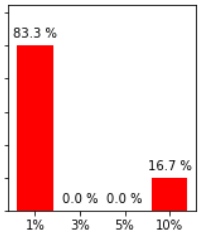	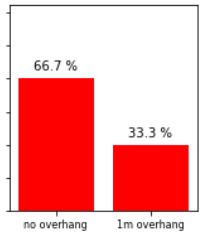
Form Factor (1:2)	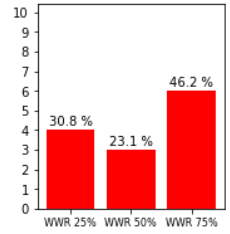	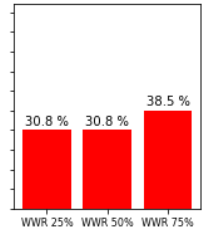	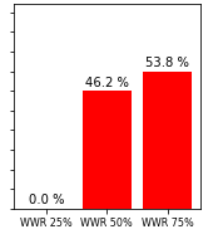	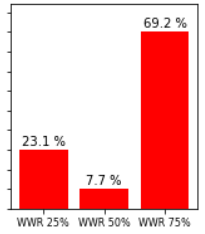	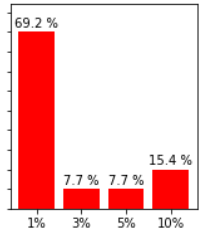	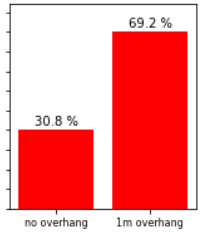
Form Factor (1:1.5)	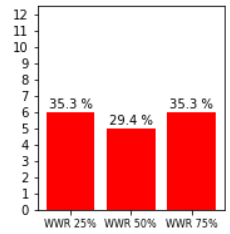	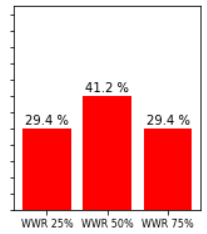	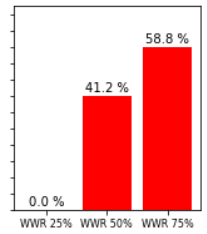	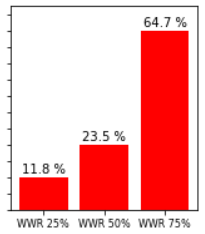	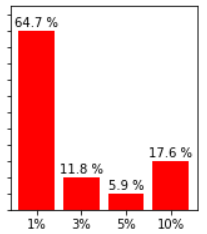	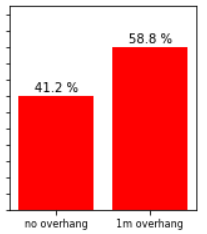

Table 3-B.1 (cont'd)

Form Factor (1:1)	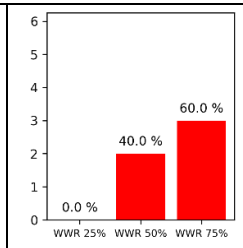	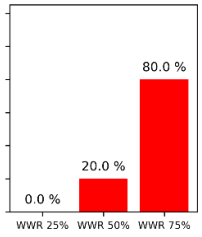	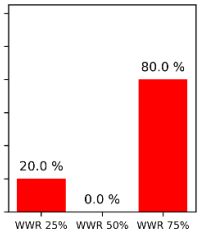	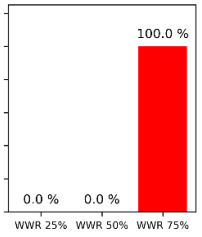	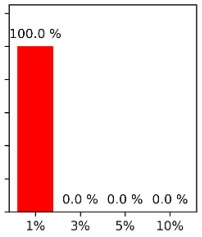	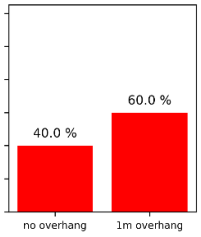
Form Factor (1.5:1)	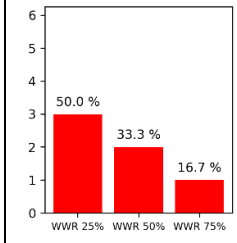	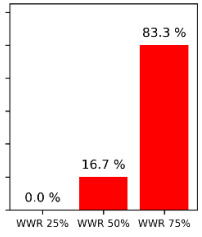	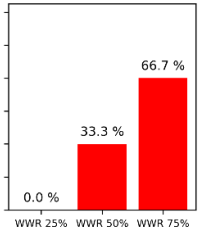	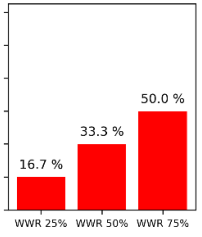	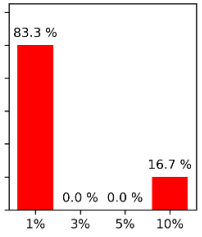	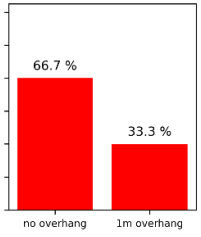
Form Factor (2:1)	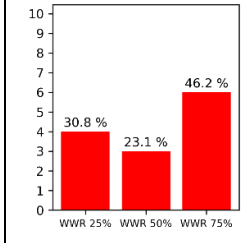	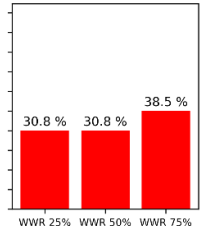	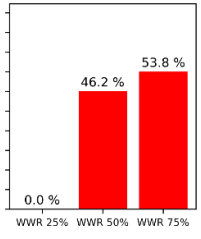	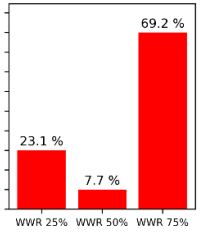	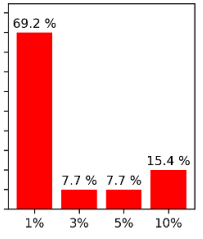	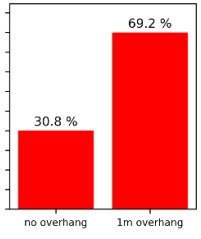
Form Factor (3:1)	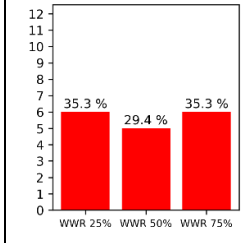	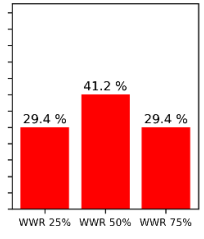	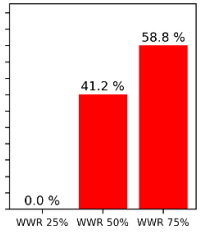	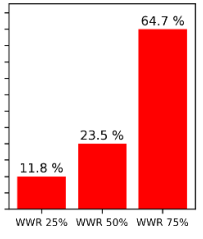	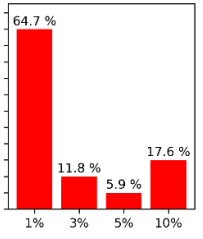	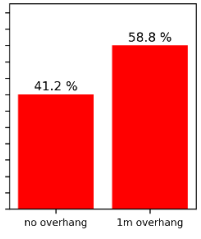

Table 3-B.1 (cont'd)

Form Factor (4:1)	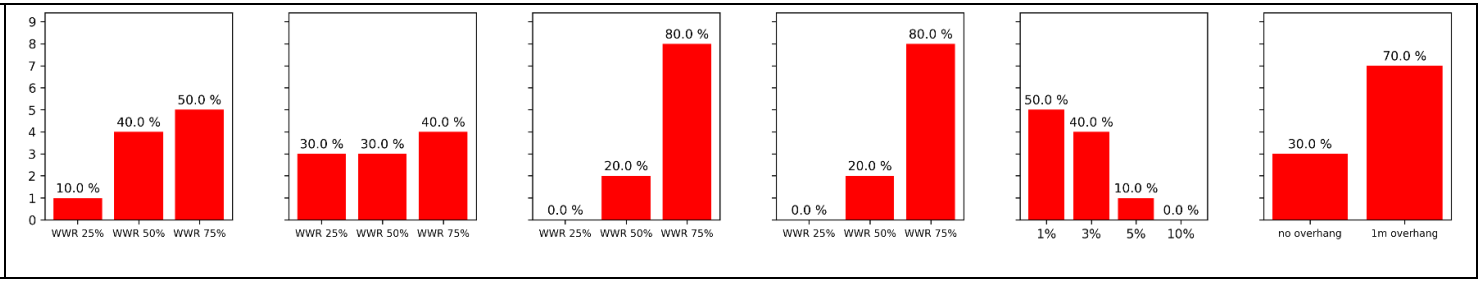

Table 3-B.2 Input variable histograms for Pareto Front 2 variable combination (EUI and View)

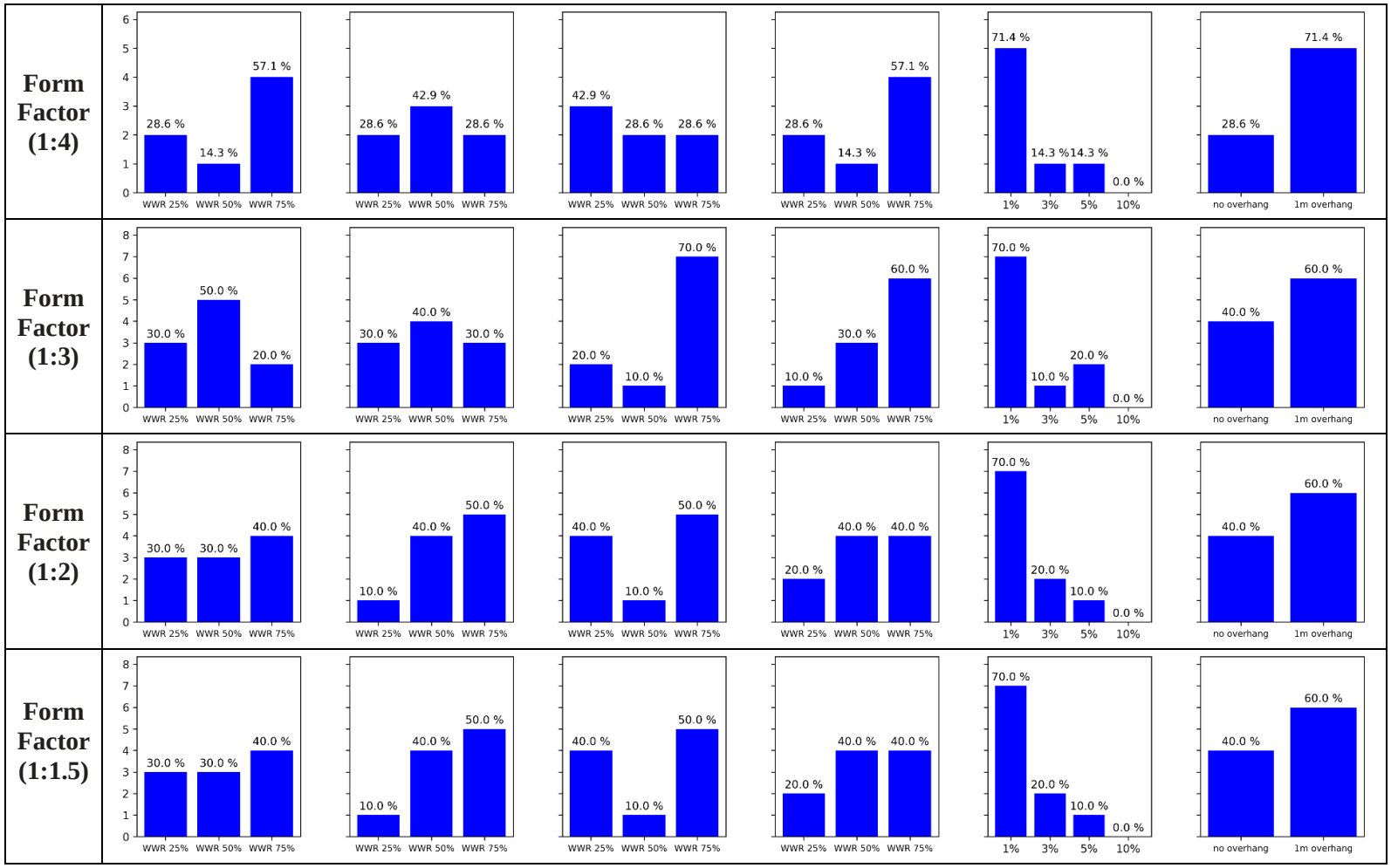

Table 3-B.2 (cont'd)

Form Factor (1:1)	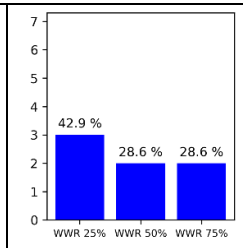	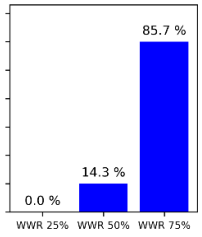	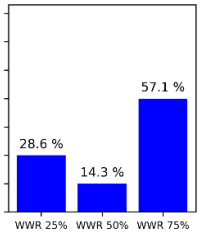	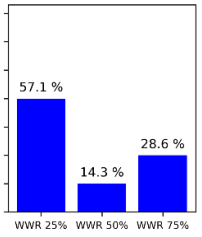	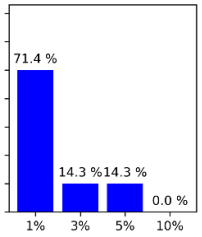	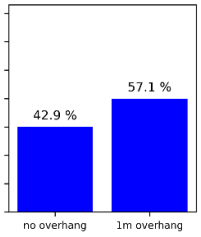
Form Factor (1.5:1)	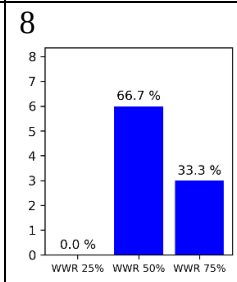	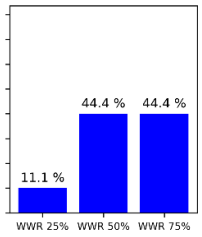	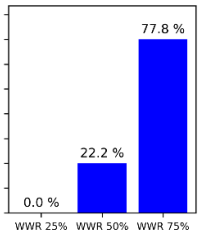	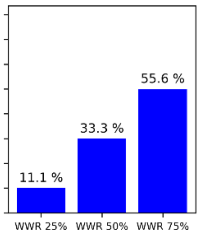	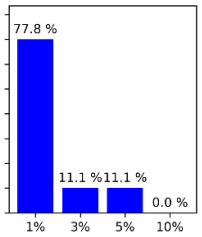	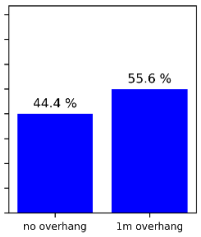
Form Factor (2:1)	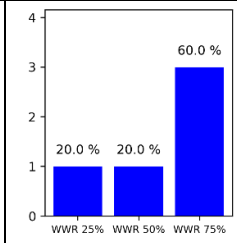	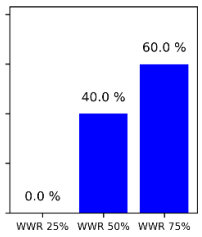	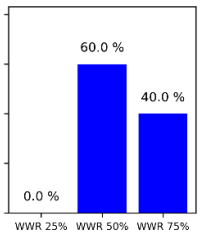	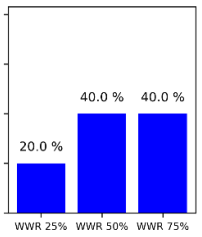	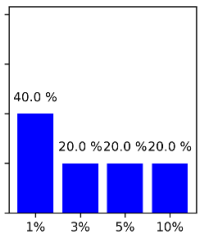	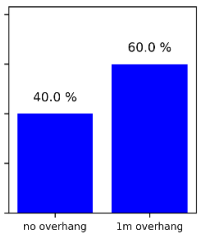
Form Factor (3:1)	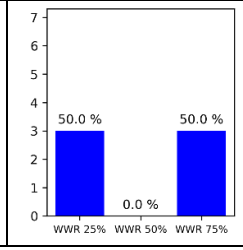	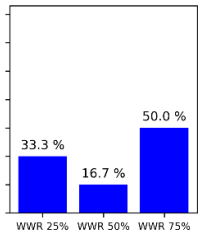	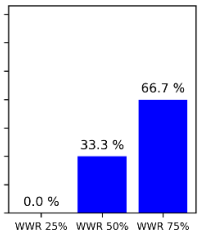	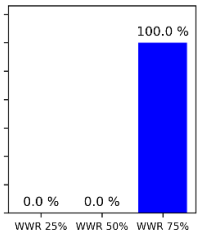	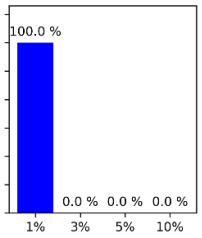	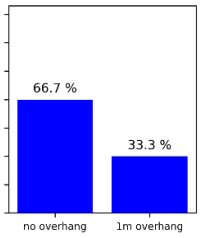

Table 3-B.2 (cont'd)

Form Factor (4:1)	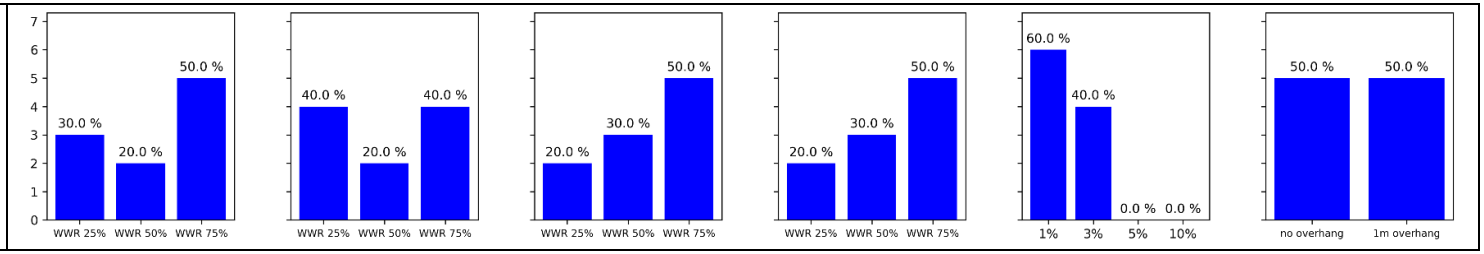

Table 3-B.3 Input variable histograms for Pareto Front 2 variable combination (EUI and PMV)

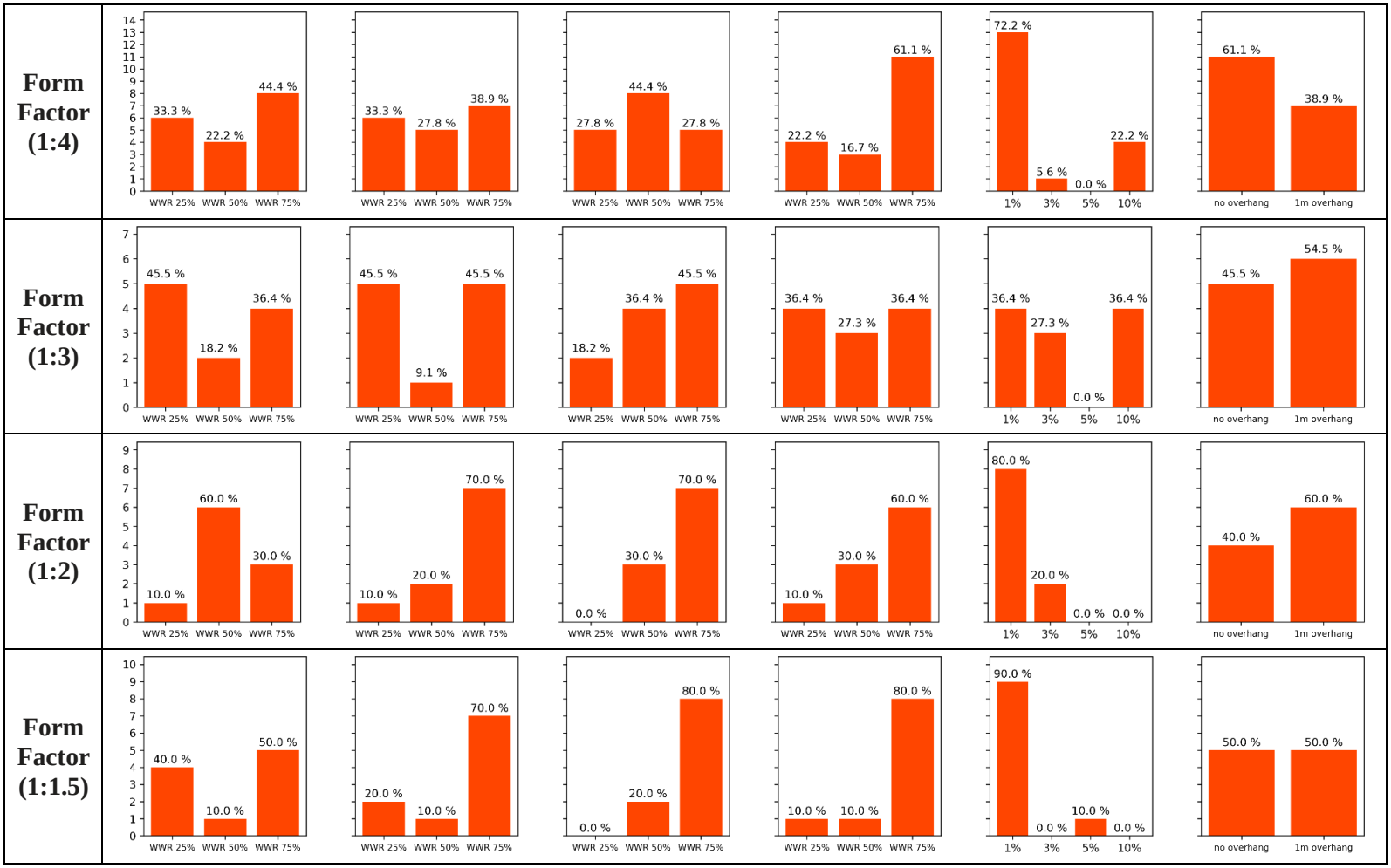

Table 3-B.3 (cont'd)

Form Factor (1:1)	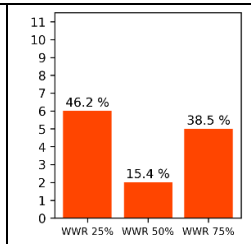	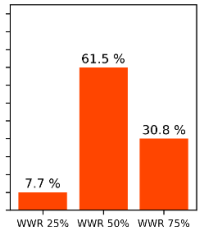	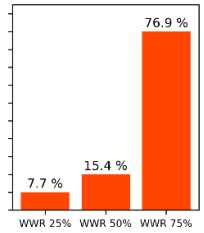	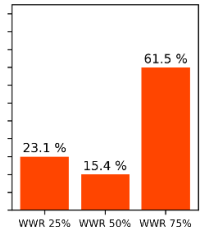	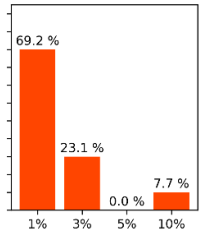	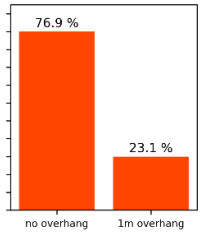
Form Factor (1.5:1)	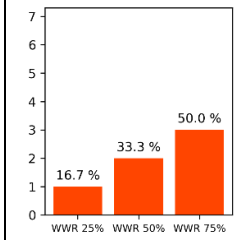	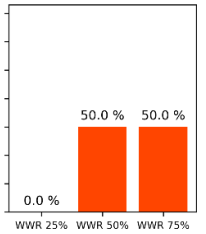	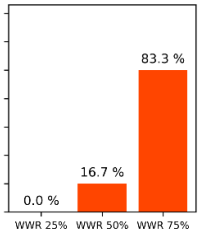	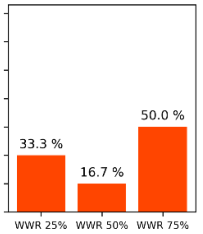	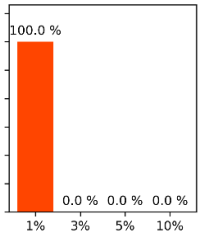	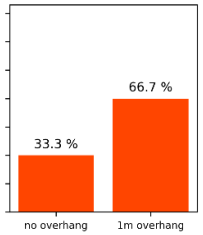
Form Factor (2:1)	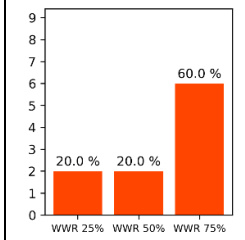	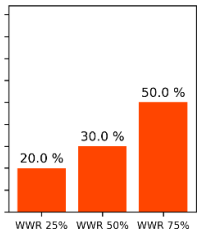	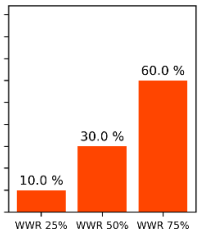	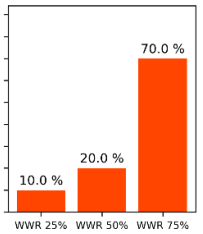	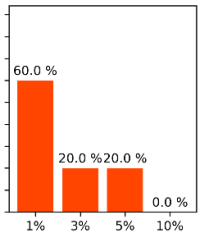	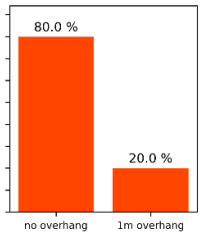
Form Factor (3:1)	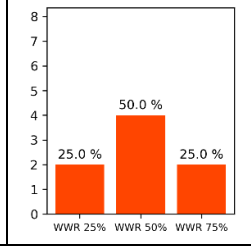	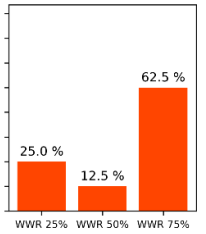	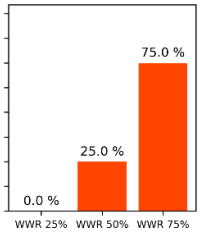	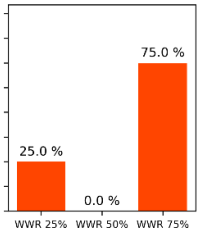	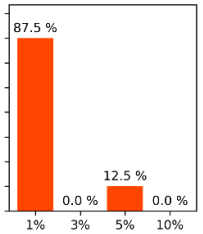	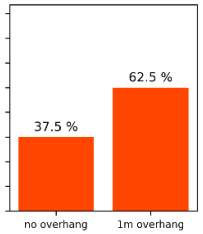

Table 3-B.3 (cont'd)

Form Factor (4:1)	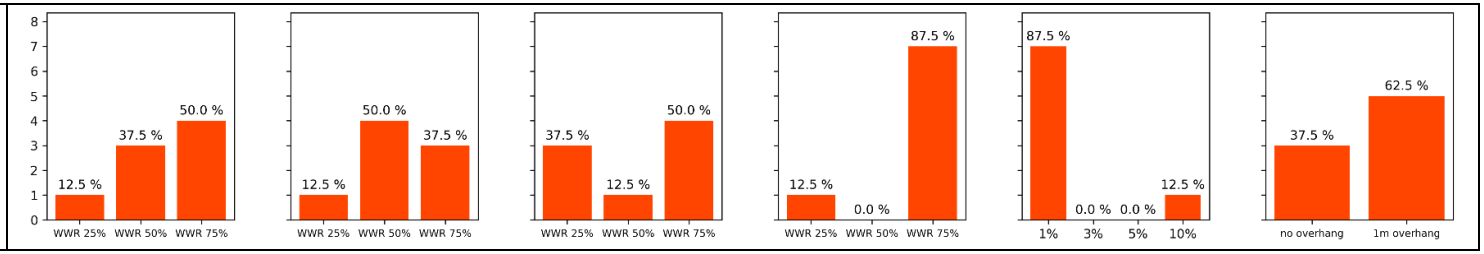

Table 3-B.4 Input variable histograms for Pareto Front 2 variable combination (UDI and View)

Form Factor (1:4)	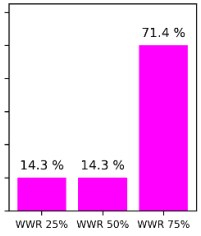	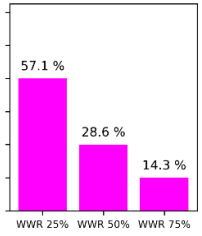	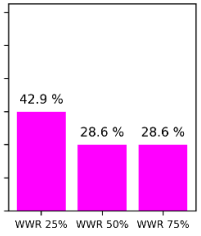	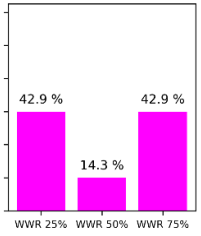	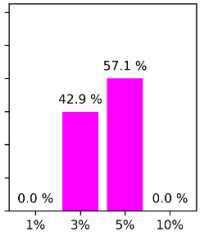	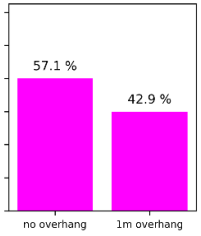
Form Factor (1:3)	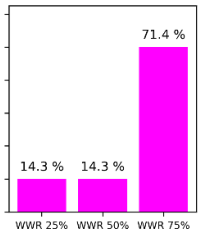	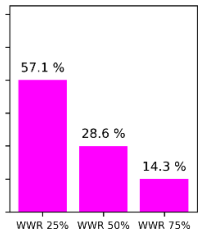	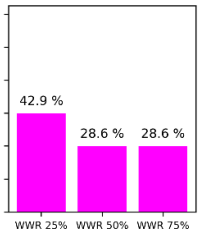	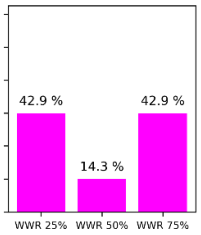	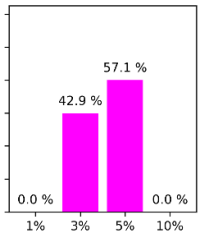	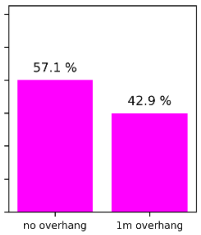
Form Factor (1:2)	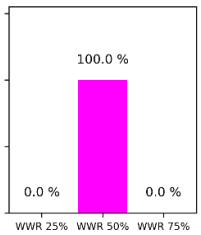	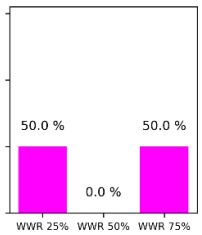	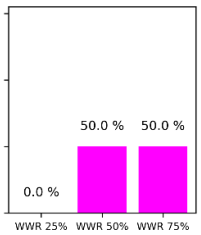	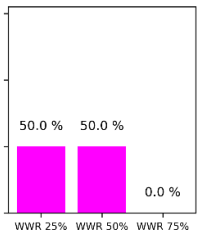	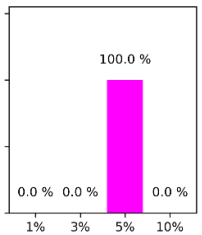	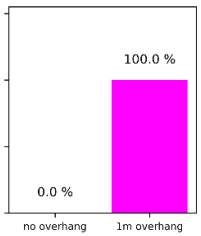
Form Factor (1:1.5)	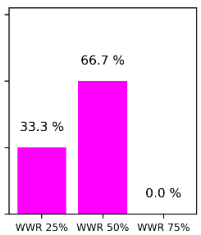	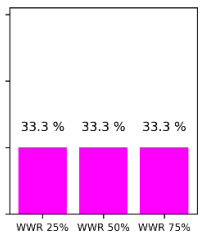	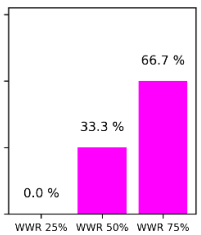	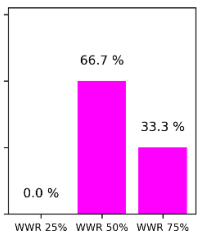	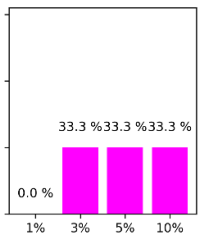	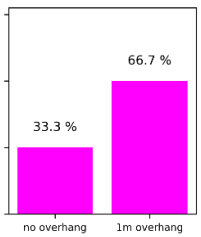

Table 3-B.4 (cont'd)

Form Factor (1:1)	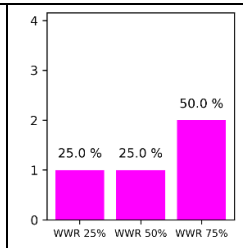	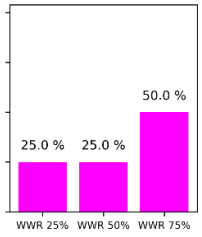	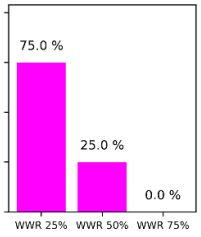	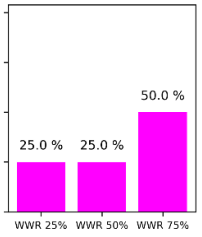	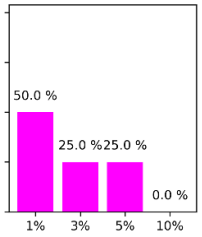	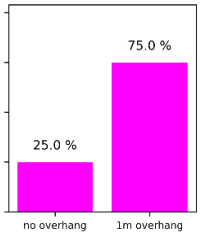
Form Factor (1.5:1)	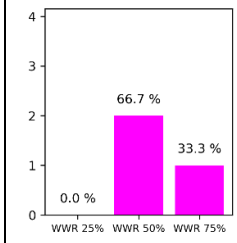	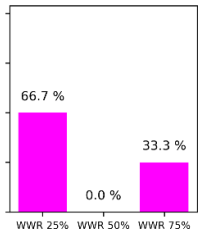	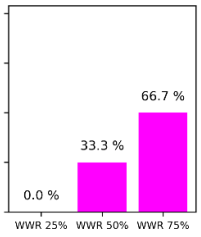	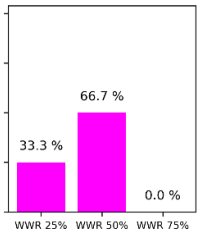	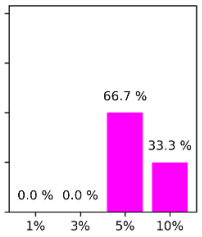	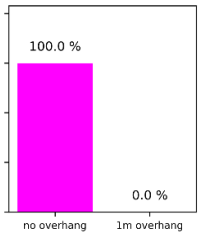
Form Factor (2:1)	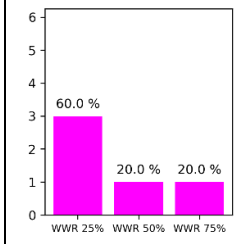	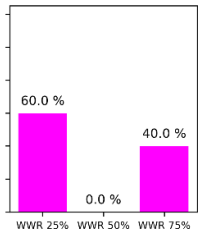	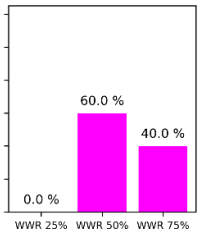	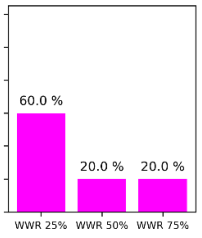	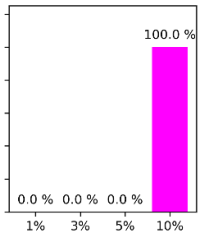	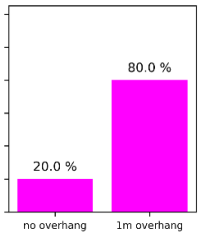
Form Factor (3:1)	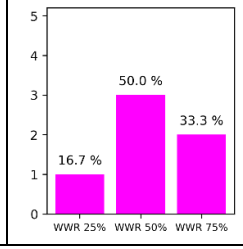	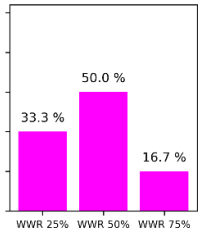	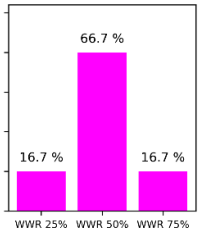	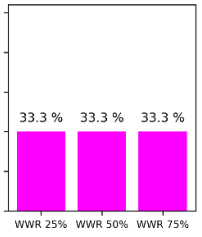	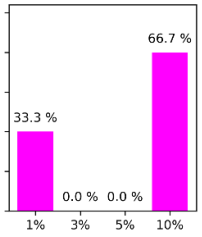	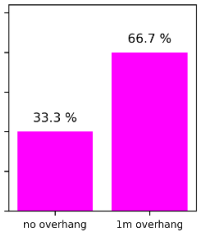

Table 3-B.4 (cont'd)

Form Factor (4:1)	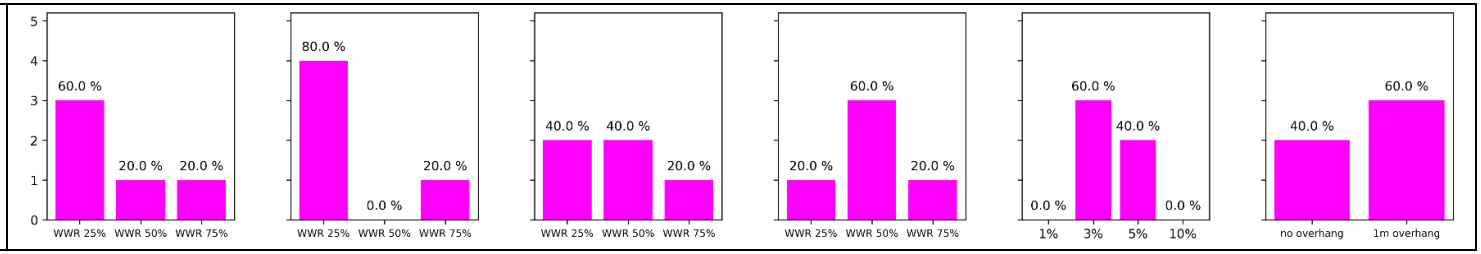

Table 3-B.5 Input variable histograms for Pareto Front 2 variable combination (UDI and PMV)

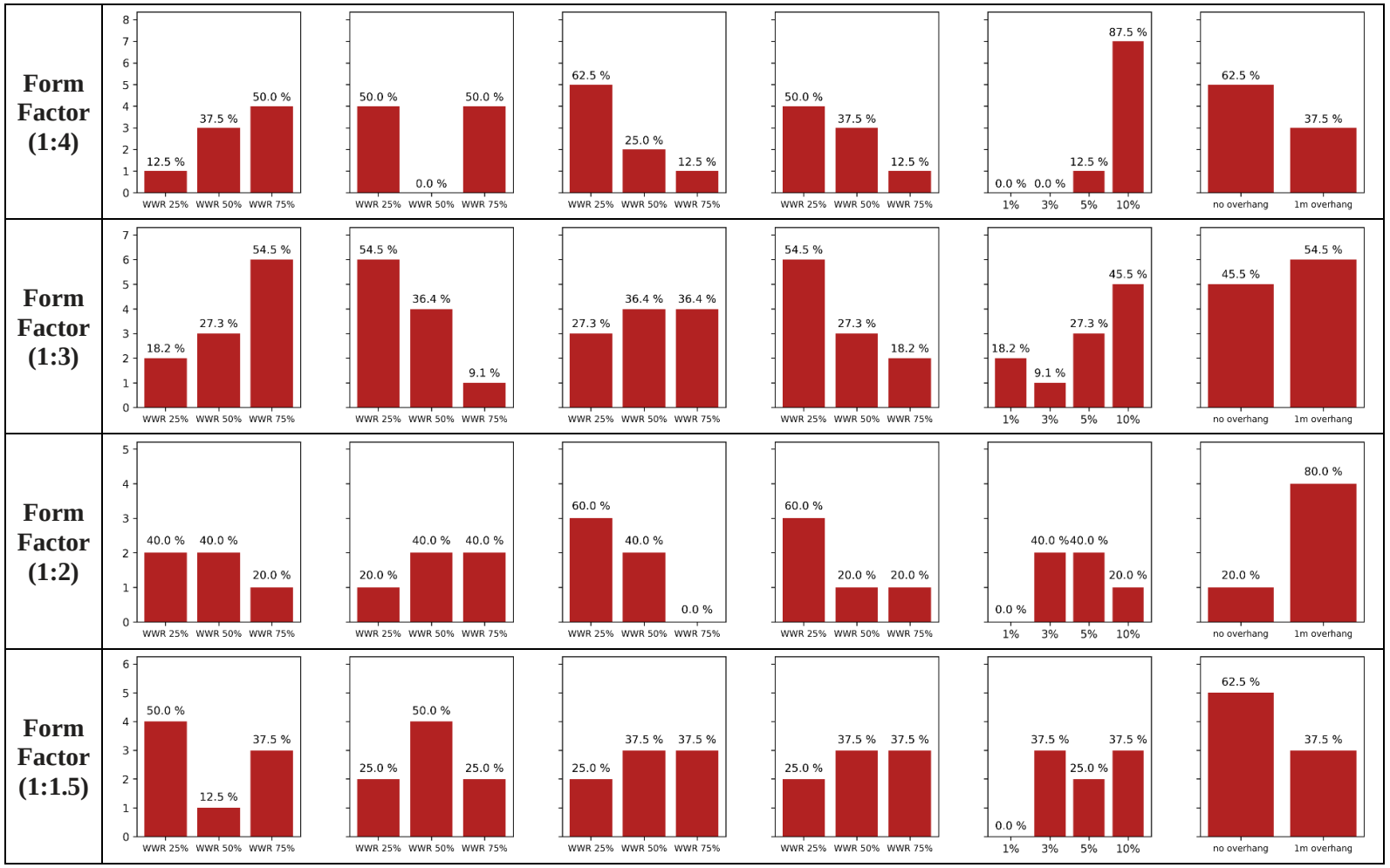

Table 3-B.5 (cont'd)

Form Factor (1:1)	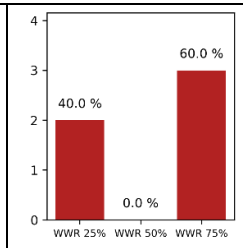	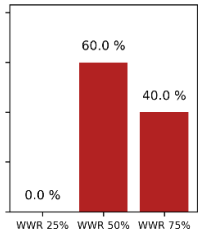	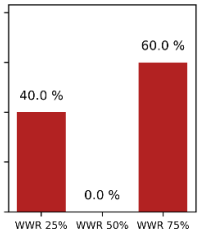	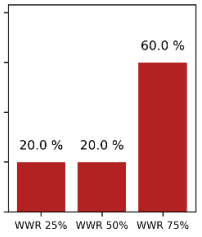	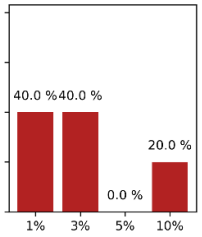	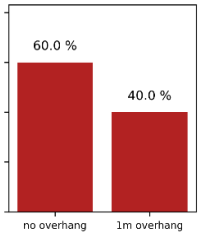
Form Factor (1.5:1)	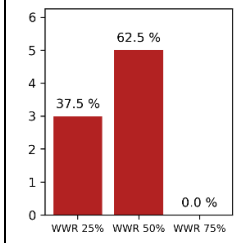	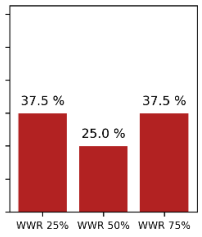	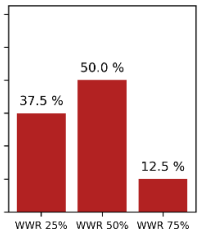	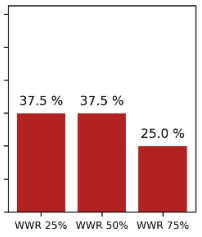	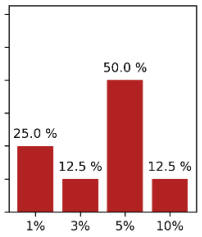	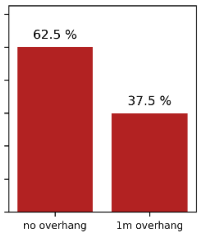
Form Factor (2:1)	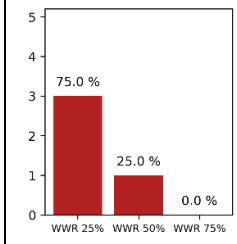	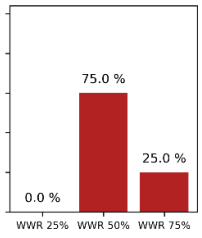	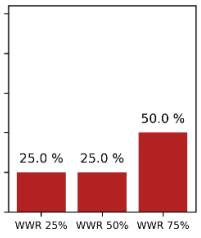	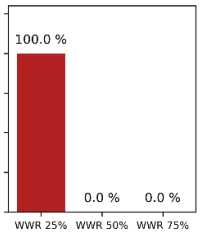	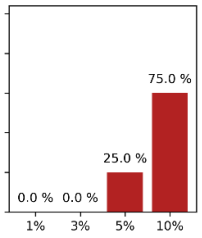	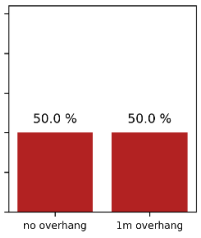
Form Factor (3:1)	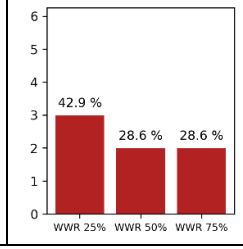	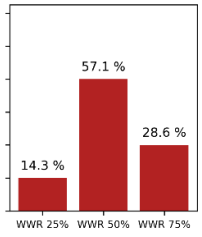	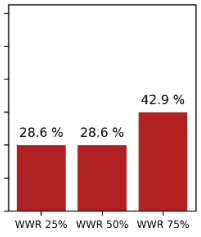	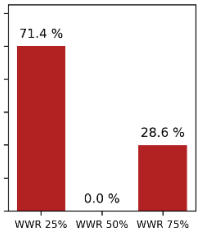	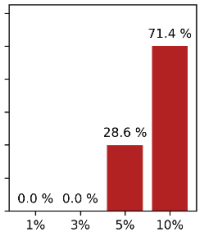	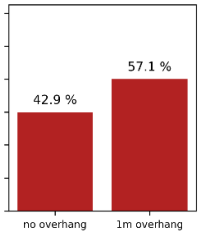

Table 3-B.5 (cont'd)

Form Factor (4:1)	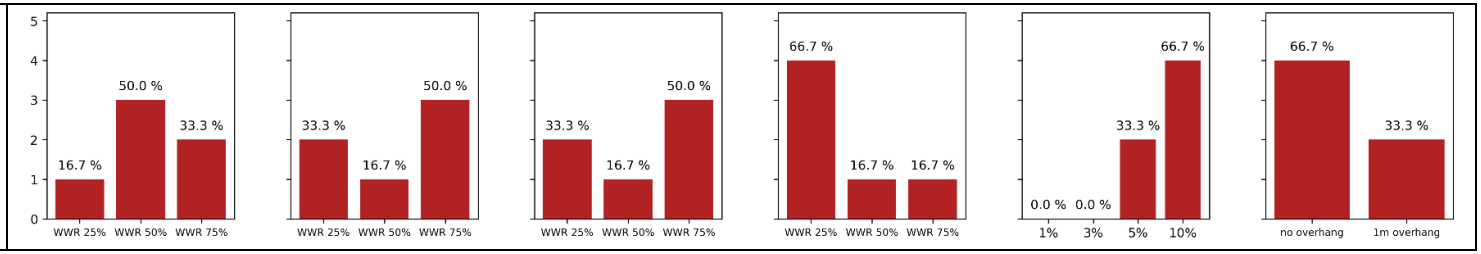

Table 3-B.6 Input variable histograms for Pareto Front 2 variable combination (View and PMV)

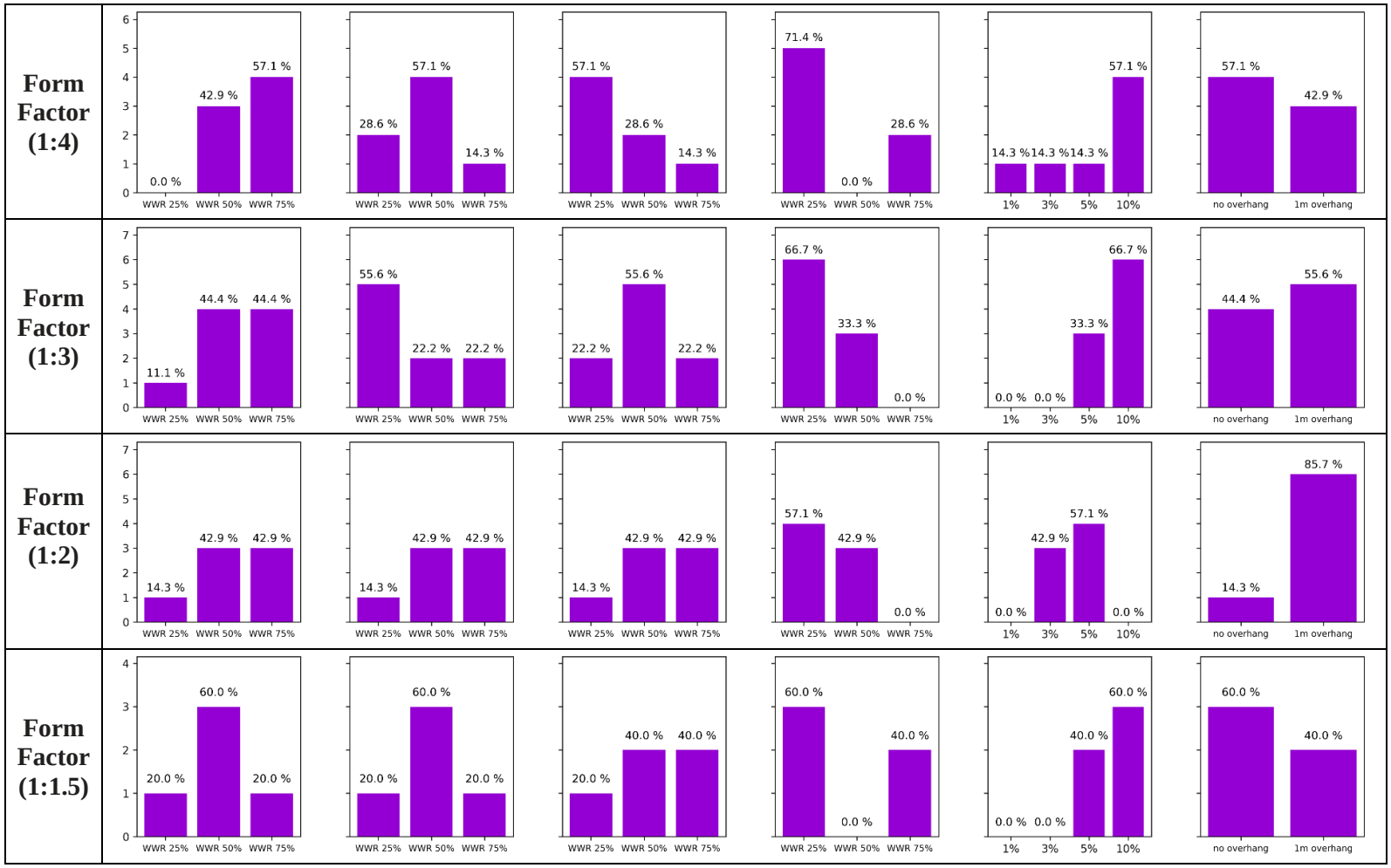

Table 3-B.6 (cont'd)

Form Factor (1:1)	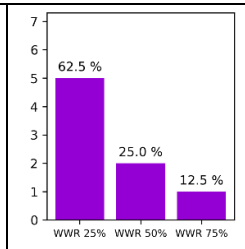	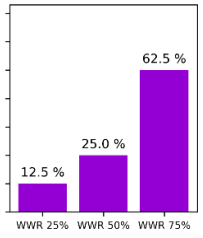	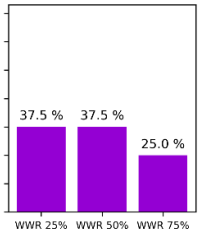	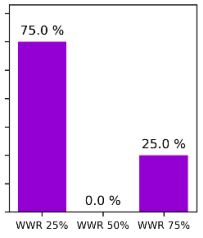	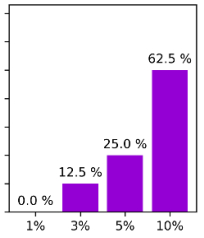	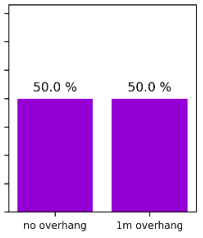
Form Factor (1.5:1)	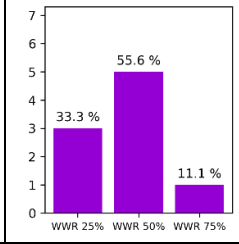	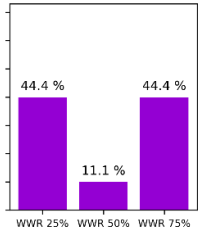	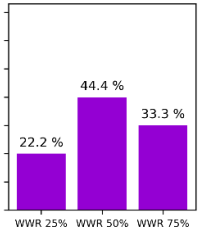	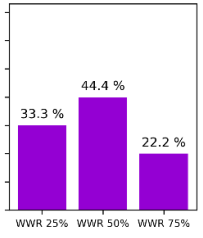	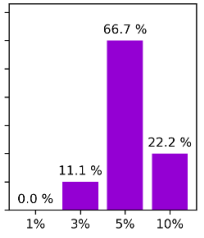	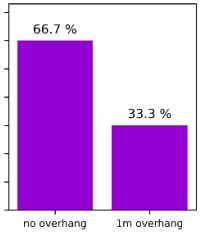
Form Factor (2:1)	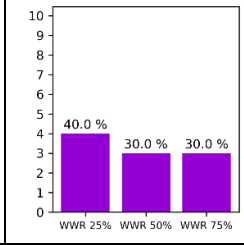	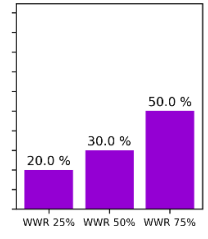	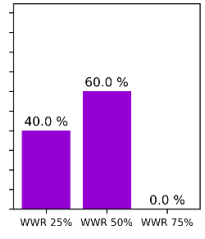	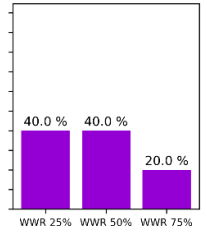	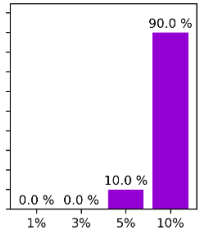	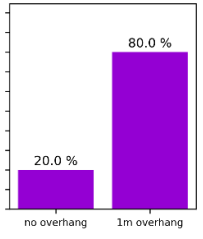
Form Factor (3:1)	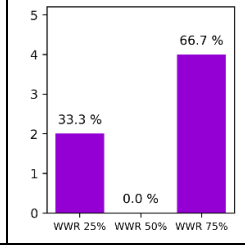	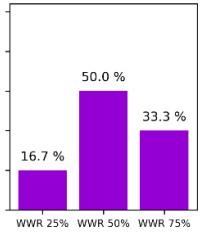	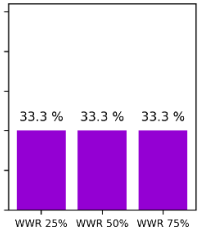	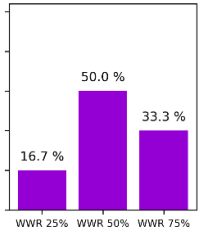	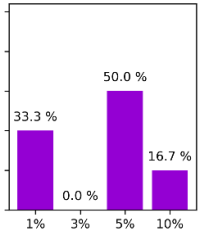	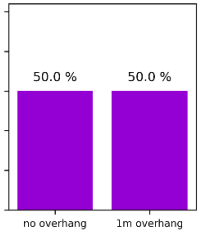

Table 3-B.6 (cont'd)

Form Factor (4:1)	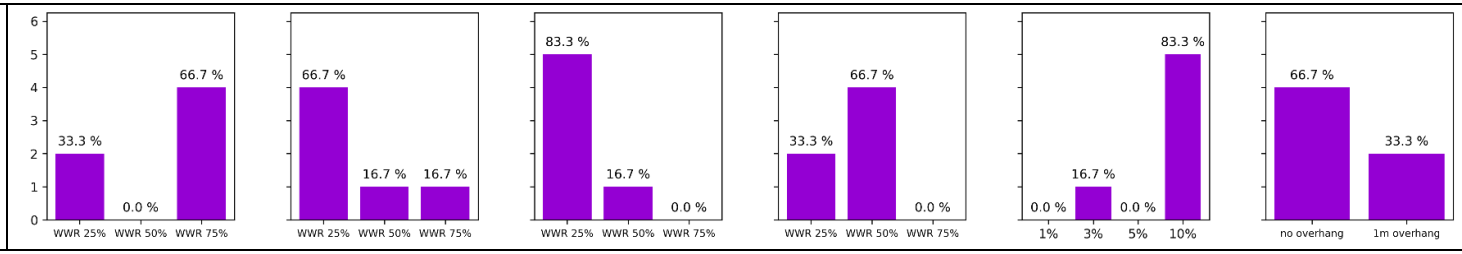

APPENDIX 3-C: THREE VARIABLE PARETO RESULTS

Table 3-C.1 Input variable histograms for Pareto Front 3 variable combination (EUI, UDI, and View)

Form Factor (1:4)	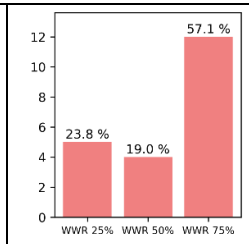	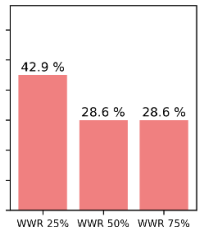	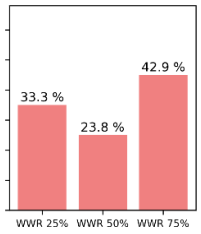	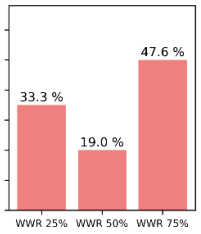	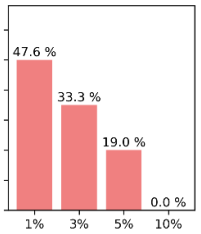	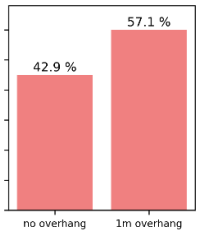
Form Factor (1:3)	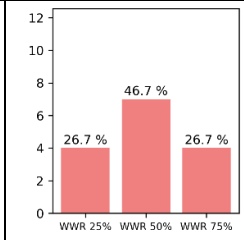	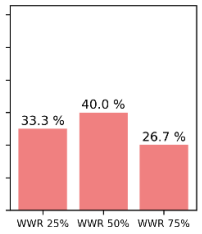	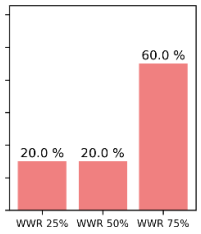	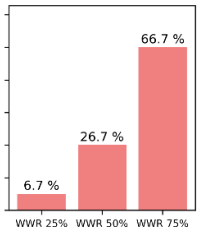	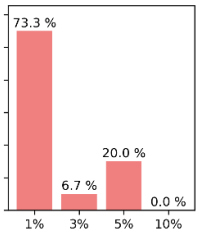	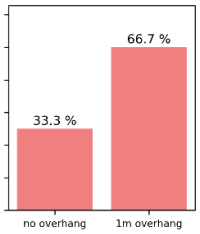
Form Factor (1:2)	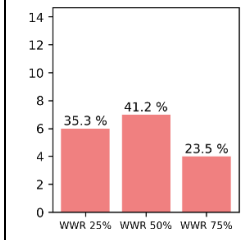	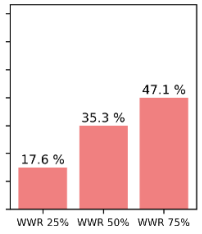	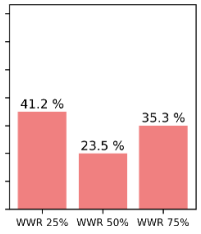	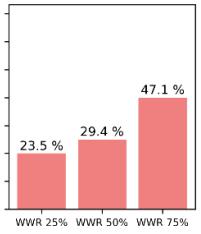	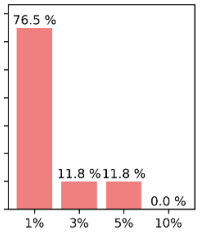	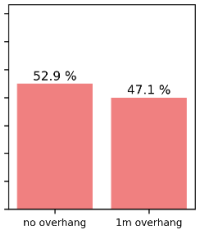
Form Factor (1:1.5)	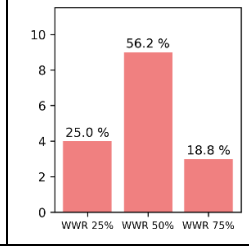	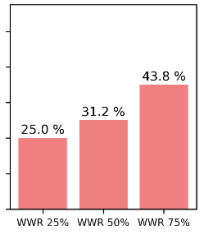	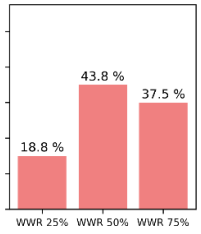	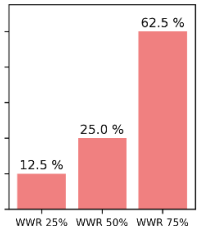	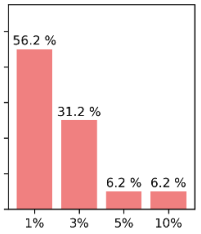	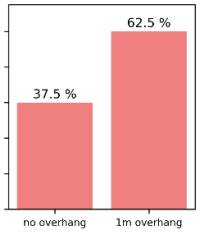

Table 3-C.1 (cont'd)

Form Factor (1:1)	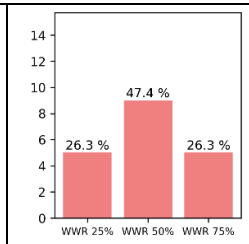	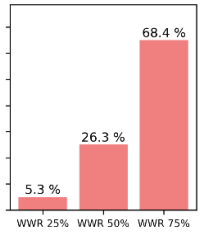	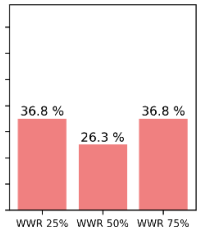	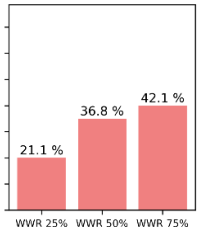	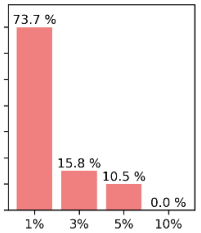	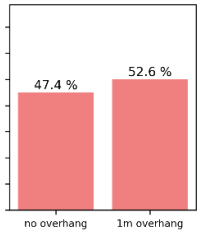
Form Factor (1.5:1)	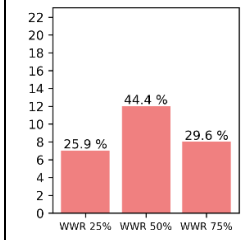	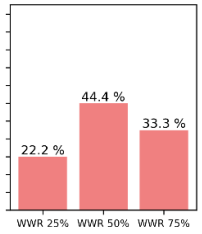	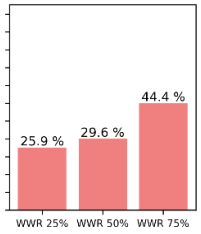	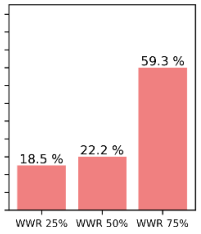	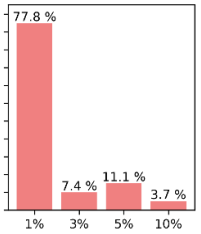	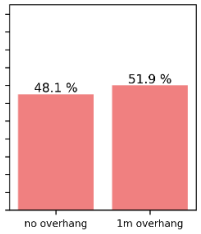
Form Factor (2:1)	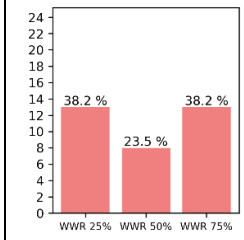	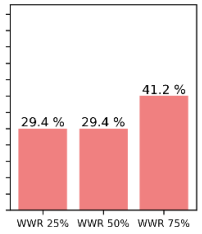	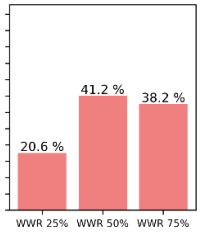	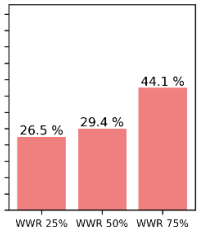	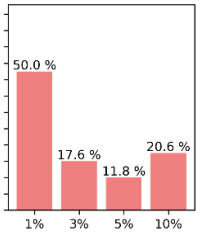	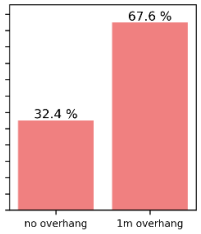
Form Factor (3:1)	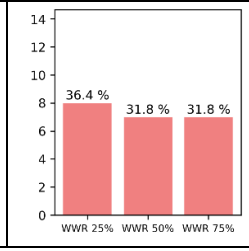	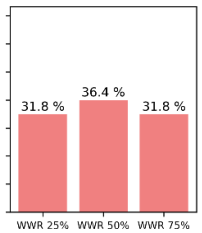	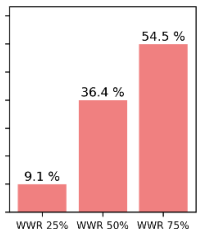	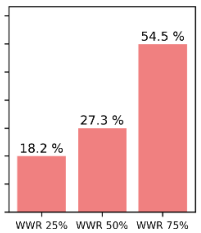	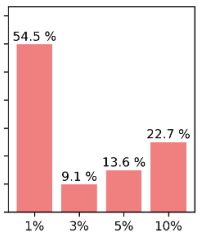	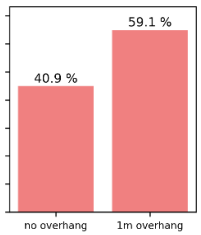

Table 3-C.1 (cont'd)

Form Factor (4:1)	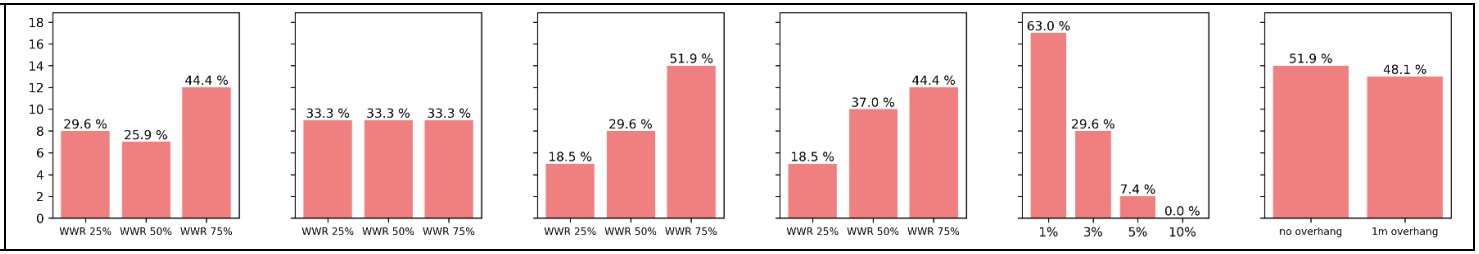

Table 3-C.2 Input variable histograms for Pareto Front 3 variable combination (EUI, UDI, and PMV)

Form Factor (1:4)	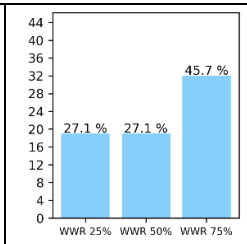	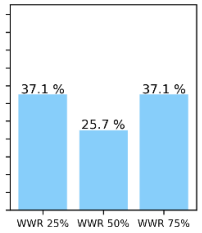	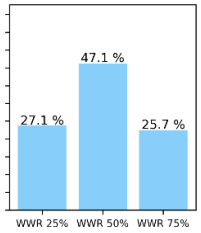	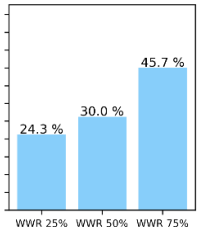	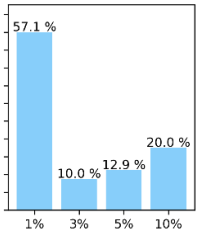	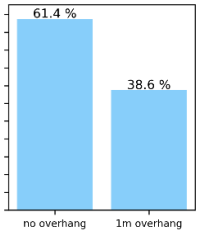
Form Factor (1:3)	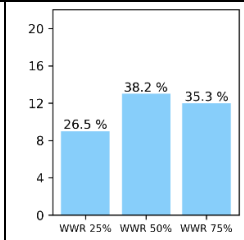	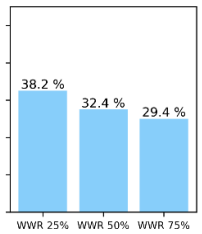	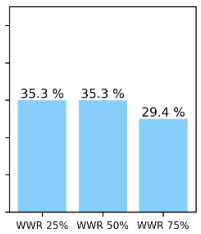	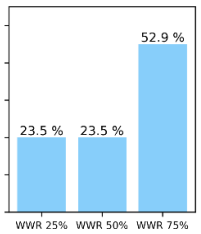	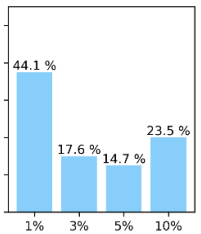	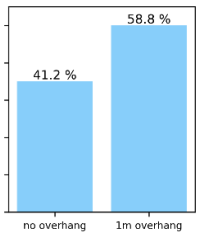
Form Factor (1:2)	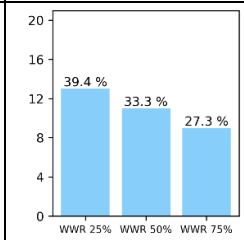	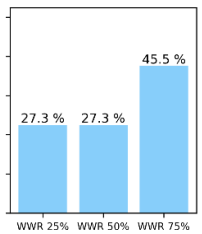	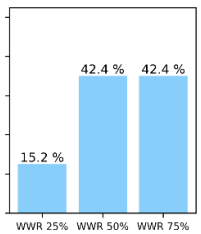	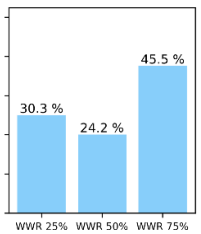	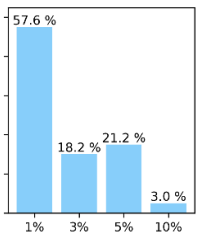	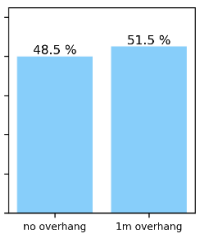
Form Factor (1:1.5)	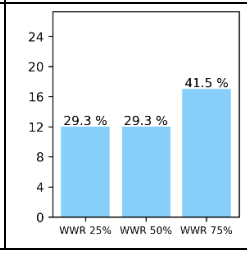	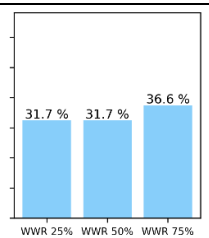	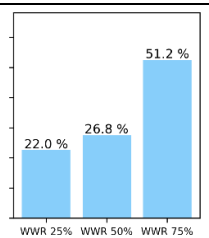	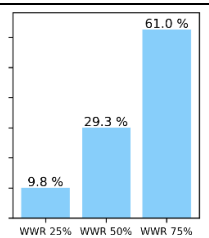	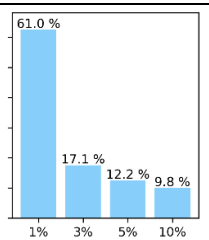	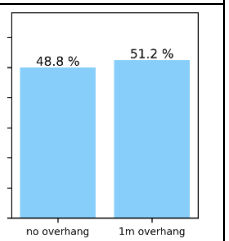

Table 3-C.2 (cont'd)

Form Factor (1:1)	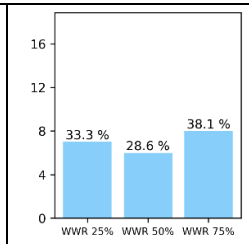	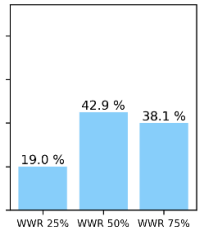	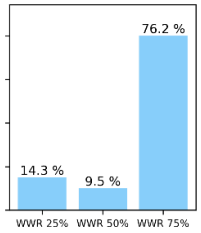	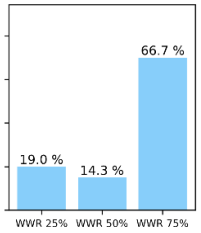	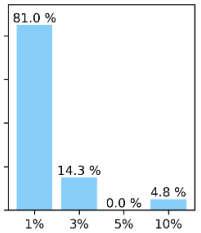	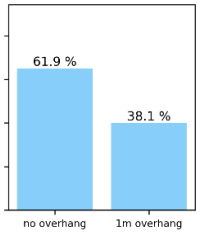
Form Factor (1.5:1)	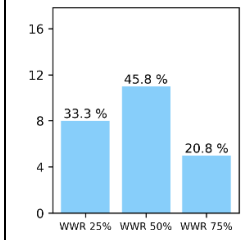	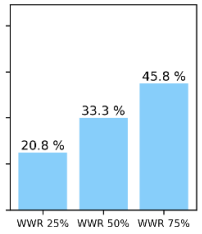	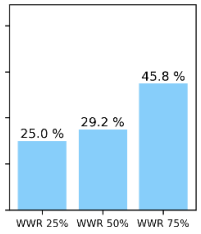	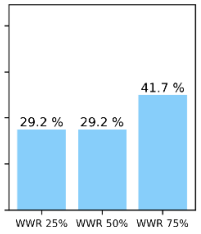	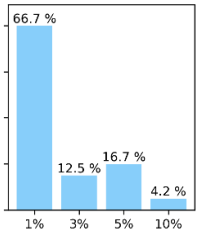	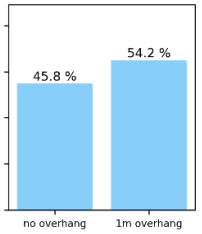
Form Factor (2:1)	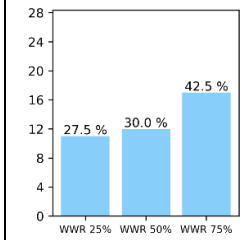	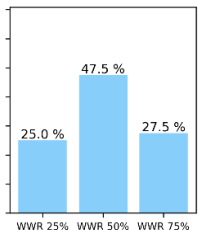	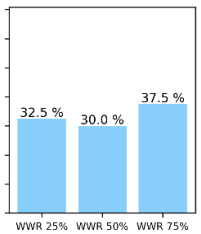	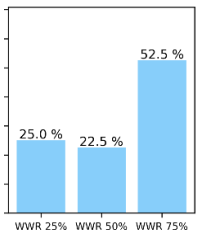	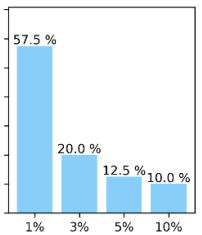	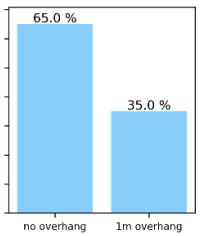
Form Factor (3:1)	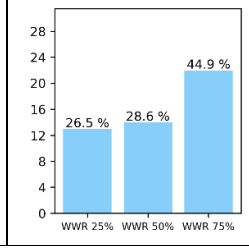	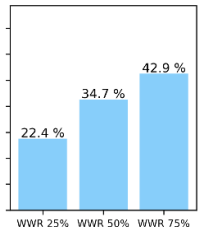	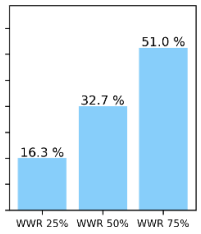	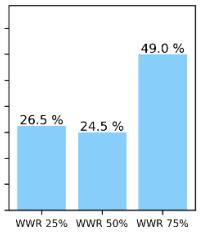	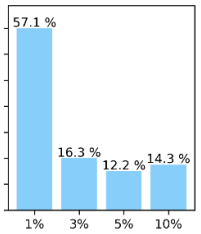	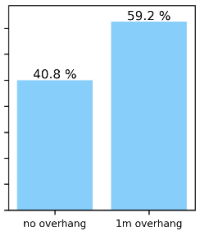

Table 3-C.2 (cont'd)

Form Factor (4:1)	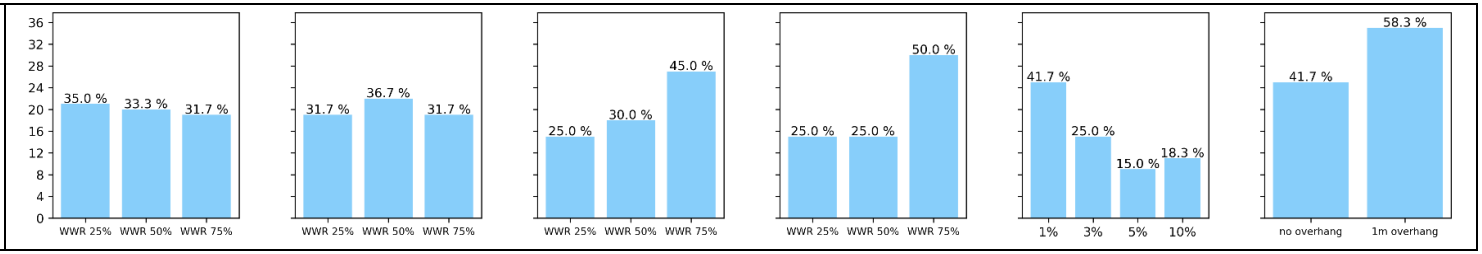

Table 3-C.3 Input variable histograms for Pareto Front 3 variable combination (EUI, View, and PMV)

Form Factor (1:4)	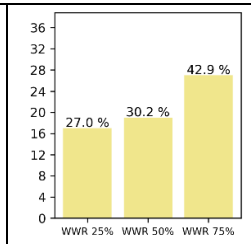	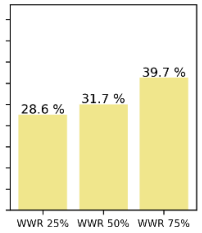	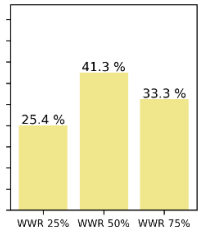	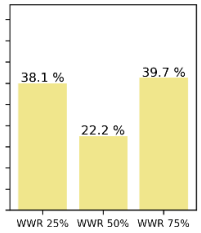	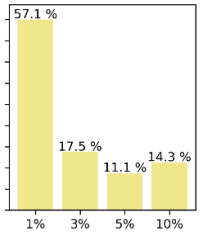	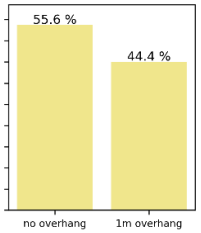
Form Factor (1:3)	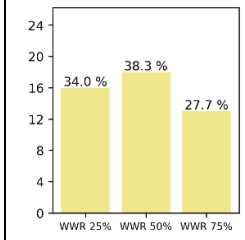	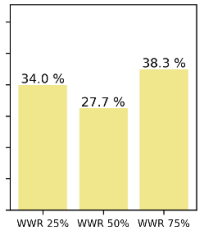	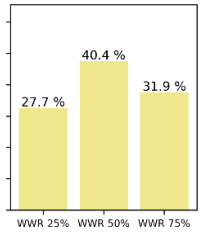	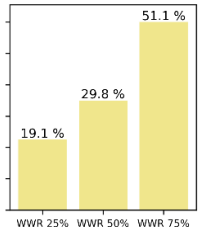	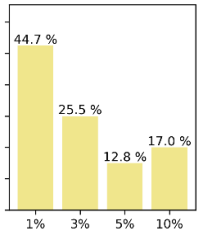	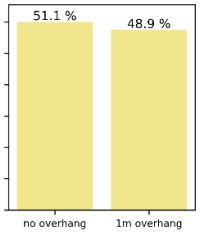
Form Factor (1:2)	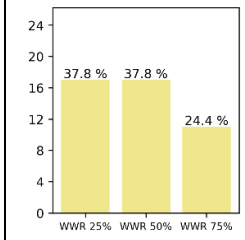	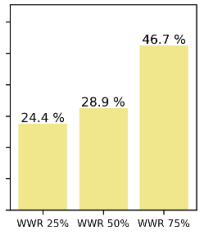	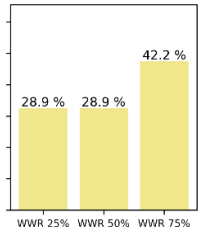	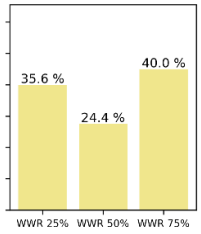	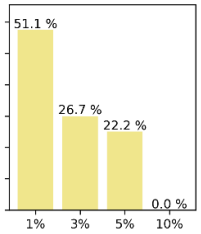	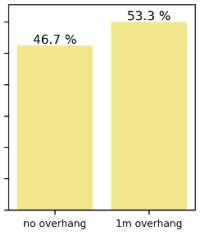
Form Factor (1:1.5)	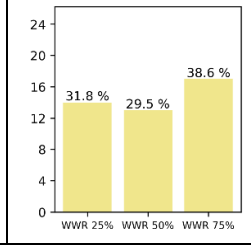	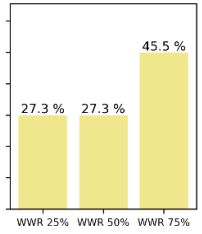	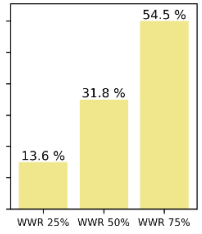	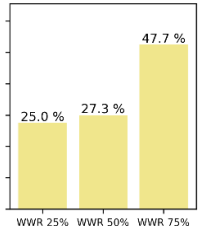	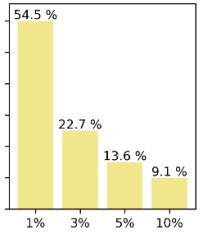	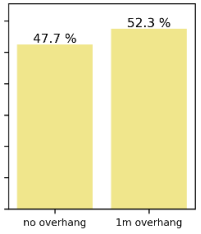

Table 3-C.3 (cont'd)

Form Factor (1:1)	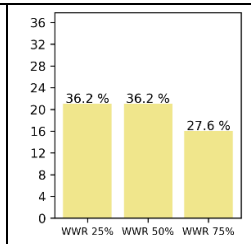	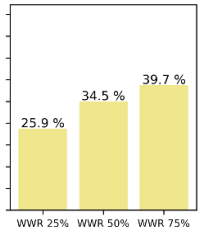	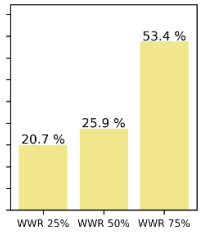	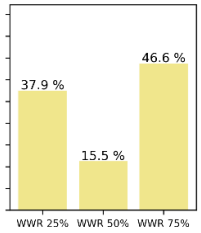	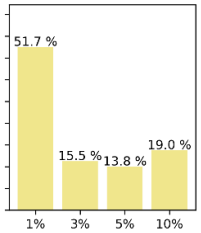	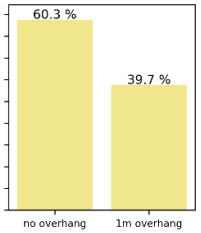
Form Factor (1.5:1)	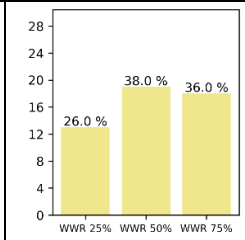	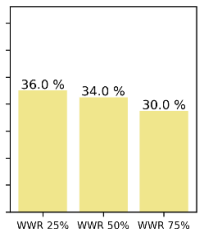	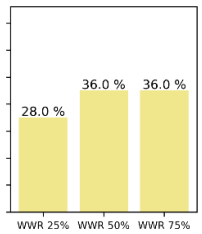	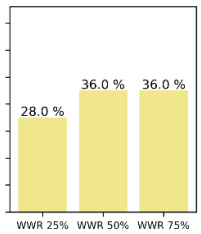	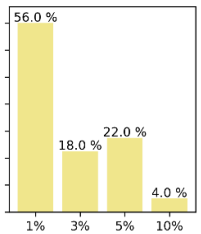	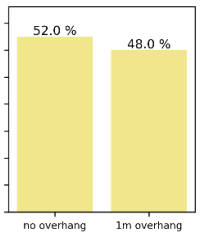
Form Factor (2:1)	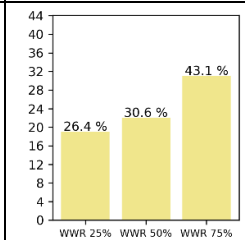	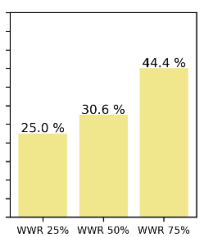	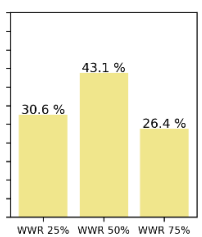	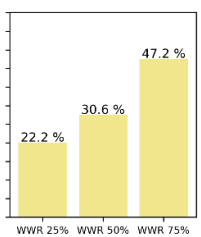	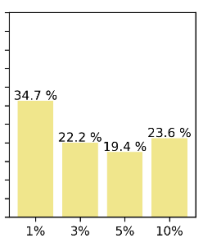	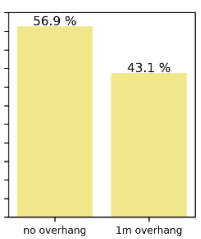
Form Factor (3:1)	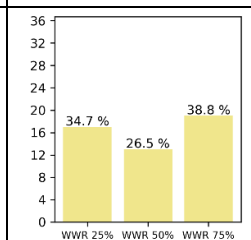	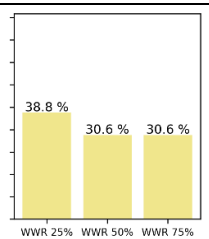	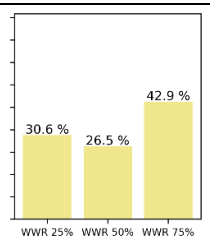	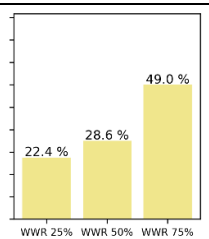	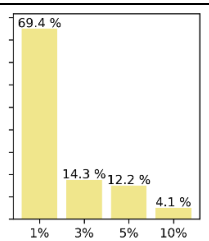	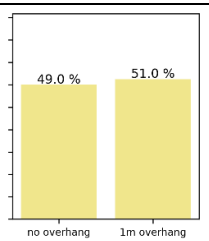

Table 3-C.3 (cont'd)

Form Factor (4:1)	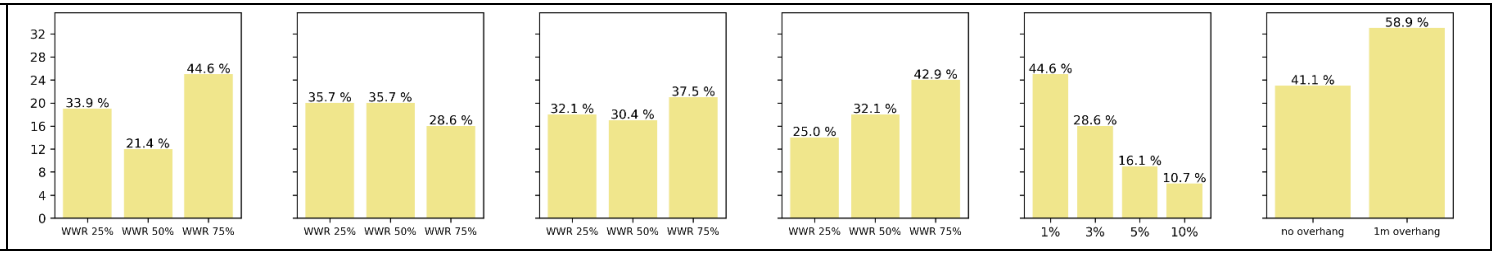

Table 3-C.4 Input variable histograms for Pareto Front 3 variable combination (UDI, View, and PMV)

Form Factor (1:4)	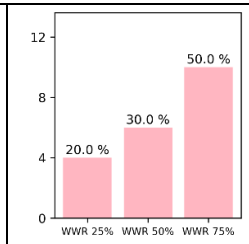	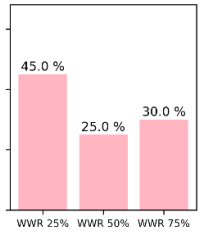	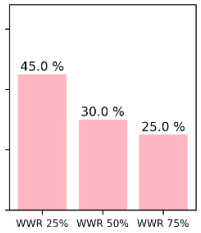	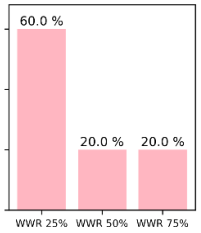	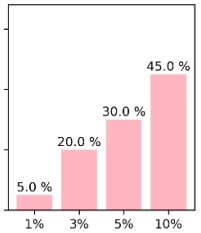	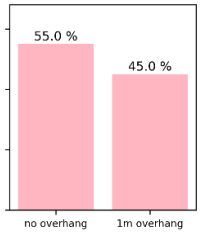
Form Factor (1:3)	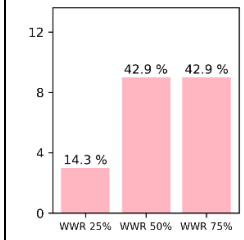	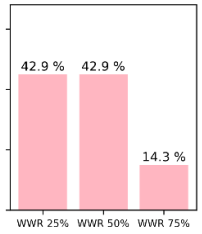	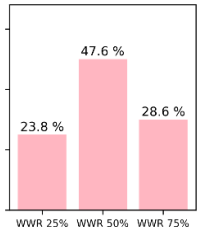	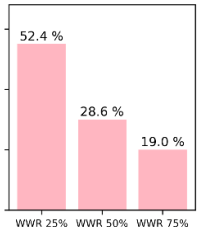	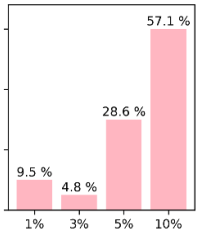	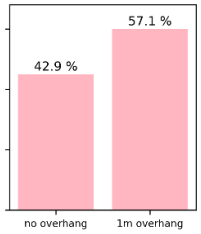
Form Factor (1:2)	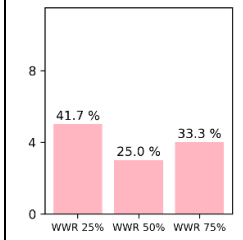	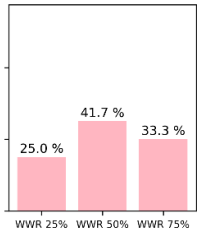	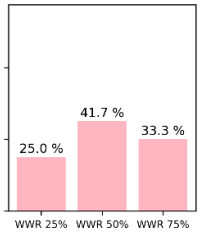	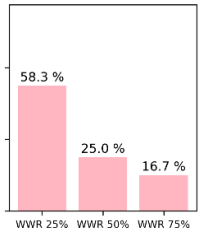	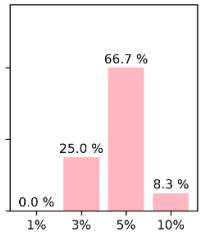	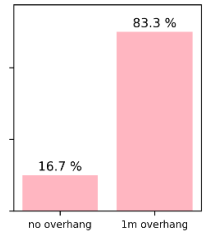
Form Factor (1:1.5)	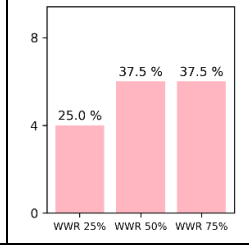	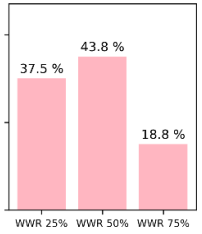	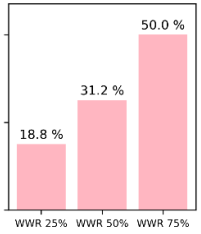	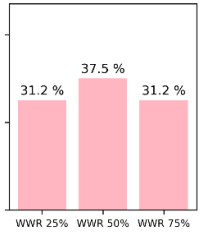	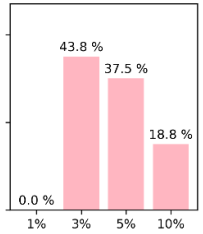	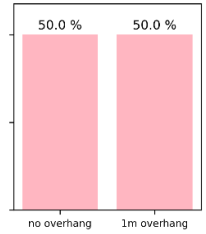

Table 3-C.4 (cont'd)

Form Factor (1:1)	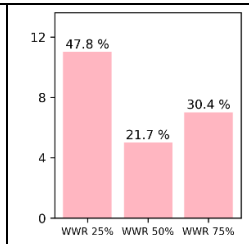	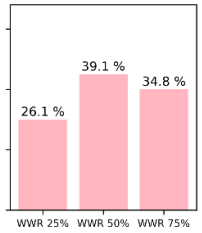	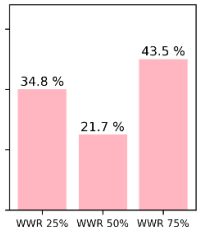	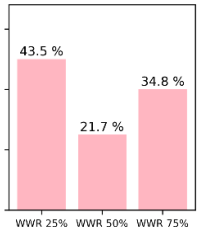	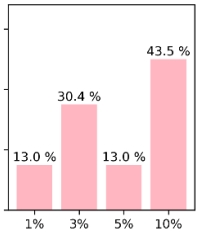	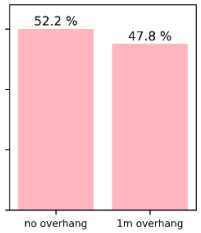
Form Factor (1.5:1)	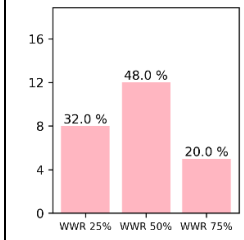	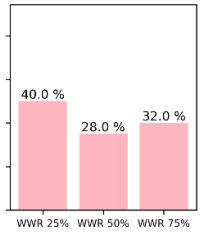	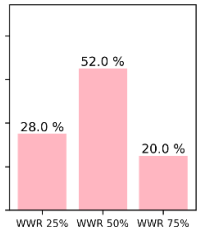	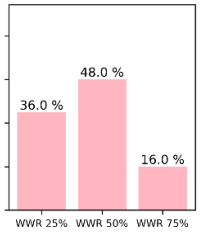	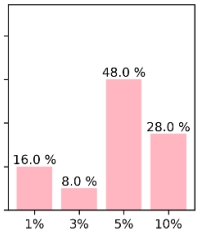	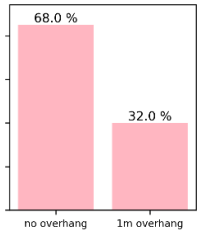
Form Factor (2:1)	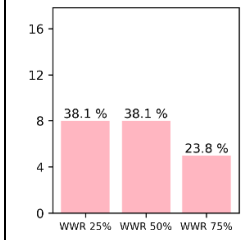	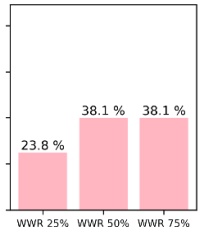	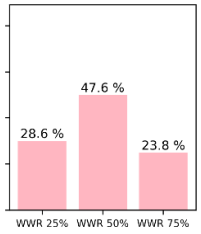	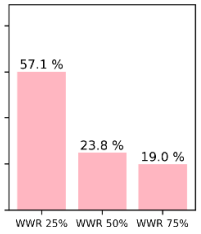	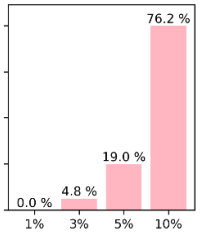	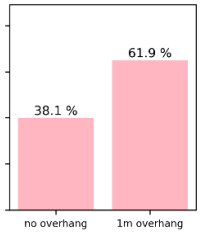
Form Factor (3:1)	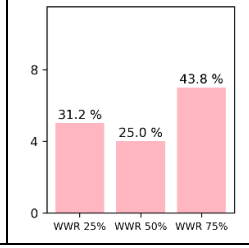	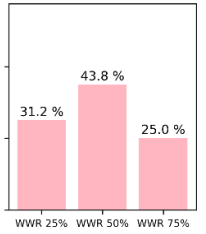	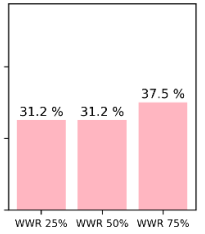	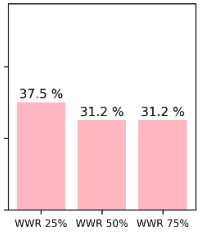	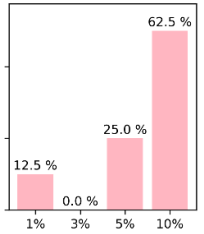	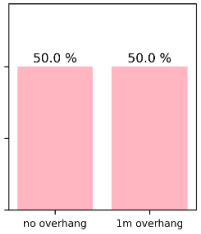

Table 3-C.4 (cont'd)

Form Factor (4:1)	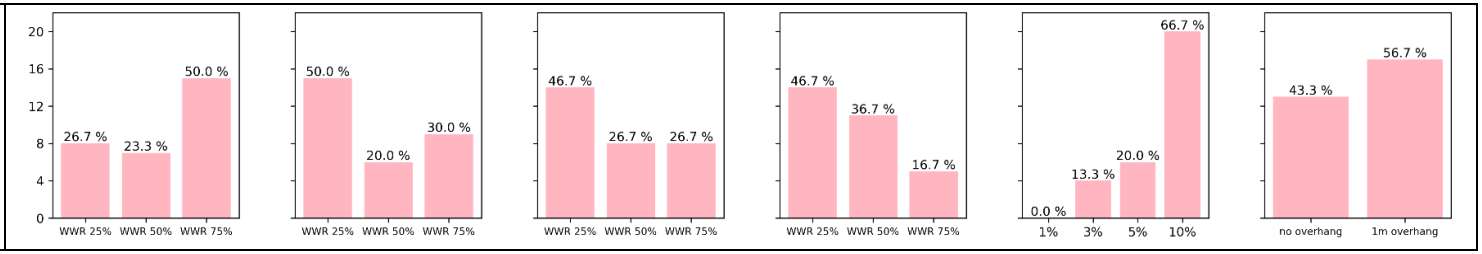

APPENDIX 3-D: FOUR VARIABLE PARETO RESULTS

Table 3-D.1 Input variable histograms for Pareto Front 4 variable combination (EUI, UDI, View, and PMV)

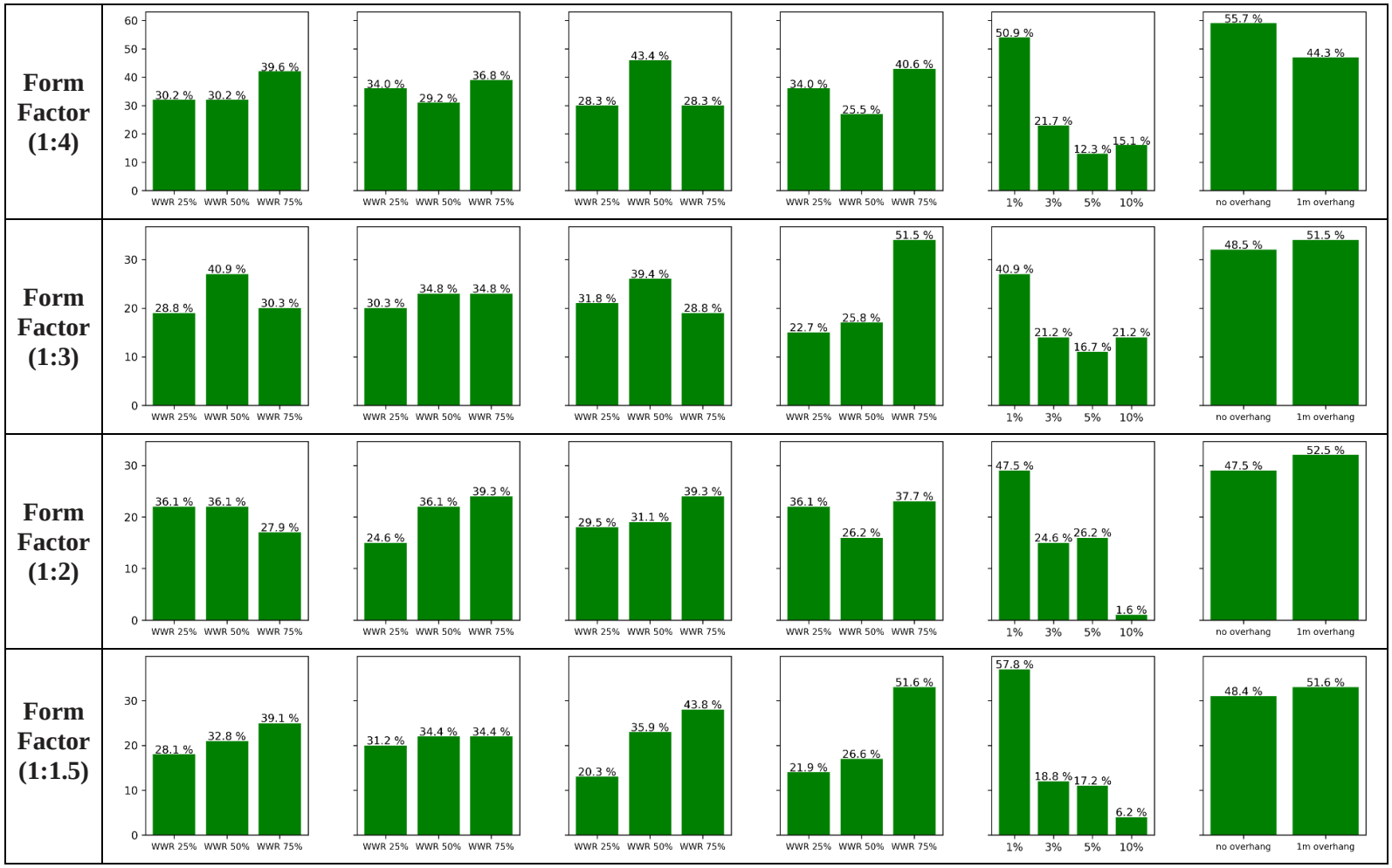

Table 3-D.1 (cont'd)

Form Factor (1:1)	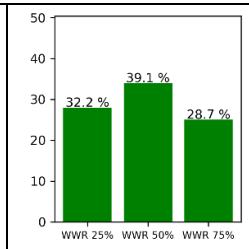	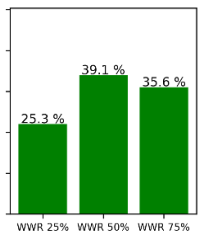	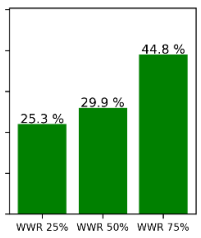	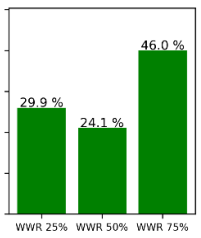	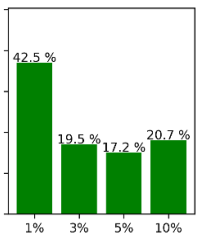	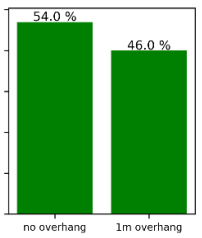
Form Factor (1.5:1)	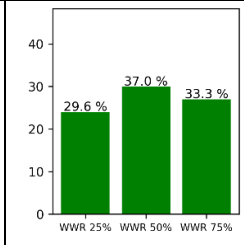	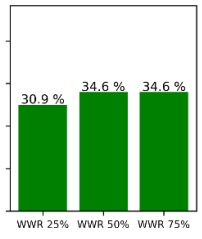	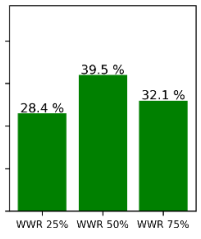	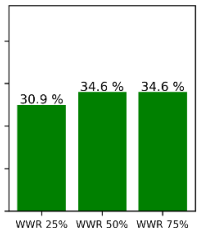	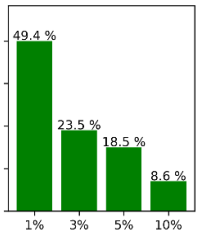	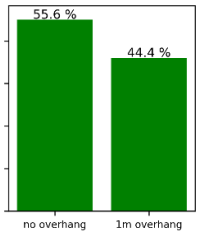
Form Factor (2:1)	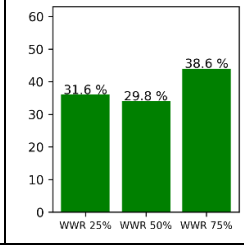	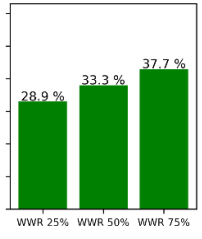	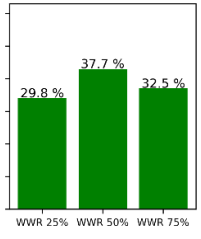	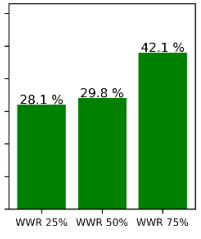	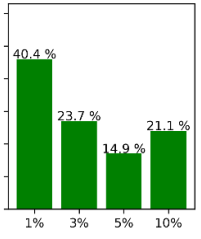	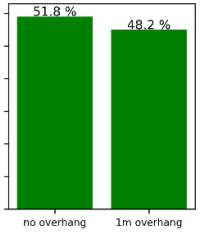
Form Factor (3:1)	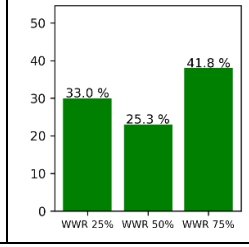	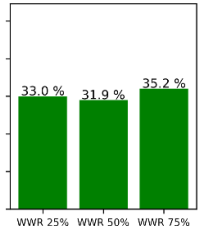	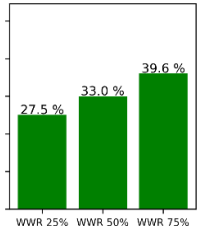	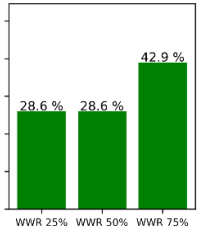	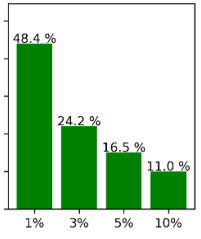	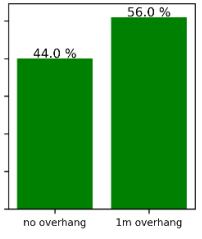

Table 3-D.1 (cont'd)

Form Factor (4:1)	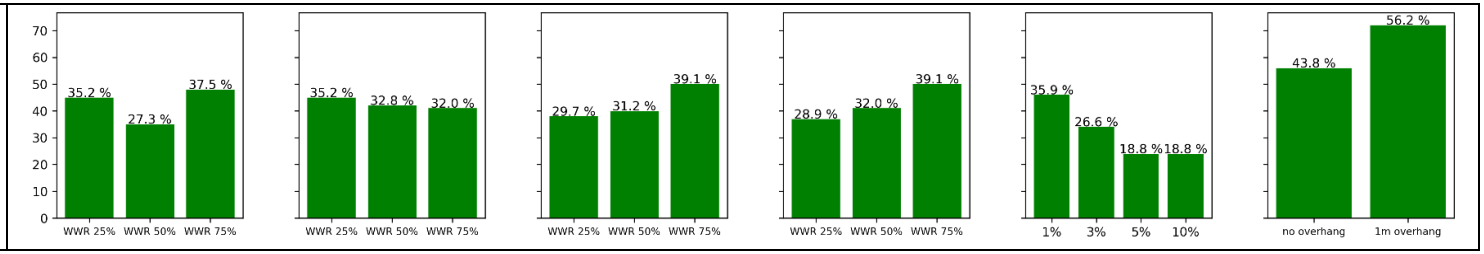

CHAPTER 4 – GRID-SCALE AGGREGATION OF LIGHTING LOADS

Published in Energy and Buildings

Citation: Vanage, S., Cetin, K., McCalley, J., & Wang, Y. (2023). Grid-Scale Demand-side Flexibility Services using Commercial Buildings Lighting Loads. *Energy and Buildings,* 113631.

ABSTRACT

Flexibility Services can be used to account for the high variability in electricity generation due to increasing renewable energy sources such as wind and solar energy. As buildings become smarter with the adoption of new technologies for sensing and control, more integration between buildings and the electric grid is possible. Building loads such as air conditioning and lighting in commercial buildings have the potential to provide these Flexibility Services. In commercial buildings, lighting accounts for approximately 10-15% of the load at time. Past studies have shown that lighting can be dimmed by 15-20% without causing visual discomfort to the occupants. Overall, this study aims to estimate the instantaneous demand reduction that can be provided due to lighting loads using prototypical building models aggregated across electric grid nodes in the Midcontinent Independent System Operator (MISO) region in the United States. Findings suggest, in a future case with 100% LED fixtures and 30% technology penetration for smart lighting controls, lighting loads can provide around 250 to 475 MW (0.21 to 0.39 % of MISO's peak load) of Flexibility Services in the MISO region. The results can be used as inputs for grid levels models to predict future generation, transmission, and distribution investments for future high renewable energy scenarios.

4.1 INTRODUCTION

The electricity generation due to renewable resources such as wind and solar combined is projected to represent 36% of the total energy generation in 2050 (EIA Energy Outlook 2022). These renewable energy generation sources depend on wind speeds and available solar radiation, which can be highly variable throughout the day. Furthermore, these generation sources do not match

exactly with electricity demand in terms of when electricity is produced versus consumed. With limited grid-level storage, electricity generation needs to be balanced with electricity demand in real-time. This variability is usually addressed using various grid-based services known as Flexibility Services (FS).

These Flexibility Services come in various forms. FS can be categorized based on how fast each can be activated to overcome the loss in generation or spike in demand, the amount of demand that can be provided by this service, and the duration for which they can remain active. FS categories include (1) transient frequency response which has the ability to compensate for the changes in under 0-20 seconds following loss of generation; (2) frequency regulation which can provide a continuous steady-state frequency control in approximately 30 seconds (remain active for 15 mins); (3) contingency reserves that can compensate for the loss of generation under 10 minutes (remain active for 30 mins); (4) load following or ramping reserves that can compensate for 30 min to 4 hour daily changes in net load; and (5) planning reserves, which are usually used to satisfy the annual peak periods (Ma et al. 2013; Ryan et al. 2014).

Currently, these FS are dependent mostly on non-renewable sources (MISO 2020), such as natural gas and oil. However, with reductions in non-renewable sources in the generation mix, compounded with more FS requirements due to increases in variable generation such as solar and wind, there is a need to provide FS using sources other than non-renewable generation sources. Further, with more renewable energy generation sources, FS will not only be needed during peak demand periods but also throughout the day. Furthermore, the transmission flow patterns significantly change with distributed renewable energy as compared to current transmission patterns dominated by non-renewable energy sources where the flow of electricity is from the

power generation plant to the consumers, therefore possibly requiring more transmission infrastructure in the future as the more distributed renewable energy is added to the gird.

Demand-side FS thus can help provide load flexibility and reduce capital investment for transmission and distribution systems by modulating loads in existing buildings to match available capacity. Various types of loads in commercial and residential buildings can potentially provide these FS. These loads can be broadly classified into two categories, including activity-driven loads (ADLs) and thermostatically controlled loads (TCLs) (Kunwar el al. 2021). ADLs are generally loads from appliances that are largely influenced by occupant activities, such as clothes washers, dryers, dishwashers, lighting, and electric vehicles. TCLs include electricity-consuming appliances such as HVAC (Heating, Ventilation and Air Conditioning) systems and water heaters, which are largely controlled by a thermostat. These different types of loads have different response times, total capacity reduction potential, time-of-day availabilities, and technology penetration levels. Thus, there is a need to study these loads separately.

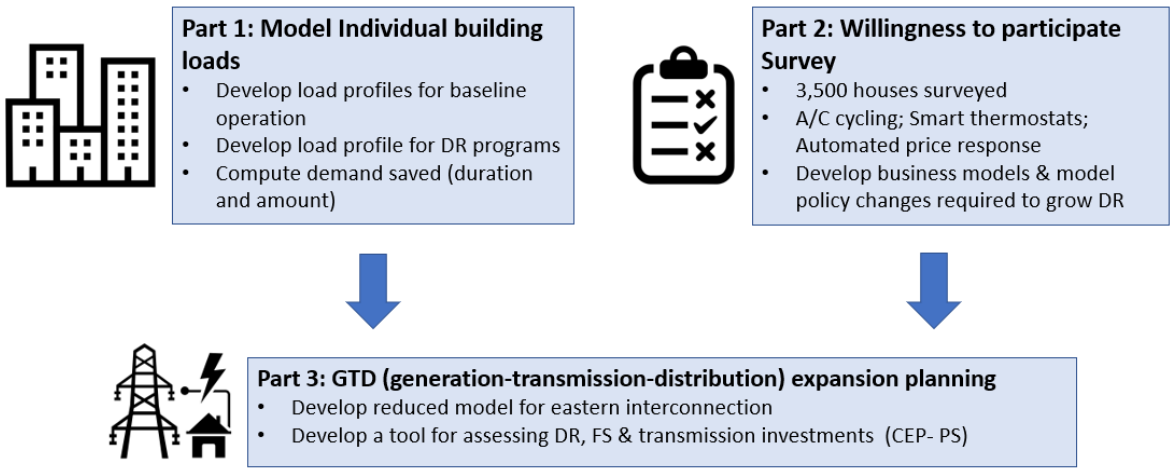

Figure 4-1 Overall Framework for Assessing Grid Level Impacts of Building Participation as Flexibility Services

The focus of the overall project was divided into three (3) main parts, as shown in Figure 4-1. A three-part framework is proposed to assess grid-level impacts of current and future potential loads,

individually and together, serving as FS. The projects were focused on residential and commercial sectors. The loads likely to represent a significant opportunity for load control but are not currently significantly utilized were chosen. In Part 1, building-scale to grid-scale models of individual loads were developed, focusing first on assessing the upper bound of the deployment opportunity of each load by time of day, day of week, and season. In Part 2, we assess the willingness of the potential building customers to participate in FS as a function of load type, time of participation, and whether the necessary technology is currently deployed. Parts 1 and 2 are then combined to determine the percentage of the available loads that customers will allow to be modulated. These are aggregated at the grid bus level as input into Part 3, GTD (generation-transmission-distribution) expansion planning software. This software co-optimizes generation, transmission, and distribution investments and operations. As discussed, the project is focused on the MISO region of the U.S. electric grid. This study, however, primarily focuses on Part 1 of the overall study, which is to estimate the flexibility provided by dimming lights to reduce lighting loads in commercial buildings at individual and grid levels.

The Illuminating Engineering Society (IES) recommends standard work plane lighting levels for various building and space types (IES Lighting Handbook 2011). However, several studies suggest that it is acceptable to reduce the lighting levels by a certain amount from the initial lighting level without occupants detecting it, also described as “detectable level”, or without it causing any significant visual discomfort, called an “acceptable level”. Most studies have evaluated these levels by reducing lighting levels gradually, and participants are asked to complete a survey to determine “detectable” and “acceptable” levels. For instance, Tenner et al. (1997) suggests that a reduction of 13% from an initial base illuminance value of 830 lux is acceptable. Similarly, two other studies (Kryszczuk and Boyce 2002; Akashi and Neches 2004) suggest that a reduction of

17% and 15-25%, respectively, from the initial base illuminance value of 1095 lux and 500 lux, is barely detectable. Further, Hu and Davis (2016) suggest reductions around 17.8 to 19.1% from the baseline values are acceptable for base illuminance levels lower than 500 lux. Various studies have highlighted the rate of dimming used for their studies, however as per Kryszczuk and Boyce (2002) who analyzed various rates of dimming between 10 lux/sec to 340 lux/sec concluded that rate of dimming does not influence the "acceptable" and "detectable" levels. The "detectable" and "acceptable" levels for various studies are summarized in Figure 4-2. The x-axis denotes the initial illuminance level used in the study and the y-axis denotes the percent reduction from the initial illuminance level that is "detectable" or "acceptable" by the participants.

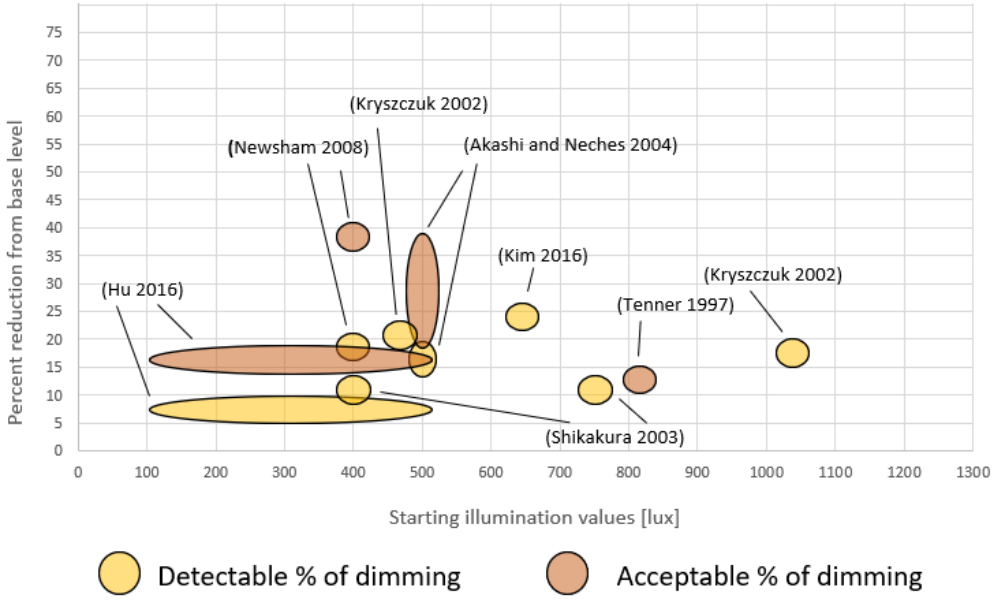

Figure 4-2 "Detectable" and "Acceptable" levels for lighting dimming based on prior literature

The divergence in the acceptable and detectable levels, as seen in Figure 4-2, across different studies, can be attributed to the differences in the experimental setup and the assumption on how their values were deduced. Across these studies, there are various initial illuminance values from which the lights are dimmed (shown as x-axis in Figure 4-2). With the experimental setup, for

instance, (Kryszczuk and Boyce 2002) asked participants to observe a black-painted target object as the illuminance levels were decreased, during which each trial subject (involved 16 participants) was asked to press a button when they detected a change. The experiment was conducted in two cases, one with distraction (of a mental task) and the other without any distraction. Hu and Davis (2016) experiment used a two-box setup, where for one box (also called the reference box) the illuminance value is one of the 5 baseline illuminance values (100, 200, 300, 400, and 500 lux) while the illuminance in the other box is a percentage increase or reduction from the baseline illuminance. The illuminance in both the boxes is randomized, and the participants are asked to select the brighter box to deduce the detectable level. For the acceptable level, the same setup is used but now the participants are given the controls to match the illuminance in box two with the reference illuminance for all 5 cases. Further, the results across the studies might differ as the experiment is subjective based on the participant's feedback using a limited number of participants. However, one similarity between all experiments in Figure 4-2 is that they were conducted in a windowless room to avoid the influence of natural daylight.

Lighting loads in commercial buildings are generally dependent on multiple factors such as space type (e.g., open office, library, surgery rooms), the operating schedule of the building, and the age of the building or the lighting efficiency. Therefore, lighting loads generally have consistent use patterns, with the stronger predictors being the day of the week (weekdays/weekends) and time of day, with some minor seasonal variations due to changes in sunrise and sunset times. Thus, lighting-based dimming as FS can be used consistently in all climate regions. Based on CBECS (2018), the total commercial building energy consumption was around 1.12 trillion kWh. Of the total electricity used by commercial buildings, lighting loads account for approximately 17 % (0.201 trillion kWh) of electricity consumption (CBECS 2018). Further, to facilitate these lighting

loads for FS, the building needs to be equipped with technologies that allow the detection of available daylight and fixtures that dim the lights based on signals from the grid. Currently, only 7-8 % of commercial buildings are equipped with technology that is likely to support demand-side FS (CBECS 2018). However, the Department of Energy's (DOE) report for the forecast of lighting technologies suggests that the connected LED lighting market will grow to include 31% of commercial buildings by 2035 (US DOE 2019). Thus, as lighting technologies are more available, lighting-based dimming in commercial buildings can contribute towards FS.

Unlike residential buildings, where significant, high-frequency sub-metered energy consumption datasets are available from various disparate sources, for commercial buildings, such extensive datasets that account for various commercial building types, ages, and climate zones, and provide end-use sub-metered data, are not available in the United States. Due to the lack of extensive and granular measured data, this study uses the DOE Commercial Reference and Prototype building models as the basis for modeling lighting-based FS in commercial buildings (U.S. DOE 2022a, U.S. DOE 2022b). The assumption for these models can be found here. (Deru et al. 2011).

To scale the individual Reference and Prototype building models and their corresponding loads to the grid level, this study used various datasets, including EIA Form 861 (U.S. EIA 2021), and building stock inventories, including the Commercial Building Energy Consumption Survey (CBECS 2012), and Commercial Building Inventories (Ma et al. 2019; Day 2020) that provide information about the number and type of buildings, age, and their areas, for specific locations of study. Each state's energy code adoption year was also used to assign the building stock to a Reference, or a Prototype building model based on a building's age. Further, the existing buildings that were built before the first energy code was adopted were matched to an appropriate Prototype building model using the age of construction and an estimate of energy use intensity (EUI) taken

from the Building Performance Database (BPD) (LBNL BPD 2019). This is done to account for energy retrofits in the older building stock that have higher EUI values. Further details on these summarized methods are provided in the methodology section.

Various research studies have estimated the demand flexibility potential for residential loads such as clothes washers, clothes dryers, and dishwashers (also known as Activity Driven Loads) (Berg, Brady et al. 2022, Kawka Emily 2022, Kunwar, et. al. 2021), and for commercial buildings, most of the studies have focused on HVAC loads for demand flexibility (Tina et. al. 2022, Cetin et. al. 2019, Tran-Quoc et. al. 2009). This study (Langevin et al. 2021) provides grid-level estimates for various grid regions throughout the USA for the residential and commercial sectors for both demand flexibility and energy efficiency. The demand flexibility estimates include precooling and appliance scheduling for residential buildings and strategies like precooling, thermostat temperature adjustment, and ice thermal storage for commercial buildings. However, very few comprehensive studies exist that provide grid-level aggregation estimates for different types of commercial buildings for lighting loads. This study also summarizes the existing research on detectable and acceptable levels of lighting dimming for DR-based events for lighting loads. This is the gap this study is focused on addressing.

Thus, this study focused on estimating the demand side FS potential of lighting loads for commercial buildings aggregated to the MISO region, which generally encompasses the Midwest region of the U.S. The scaling of such FS provided by lighting loads to the grid level can be used to predict the upper bound of load reduction by the time of day and day of the week. It can also be used as an input into grid models focused on predicting future GTD (generation-transmission-distribution) investments (Li and McCalley 2017; Zhou, Wang, and McCalley 2011). In addition, the framework used herein to assess individual loads can be used to evaluate the potential for FS

support for other types of building loads at the building- and grid scale. This paper is organized as follows: Section 4.2 discusses the methodology for modeling building-level loads; Section 4.3 focuses on aggregating building-level loads to grid level; Section 4.4 and Section 4.5 discuss the building-level and aggregated grid node level results for the MISO region. Section 4.6 discusses the conclusions and limitations of the study.

4.2 BUILDING LEVEL MODELING

Lighting-based FS was modeled using both the DOE Reference and Prototype building models (U.S. DOE 2022a, U.S. DOE 2022b) to capture the variations in building types across the entire commercial building stock. The US DOE Reference and Prototype building models are sub-categorized into two types of residential apartments and 14 commercial building types, such as office buildings, primary and secondary schools, retail buildings, hospitals and others as shown in Figure 4-3. These buildings are shown in Table 4-3 with their Lighting Power Densities (LPD). These models have different assumptions for space utilization, occupancy, equipment and lighting loads, and HVAC system types used for heating and cooling (Deru et al. 2011). Hospital and outpatient buildings are excluded from this study with the assumption that these buildings are considered critical, and any lighting reduction under IES guidelines might need detailed evaluation of these building types.

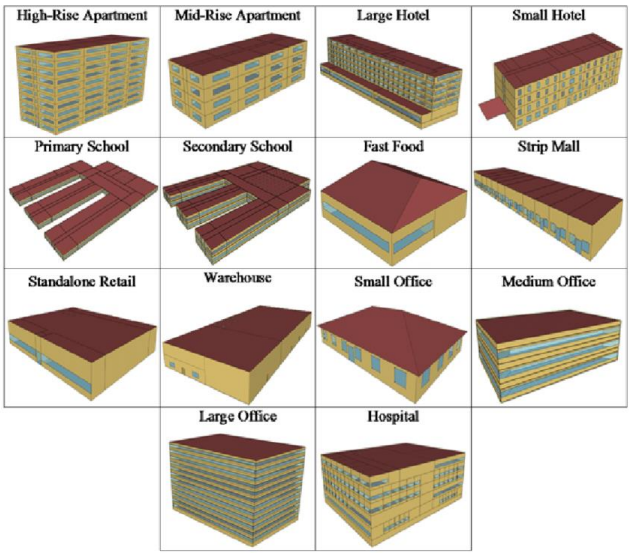

Figure 4-3 DOE Reference building models

The Prototype building models were used for all buildings built after the adoption of the ASHRAE 90.1-2004 and the Reference building models were used for buildings built before this time. The year for ASHRAE 90.1 code adoption for various versions for different states is summarized by Livingston et al. (2014). For buildings that were constructed between 1980 and the first code adoption year of that particular state, the post-1980 Reference building models were used. For buildings constructed before 1980, the pre-1980 Reference building models were used. Table 4-1 outlines each of the building energy models used and some of their characteristics. Figure 4-4 compares the EUI for Prototype building models with the EUI data available for office buildings in Building Performance Database (BPD).

Table 4-1 Building models used and description

U.S. DOE Building Energy Model Version	Daylighting Control in Energy Model	US DOE building energy model type	Is BPD[a] used to redistribute the areas?
Pre – 1980	No daylighting controls for any zones	Reference	Yes
Post - 1980	No daylighting controls for any zones	Reference	Yes
ASHRAE 90.1-2004	No daylighting controls for any zones	Prototype	No
ASHRAE 90.1-2007	No daylighting controls for any zones	Prototype	No
ASHRAE 90.1-2010	Daylighting controls in some zones	Prototype	No
ASHRAE 90.1-2013	Daylighting controls in some zones	Prototype	No

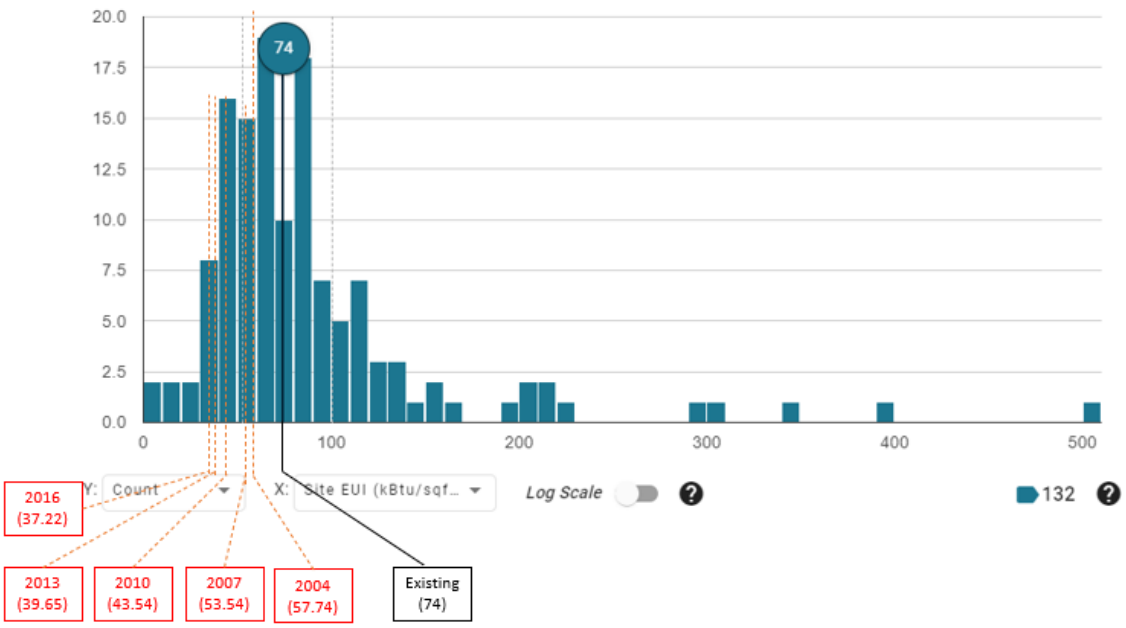

Figure 4-4 EUI for Prototype building models compared with EUI data from BPD for office buildings

Zones in all commercial buildings can be categorized based on whether daylighting controls are present (lighting loads are reduced using daylighting controls when sufficient daylight is available) and if lighting loads for a particular zone will be available for use in FS. As specified in Table 4-1, the post-1980 and pre-1980 Reference building models do not have daylighting controls for any zones. Similarly, the ASHRAE 90.1-2004 and 90.1-2007 Prototype building models do not have daylight controls, while the ASHRAE 90.1-2010 and 90.1-2013 Prototype building models have daylight controls for some perimeter zones. The amount of lighting load reduced for daylighting control in Prototype models (ASHRAE 90.1-2010 and 90.1-2013) is determined using daylight reference points (points where horizontal illuminance values are calculated), daylight illuminance setpoint values at reference points (lighting level at the reference point when the electric lighting is operating at full input power), fraction of lighting controlled by the reference point, and the control type (stepped, continuous).

There are also some zones for which lighting-based FS is not considered, such as classrooms in primary and secondary school education buildings as these zones are assumed to be critical. The hospital building and outpatient care buildings are not considered for FS and are also not considered in this study. Thus, all the zones can be divided into 4 types as shown in Figure 4-5.

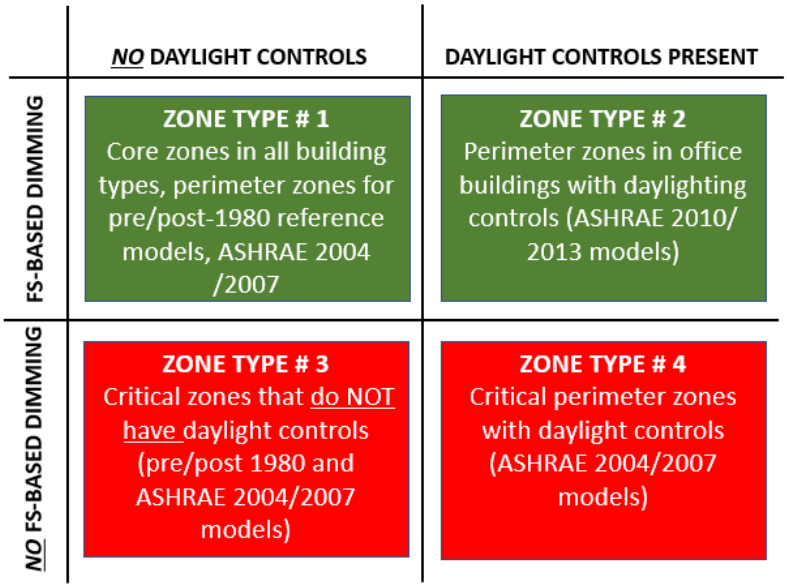

Figure 4-5 Categorization of zones based on if the zones have daylighting controls and if FS based lighting dimming is considered *(Note: Green zones provide FS based savings; Red zones do NOT provide FS based dimming)*

Zone Type #1 (such as all zones in pre-1980, post-1980, ASHRAE 90.1-2004, and 2007, core zone in ASHRAE 90.1-2010 and 2013 for all building types) do not have any daylighting controls, but lighting-based FS is considered in these zones. Thus, for Zone Type #1, the only reduction in lighting load is for FS services. Based on a literature review of "detectable" and "acceptable" lighting levels, dimming of 20% from the base illumination level is assumed as an acceptable level for this study (Figure 4-2). For Zone Type #1, if lighting levels are 500 lux under normal operating conditions, the acceptable level for FS-based dimming would be 400 lux (i.e., 20% reduction). In all cases, the lighting power was assumed to be linearly proportional to the light produced (lux) by the lighting fixture (Raziei and Mohscnian-Had 2013; Karpilow, Henze, and Beamer 2020). For

example, Figure 4-6 (a) shows the difference between the lighting power for a baseline case without FS-based dimming and with FS-based dimming for an ASHRAE 90.1-2004 small office building. The demand saved for FS is the difference between the baseline model without dimming controls and the baseline model with 20% DR-based dimming.

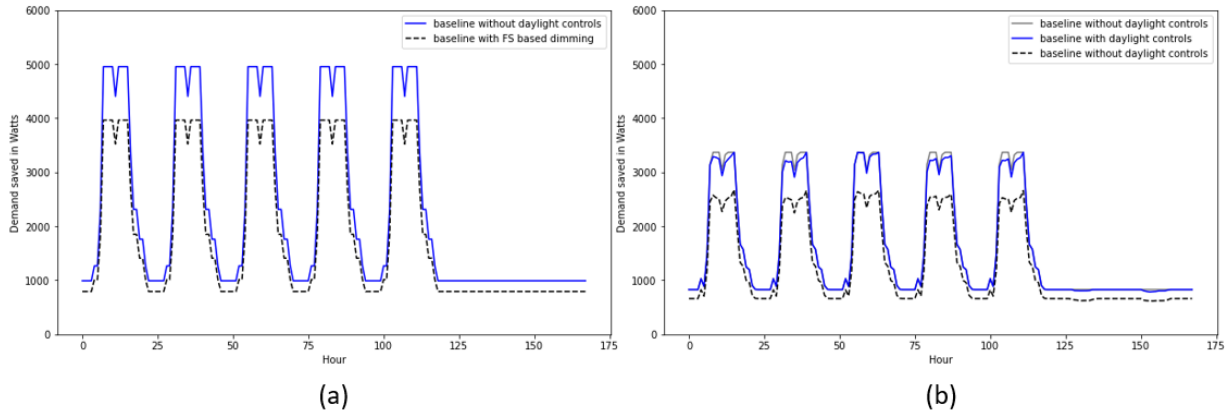

Figure 4-6 FS-based dimming for an (a) ASHRAE 90.1-2004 small office building with Zone Type #1 core and perimeter zones and (b) ASHRAE 90.1-2010 small office building for Zone Type #1 core zone and Zone Type #2 perimeter zones) (*Note: For the core zones of both ASHRAE 90.1-2004 and ASHRAE 90.1-2010 model 20% dimming is assumed)*

For Zone Type #2 (perimeter zones in ASHRAE 90.1-2010 and 2013 for DOE buildings that have daylighting controls) which use daylighting controls and are considered for FS-based dimming, it is important to distinguish between the dimming due to the already existing daylight controls, for which the reduction in lighting power is already utilized as an energy-saving measure, and lighting power reduction for FS based lighting dimming which is due to the reduction in the acceptable level by 20 %. This can be seen as three different cases. (i) If the daylight illuminance setpoint value at the reference point (which controls the entire zone) is 500 lux and the available daylight at that timestep is 700 lux, the lighting power is reduced to zero using daylight controls and there is no opportunity for FS-based dimming as the lighting is already off due to daylighting controls. (ii) For cases where the available daylight is less than 500 lux but more than 400 lux (which is 20 % lower than 500 lux). As the available daylight is still higher than 400 lux, which is the acceptable

lighting level during the FS event is acceptable, the artificial lighting is fully switched off. This provides FS based savings somewhere between lux and 100 lux. (iii) For cases when the available daylight is less than 400 lux, e.g., 150 lux, the daylighting control would reduce the power consumption such that the remaining needed lighting (i.e., 250 lux in this example) is provided by the artificial electric lighting, which provides the maximum allowable FS based lighting savings of 100 lux (which is 20% of 500 lux). These cases for Zone Type #2 are highlighted in Figure 4-7.

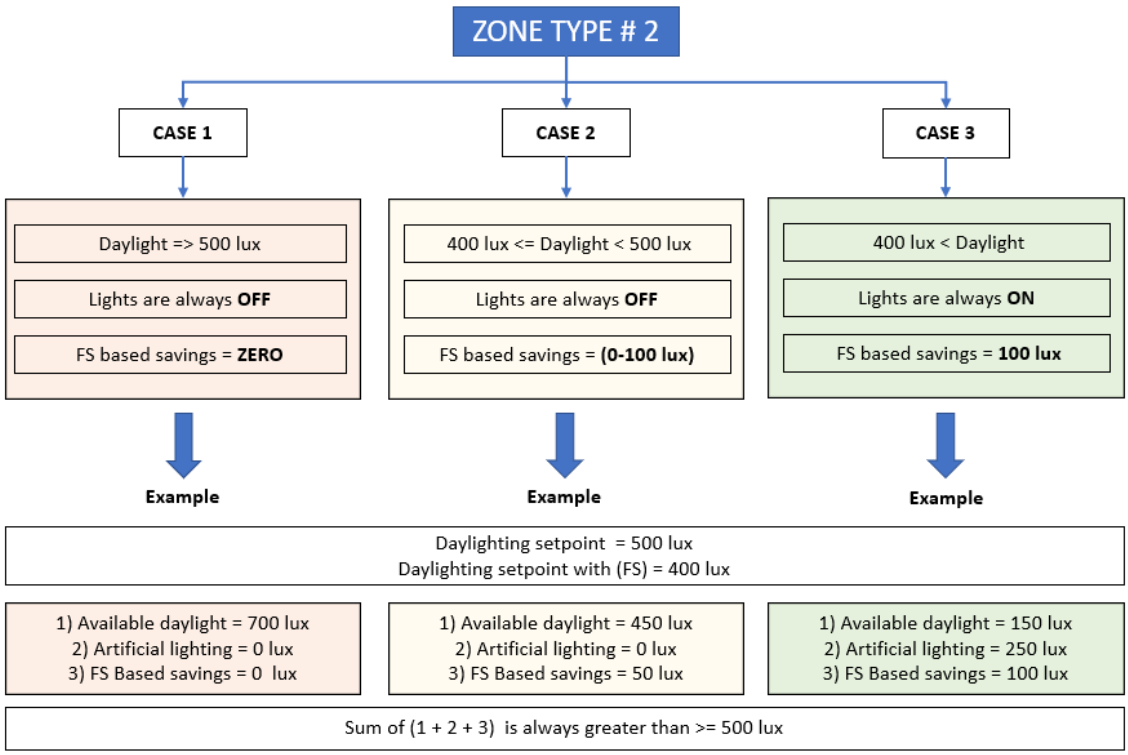

Figure 4-7 Cases for FS savings for Zone Type #2 (perimeter zones in office buildings with daylight controls) based on available daylight

The figure 4-8 below shows a plot of how the annual values are converted to a 24-hour boxplot. Figures 4-12a and 4-12b thus only show the maximum and minimum (yellow and blue line respectively). As the pre-1980/post-1980, ASHRAE 90.1-2004, and ASHRAE 90.1-2007 building energy models do not have any perimeter zones with daylighting controls, thus the minimum and

maximum demand reduction are the same. However, building energy models following ASHRAE 90.1-2010 and ASHRAE 90.1-2013 have daylighting controls for some of their perimeter zones and thus have a different minimum and maximum value. The minimum values for demand saved for lighting-based FS thus represent a case where daylighting controls dimmed most of the lights and lighting therefore was either not available for FS, or it represented a smaller portion of lighting. For the maximum demand saved case, lighting was more available for FS-based dimming as they were not switched off due to less available daylight during this period.

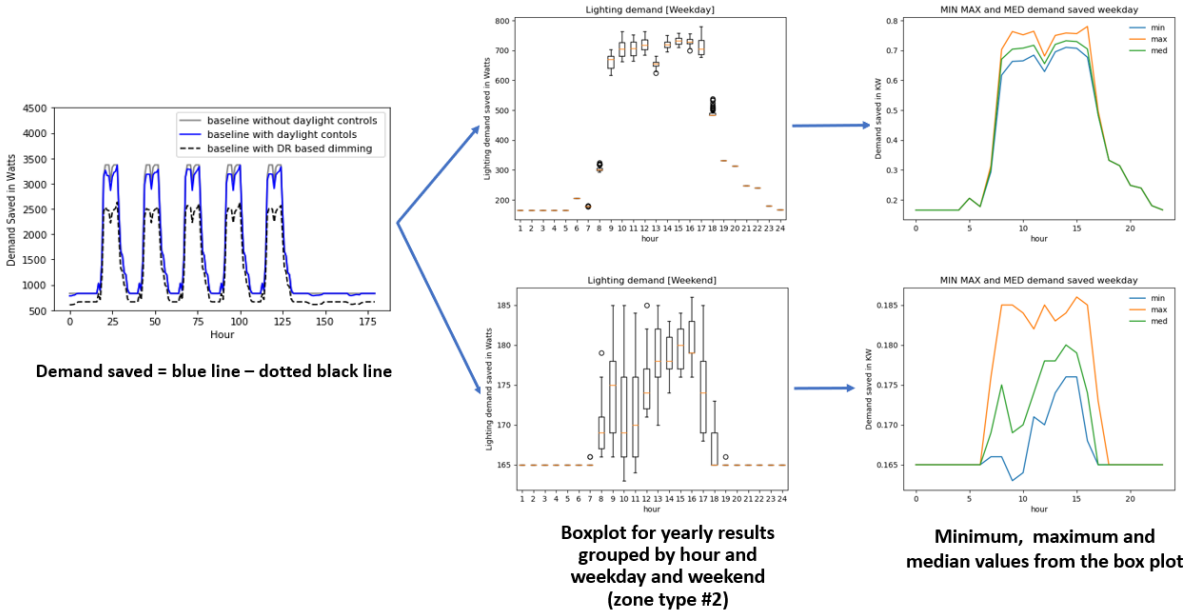

Figure 4-8 Conversion of annual lighting results to an hourly profile for Zone Type #2

This logic was applied to the models in EnergyPlus using the EMS (Energy Management System) program for all Zone Type #2. Figure 4-6 (b) shows the demand saving due to FS for an ASHRAE 90.1-2010 Prototype building. The difference between the zone lighting power after daylighting (in blue solid line) and the lighting power after dimming (dashed black line) is the lighting load saved for FS. Figure 4-6 (b) also shows the baseline lighting power without daylighting controls (solid line in gray) to highlight the dimming associated with daylighting controls.

Zone Type #3 (all critical core zones such as classrooms in pre-1980, post-1980, ASHRAE 90.1-2004, and 2007 for all building secondary and primary buildings) does not have any daylighting controls to adjust lighting levels and they are not considered for dimming as FS due to being important. Similarly, Zone Type #4 (all critical core zones such as classrooms in ASHRAE 90.1-2010 and 2013 for all building secondary and primary buildings) uses daylighting control but are not considered for dimming as FS due to being important. Therefore, all zones that fall under Zone Type #3 and #4 do not contribute to any lighting load savings for FS. The lighting load reduced for FS for all Zone Types are combined at an hourly level over a period of one year for each building type. The lighting load reduction is then aggregated by hour for weekdays and weekends.

4.3 GRID LEVEL MODELING

4.3.1 Datasets for grid-level modeling

Commercial Building Inventories

The Commercial Building Inventories (Day 2020) dataset provides modeled data for commercial buildings by building type, age, and building area for all the cities and counties in the United States. The dataset is modeled using CoStar Realty Information data and FEMA Hazus building stock data (FEMA Hazus) through a process described in (Ma et al. 2019). The study suggests an overlap between the CoStar and the FEMA Hazus dataset, and some buildings may be represented twice. Thus, only CoStar data was used for this study as it is more detailed than the FEMA Hazus dataset.

City and County Energy Profiles

The City and County Energy Profiles data provides modeled electricity and natural gas consumption and expenditures, and associated emissions for all the cities in the United States (Day 2020). This dataset was used to compare the total energy consumption for commercial buildings from this dataset to the energy consumption of the county aggregated model of DOE Reference

and Prototype building models developed in this work. As the CoStar dataset, which is used to represent the building stock, is a subset of the entire building stock dataset, the City and County Energy Profiles energy consumption data was used to magnify the existing data and ultimately account for all the buildings in each county.

Building Performance Database

The Building Performance Database (BPD) contains information related to building characteristics such as age, building type, climate zone, heating and cooling characteristics, and energy-related characteristics such as the source and site Energy Use Intensity (EUI) for a large number of residential and commercial buildings in the U.S (LBNL BPD 2019). For this study, the BPD Application Programming Interface (API) is used to obtain summary statistics of EUIs of U.S. commercial buildings filtered by age, building type, and climate zone. The intended purpose of these summary statistics is to compare the EUIs of the DOE Reference and Prototype building models with buildings built before energy code adoption in order to estimate the older buildings in the database that have lower EUIs due to energy-related retrofits.

4.3.2 Scaling individual model to the MISO region

The Commercial Building Inventory data was split into five regions namely West, Midwest, Northwest, South Central, and South Atlantic. EIA Form-861 (US EIA 2021) contains information on which counties are in the MISO region. Both the Commercial Building Inventory data and the EIA Form-861 are used to filter building stock data associated with counties in the MISO regions. The energy code adoption year for each state (Livingston et al. 2014) and the year built for the building stock were used to aggregate the building areas into six groups based on the ASHRAE energy code version as per Table 1 for 12 building types (hospital and outpatient buildings are excluded) and for each county in the MISO region. Initially, the area was aggregated only based

on the year of construction and did not account for any energy retrofits in the older buildings built before the code adoption.

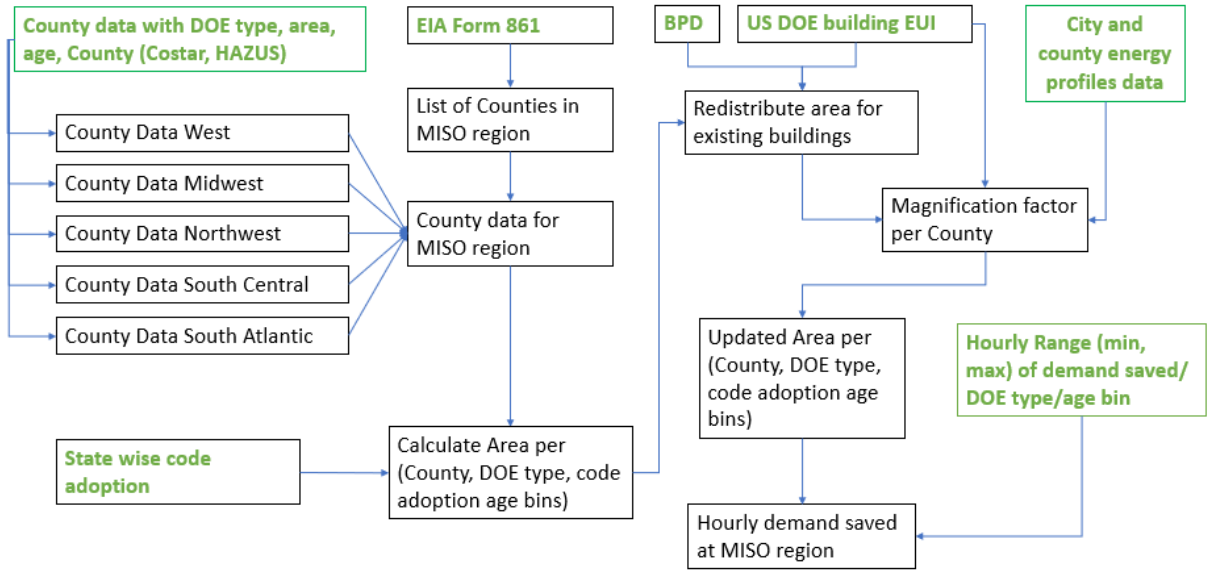

Figure 4-9 Steps to scale individual Reference and Prototype building energy models to the MISO region *(Note: CoStar- Commercial real estate building dataset, HAZUS - Building hazards database, BPD - Building Performance Database)*

To account for energy retrofits in building groups built before code adoption (e.g., pre-1980, post-1980), BPD summary statistic data was used. The BPD summary statistic data includes the site EUI values for the 0th, 25th, 50th, 75th, and 100th percentile for the data filtered based on age, climate zone, and building type. Various studies have used a Weibull distribution function to determine a corresponding EUI for these percentile values (e.g., Geraldi and Ghisi 2020). Thus, the EUI distribution function and the EUIs calculated for the Reference and Prototype building models were used to redistribute the older buildings into groups that better match their EUIs to account for retrofits that may have occurred. For example, to redistribute the area for an office building built before 1980 in ASHRAE Climate Zone 5A, BDP data was used to estimate the distribution function of the EUI of all available office buildings in the BDP database filtered by age group, climate zone, and building type.

As the CoStar dataset is a subset of the building stock in the City and County Energy Profiles data, energy consumption data by county was used to magnify and ultimately account for all the buildings in each county. Further, the redistributed building areas for all Reference and Prototype building models for all code versions for each county were combined to calculate the demand savings for each hour across a year-long period for each county. The complete steps to aggregate building-level loads to the MISO level are shown in Figure 4-9.

Each county was then assigned to a grid node. The reduced model for the MISO region was developed following Newlun et al. (2021). The reduced MISO node model consists of 158 nodes, as shown in Figure 4-10. For the assignment of a county or a group of counties to a node, the peak load at each bus is calculated using the peak load for MISO (121 GW, which was the peak load for the high-temperature summer of 2019) multiplied by the load distribution factors (LDFs) at each node. The LDFs at each node are obtained from a 2024 Heavy Summer MTEP power flow case. The MISO peak load in 2019 was used instead of a recent year to choose a pre-pandemic year.

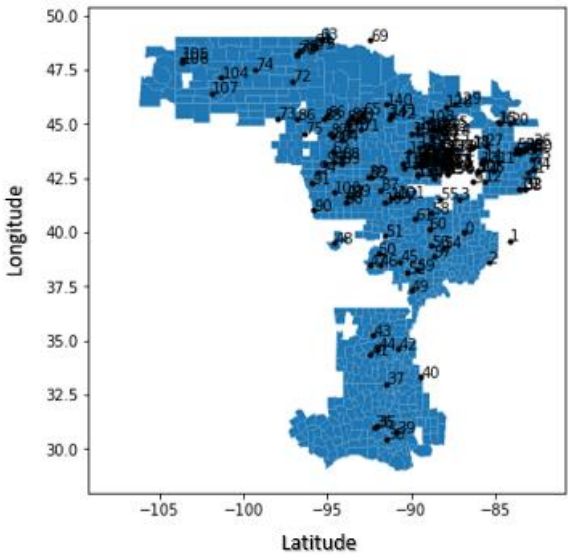

Figure 4-10 MISO grid reduced node model developed by Newlun et al. (2021) *(Note: each of the counties in the MISO region are shown in blue; each of the grid nodes is labeled numerically and represented using a black dot in the figure)*

The average load for each county is calculated using total annual energy consumption for each county taken from (Day 2020) across 8760 hours. Initially, load from each county was assigned randomly to one of the five closest nodes based on distance. The distance between each county and bus combination was calculated using the latitude and longitude of the centroid of the county and the bus. For each node, a group of counties is assigned, and the sum of the load for all the counties in the group is compared to the load at the node. As several combinations for assignments is possible with more than 850 counties and 158 busses, the assignment was optimized using a genetic algorithm-based optimization (PyPI Geneticalgorithm) such that the difference between the load at each node and the sum of loads for the randomly assigned counties to that node is minimized, as shown in Figure 4-11.

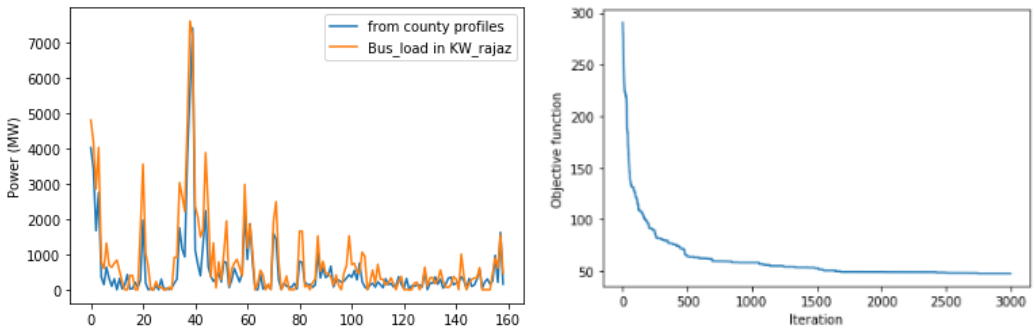

Figure 4-11 County to node assignment for 158 nodes in the MISO region using Genetic Algorithm

To account for the amount of demand flexibility that can be provided at present and in the future depends on various factors such as the (a) LPD of the lighting systems (whether the fixtures are LED, or a combination of various technologies), (b) percent of buildings that have daylighting controls, (c) technology penetration for lighting fixtures that provides the lighting fixture the ability provide a dimming response based on a signal and (d) customer willingness to participate in the FS programs now and in the future. Three cases are thus developed, as outlined in Table 4-2. Case 1 is used to show lighting demand saving associated with FS for the building stock that was developed based on Figure 4-9, which includes buildings assigned to a Reference or Prototype building model based on age and energy code adoption. Case 2 is where all the lighting in all buildings is considered to be LEDs and Case 3 is where all buildings have 100 % percent LEDs, and 100 % daylighting controls for all the zones that have daylighting in ASHRAE 90.1-2013 model.

Table 4-2 Nomenclature for various test cases for aggregation

Case	Description	Technology penetration		
		10% (current)	30% (2035)	100% (ideal)
Case 1	Building stock developed in Figure 4-9	Case_1_TP_10%	Case_1_TP_30%	Case_1_TP_100%
Case 2	Case 1 with (100 % LED retrofit)	Case_2_TP_10%	Case_2_TP_30%	Case_2_TP_100%
Case 3	Case 1 with (100 % LED retrofit + 100 % daylighting controls)	Case_3_TP_10%	Case_3_TP_30%	Case_3_TP_100%

For all cases, three technology penetration scenarios are shown in Table 4-2, including, (1) the current (present-day) case with 10% technology penetration, (2) the future case in 2035 with 30% technology penetration, and (3) the ideal case in the future with 100% technology penetration. The customer's willingness to participate is assumed to be 100 % in this study as such data for commercial buildings does not exist currently.

Table 4-3 shows the LPD of all the Reference and Prototype buildings by ASHRAE energy code versions. The LPD for ASHARE 90.1 -2019 is assumed to have all LED fixtures and is used as a reference to convert the LPD for other energy code versions to 100% LED for Cases 2 and 3. For instance, the LPD for a small office building for Pre-1980 and Post–1980 models is 19.48 W/m2. To account for 100% LED in Case 2 the lighting demand savings for the small office buildings, The LPD Pre-1980 and Post–1980 small office building is multiplied by a factor of 0.353 (i.e. 6.89/19.48 is taken from Table 3). Similarly, factors are used to convert all building type and energy code version models to 100 % LED for Case 2 and Case 3. The values in Table 3 are the average LPDs by zone area for each building type and building energy code versions.

Table 4-3 Average Lighting Power Densities (LPDs) in (W/m^2) for Reference and Prototype building models by energy code version

Building Type	Pre/post - 1980	90.1-2004/2007	90.1-2010	90.1-2013	90.1-2019 (reference to convert other code versions to 100% LED)
Small Office	19.48	10.76	9.68	8.83	6.89
Medium Office	16.89	10.76	9.68	8.83	6.89
Large Office	16.14	10.76	9.68	8.83	6.89
Stand-alone Retail	32.32	16.74	16.30	14.16	10.19
Strip Mall	38.47	19.58	19.08	17.18	12.99
Primary School	19.55	12.78	11.27	11.33	7.37
Secondary School	15.17	12.20	10.26	10.20	7.35
Small Hotel	16.23	10.42	8.31	9.40	4.92
Large Hotel	16.70	10.76	10.40	9.36	5.34
Warehouse	6.63	8.72	7.56	7.52	4.83
Quick Service Restaurant	31.95	17.76	10.12	10.01	8.02
Full-Service Restaurant	24.38	19.96	9.87	10.52	7.90

In the following sections, the aggregated results are shown both at the node level as well as for the entire MISO region for all three cases and all building technology penetration scenarios. The node-level results are shown using a bubble plot over the MISO region while the node-level results represent the maximum demand that can be saved on weekdays at 2 pm. The MISO level results are calculated by adding the demand savings values at all the nodes for weekdays and weekends separately. Thus, the results show that the minimum and maximum lighting-based demand can be saved throughout the MISO region on weekdays and weekends.

4.4 RESULTS FOR BUILDING LEVEL LOADS

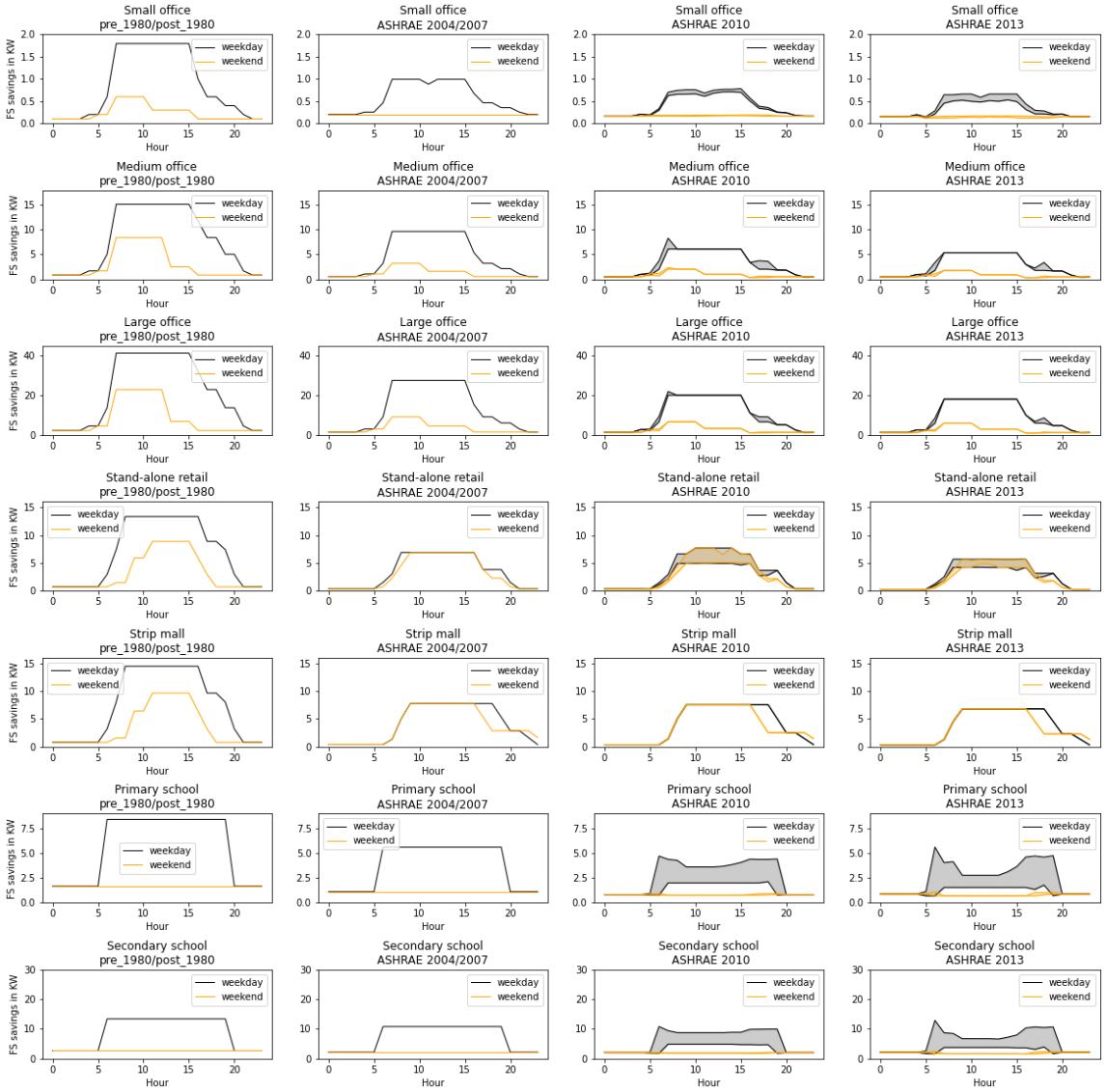

Figure 4-12a Median lighting demand saved due to FS (in kW) by building type and building code version for weekdays and weekends for DOE Prototype and Reference building models for the entire year *(Note: the shaded parts for ASHRAE 90.1-2010 and ASHRAE 90.1-2013 models represent the range between maximum and minimum lighting demand savings)*

Figures 4-12a and 4-12b show the hourly lighting demand that can be reduced due to lighting-based dimming (lighting load reduced from daylighting controls not included) at the building level by hour over a period of one year. The same procedure is repeated for all Reference and Prototype

building models and all code versions, to determine the maximum and minimum lighting load that can be used as FS by hour for weekdays and weekends.

The pre-1980/post-1980, ASHRAE 90.1-2004, and ASHRAE 90.1-2007 building energy models do not have any perimeter zones with daylighting controls, thus the minimum and maximum demand reduction are the same. However, building energy models following ASHRAE 90.1-2010 and ASHRAE 90.1-2013 have daylighting controls for some of their perimeter zones. The minimum values for demand saved for lighting-based FS thus represent a case where daylighting controls dimmed most of the lights and lighting therefore was either not available for FS, or it represented a smaller portion of lighting. For the maximum demand saved case, lighting was more available for FS-based dimming as they were not switched off due to less available daylight during this period.

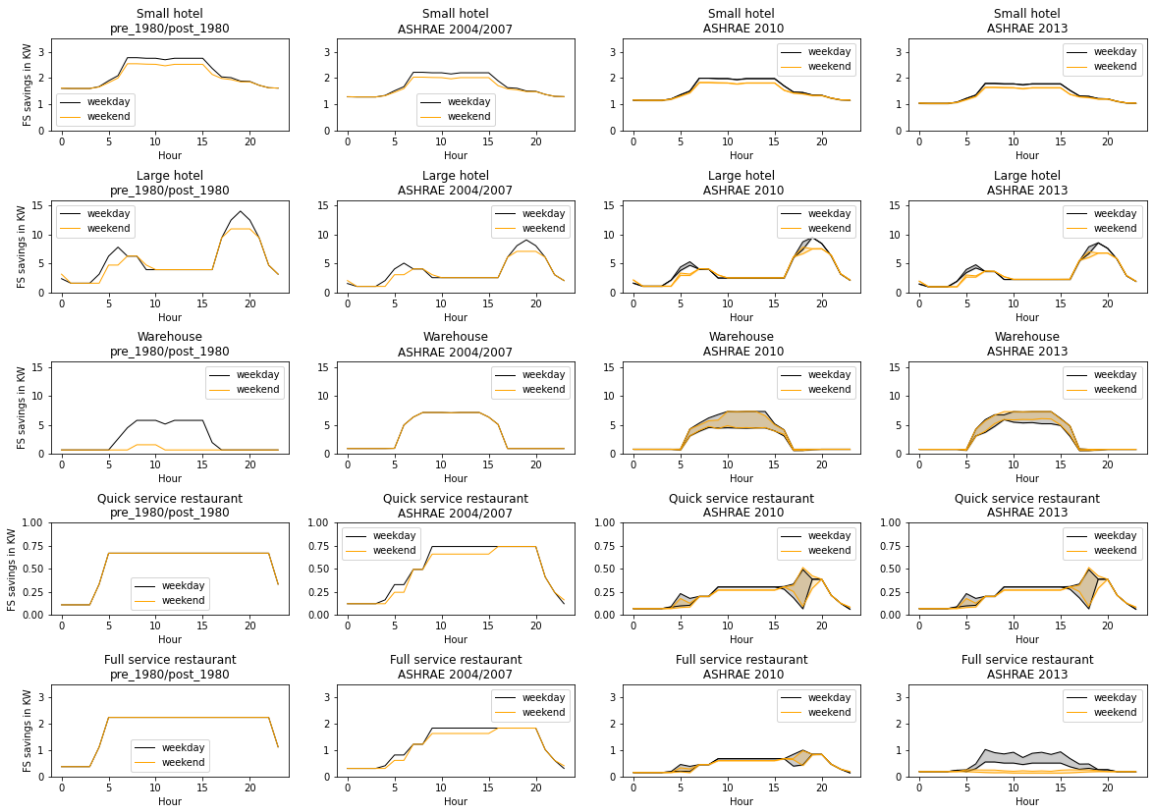

Figure 4-12b Median lighting demand saved due to FS (in kW) by building type and building code version for weekdays and weekends for DOE Prototype and Reference building models for the entire year *(Note: the shaded parts for ASHRAE 90.1-2010 and ASHRAE 90.1-2013 models represent the range between maximum and minimum lighting demand savings)*

4.5 AGGREGATED GRID-LEVEL RESULTS

Figure 4-13 shows the maximum lighting demand available for FS across the 158 nodes in the MISO grid reduced models for all 3 Cases and 3 technology penetration scenarios at 2 pm in the afternoon. 2 pm was chosen to show in the bubble plot since the lighting-based demand savings is at a maximum between 9 am to 3 pm. Thus, the use of data between 9 am and 3 shows similar results. Lighting demand that can be used for FS reduces (from top to bottom in Figure 4-13) as there are more LED lights in use (Case 2), and there are more LED lights with daylighting controls (Case 3). The lighting available for FS increases (left to right in Figure 8) as more lighting fixtures have the ability to respond to a grid signal and dim the lights to participate in FS.

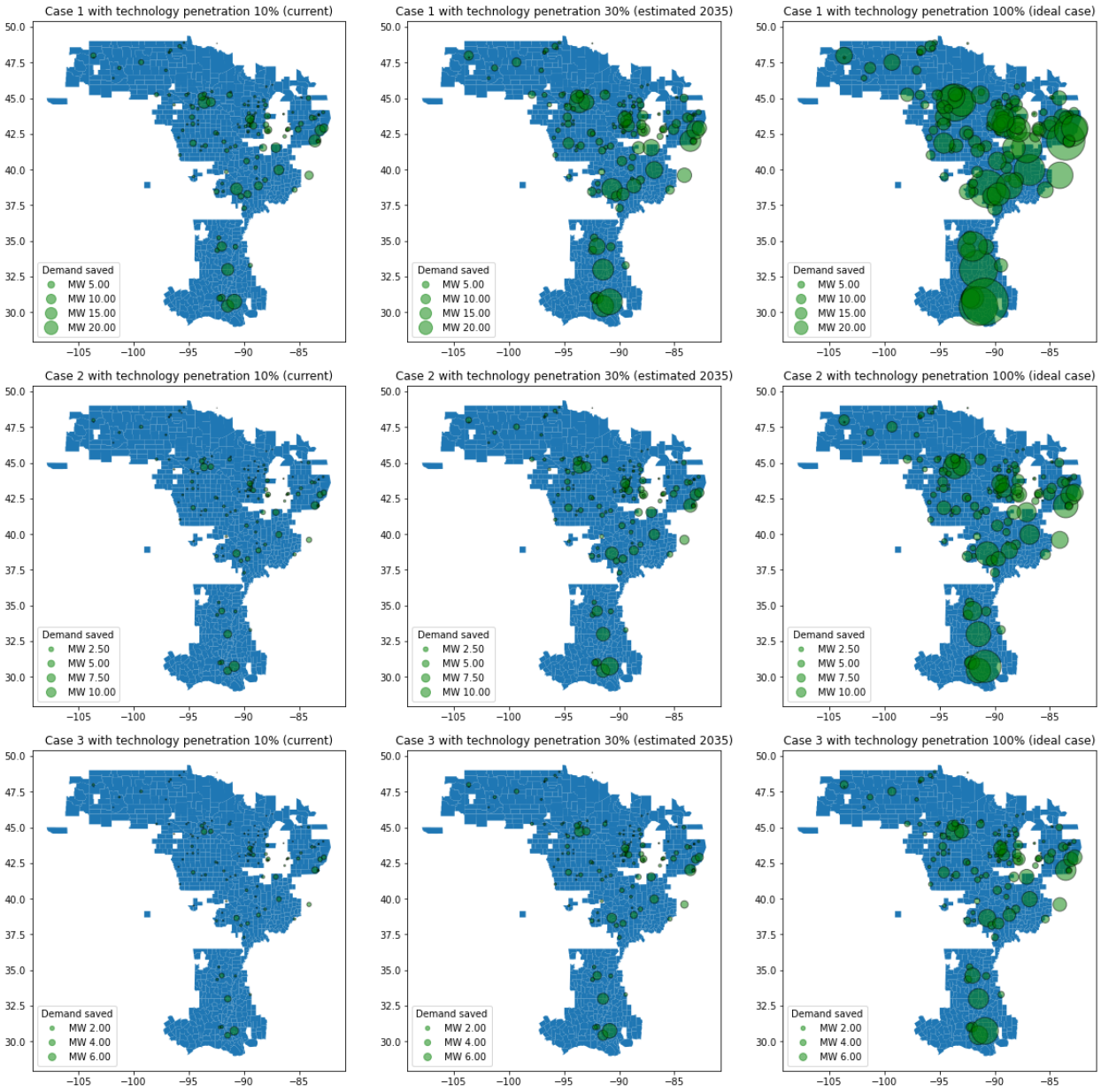

Figure 4-13 Maximum aggregated demand saved due to lighting-based FS for Case 1 (first row), Case 2 (second row) and Case 3 (third row) (see Table 2), at technology penetration scenarios of 10% (left column), 30% (center column) and 100% (right column) at grid nodes at 2 pm in the afternoon on weekdays

Figure 4-14 shows the hourly profile for lighting demand that can be used as FS for weekdays and weekends for the entire MISO region. Similar to Figure 7, Case 2 (100% LED) and Case 3 (100% LED and daylight control) reduce the amount of lighting load available for FS. In addition, the amount of lighting load available for FS increases with technology penetration. Table 4-4 shows

the magnitude and percent of electricity demand that is available for all the cases as a percentage of peak MISO load in 2019. Thus, flexibility services can be provided by lighting loads, both by newer and the older buildings in the building stock by installing fixtures with dimming-based controls. The older higher LPD lighting fixtures can provide more demand flexibility than newer lighting fixtures with low LPD.

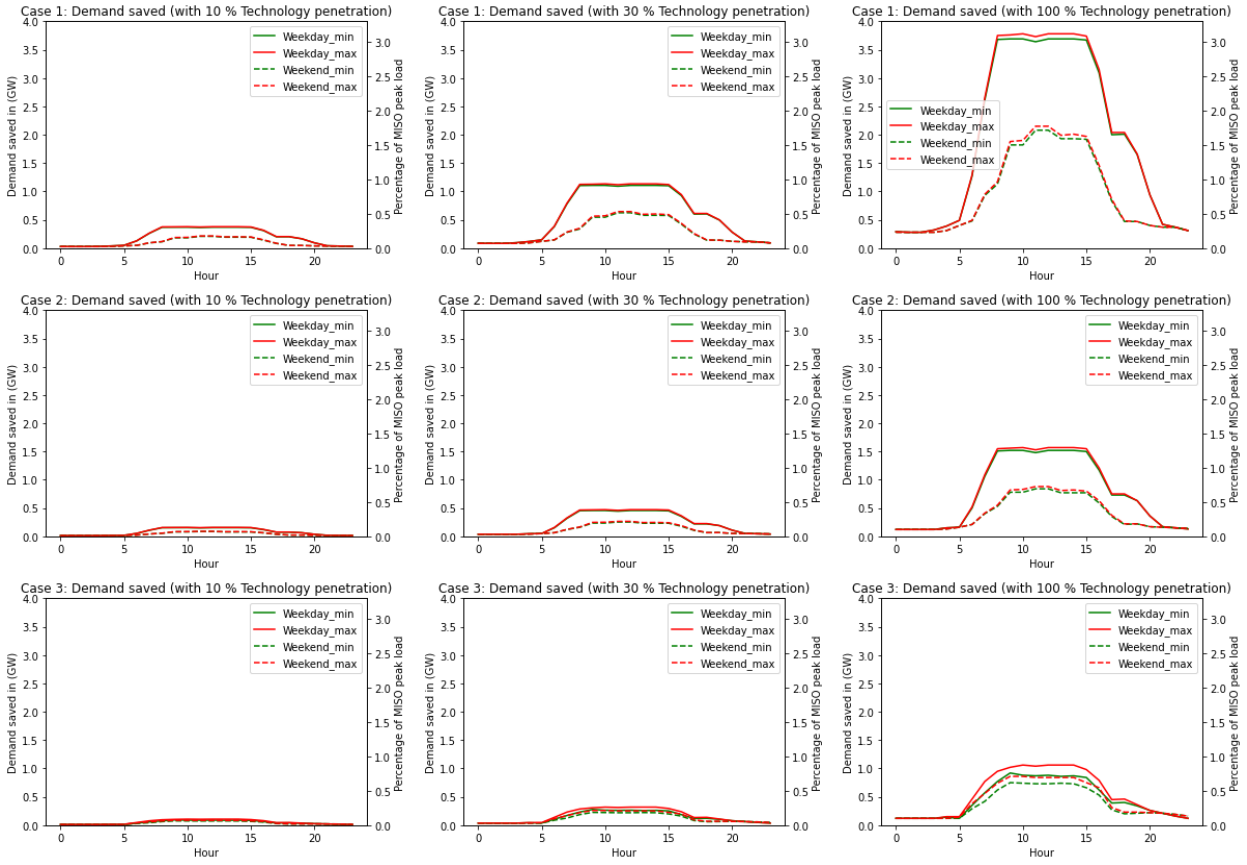

Figure 4-14 Maximum and minimum aggregated demand saved due to lighting-based FS for all three cases in table 3 at an hourly level for the entire MISO region for weekdays and weekends

Table 4-4: Available lighting loads for FS at the MISO level as a percent of total peak MISO loads

Case	Sub case	Peak load (in MW)			MISO (in GW)	% of MISO load		
		TP_10%	TP_30%	TP_100%		TP_10%	TP_30%	TP_100%
Case_1	Weekday - Min	369	1107	3690	121	0.30	0.91	3.05
	Weekday - Max	378	1134	3780	121	0.31	0.94	3.12
	Weekend - Min	208	624	2080	121	0.17	0.52	1.72
	Weekend - Max	215	645	2150	121	0.18	0.53	1.78
Case_2	Weekday - Min	152	456	1520	121	0.13	0.38	1.26
	Weekday - Max	157	471	1570	121	0.13	0.39	1.30
	Weekend - Min	84	252	840	121	0.07	0.21	0.69
	Weekend - Max	88	264	880	121	0.07	0.22	0.73
Case_3	Weekday - Min	92	276	920	121	0.08	0.23	0.76
	Weekday - Max	106	318	1060	121	0.09	0.26	0.88
	Weekend - Min	75	225	750	121	0.06	0.19	0.62
	Weekend - Max	86	258	860	121	0.07	0.21	0.71

4.6 CONCLUSIONS

The percentage of electricity generated from variable sources such as wind and solar is projected to rise in the future. One of the ways to balance the demand and supply in the electric grid is through adjusting the load on the electric grid (i.e., the demand side). This study is focused on estimating the Flexibility Services that can be provided by the lighting load in commercial buildings. Based on the literature review, it was found that lighting load can be reduced by 20% from the baseline illuminance level without causing any significant discomfort to occupants. Thus, this study first uses Reference and Prototype building energy models to estimate the lighting load that can be used for FS due to various building types and their energy code versions. The study also accounts for daylighting controls that can either dim or completely turn off the lights when sufficient daylight is present. The building level loads are further aggregated to various nodes of the electric grid for the MISO region.

The study discusses various cases in the present and future with a range of levels of LED lighting fixture adoption and availability of technology that can use the existing lighting infrastructure to

provide FS. Overall, results suggest that for a case with all LEDs and a 30% technology penetration, these smart lighting fixtures can provide approximately 300 to 600 MW (0.25 to 0.5 % of MISO peak load) of lighting-based FS. For the case with 100 % LEDs that also use perimeter zone daylighting controls can provide around 300 – 400 MW (0.25 to 0.33 % of MISO peak load) of lighting-based FS. Reducing these peaks loads can help to reduce the need for high cost and carbon emitting peaking plants resulting in a cleaner and affordable grid. Further, the use of daylighting controls reduces overall energy consumption of the buildings which is a strong benefit from an emissions standpoint. However, this also reduces the amount of load used by lighting that can support FS. Similarly, as the current higher Lighting Power Density (LPD) lighting fixtures that can provide more demand flexibility are replaced with lower LPD lighting fixtures, this will also reduce consumption, which is beneficial, but at the same time reduce the available demand flexibility from lighting. We also note that demand-side lighting FS in commercial buildings also aligns with typical solar energy generation profiles. Thus, likely it can be used to offset losses in solar generation due to intermittent causes such as the sun being obstructed by clouds. Moving forward, these results at each node can be used for grid models focused on predicting future generation, transmission, and distribution infrastructure.

There are some limitations to this study, as well as opportunities for future work. The first relates to the “acceptable” and “detectable” limits for lighting dimming. Most studies that provide this are older and the impact on vision or loss of productivity over long term dimming is not extensively studied. In addition, these studies did not account for external daylight. Newer studies could be further used to determine the maximum amount of time the lighting loads can be lowered, as well as how daylight impacts these results. The second relates to the building stock data used. The building stock was approximated using the two datasets, the CoStar Realty Information data and

FEMA Hazus building stock. However, while these datasets represent, to the authors' knowledge, the most comprehensive datasets available for buildings, they do not necessarily represent the entire building stock. Development of building stock data at the county level would improve the accuracy of aggregation efforts. Third, is the limitations on knowing the growth in availability and costs of LED lights, daylight and occupancy controls, and other technologies, as well as changes to regulations and mandates which might impact adoption rates, and or willingness to participate. Technology adoption rates and willingness to participate in FS for commercial buildings should be studied further to better refine these growth estimates for future scenarios.

REFERENCES

Akashi, Yukio, and Jason Neches. 2004. “Detectability and Acceptability of Illuminance Reduction for Load Shedding.” *Journal of the Illuminating Engineering Society* 33 (1): 3–13. https://doi.org/10.1080/00994480.2004.10748422.

Augustine, C.; Bain, R.; Chapman, J.; Denholm, P.; Drury, E.; Hall, D.G.; Lantz, E.; Margolis, R.; Thresher, R.; Sandor, D.; Bishop, N.A.; Brown, S.R.; Cada, G.F.; Felker, F.; Fernandez, S.J.; Goodrich, A.C.; Hagerman, G.; Heath, G.; O’Neil, S.; Paquette, K. 2012. “Renewable Electricity Generation and Storage Technologies. Vol 2. of Renewable Electricity Futures Study. NREL/TP-6A20-52409-2.” Vol. 2. Golden, CO.

Berg, Brady, et al. "Occupant-Driven End Use Load Models for Demand Response and Flexibility Service Participation of Residential Grid-Interactive Buildings." Available at SSRN 4108846 (2022).

Cetin, Kristen S., et al. "Development and validation of an HVAC on/off controller in EnergyPlus for energy simulation of residential and small commercial buildings." Energy and Buildings 183 (2019): 467-483.

Deru, Michael, Kristin Field, Daniel Studer, Kyle Benne, Brent Griffith, Paul Torcellini, Bing Liu, et al. 2011. “U.S. Department of Energy Commercial Reference Building Models of the National Building Stock.” *Publications (E)*, no. February 2011: 1–118. http://digitalscholarship.unlv.edu/renew_pubs/44.

EIA 2020, Energy Consumption by sector. Available:https://www.eia.gov/totalenergy/data/browser/?tbl=T02.01#/?f=A&start=2003&end=2020&charted=3-6-9-12

FEMA Hazus building stock data Available: https://www.fema.gov/summary-databases-hazus-multi-hazard

Geraldi, Matheus Soares, and Enedir Ghisi. 2020. “Mapping the Energy Usage in Brazilian Public Schools.” *Energy and Buildings* 224: 110209. https://doi.org/10.1016/j.enbuild.2020.110209.

Geneticalgorithm, Python Package Index - PyPI. Available at: https://pypi.org/project/geneticalgorithm/

Hu, Wenye, and Wendy Davis. 2016. “Dimming Curve Based on the Detectability and Acceptability of Illuminance Differences.” *Optics Express* 24 (10): A885. https://doi.org/10.1364/oe.24.00a885.

IES LIGHTING HANDBOOK The IES Lighting Handbook: Reference and Applications, Tenth Edition” (2011).

Karpilow, Alexandra, Gregor Henze, and Walter Beamer. 2020. “Assessment of Commercial Building Lighting as a Frequency Regulation Resource.” *Energies* 13 (3): 1–14.

https://doi.org/10.3390/en13030613.

Kawka, Emily. Data-Driven Modeling and Analysis of Residential Building Energy Consumption and Demand Flexibility. Michigan State University, 2022.

Kryszczuk, Krzysztof M., and Peter R. Boyce. 2002. “Detection of Slow Light Level Reduction.” *Journal of the Illuminating Engineering Society* 31 (2): 3–10.https://doi.org/10.1080/00994480.2002.10748387.

Kunwar, Niraj, Soham Vanage, and Kristen Cetin. 2021. “Residential Occupant-Dependent Appliance Power and Time-Of-Use Estimation for Grid Demand Response Applications.” *ASHRAE Transactions* 127 (1).

Langevin, Jared, et al. "US building energy efficiency and flexibility as an electric grid resource." Joule 5.8 (2021): 2102-2128.

Lawrence Berkeley National Laboratory “Building Performance Database (BPD),” 2019. Available: https://bpd.lbl.gov/.

Li, Yifan, and James D. McCalley. 2017. “An Innovative Disjunctive Model for Value-Based Bulk Transmission Expansion Planning.” *Electric Power Systems Research* 143: 7–13. https://doi.org/10.1016/j.epsr.2016.09.004.

Livingston, O V, P C Cole, D B Elliott, and R Bartlett. 2014. “Building Energy Codes Program: National Benefits Assessment.” *Pacific Northwest National Laboratory, Richland, Washington*, no. March: 1992–2040.

M. Day 2020, “City and County Commercial Building Inventories. National Renewable Energy Laboratory,” U.S. Dept. of Energy Office of Energy Efficiency &Renewable Energy, 2020. Available: https://catalog.data.gov/dataset/city-and-county-commercial-building-inventories.

Ma, Ookie, Nasr Alkadi, Peter Cappers, Paul Denholm, Junqiao Dudley, Sasank Goli, Marissa Hummon, et al. 2013. “Demand Response for Ancillary Services.” *IEEE Transactions on Smart Grid* 4 (4): 1988–95. https://doi.org/10.1109/TSG.2013.2258049.

Ma, Ookie, Ricardo Oliveira, Evan Rosenlieb, Megan Day, Ookie Ma, Ricardo Oliveira, Evan Rosenlieb, and Megan Day. 2019. “Sector-Specific Methodologies for Subnational Energy Modeling Sector-Specific Methodologies for Subnational Energy Modeling,” no. November. https://www.nrel.gov/docs/fy19osti/72748.pdf.

MISO 2020, Available: https://cdn.misoenergy.org/MISO%20FORWARD_2020433101.pdf

Newlun, Cody J., James D. McCalley, Rajaz Amitava, Ali Jahanbani Ardakani, Abhinav Venkatraman, and Armando L. Figueroa-Acevedo. 2021. “Adaptive Expansion Planning Framework for MISO Transmission Planning Process.” *2021 IEEE Kansas Power and Energy Conference, KPEC 2021*. https://doi.org/10.1109/KPEC51835.2021.9446221.

Kunwar, Niraj, Soham Vanage, and Kristen Cetin. "Residential Occupant-Dependent Appliance Power and Time-Of-Use Estimation for Grid Demand Response Applications." ASHRAE Transactions 127.1 (2021).

Raziei, Seyed Ataollah, and Hamed Mohscnian-Had. 2013. “Optimal Demand Response Capacity of Automatic Lighting Control.” *2013 IEEE PES Innovative Smart Grid Technologies Conference, ISGT 2013*, 1–6. https://doi.org/10.1109/ISGT.2013.6497854.

Ryan, James, Erik Ela, Damian Flynn, and Mark O’Malley. 2014. “Variable Generation, Reserves, Flexibility and Policy Interactions.” In *Proceedings of the Annual Hawaii International Conference on System Sciences*, 2426–34. IEEE. https://doi.org/10.1109/HICSS.2014.304.

Tenner, A. D., Begemann, S. H. A., & Beld, van den, G. J. (1997). Acceptance and preference of illuminances in offices. In the European Lighting Conference (pp. 130-143)

Tina, Giuseppe Marco, Stefano Aneli, and Antonio Gagliano. "Technical and economic analysis of the provision of ancillary services through the flexibility of HVAC system in shopping centers." Energy 258 (2022): 124860.

Tran-Quoc, T., et al. "Air conditioner direct load control in distribution networks." 2009 IEEE Bucharest PowerTech. IEEE, 2009.

U.S. Department of Energy, Energy Savings Forecast of Solid-State Lighting in General Illumination Applications, accessed August 19, 2019

U.S.DOE 2022a Commercial Prototype Building Models. Available: https://www.energycodes.gov/prototype-building-models#Commercial

U.S.DOE 2022b Commercial Reference Building Models. Available: https://www.energy.gov/eere/buildings/commercial-reference-buildings

U.S. EIA 2018 Commercial Buildings Energy Consumption Survey. Available: https://www.eia.gov/consumption/commercial/data/2018/

Zhou, Ying, Lizhi Wang, and James D. McCalley. 2011. “Designing Effective and Efficient Incentive Policies for Renewable Energy in Generation Expansion Planning.” *Applied Energy* 88 (6): 2201–9. https://doi.org/10.1016/j.apenergy.2010.12.022.

CHAPTER 5 – CONCLUSIONS AND RESEARCH CONTRIBUTIONS

5.1 Conclusions

This research focuses on energy savings, demand reduction, and visual comfort improvements due to lighting and shading controls in commercial buildings. The first step was to investigate the kind of control strategies that already exist in the recent literature and the metrics used to implement the control strategy, then evaluate their performance post-implementation. Based on the literature review, various control strategies for lighting and shading controls in buildings already exist. The results of these studies are usually presented as case studies using either actual buildings or simulations using box models. However, comparing shade and lighting control strategies across different studies for generalized conclusions is still very challenging as most existing studies use different baseline model assumptions for some variables such as room sizes (depth and width), window size (height, width, and WWR (with/without split windows)), window orientation (simultaneous windows in two directions), glazing material properties, shade material properties, and climate zones of the building.

Thus, the first part of this study focused on comparing the existing control strategies using a common baseline model. A DOE Prototype building model for small office buildings was chosen as it is the most common commercial building in the United States based on the building size and use type. Controls were modeled for four different categories including (a) Baseline Model (model with and without shades/ no lighting control), (b) Manual Control Strategy, (c) Independent Control Strategy using solar radiation and glare and (d) a novel control strategy developed by the author, called the Integrated Control Strategy. This combines the Independent Control Strategy with other variables such as Work Plane Protection Position (WPP), occupancy-based control, and HVAC state to select appropriate shading and lighting level targets. The performance metrics used for comparing these control strategies include visual comfort metrics such as view to the outside,

glare conditions, and energy use metrics such as cooling, heating, lighting, and total EUI. Sensitivity analysis for two variables namely zone orientation (N, W, E and S) and ASHRAE climate zones (CZ2A, CZ4A, CZ5A, and CZ7) was provided when comparing the control strategies. The conclusions of this study suggest that a complex rule-based shading strategy such as an Integrated Control Strategy, which uses HVAC state, occupancy sensors, and time of day for controls, only performs slightly better in terms of both energy use and visual comfort than a control strategy that uses glare to control the shades. Thus, if the addition of sensors is needed to support complex shading and lighting control strategies, these sensors may benefit from being used for multiple purposes such as occupancy detection and HVAC controls in order to justify their use.

The results for the first part were used to select a control strategy for further sensitivity analysis. The control strategy chosen was an Independent Control Strategy (IDS) using glare. The other aspect identified in the first part is that variables such as climate zones impact energy use significantly but not visual comfort. Building-related variables such as Window-to-Wall Ratio (WWR), orientation of the windows, shade properties, glazing properties, and presence of shade overhangs are some of the variables that significantly affect both visual comfort and the energy performance of the building. To investigate the impact of these variables on the control strategy, the prior model was updated further to build a parametric simulation model using six (6) input variables, including WWR for all four orientations, shade material openness factor, and the length overhang depth to evaluate the best-case scenarios based on four performance metrics Useful Daylight Illuminance (UDI), Energy Use Intensity (EUI), view to the outside, and improvement and thermal comfort. To evaluate the impact of additional variables, this process was repeated nine (9) times for different building form factors to estimate the variation in results as the building form factor changed. The study concludes that the best solution for two (2) variable combinations such

as with one of the variables involving EUI (such as EUI and UDI, EUI and View, EUI, and PMV) the solution) is predominantly a low 1% openness factor for shade openness factor combined with high WWR values (such as 75 % and 50%) for the South and West facing direction. The other set of optimum solutions involves a high shade openness factor (5% and 10 %) openness factor for shade openness factor combined with low WWR values (such as 25 % and 50%). For the north-facing direction, the optimum values for results do not show any particular pattern. For the variable shade overhang depth, no overhangs are slightly preferable for square buildings whereas overhangs with 1 meter depth are preferable for more rectangular buildings. However, the difference is very close to 50-50. Therefore, the variation in result between building form factors is only slightly different.

In addition to the four (4) performance metrics, (Energy based (EUI) and comfort based (UDI, view and thermal comfort)) used in Focus Area 2, the demand reduction potential using building controls is projected to play an important role in future as the percentage of electricity generated from variable sources such as wind and solar is projected to rise in the future. For the grid to be balanced, the electric demand and supply need to match in real time. Though there are various ways of achieving this, one cost-effective method is to reduce existing building loads when the electric grid is strained, also known as Demand-Side Flexible Services. To simplify this study, only lighting controls are considered, as shading was always assumed to be open. The potential for lighting loads as Flexibility Services was estimated for 10 different types commercial buildings using DOE Reference and Prototype building models as opposed to just the small office building on Focus Area 1 and 2.

Based on the literature review, it was found that lighting load can be reduced by 20% from the baseline illuminance level without causing any significant discomfort to occupants. The study also

accounts for daylighting controls that can either dim or completely turn off the lights when sufficient daylight is present. The building level loads for these 10 commercial buildings are further aggregated to various nodes of the electric grid for the MISO region. Overall, results suggest that for a case with all LED lighting in commercial buildings and a 30% technology penetration, these smart lighting fixtures can provide approximately 300 to 600 MW (0.25 to 0.5 % of MISO peak load) of lighting-based FS. For the case with all % LED lighting that also use perimeter zone daylighting controls can provide around 300 to 400 MW (0.25 to 0.33 % of MISO peak load) of lighting-based FS. Thus, using lighting loads as a Demand-side FS can reduce peak loads, which can help to reduce the need for high-cost and high-carbon emitting peaking plants resulting in a cleaner and affordable grid.

5.2 Research Contributions

The goal of this research study is to investigate energy savings, demand reduction, and visual comfort improvements due to lighting and shading controls in commercial buildings. A meta-analysis that can quantify and estimate the visual comfort and energy savings improvements for shading and lighting controls across different existing control strategies can be very challenging as these studies have different assumptions for baseline models and use different metrics for comparing the results. This portion of this research represents a significant contribution as it provides a performance comparison between existing control strategies with same building inputs. In addition to the control strategies, the study also provides different baseline cases such as shades always open, shades always closed, and manual control strategy to which the results for complex shading controls can be compared. The developed methodology can be used by design teams to estimate energy savings and visual comfort improvements based on their respective baseline case.

The control strategies are compared using an ASHRAE 90.1-2004 baseline model, for which EUI compares to the existing building stock. However, the Lighting Power Density (LPD) for the model is assumed to be 6.88 W/m^2 with all LED lighting, as replacing LED lighting is the easiest retrofit for energy saving before implementing any controls. Thus, the results of this study are very relevant for retrofit projects that are planning control upgrades when selecting different controls strategies. For new construction projects, energy savings will be lower than predicted in this research due to a likely more efficient building envelope and more efficient equipment. However, as this research assumes LED lighting for the model, the lighting energy saving, and visual comfort results are applicable for both retrofit and the new construction projects.

For the development of the parametric model, previous studies that have used parametric/optimization models with shading systems such as roller shades are limited. Most studies have focused on using horizontal and vertical louvers. Further, studies that have used a parametric model for a roller that switches between different shade positions based on a control strategy are rare. This study uses roller shades with three shade positions (fully open, 50 percent closed, and fully closed) and uses a daylighting model that controls shade in all four orientations independently for each timestep. As the amount of daylight entering the space from different orientations varies throughout the day, using an automated shading control strategy for roller shades that can operate in multiple positions independently for different orientations is crucial.

Literature reviews for parametric and optimization studies for daylighting models usually use only two output metrics, Energy Use Intensity (EUI) and one daylighting metric, typically Useful Daylight Illuminance (UDI) or Daylight Autonomy (DA). A few studies have also used Spatial Daylight Autonomy (sDA) and Annual Sunlight Exposure (ASE) as the output metrics for visual comfort. This study uses a glare-based daylighting control strategy (shades are lowered if

DGPs>0.35) with multiple output metrics including Energy Use Intensity (EUI), Useful Daylight Illuminance (UDI), view to the outside, and percent improvement in thermal comfort. Thus, the parametric model adds to the existing knowledge of roller shade-based systems while selecting the best solution, considering more performance metrics than past studies. The results also present the best solution for a combination of two/three variables. For instance, this project uses four performance metrics UDI, EUI, view and thermal comfort. The study provides the best solution for combination for two variable such as best solution for UDI and EUI, the best solution EUI and view and so on. Similarly, the study also presents the best solution for combination of three (such as UDI, EUI and view or EUI, UDI and Thermal comfort and so on) variables. The results presented thus can help a design team to choose a set of input variables based on their goal for a particular project. As the input variables used in the parametric model, such as building form factor, WWR, shade properties, and depth of shade overhang, are decided during the preliminary design phase of the project, these variables are harder to change after building construction is complete. As the model uses ASHRAE 90.1-2019 standard assumptions for the baseline model, the research is useful for estimating energy saving and visual comfort improvements for new construction projects.

Finally, by estimating demand flexibility using lighting loads for different commercial buildings, the developed building- and grid-scale estimates for each grid node can be used for grid models focused on predicting future generation, transmission, and distribution infrastructure performance and needs. The study presents three scenarios that provide high and low estimates for the potential for using lighting loads as demand side-flexibility services. As HVAC loads for flexibility services is extensivity studied as flexibility services, the same amount of attention is currently not given for lighting loads; this study addresses this gap.

5.3 Limitations and Future Work

Ladybug tools are used to model the control strategies and develop the parametric model. This front-end tool allows the user to develop daylighting and energy simulation models using one common set of tools. The Ladybug tool uses EnergyPlus for energy simulation and RADIANCE for daylighting simulation. It also supports cloud-based computation, allowing the ability to run very large parametric models (such as the models used in this research) faster. However, despite using the latest available tools and analyzing the current literature for opportunities, there are some assumptions and limitations to the current study.

First, the minimum timestep for the analysis is one hour due to the significant time taken for RADIANCE simulation for granular timesteps. Studies with more granular timesteps for daylighting and energy simulation can highlight the incremental saving of complex shading and lighting strategies by capturing fluctuating weather conditions. Second, the occupancy schedule used in Integrated Control Strategy (IGS) is based on the DOE model Prototype Building model's hourly occupancy schedule. A stochastic model or a case study which accounts for occupancy at a finer timestep can better highlight the impact of occupancy when used as IGS. The third limitation is that while using the Ladybug tool's cloud computing option allows the author to develop a large parametric model, even with cloud-based tools, it can still be very difficult to add every variable that influences the model's performance. Further, cloud-based tools currently only allow for the development of parametric models and not optimization-based models. Implementing Optimization based algorithms with cloud-based computing can allow for more variables to be incorporated into the simulation for a more fine-tuned result. This study also explored WWR, shade properties, and shade overhang depth as a few variables. However, other variables, such as glazing type, minimum windowsill heights, and different climate zones, can provide further insight

for the impact. For future work the author proposes to also study the impact of daylighting and it controls on different types of commercial buildings (e) The shade depth variable can be optimized for each orientation instead of using the same shade depth for all directions (that converts one variable into four additional variables, increasing the number of simulations significantly). (f) The study only considers form factors with rectangular shapes. However, buildings with non-rectangular shapes such as U-shaped, T-shaped, H-shaped, trapezoidal, and other free-form building shapes combined with the effect of daylight and energy performance are not well studied. If such non-rectangular building shapes with multiple stories are analyzed, the shading effect of parts of the same building over other parts of the building must be carefully evaluated.

For limitations and future work for the demand flexibility part of this research, the first relates to the "acceptable" and "detectable" limits for lighting dimming. Most studies that provide this are older, and the impact on vision or loss of productivity over long-term dimming has not been extensively studied. In addition, these studies did not account for external daylight. Newer field studies that could quantity and verify these acceptable and detectable levels can be used to determine the maximum amount of time the lighting loads can be lowered and how daylight impacts these results. The second relates to the building stock data used. The building stock was approximated using the two datasets, the CoStar Realty Information data and the FEMA Hazus building stock. However, while these datasets represent, to the authors' knowledge, the most comprehensive datasets available for buildings, they do not necessarily represent the entire building stock in the U.S. Developing building stock data at the county level would improve the accuracy of aggregation efforts. Efforts to build a robust dataset for commercial building will help refine the grid levels. Third is the limitations on knowing the growth in availability and costs of LED lights, daylight and occupancy controls, and other technologies, as well as changes to

regulations and mandates which might impact adoption rates and or willingness to participate moving forward. Technology adoption rates and willingness to participate in FS for commercial buildings should be studied further to refine these growth estimates for future scenarios. Further, the current study only develops estimates for lighting controls, but a combination of lighting and shading control can provide better estimates and should be considered for future work.

CHAPTER 6 – PUBLICATIONS

6.1 Journal Publications

Vanage, S., Dong, H., & Cetin, K. (2023). Visual comfort and energy use reduction comparison for different shading and lighting control strategies in a small office building. *Solar Energy*, 265, 112086.

Vanage, S., Cetin, K., McCalley, J., & Wang, Y. (2023). Grid-Scale Demand-side Flexibility Services using Commercial Buildings Lighting Loads. *Energy and Buildings*, 113631.

Vanage, S., Dong, H., Kunwar, N. & Cetin, K. (2023). Parametric model development for building input variables for lighting and shading controls for different building form factors *(to be submitted to Journal Energy)*

6.2 Conference proceedings

Vanage, S., Hao Dong, and Kristen Cetin. "Energy and demand saving potential due to integrated HVAC, lighting, and shading controls in small office building." *Construction Research Congress 2022*. 2022.

Vanage, S., Kunwar, N., Malekpour, D., & Cetin, K. (2022, January). Co-Simulation and Validation of Automated Shading Devices using EnergyPlus and Radiance to Optimize Building Energy Use. In *ASHRAE winter conference* papers.

Vanage, S., Niraj Kunwar, and Emily Kawka. "Aggregation of Lighting Demand Response for the Midcontinent Independent System Operator (MISO) Region." *ASHRAE Transactions* 127 (2021): 484-491.

Vanage, S., Amitava, R., Kawka, E., Morton, A., Newlun, C., & Kristen Cetin PhD, P. E. (2021). Framework for Assessing Grid-Level Impacts of Building Participation in Flexibility Services. *ASHRAE Transactions*, 127, 23-26.

Vanage, S.; Cetin, Kristen; McCalley, James; Yu Wang " Estimating Demand Flexibility using Cooling Loads in Commercial Office Buildings." *ASHRAE Transactions*. 2022, Vol. 128 Issue Part2, p23-26. 4p

Vanage, S., Kawka, E., Cetin, K., Amitava, R., Newlun, C., & McCalley, J. (2021, April). Impact of Demand Response on Flexibility Services and Transmission Investment. In 2020 52nd *North American Power Symposium (NAPS)* (pp. 1-6). IEEE.

6.3 Other Publications

Dong, Hao, **Soham Vanage**, and Kristen Cetin. "Review of Ice Thermal Energy Storage (ITES) using Conventional Control Strategies in Commercial Buildings." *ASHRAE Transactions* 129 (2023).

Shrestha, S., Desjarlais, A. O., Jogineedi, R., Biswas, K., Bingham, L., Weiss, B., & **Vanage, S.** (2023). Transformative Efficiency and Automation in Modular Homes (TEAMH). *Oak Ridge National Lab (ORNL)*, Oak Ridge, TN (United States).

Dong, Hao, **Soham Vanage**, and Kristen Cetin. "Energy Use Sensitivity Analysis of Sensor Placement in Small Office Buildings with Dynamic Shading and Lighting." *ASHRAE Annual Conference* 2022. 2022.

Berg, B., Kunwar, N., **Vanage, S**., Cetin, K., Ardakani, A. J., McCalley, J., & Wang, Y. (2022). Occupant-Driven End Use Load Models for Demand Response and Flexibility Service Participation of Residential Grid-Interactive Buildings. Available at SSRN 4108846.

Kunwar, Niraj, **Soham Vanage**, and Kristen Cetin. "Residential Occupant-Dependent Appliance Power and Time-Of-Use Estimation for Grid Demand Response Applications." *ASHRAE Transactions* 127.1 (2021).

Kunwar, N., **Vanage, S.,** Peruski, E., Mitra, D., & Cetin, K. (2020). Occupant-Dependent Residential End Use Load Profiles for Demand Response Under High Renewable Energy Scenarios. *ASHRAE Transactions*, 126(2), 3-6.